The University Of Sheffield.

Deciphering the mechanisms linking DNA damage repair, chromatin modification and autophagy in Huntington's disease

Nelma Margarida Pereira Palminha

A thesis submitted in partial fulfilment of the requirements for the degree of Doctor of Philosophy

Department of Molecular Biology & Biotechnology
University of Sheffield

September 2021

Declaration

I, Nelma Margarida Pereira Palminha, confirm that the Thesis is my own work. I am aware of the University's Guidance on the Use of Unfair Means (www.sheffield.ac.uk/ssid/unfair-means). This work has not previously been presented for an award at this, or any other, university.

Acknowledgements

Firstly, I would like to express my gratitude to my supervisor, Prof Sherif El-Khamisy. Thank you for the all the guidance, wisdom and support you have given me throughout these 4 years. I will be forever grateful to you for this opportunity and for believing in me.

To Dr Laura Ferraiuolo and Dr Cleide dos Santos Souza, thank you for generating the GABAergic neurons, and for providing me with training and knowledge in iNPC differentiation. Also, thank you for preforming the immunofluorescence screening using the Opera system and analysis with Harmony software.

I would also like to thank Dr Swagat Ray for all the support and advice given throughout these years. To Dr Chunyan Liao thank you for your help in maintaining my cells when needed and for all the help during my time in the lab. To Dr Mateusz Jurga, thank you for also helping me with cell maintenance and Western blotting, and for all the good moments in the lab.

A special thanks to soon-to-be Dr Nelly Berrueta Ramirez, my Nena and PhD sister, for all the useful discussions, dancing and laughing. To soon-to-be Dr Arwa Abugable, thank you for helping with cell maintenance, and immunoblotting, as well as for our lovely discussions about troubleshooting IPs and for the chocolates. To all members of the El-Khamisy lab, past and present: thank you for all your support.

To my dear friends Marta, Ricardo, Rita and Rogério (Gang das Manas) and to Cristiana, Filipe and Madalena (Sheffield's Portuguese crew), thank you for always being there for me no matter what. You have kept me sane during these insane years. You are my pillars and the best friends anyone could ever ask for.

To my parents, I express my immense gratitude. If I am here writing these words, it is all thanks to you and your infinite support. I am proud to be your daughter.

Finally, I acknowledge the open access license that covers the use of BioRender, allowing me to create some of the diagrams for this thesis.

Abstract

Huntington's disease (HD) is a neurodegenerative disorder caused by CAG repeat expansion in the huntingtin *(HTT*) gene, with no current treatments available. Neurodegeneration is often associated with defects in DNA damage response (DDR) pathways. Several studies have suggested a common pathogenic mechanism driven by faulty DDR processes in polynucleotide expansion disorders. One form of DNA breakage is topoisomerase I (TOP1)-linked DNA breaks which arise from normal brain function and constitute a threat to neuronal survival. TOP1-DNA breaks cause neurodegeneration in several disorders, including spinocerebellar ataxia with axonal neuropathy-1 (SCAN1), ataxia telangiectasia (A-T) and in amyotrophic lateral sclerosis (ALS). Whether TOP1-DNA breaks are sources of genomic instability in HD is unknown. Evidence also suggests a crosstalk between defective DNA repair, accumulation of toxic protein aggregates and autophagy, which has been shown to be involved in the pathogenesis of *C9orf72*-ALS. Whether and how these mechanisms are connected in the context of HD is unclear.

To address these issues, I examined the recruitment of DDR factors in response to DNA damage, analysed histone H2A ubiquitination and tested whether defective autophagy mechanisms are responsible for altering DNA repair signalling in HD models. I report defective 53BP1 foci formation in human cells ectopically expressing mutant HTT, HD primary human fibroblasts and primary GABAergic striatal neurons derived from HD patients after treatment with the TOP1 inhibitor, camptothecin (CPT), suggesting HD cells lack efficient DDR signalling in response to TOP1-induced DNA breaks. Defective 53BP1 recruitment was caused by reduced H2A ubiquitination due to limited availability of RNF168. The reduced RNF168 activity was caused by increased p62 interaction, a protein involved in selective autophagy. Depletion of p62 or disruption of the interaction between RNAF168 and p62 restored 53BP1 recruitment and subsequent DNA repair in HD cellular models, providing new opportunities for therapeutic interventions. These findings are reminiscent to what was described for p62 accumulation caused by *C9orf72* expansion in ALS/FTD and suggest a common mechanism by which protein aggregation perturb DNA repair signalling.

Table of contents

List of Figures

List of tables

Abbreviations

% – percent
53BP1 – p53-binding protein 1
5mc – 5 methyl-cytosines
8-oxoG – 8-oxoguanine
AIF – apoptosis-inducing factor
ALS – Amyotrophic lateral sclerosis
AOA – Ataxia oculomotor apraxia
AOA1 – Ataxia with oculomotor apraxia type-1
AP site – Apurinic site
APE1 – AP-endonuclease 1
APLF – Aprataxin and PNKP-like factor
APTX – Aprataxin
APTX – Aprataxin
A-T – Ataxia telangiectasia
ATLD – Ataxia telangiectasia-like disease
ATM – Ataxia telangiectasia mutated
ATXN3 – Ataxin-3
BARD1 – BRCA1-associated RING domain
BDNF – Brain-derived neurotrophic factor
BER – Base excision repair
BRCA1 – Breast cancer type 1 susceptibility protein
BSA – Bovine serum albumin
BURD - BRCT-domain-associated ubiquitin-dependent recruitment
C9orf72 – chromosome 9 open reading frame 72
CAG – Cytosine-adenine-guanine
CBP – CREB-binding protein
CNS – Central nervous system
Co-IP – Co-immunoprecipitation
CPP – Cell penetrating peptide
CPT – Camptothecin
CREB – cAMP-response element
DAPI – 4,6-diamidino-2-phenylindole
DDR – DNA damage response
dH_2O – Distilled water
DKK-1 – Dickkopf-1
DMEM – Dulbecco's Modified Eagle's Medium
DMSO – Dimethyl sulfoxide
DNA – Deoxyribonucleic Acid
DNA-PK – DNA-dependent Protein Kinase
DPR – Dipeptide repeats
DRH – DNA repair hotspot
DRPLA – Dentatorubral-pallidoluysian atrophy
DRPLA – Dentatorubral-pallidoluysian atrophy
DS – Donkey serum
DSB – Double-strand break
DSBR – Double-strand break repair
DUB - Deubiquitinase
E1 – Ubiquitin-activating enzyme
E2 – Ubiquitin-conjugating enzyme
E3 – Ubiquitin ligase
FA – Fanconi anaemia
FBS – Foetal bovine serum
GABA – Gamma-aminobutyric acid
GeM-HD – Genetic Modifiers of Huntington's disease
GoF – Gain-of-function
GWAS – Genome-wide association studies
h – hour
H2AK15ub – Ubiquitinated H2A at lysine 15
H_2O_2 – Hydrogen peroxide
HAP1 – Huntingtin-associated protein 1
HD – Huntington's disease
Hdh - HD gene homolog
HEAT – Huntingtin, Elongation Factor 3, PR65A scaffolding subunit of protein phosphatase 2A, and Target of rapamycin (TOR) kinase
HEK293 – Human embryonic kidney 293
HIV-1 – Human immunodeficiency virus 1
HR – Homologous recombination
HTT – Huntingtin
ICL – Interstrand crosslink
IF – Immunofluorescence
IP – Immunoprecipitation
iPSC – induced pluripotent cell
K - Lysine
LB – LIM protein-binding
LIM – LIN-11, Isl1 and MEC-3
LoF – Loss-of-function
Me2 – Dimethylated
MEF – Mouse embryonic fibroblasts
MEM – Minimum Essential Medium Eagle
min – minute
MIU1 – Motif interacting with ubiquitin 1
MMR – Mismatch repair

MRC5 – Medical Research Council strain 5
MRN - MRE11, RAD50 and NBS1
mRNA – messenger RNA
MSN – medium spiny neuron
mtHTT – mutant huntingtin
NEAA – Nonessential amino acids
NER – Nucleotide excision repair
NES – Nuclear export signal
NES – Nuclear export signal
NHEJ – Non-homologous end joining
NLS – Nuclear localization signal
NPC – Neural progenitor cell
NuRD – Nucleosome Remodelling and histone Deacetylation
$O_2^{\bullet-}$ – Superoxide
OGG1 – 8-oxoG DNA glycosylase
PARP1 – poly (ADP-ribose) polymerase 1
pATM – Phosphorylated ATM
PBS - Phosphate Buffered Saline
PDB – Protein-linked DNA breaks
PEI – Polyethylenimine
PIKK – Phosphoinositide 3-kinase (PI3K)-related kinases
PNKP – Polynucleotide kinase 3'-phosphatase
PolyQ – Polyglutamine
Polβ – Polymerase β
PPI – Protein:protein interaction
PRC1 – Polycomb repressive complex 1
PTD – Protein transduction domain
PTM – Post-translational modification
RA – Retinoic Acid
PMN – Purmorphamine
REST/NRSF – Repressor element-1 transcription factor/neuron restrictive silencer factor
RING – Really interesting new gene
RNA - Ribonucleic Acid
RNF168 – RING finger protein 168
RNF8 – RING finger protein 8
RNS – Reactive nitrogen species
ROS – Reactive oxidative species
RPA – Replication protein A
RRE – RNA repeat expansion
rRNA – Ribosomal RNA
RT – Room temperature
S – Serine
s.e.m. – Standard error of mean
SAR-seq – synthesis associated with repair sequencing
SASP – Senescence-associated secretory phenotype
SA-β-gal –Senescence-associated-β-galactosidase
SBMA – Spinal and bulbar muscular atrophy
SBMA – Spinal and bulbar muscular atrophy
SCA – Spinocerebellar ataxia
SCAN1 - Spinocerebellar ataxia with axonal neuropathy 1
SDS – Sodium dodecyl sulfate
SDS-PAGE – SDS-polyacrylamide gel electrophoresis
SETX – Senataxin
SHH – Sonic hedgehog
siRNA – small interfering RNA
SNP – Single nucleotide polymorphism
SQSTM1 – Sequestosome 1
SSB – Single-strand break
SSBR – Single-strand break repair
ssDNA – Single-stranded DNA (ssDNA)
TAT – Transactivator
TBS – Tris Buffered Saline
TBST – TBS/Tween-20
TCR – Transcription-coupled repair
TDP1 – Tyrosyl-DNA phosphodiesterase 1
TOP1 – Topoisomerase I
TOP1cc – TOP1 cleavage complex
TR-FRET – Time resolved fluorescence resonance energy transfer
TWAS – Transcriptome-wide association study
Ub – Ubiquitin
UBA – ubiquitin-associated
UDR – Ubiquitin-dependent recruitment
UIM – Ubiquitin-interacting motif
VCP – Valosin-containing protein
WB – Western blotting
XLF – XRCC4-like factor
XRCC4 – X-ray repair cross-complementing protein 4

Chapter 1: General introduction

1.1. Introduction to DNA damage response and repair

Exogenous and endogenous sources of DNA damage threaten genomic integrity of cells on a daily basis (Chaudhuri and Nussenzweig, 2017). The human body is in constant contact with potentially dangerous environmental hazards, including UV light due to sun exposure, toxic chemicals (cigarette smoke and alcohol), and in extreme cases, exposure to ionizing radiation and use of chemotherapeutical drugs. Although external stimuli can be preventable, internal threats resultant from by-products of normal cell functioning pose a greater danger to the integrity of the genome as these are inevitable events. These include transcription, replication and mitochondrial respiration. The latter promotes reactive oxidative species (ROS) production and oxidation events. Per day, each cell of the human body endures tens of thousands of DNA damaging events (Jackson and Bartek, 2009).

To preserve DNA integrity, cells have evolved an elaborate network of signalling transducing pathways – The DNA damage response (DDR) – that detect the damage and orchestrate the appropriate activation of DNA repair mechanisms (Jackson and Bartek, 2009). Each DNA repair pathway is specific to a type of genomic lesion, somewhat like a toolkit, where each "tool" (DNA repair pathway) has a specific function (Figure 1.1.1). The mismatch repair (MMR) pathway is selectively activated to repair base mismatches, common endogenous lesions that occur during replication (Li, 2008). Breakage of a single strand of the DNA phosphodiester backbone, or single-strand break (SSB) require SSB repair (SSBR) mechanisms for their processing (Caldecott, 2008). Damaged bases, as the ones induced by ROS-mediated oxidation, can generate SSBs since their processing by base excision repair (BER) produces a nick into the DNA backbone to excise the modified base (David, O'Shea and Kundu, 2007). Bulky DNA lesions and pyrimidine dimers resultant from UV light are repaired via nucleotide excision repair (NER) (Tresini *et al.*, 2016). As for interstrand crosslinks (ICL), they are resolved by the Fanconi anaemia (FA) pathway (Moldovan and D'Andrea, 2009). Lastly, double-strand breaks (DSBs) activate either non-homologous end-joining (NHEJ) or homologous recombination (HR) pathways (Ceccaldi, Rondinelli and D'Andrea, 2016).

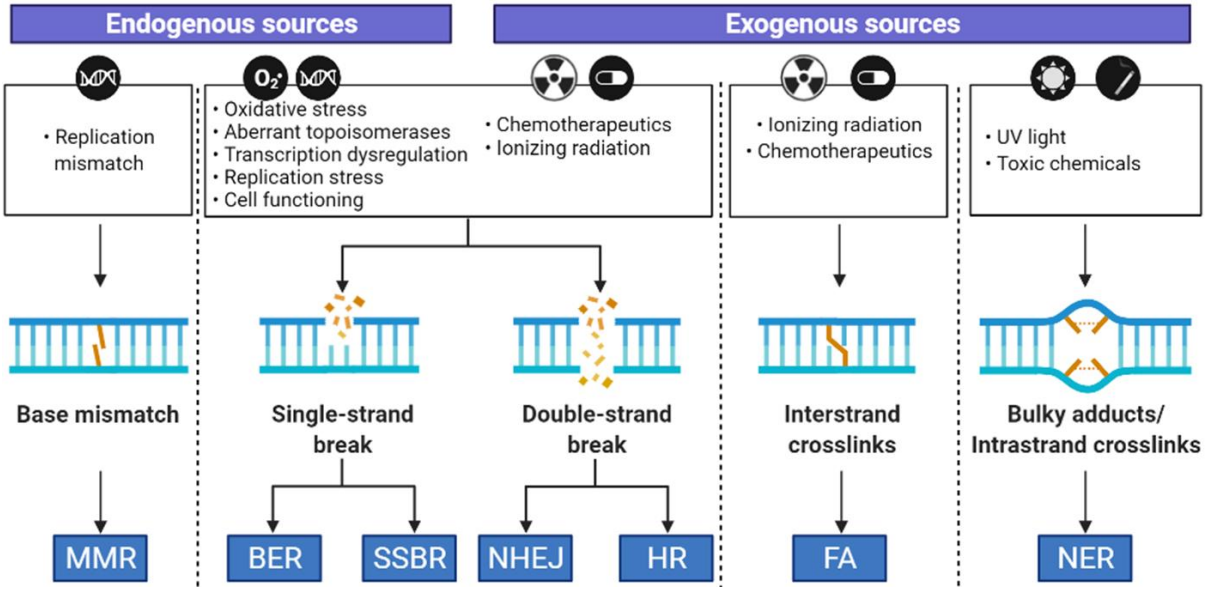

Figure 1.1.1 – Different DNA lesions activate specific DNA repair pathways

Endogenous (replication, transcription, oxidative stress, abortive topoisomerases, and other activities of normal cell function) and exogenous (ionizing radiation, chemotherapeutics, UV light and other toxic chemicals) sources of damage contribute to the generation of various DNA lesions that compromise genomic integrity. Each of these DNA lesions activate a specific DNA repair pathway to fix the damage and restore genomic homeostasis. Base mismatches introduced by replication errors activate the mismatch repair pathway (MMR). Single-strand breaks can either be repaired by base excision repair (BER) or single-strand break repair (SSBR) pathways. The two mostly known pathways involved in the repair of double-strand breaks are non-homologous end-joining (NHEJ) and homologous recombination (HR). DNA crosslinks are repaired by the Fanconi anaemia (FA) pathway and bulky lesions induced by UV light are repaired by the nucleotide excision repair (NER) pathway. (Adapted from (Burgess *et al.*, 2020); created with BioRender.com).

To simplify, the DDR is coordinated by sensors, transducers, mediators and effectors (Figure 1.1.2) (Shiloh and Ziv, 2013). The first step in DDR activation is the recognition of altered DNA structures as damaging events. DNA damage sensors detect the damage and activate the DDR kinases responsible for transducing the DDR signalling cascade via series of protein phosphorylation events (Maréchal and Zou, 2013). DNA damage signalling cascade is coordinated by three phosphoinositide 3-kinase (PI3K)-related kinases (PIKKs) – ataxia telangiectasia mutated (ATM) and DNA-dependent protein kinase (DNA-PK) are involved in DSB repair and ataxia telangiectasia and Rad3 related (ATR) mediates replication stress response (Blackford and Jackson, 2017).

After the occurrence of DSBs, the MRE11, RAD50 and NBS1 (MRN) complex is rapidly recruited to the chromatin, where it acts as a major DSB sensor for ATM, leading to the relocation of ATM to the sites of damage (Uziel *et al.*, 2003; Shiloh and Ziv, 2013). In turn, ATM transits from inactive dimers to active monomers through autophosphorylation of its serine (S) 1981 (Bakkenist and Kastan, 2003). Alternatively, DSBs can also be sensed by the Ku heterodimer (Ku70/Ku80), leading to the formation of DNA-PK complex. ATR is the kinase transducer for replication stress response and its relocation to the damage sites requires the binding of the replication protein A (RPA) to extended stretches of single-stranded DNA (ssDNA) (Blackford and Jackson, 2017).

Once activated, the DDR kinases phosphorylate a myriad of substrates. These include mediators, whose role is to recruit and assemble factors at the damage sites into foci to facilitate the repair. In addition, DDR kinases are also responsible for activating effectors that are involved in different cellular mechanisms (Harper and Elledge, 2007). Ultimately, the DDR signalling cascade leads to the activation of several cellular processes responsible for maintaining the stability of the genome, including DNA repair, cell cycle regulation and induction of apoptosis (Maréchal and Zou, 2013).

Curiously, a certain level of redundancy is also observed among DDR kinases, as they target the same downstream substrates. For example, despite being associated with different repair pathways, all three master DDR kinases, ATM, ATR and DNA-PK, phosphorylate the histone variant H2AX at S139 (γH2AX) and the tumour suppressor p53 (Blackford and Jackson, 2017).

	Double-strand break		Replication stress
			
Sensor	Ku70/Ku80	MRN	RPA
Transducer	DNA-PK	ATM	ATR
Mediator	γH2AX	γH2AX 53BP1 BRCA1	γH2AX
Effector	CHK2 p53	CHK2 p53	CHK1 p53
Cellular response	NHEJ repair Cell cycle arrest Apoptosis	NHEJ repair (53BP1) HR repair (BRCA1) Cell cycle arrest Apoptosis	Cell cycle arrest

Figure 1.1.2 – The composition of the DNA damage response signalling cascade

The DNA damage response (DDR) is a transducing signalling cascade that involve the tight coordination between different factors. The DNA damage sensors detect the abnormal DNA structures such as double-strand breaks or those induced during replication stress. The sensors promote the recruitment of signalling transducing master kinases that coordinate the DDR by initiating a cascade of phosphorylation events that promote the recruitment and activation of signalling mediators and effectors. The DDR conclude in the activation of different cellular responses, including DNA repair, cell cycle arrest and apoptosis. Adapted from (Kok *et al.*, 2021).

1.2. Double-strand break repair signalling

DSBs are the most deleterious types of damage due to their high mutagenic potential and ability to induce premature cell death. The two most widely studied repair pathways involved in DSB repair are the classical NHEJ (herein NHEJ) and HR. In addition, two alternative pathways have also been identified in DSB repair: single-strand annealing and alternative end-joining (Ceccaldi, Rondinelli and D'Andrea, 2016).

NHEJ and HR are two mutually exclusive pathways that are tightly regulated by cell cycle. HR occurs only during S and G2 phases of the cell cycle, because it requires the presence of a sister chromatid to use as a template for the repair of the damaged strands. NHEJ, on the other hand, can be activated during all cell cycle and acts predominantly in G0/G1 phases. (Schwertman, Bekker-Jensen and Mailand, 2016; Chang *et al.*, 2017). Therefore, in non-replicating cells, such as postmitotic neurons, NHEJ pathway plays a crucial role in maintaining genome stability (Iyama and Wilson, 2013; Massey and Jones, 2018).

NHEJ starts with the tethering of Ku70/Ku80 heterodimer onto the DSB-flanking DNA ends. The binding of the Ku heterodimer to DNA creates a platform for the binding of the catalytic subunit of DNA-PK (DNA-PKcs). DNA-PKcs attaches to Ku80 subunit, forming the DNA-PK complex. DNA-PK then induces a cascade of events by phosphorylating a series of substrates that culminate in the recruitment of end-processing factors and/or ligase complexes (Chang *et al.*, 2017). The majority of DSBs generate ends incompatible for direct ligation due to 5'- or 3'-single-stranded overhangs. Artemis is an endonuclease involved in the processing of such incompatible termini by resecting the DNA-overhangs to create blunt-ends or microhomologous regions to facilitate end-joining (Chang, Watanabe and Lieber, 2015). Other nucleases involved DNA end processing for NHEJ are the polynucleotide kinase 3'-phosphatase (PNKP) and the aprataxin and PNKP-like factor (APLF) (Chang *et al.*, 2017). Processed ends are then stabilized by the X-ray repair cross-complementing protein 4 (XRCC4)/ XRCC4-like factor (XLF) complex, promoting the recruitment and activity of DNA ligase IV to re-ligate the broken DNA ends (Brouwer *et al.*, 2016). Because almost no homology is required to repair DSBs by NHEJ, this pathway is considered error-prone (Ceccaldi, Rondinelli and D'Andrea, 2016).

In opposition, HR is an error-free event. HR is initiated by the attachment of the MRN complex to the proximal regions of the DSBs. This leads to the recruitment and activation of ATM, triggering a cascade of signalling events that promotes the recruitment of a complex formed by

breast cancer type 1 susceptibility protein (BRCA1) and BRCA1-associated RING domain (BARD1). Next, the association between the BRCA1/BARD1 complex with CtBP-interacting protein (CtIP) and with the MRN (BRCA1-C complex) induces the endonuclease activity of MRE11, initiating end resection (Sartori *et al.*, 2007). Extensive 5'-3' end resection occurs after MRN-mediated recruitment of a complex of helicases comprised of BLM, EXO1 and DNA2. Simultaneously, the exonuclease activity of MRE11 proceeds to clip the DNA in the 3'-5' direction (Mozaffari, Pagliarulo and Sartori, 2021). This extensive DNA-end processing mediated by the BRCA1-C complex promotes the displacement of the Ku70/Ku80 heterodimer. Concurrently, 5'-3' resection generates long stretches of ssDNA that are targeted by RPA, activating ATR and checkpoint activation. The BRCA1/BARD1 complex then interacts with PALB2, which promotes BRCA2 recruitment and consequent replacement of RPA with RAD51 at the ssDNA overhangs (Esashi *et al.*, 2007). The RAD51-ssDNA filaments perform homology search and strand invasion (Renkawitz, Lademann and Jentsch, 2014). DNA polymerases then use the homologous invaded strands as templates to fill in the gaps and the repair is finalised by the ligation of the newly synthesized stretches and re-annealing of DNA duplex (Aleksandrov *et al.*, 2020).

1.2.1. Histone post-translational modifications and the orchestration of double-strand break repair

The appropriate recruitment of DDR factors happens in a highly orchestrated manner, regulated by large-scale changes in the chromatin landscape (Clouaire *et al.*, 2018). All four core histones that constitute the nucleosome – H2A, H2B, H3 and H4 – and linker histone H1 are subjected to strictly controlled events of phosphorylation, acetylation, methylation, ubiquitination and SUMOylation during DSB repair. These DSB-induced chromatin post translational modifications (PTM) ensure proper remodelling and accessibility of the chromatin necessary for the recruitment of DNA repair proteins and creates anchoring locations for the stabilization and retention of said repair proteins at the damaged sites (Schwertman, Bekker-Jensen and Mailand, 2016; Aleksandrov *et al.*, 2020).

The first steps of DSB repair involves sensing of the damaged chromatin by the MRN complex, followed by MRN-dependent recruitment and activation of ATM (Uziel *et al.*, 2003; Tobias *et al.*, 2013). Activated ATM (pATM) then phosphorylates a series of substrates leading to the recruitment of downstream factors, including the phosphorylation of H2AX at the sites of DNA breaks (Burma *et al.*, 2001; Lavin, Delia and Chessa, 2006; Biton *et al.*, 2007; Shiloh and Ziv, 2013).

Once phosphorylated, the DSB marker γH2AX is the main mediator for the recruitment and clustering of repair and signalling factors into foci at DSB sites (Harper and Elledge, 2007). Firstly, γH2AX serves as a platform for the recruitment of MDC1. The SDT domain of MDC1 is phosphorylated by CK2, creating a binding site for NBS1 (Jungmichel and Stucki, 2010). By recognizing γH2AX, phosphorylated MDC1 brings the now bound MRN complex to the damage sites, promoting further ATM recruitment and activation, creating a positive feedback loop, leading to γH2AX bidirectional propagation from the break site for a few megabases (Iacovoni *et al.*, 2010). Newly recruited pATM binds to and phosphorylates MDC1 (pMDC1), promoting its oligomerization at the breaks (Luo, Yuans and Lous, 2011). The ATM-mediated pMDC1 also serves as a platform for the binding of Really Interesting New Gene (RING)-containing E3 ubiquitin ligases, starting a cascade of histone ubiquitination events that orchestrates DSB repair (Huen *et al.*, 2007).

The choice between NHEJ and HR is highly dependent on cell cycle, type of DNA break and chromatin landscape (Chapman, Taylor and Boulton, 2012; Chang *et al.*, 2017; Clouaire *et al.*,

2018). Notably, histone ubiquitination is critical in determining the choice of DSB repair pathway (Schwertman, Bekker-Jensen and Mailand, 2016).

First, pMDC1 is recognized by the FHA domain of RING finger protein 8 (RNF8) (Huen *et al.*, 2007). RNF8 associates with UBC13 and incites its E2 ubiquitin conjugating activity, driving K63-linked polyubiquitination of the linker histone H1 (Huen *et al.*, 2007; Mailand *et al.*, 2007; Wang and Elledge, 2007; Thorslund *et al.*, 2015). H1 polyubiquitination signals for the sequential recruitment of RNF168 to the chromatin, which in turn monoubiquitinates histone H2A at lysine (K) 13 and K15 residues (Mattiroli *et al.*, 2012; Fradet-Turcotte *et al.*, 2013; Wilson *et al.*, 2016). RNF168 recognises the product of its own activity, accumulating at the sites of damage and amplifying H2AK13/K15 monoubiquitination (H2AK13/K15ub). H2AK13/K15ub signal is further extended to K63-ubiquitin chains by RNF8/UBC13 (Mattiroli *et al.*, 2012). RNF168-mediated ubiquitination of H2AK13/K15 relaxes the chromatin and exposes dimethylated H4K20 and H3K79 (H4K20me2 and H3K79me2), creating a binding site for the recruitment and stabilization of p53-binding protein 1 (53BP1) (Huyen *et al.*, 2004; Pei *et al.*, 2011; Hu *et al.*, 2017).

RNF8 also promotes RNF168 recruitment by inducing chromatin remodelling in a manner independent of its canonical ubiquitin-ligase activity. RNF8 acts through association with CHD4, the catalytic subunit of the Nucleosome Remodelling and histone Deacetylation (NuRD) complex (Luijsterburg *et al.*, 2012). The methyltransferase KMT5A is also a target of RNF8 (Lu *et al.*, 2021). KMT5A (or SET8) is mainly known for catalysing methylation of H4K20, which is then extended to H4K20me2 by SUV420, promoting the recruitment of 53BP1 (Hsiao and Mizzen, 2013). A recent report showed that RNF8-mediated ubiquitinated KMT5A binds to RNF168 and facilitates H2AK15 ubiquitination, further aiding 53BP1 chromatin retention (Lu *et al.*, 2021).

53BP1 favours the choice towards NHEJ pathway (Figure 1.2.1) (Zimmermann and De Lange, 2014). 53BP1 distributes along the DSB-flanking chromatin, where it recognises H4K20me2 and H3K79me2 via its Tudor domain and binds ubiquitinated H2AK15 (H2AK15ub) through its ubiquitin-dependent recruitment (UDR) motif (Fradet-Turcotte *et al.*, 2013; Kocyłowski *et al.*, 2015; An *et al.*, 2018). Chromatin-bound 53BP1 then promotes the recruitment of RIF1 and PTIP (Callen *et al.*, 2020). RIF1 and PTIP recruitment and binding to 53BP1 is dependent on ATM-mediated phosphorylation of distinct S/TQ motifs of 53BP1 (Callen *et al.*, 2013; Chapman *et al.*, 2013). Once 53BP1/RIF1/PTIP complex is formed, the Shieldin complex

(REV7, RINN1, RINN2 and RINN3) is recruited to DSBs via RIF1, while Artemis is recruited via PTIP. Shieldin and Artemis then act as effectors in protecting DNA ends from extensive resection and in microprocessing the DSB ends, respectively, to facilitate end-joining (Wang *et al.*, 2014; Gupta *et al.*, 2018). This way, 53BP1 enables DSB repair via NHEJ by inhibiting DNA resection and generation of ssDNA necessary for HR to occur. (Huyen *et al.*, 2004; Pei *et al.*, 2011; Fradet-Turcotte *et al.*, 2013; Wilson *et al.*, 2016).

H4K20me2 also serves as a docking site for the binding of several 53BP1 competitors. The Polycomb-group protein L3MBTL1 possesses the same capacity as 53BP1 to bind to H4K20me and H4K20me2, thus antagonizing 53BP1 chromatin retention (Acs *et al.*, 2011). DNA damage-induced RNF8-RNF168 activities facilitate the recruitment of the AAA-ATPase valosin-containing protein (VCP or p97) to DSB sites, where it displaces L3MBTL1 and unmasks H4K20me2 for the binding of 53BP1 (Acs *et al.*, 2011). TIP60 is an acetyltransferase complex that also regulates 53BP1 recruitment to the chromatin. TIP60 binds H4K20me2 via MBTD1 subunit, leading to H2AK15 acetylation. H2AK15 acetylation opposes to RNF168-mediated ubiquitination of this same residue, and therefore supports HR by preventing 53BP1 binding to DNA (Jacquet *et al.*, 2016). In addition, TIP60 is also responsible for H4K16 acetylation, which disrupts the binding of 53BP1 to H4K20me2 (Tang *et al.*, 2013).

Alternatively, H2A ubiquitination by the RNF8-RNF168 pathway recruits BRCA1 to the chromatin, which is known to promote HR (Stewart *et al.*, 2009). BRCA1 exists in different complexes (BRCA1-A, BRCA1-B, BRCA1-C and BRCA1-P) with distinct functions (Her *et al.*, 2016; Krais *et al.*, 2021). RAP80 is part of the BRCA1-A complex and recognises K63-linked ubiquitin chains on H2A with its ubiquitin interacting motif (UIM), bringing the BRCA1-A complex (BRCA1/BARD1/RAP80/Abraxas/BRCC36) to DSBs (Wang and Elledge, 2007). Once at the damage sites, BRCA1-A complex restricts end-resection through BRCC36-mediated cleavage of K63 ubiquitin chains (Coleman and Greenberg, 2011; Ng *et al.*, 2016). This suggests the RNF8-RNF168 pathway is essentially pro-NHEJ by blocking DNA end resection. A different study has demonstrated that RNF8 knockout and consequent depletion of UBC13 activity from mouse embryonic fibroblasts (MEFs) abrogated both 53BP1 and BRCA1 recruitment into repair foci. Interestingly, targeting RNF168 to the sites of damage restored 53BP1 foci formation in the absence of RNF8, but not BRCA1 (Hodge *et al.*, 2016). This study emphasised that BRCA1 recruitment to DSBs is dependent on RNF8/UBC13-mediated K63-linked ubiquitination, but not on RNF168. On the other hand, 53BP1 and consequently NHEJ depends on RNF168-induced monoubiquitination of H2AK15 and

dispenses RNF8/UBC13 activity. In agreement, a recent study showed that persistent retention of RNF8 at the chromatin hinders 53BP1 recruitment and benefits HR-mediated DSB repair (Singh *et al.*, 2019). Ataxin-3 (ATXN3) and p97 extract RNF8 from the chromatin by inducing RNF8 proteasomal degradation, facilitating 53BP1 chromatin attachment in an RNF168-dependent way (Singh *et al.*, 2019). The suggested model highlights the choice between NHEJ and HR pathways depends on the timely orchestration of RNF8 turnover. RNF168 recruitment needs RNF8-induced K63-linked H1 ubiquitination as a priming event (Thorslund *et al.*, 2015). Once RNF168 is at the chromatin, RNF8 is removed for 53BP1 attachment, which consequently inhibits DNA end resection and HR (Singh *et al.*, 2019) (Figure 1.2.1).

It is unclear whether there is a separation of function between RNF8 and RNF168, where RNF8 tilts the balance towards HR, while RNF168 favours NHEJ. Or instead, whether RNF8-RNF168 pathway is entirely pro-NHEJ by facilitating the recruitment of two independent anti-resection complexes – RNF8-induced BRCA1-A complex and RNF168-dependent 53BP1/RIF1/PTIP complex. Nonetheless, the interplay between 53BP1- and BRCA1-related mechanisms is highly complex and the way they control DSB repair is not fully understood.

Recently two studies have highlighted the role of RNF168 in mediating HR by inducing the recruitment of BRCA1-P complex (BRCA1/PALB2/BRCA2/RAD51) (Becker *et al.*, 2021; Krais *et al.*, 2021). BARD1 recognises RNF168-induced H2AK15ub via its newly identified BRCT-domain-associated ubiquitin-dependent recruitment (BURD) motif (Becker *et al.*, 2021). This allows the recruitment of BRCA1 and subsequent accumulation of PALB2, BRCA2 and RAD51 at the DSBs through interaction between the coiled coil domains of BRCA1 and PALB2 (Krais *et al.*, 2021). Additionally, BARD1 also binds to unmethylated H4K20, which contrasts with 53BP1 (Becker *et al.*, 2021). H4K20 methylation state changes throughout cell cycle progression, thus evidencing the choice of DNA repair pathway is governed by differences in the chromatin landscape that depend on DNA damage and cell cycle (Shoaib *et al.*, 2018; Becker *et al.*, 2021).

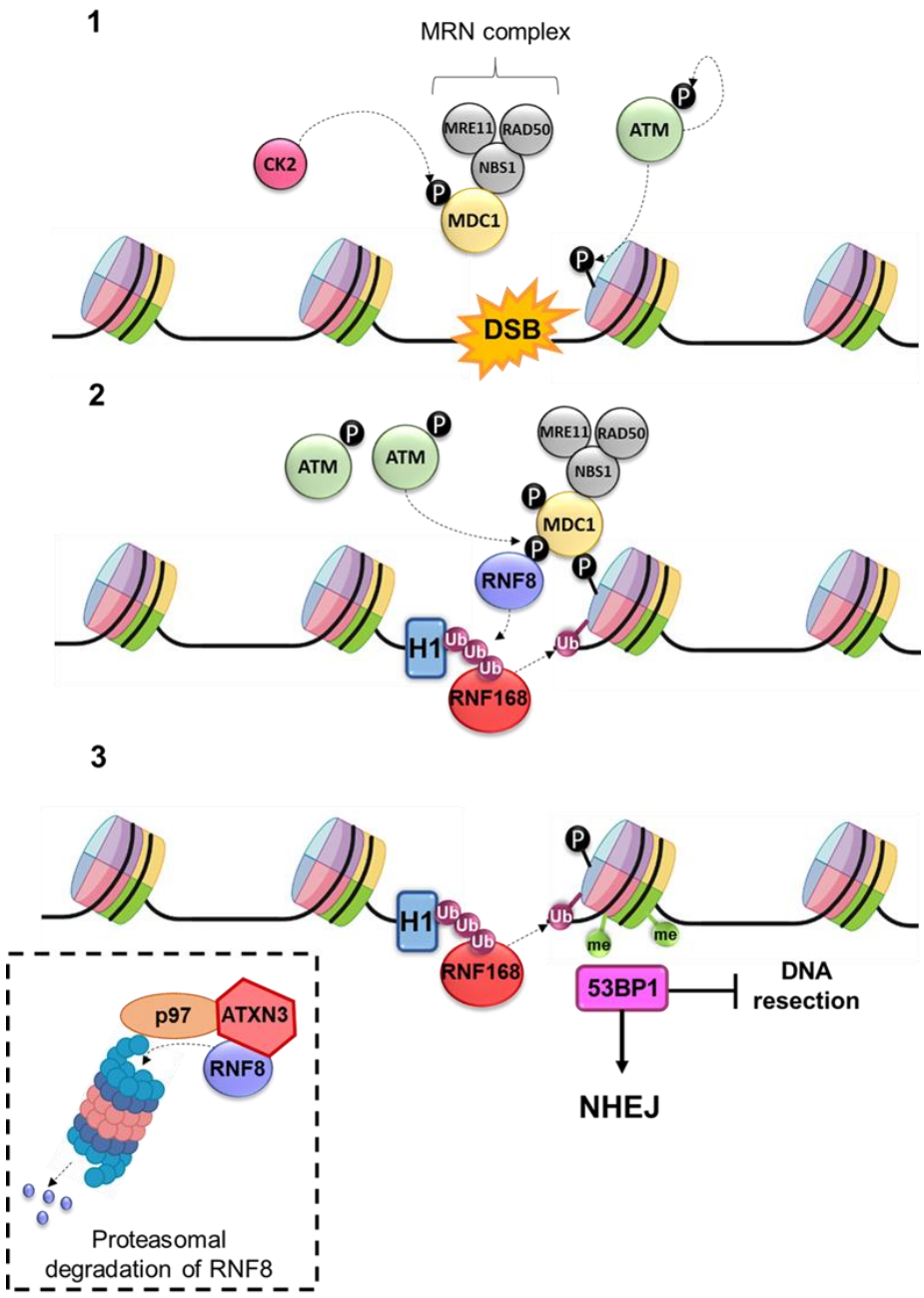

Figure 1.2.1 Histone modification events that mediate 53BP1 recruitment

1- After a DSB, MRN complex senses the damage and recruits ATM. ATM is activated through autophosphorylation and phosphorylates S139 of H2AX (γH2AX), leading to the recruitment of MDC1. Phosphorylation of MDC1 by CK2 creates a binding site for NBS1.

2- MDC1 recognizes γH2AX through its BRCT domain, bringing the MRN complex to the sites of damage. This promotes further ATM recruitment and activation, leading to phosphorylation of MDC1 by ATM. Phosphorylated MDC1 is recognized by the FHA domain of RNF8, which in turn ubiquitinates H1 via K63-linked chains. RNF168 then recognizes ubiquitination H1 and monoubiquitinates H2AK13/K15.

3- RNF8 is then removed by ATXN3/p97 complex and degraded by the proteasome. This supports the specific recognition of H2AK15ub and methylated H4K20 and H3K79 by 53BP1, promoting NHEJ repair pathway by preventing DNA resection. Adapted from (Bartocci and Denchi, 2013).

1.3. Maintenance of genome integrity in the nervous system

Preserving neural homeostasis is fundamental to the functioning of the central nervous system (CNS) and depends mainly on the ability to sustain the integrity of the neuronal genome. The mature brain is composed essentially by postmitotic neurons (Chow and Herrup, 2015). Since mature neurons are not replicating cells, they do not suffer from replication stress and have limited DNA repair pathways on which they can rely on. For example, neurons cannot use HR pathway to repair DSBs, since it needs a sister chromatid to use as a template, which is only available during S and G2 phases of the cell cycle (McKinnon, 2013). Therefore, neurons are long-lived cells that cannot be replaced and need to sustain constant damage throughout organismal lifetime. It is vital for neurons to be well-equipped with mechanisms that ensure the protection of the neural genome.

Neurons have evolved several strategies to protect their genome and guarantee longevity. Two independent studies have recently developed a method to map the location of endogenous DNA damage and repair, by identifying sites of DNA synthesis associated with DNA repair through sequencing of EdU-labelled DNA – synthesis associated with repair sequencing (SAR-seq) (Wu *et al.*, 2021), or Repair-seq (Reid *et al.*, 2021). These studies revealed that postmitotic neurons have privileged genomic sites in which DNA repair is prioritised. These sites were called DNA repair hot spots (DRH) (Reid *et al.*, 2021). Almost 61,200 DRH peaks, that covered about 2% of the neuronal genome, were detected. These DRHs occurred within gene bodies, 5' untranslated regions, intergenic and intronic regions, as well as in open chromatin regions, particularly promoters (Reid *et al.*, 2021). SAR-seq analysis also revealed enrichment for DNA repair at sites of open chromatin, but these were observed in neuronal enhancers and not promoters (Wu *et al.*, 2021). These differences might be due to lack of comparison of Repair-seq peaks with other markers of active enhancers, such as H3K4me1 and MLL4, as performed by Wu *et al.*, (2021). Further gene ontology analysis showed DRH-containing genes are involved in neuronal functions. DRH were also enriched with H2A isoforms and RNA binding proteins. Interestingly, after inducing DNA damage, there was redistribution of several DRHs, while some hotspots remained stable. The stable DRHs happened mainly in evolutionary conserved constrained elements of the genome and in regions enriched with methylated CpG sites, which are associated with the epigenetic clock. (Reid *et al.*, 2021). Analysis by SAR-seq further demonstrated the repair sites were spots of SSBs (Wu *et al.*, 2021). Also, in agreement with Reid *et al.*, (2021) findings, SAR-seq peaks and SSBs co-localised at CpG dinucleotides and were associated with sites of demethylation of 5 methyl-

cytosines (5mc) (Wu *et al.*, 2021). Demethylation of 5mc at gene promoters are sources of ROS (Sengupta *et al.*, 2020). Therefore, the presence of DRH in these regions might protect neurons from one of the most occurrent endogenous hazards to neuronal genome.

These regions could play an important role in the progression of neurodegenerative disorders, since DRHs might be more vulnerable to the decline and dysregulation of DNA repair mechanisms characteristic of several neurodegenerative diseases. Interestingly, in the striatum of Huntington's disease (HD) mice, decreased active enhancers were shown to associate with downregulation of genes associated with neuronal activity (Achour *et al.*, 2015). This was accompanied by reduced RNA polymerase II occupancy at enhancers, leading to decreased transcription of enhancer RNA and consequent decreased expression of the target genes (Achour *et al.*, 2015; Le Gras *et al.*, 2017). It would be interesting to know whether this is caused by HD-associated decline of DNA repair and consequent increased SSB burden at DRHs.

1.3.1. Endogenous sources of DNA lesions in the mature brain

During neurogenesis, most of the damage results from replication stress due to the rapid proliferation rates involved in the development of the brain (Chow and Herrup, 2015). In the mature brain four main sources can damage neuronal genome, which can also be present in the developing brain: (i) oxidative stress, caused by increased ROS resulting from the high respiratory rates required for neuronal functioning; (ii) transcription-associated DNA damage, as a result from the elevated transcriptional activity associated specially with long neurons; (iii) aberrant activity of topoisomerases, which can become irreversibly trapped onto the DNA strand, leading to accumulation of DNA damage and activation of DDR pathways; and (iv) normal neuronal activity, which also involves the production of DNA damage.

As the organism ages, these lesions tend to gradually accumulate in the neuronal genome. During normal ageing there is a slow regression of the brain physiological functions, which manifests as a decline in cognitive performance, memory and learning capacities, attention, sensory perception (vision, hearing, touch, smell and taste) and motor coordination (Pal and Tyler, 2016; Mattson and Arumugam, 2018; Sikora *et al.*, 2021). However, in a neurodegenerative setting, these same brain processes associated with age, decay at a much rapid rate (Figure 1.3.1). As a matter of fact, accelerated ageing is a characteristic of neurodegenerative disorders, including HD (Horvath *et al.*, 2016; Machiela *et al.*, 2020; Alcalá-Vida *et al.*, 2021).

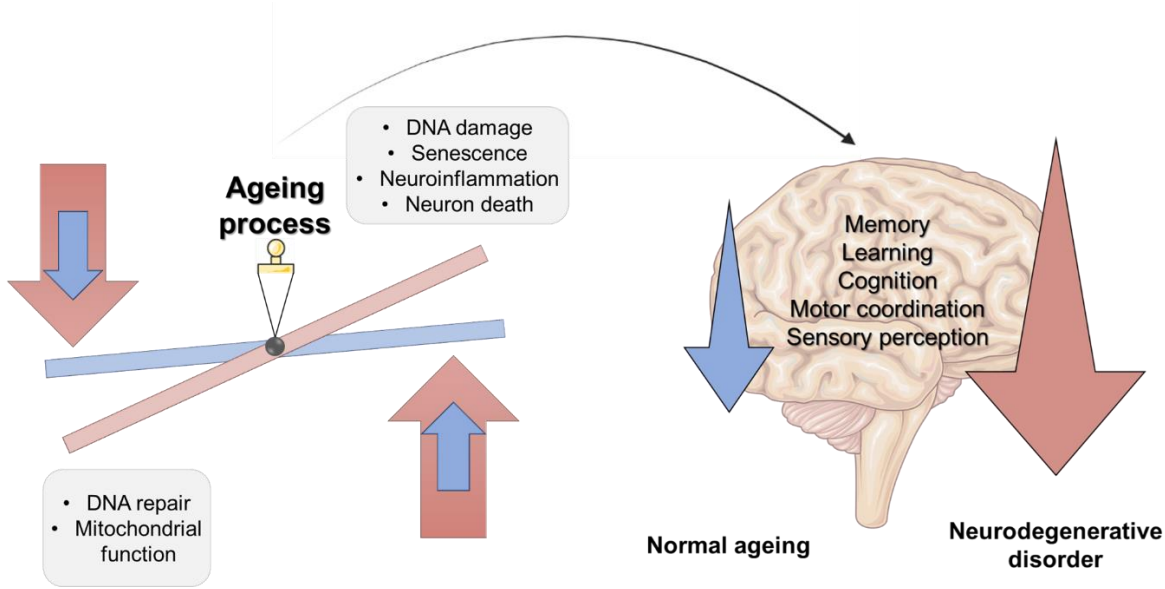

Figure 1.3.1 – DNA damage-induced decay of brain function during normal ageing and in neurodegenerative disorders

During the physiological ageing process (blue arrows), there is a slow decrease of neuronal DNA repair capacity and mitochondrial function. This leads to a gradual accumulation of DNA damage, together with increase of cellular senescence, neuroinflammation, and an increase in neuron death. The progressive neuronal death contributes to the gradual deterioration of brain function, which manifests as a decay in memory, learning, cognition, motor function and sensorial perception, typically associated with normal ageing. In a pathological setting (red arrows), the disease-associated insults exaggerate the ageing process, and the decay of brain function happens in a much rapid rate, further contributing to the progression of specific neurodegenerative disorders.

1.3.1.1. Oxidative stress in neurons

The brain consumes about 20% of the total oxygen in circulation to produce the energy necessary for the CNS functioning (Madabhushi, Pan and Tsai, 2014). The CNS is therefore exposed to the by-products of mitochondrial oxidative phosphorylation, including ROS and reactive nitrogen species (RNS). 5g of ROS per day leak from the electron transport chain. Superoxide ($O_2^{\bullet-}$) and hydrogen peroxide (H_2O_2) are the predominant ROS produced (Hayyan, Hashim and Alnashef, 2016). Other sources of ROS include oxidative demethylation of histones and of 5mc of CpG dinucleotides at promoters during transcriptional activation (Sengupta *et al.*, 2020).

These families of highly reactive free radicals have hazardous effects when not properly counterbalanced by the antioxidative response system. Excessive ROS production generates oxidative stress, which contributes to neuronal disfunction and degeneration due to extensive protein and lipid peroxidation (Salim, 2017). DNA base oxidation is also a common event induced by ROS. Guanine is particularly susceptible to oxidation given its decreased redox capacity, generating 8-oxoguanine (8-oxoG), a DNA adduct commonly used as a marker of oxidative stress (David, O'Shea and Kundu, 2007). BER is the main pathway involved in the removal of such DNA adducts and requires the recognition and base removal of the 8-oxoG from the DNA backbone by 8-oxoG DNA glycosylase (OGG1), creating an apurinic site (AP site). The AP sites are processed by AP-endonuclease 1 (APE1), generating SSBs, which are ligated by DNA ligases I or III (Shaikh and Martin, 2002; David, O'Shea and Kundu, 2007).

An increase of DNA adducts is a frequent finding in ageing organisms and in neurodegenerative settings. 8-oxoG tend to accumulate at promoter regions due to their high guanine content, promoting the activation of proinflammatory and immediate early response genes (Fleming, Ding and Burrows, 2017).

Neuroinflammation is a common finding in neurodegenerative disorders, including HD. Recently a study detected elevated levels of pro-inflammatory cytokines in the plasma of HD carriers. In addition, the authors observed increased ROS release by HD microglia, thus showing oxidative stress and hyperactivation of inflammation is involved in HD neuropathology (O'Regan *et al.*, 2021).

Logically, persistent DNA damage leads to constant activation of the DDR mechanisms. Over time, cell cycle dynamics are altered due to the constant need for arresting the cell cycle to promote DNA repair (Crane *et al.*, 2019). When cells are not able to handle the lack of cell

cycle regulation, they can ultimately stop replicating, entering in cellular senescence (Petr *et al.*, 2020). Neurodegenerative diseases such as HD, Alzheimer's disease, Parkinson's disease and amyotrophic lateral sclerosis (ALS) display increased senescence-like phenotypes, yet another link between ageing and late-onset neurodegenerative disorders (Hou *et al.*, 2019). Neural stem cells and medium spiny neurons (MSNs) derived from HD patients exhibit senescence features, such as increased expression of the senescence inducer $p16^{INK4}$ and high SA-β-gal activity. Furthermore, the senescent features developed during neuronal differentiation and persisted in the fully matured HD neurons, suggesting senescence is an early event set in HD brains (Voisin *et al.*, 2020).

Another consequence of the increased oxidative damage is hyperactivation of poly (ADP-ribose) polymerase 1 (PARP1), a protein involved in the recruitment repair proteins by catalysing the addition of PAR chains (Wei and Yu, 2016). Hyperactivation of PARP1 can be detrimental to the cells by increasing energy consumption. This causes NAD^+ imbalance and consequent SIRT1 deactivation, since both PARP1 and SIRT1 depend on NAD^+ for their activities (Fang *et al.*, 2014). SIRT1 is a class III histone deacetylase and plays a role in many biological processes, including DNA repair and telomere stability, by influencing chromatin dynamics and stability through histone deacetylation. Other functions of SIRT1 include autophagosome maturation, thus endorsing autophagy (Rahman and Islam, 2011; Lin and Fang, 2013). SIRT1 also promotes mitochondrial function through deacetylation of the mitochondria regulator, PGC-1α (Ventura-Clapier, Garnier and Veksler, 2008). Furthermore, increased PARP1 activation can also promote cell death by parthanatos, a programmed cell-death driven by the nuclear translocation of apoptosis-inducing factor (AIF) from the mitochondria. This cell death mechanism is independent on caspase activity and is promoted by PARylation (Kam *et al.*, 2018; Wang and Ge, 2020).

Post-mortem brain tissues from HD patients have shown increased PARP1 expression and reduction of PARP1 activity ameliorated neuropathology in R6/2 HD mice (Vis *et al.*, 2005; Cardinale *et al.*, 2015; Paldino *et al.*, 2017). In addition, the activity of SIRT1 was also found to be decreased in HD mice brains (Tulino *et al.*, 2016). This decreased SIRT1 activity was caused by an age-dependent impairment in SIRT1 phosphorylation, specifically in the striatum of R6/2 HD mice brains, while SIRT1 activity remained unchanged in the cerebellum. Since both PARP1 and SIRT1 compete for NAD^+ and elevated PARP1 activity is associated with energetic deficits, it would be interesting to ascertain whether there is a correlation between elevated PARP1 and decreased SIRT1 activities in HD. Moreover, abnormal mitochondrial

function, bioenergetics and decreased mitochondria biogenesis have been widely described in tissues from HD patients, concurrent with increased ROS levels and oxidative DNA damage (Tabrizi *et al.*, 1999; Milakovic and Johnson, 2005; Ayala-Peña, 2013; Askeland *et al.*, 2018; Jędrak *et al.*, 2018). SIRT1 enhances mitochondrial activity by deacetylating and activating PGC1-α (Watroba and Szukiewicz, 2016). In agreement with an energetic imbalance in HD, PGC1-α expression was also found to be repressed in the striatum of HD human and mice brains (Cui *et al.*, 2006). Therefore, a feedforward effect is possible, whereby in the striatum of HD brains, defective mitochondrial dynamics and structure cause oxidative DNA damage promoting PARP1 hyperactivation. This creates an energy imbalance, due to high consumption of NAD^+, leading to reduced SIRT1 deacetylase activity, which further feeds into the existing mitochondrial defects. Besides, a recent study indicates a possibility that these phenotypes might be exacerbated with ageing (Machiela *et al.*, 2020). HD-like phenotypes, including increased sensitivity to oxidative stress and DNA damage, were found in primary HD striatal neurons after accelerating ageing with progerin treatment. This further endorses the idea that the ageing process supports the onset and progression of HD (Machiela *et al.*, 2020). This study also showed absence of ROS production in response to oxidative stress in immature neurons, which might provide some insights regarding the differences between congenital and age-related neurodegenerative disorders, which will be discussed later.

1.3.1.2. Transcription-induced DNA damage in neurons

Neurons exhibit high transcriptional activity, which triggers topoisomerase-mediated cleavage activity to relax the helical tension of the DNA backbone generated during transcription (Cristini *et al.*, 2019). Topoisomerase I (TOP1) induces temporary SSBs to unwind the supercoiled DNA and allow neuronal gene expression. During its catalytic activity, TOP1 becomes covalently attached to the 3'-end of the DNA nick, resulting in transient TOP1 cleavage complexes (TOP1cc), which are protein-linked DNA breaks (PDB) (Pommier *et al.*, 2003). Consequently, these PDB occur as a natural by-product of TOP1 activity in the brain (Sordet *et al.*, 2010; McKinnon, 2016).

TOP1cc occur frequently in postmitotic neurons and can become irreversibly trapped due to physiological or pathological conditions (Berger *et al.*, 2017). Common DNA alterations, such as base oxidation, alkylation, base mismatch and DNA nicks contribute to stabilise TOP1cc on the chromatin (Pourquier, Pilon, *et al.*, 1997; Pourquier, Ueng, *et al.*, 1997). Additionally, TOP1cc can also be trapped by camptothecin (CPT), a chemotherapeutic drug that targets

DNA-bound TOP1 (Pommier, 2006). Persistent TOP1cc are sources of transcription-blocking lesions that can be converted into DSBs, which if unresolved, can lead to premature neuronal cell death (Cristini *et al.*, 2016).

R-loops are another source of transcription-dependent DNA damage. R-loops are three-stranded structures formed by RNA:DNA hybrids. R-loops are generated during transcription, following a "thread back" model, whereby the newly transcribed messenger RNA (mRNA), as it exits the RNA polymerase, re-anneals to the template DNA strand to which is complementary, while displacing the single-stranded non-template DNA (Aguilera and García-Muse, 2012). Physiological R-loops play a role in several cellular processes, including immunoglobulin class switch recombination, replication of mitochondrial DNA, regulation of gene expression and in transcription initiation and termination (García-Muse and Aguilera, 2019). However, unbalanced R-loop homeostasis and/or the formation of unscheduled R-loops can result in increased genomic instability. R-loops can be a source of transcription stress, leading to stalling or backtracking of the RNA polymerase. In addition, R-loops are sources of replication stress by inducing replication fork stalling and by causing transcription-replication collisions (García-Muse and Aguilera, 2019; Rinaldi *et al.*, 2021).

Cells evolved mechanisms to maintain R-loop homeostasis. These mechanisms prevent the harmful effects of R-loops by either preventing their accumulation of by removing them (Rinaldi *et al.*, 2021). Factors involved in the processing and export of mRNA have shown to play a protective role against R-loop accumulation. In particular, the transcription/export (THO/TREX) complex, a conserved multiprotein complex involved in transcription elongation, mRNA processing and nuclear export, was shown to prevent R-loop accumulation (Huertas and Aguilera, 2003; Gómez-González *et al.*, 2011; Katahira, 2012). Additionally, DNA topology also plays an important role in preventing R-loops. Negative-supercoiling of the DNA duplex favours R-loop formation. Indeed, depletion of TOP1 was shown to simultaneously increase negative supercoiling and R-loop formation in bacteria, yeast and human cells (El Hage *et al.*, 2010; Manzo *et al.*, 2018).

R-loop specific nucleases and helicases are factors involved in R-loop resolution. RNase H1 and H2 are ribonucleases that degrade the RNA moiety in DNA:RNA hybrids. Evidence supporting the role of RNase H enzymes in resolving R-loops include studies showing that depletion of these enzymes result in R-loop accumulation. Also, overexpression of RNase H1 is often shown to be sufficient to eliminate R-loops (Huertas and Aguilera, 2003; Wahba *et al.*,

2011; Lin and Wilson, 2012; Zhao *et al.*, 2018). Helicases involved in the unwinding of the DNA:RNA hybrids have also been implicated in R-loop resolution. Among these factors is the helicase senataxin (SETX), which removes R-loops at transcription termination sites (Skourti-Stathaki, Proudfoot and Gromak, 2011). Additional RNA/DNA helicases involved in R-loop removal include DDX19, AQR and RECQL5, whereby depletion of these factors result in R-loop accumulation (Sollier *et al.*, 2014; Li *et al.*, 2015; Hodroj *et al.*, 2017). Furthermore, FANCM, a member of the FA pathway with ATPase and translocase activities, was also shown to be implicated in R-loop resolution in a manner dependent of its translocase activity (Schwab *et al.*, 2015).

Provided that neurons are heavily transcriptionally active, the co-occurrence of transcription-induced TOP1cc and R-loops is highly probable (Cristini *et al.*, 2019). During transcription, as RNA polymerase advances along the DNA strand, it creates positive supercoiling ahead the transcription bubble, which blocks transcription elongation, and negative supercoiling behind the transcription machinery (Pommier *et al.*, 2003; Baranello *et al.*, 2016). TOP1 releases the positive torsional stress (Baranello *et al.*, 2016). However, trapping of TOP1cc onto DNA, for example due to increased levels of oxidative DNA damage, block transcription and stabilize negative supercoils (Sordet *et al.*, 2010; Cristini *et al.*, 2019). In turn, negative supercoils promote DNA melting, which favours mRNA invasion into the DNA duplex, thus facilitating R-loop formation (Aguilera and García-Muse, 2012). The processing of these two transcription-blocking lesions requires the formation of SSBs. The displaced ssDNA in R-loops is prone to deamination and oxidative damage, triggering BER and consequent SSBs formation. In addition, R-loops can activate TC-NER. R-loop processing by TC-NER involves activities of the flap-encoducleases XPG or FEN1 and XPF, which cleave the ssDNA stretch in R-loops at the 5’ and 3’ extremities, respectively (Gregersen and Svejstrup, 2018; Cristini *et al.*, 2019). In turn, the repair of TOP1cc involves TOP1 proteolysis by the ubiquitin-proteasome system, followed by tyrosyl–DNA phosphodiesterase-1 (TDP1)-mediated excision, which generates an intermediate SSB (Katyal *et al.*, 2007, 2014). Therefore, co-existence of R-loops and/or TOP1cc on opposite strands at close proximity can lead to the formation of transcriptional DSBs in neurons, which contribute to neuronal degeneration (Cristini *et al.*, 2020).

Increased oxidative stress also interferes with transcription. The intermediates generated by BER during the repair of oxidative DNA, AP-sites and SSBs, have the potential to stall transcription elongation if not quickly resolved (Lans *et al.*, 2019). Persistently blocked RNA

polymerase II is highly cytotoxic for neurons for the following reasons: (i) it reduces transcription; (ii) it promotes the accumulation of R-loops, which generates DSBs if in the presence of co-transcriptional TOP1cc (Cristini *et al.*, 2019); and (iii) stalled RNA polymerase II and stabilised R-loops can cause clashes with ongoing transcription machineries, also leading DSB formation. DSBs render neurons to ATM hyperactivation and consequent triggering of p53-mediated apoptotic mechanisms, causing premature neuronal death (Ditch and Paull, 2012; Poetsch, 2020).

An early study has reported drastic changes in the transcriptional profile of genes vital for neuronal function, in an age-dependent manner (Lu *et al.*, 2004). The expression of genes associated with synaptic transmission, vesicular transport, neuron survival and mitochondrial activity was downregulated after the age of 40. Moreover, promoter genes in the aged cortex showed increased levels of 8-oxoG. Further treatment with H_2O_2 and an $FeCl_2$ confirmed that the promoters of the age-dependent downregulated genes were prone to oxidative damage. The damage to the promoters of these genes was then counteracted by expression of the BER enzyme, OGG1. This indicates accumulation of DNA lesions together with a decline of DNA repair capability are behind the deterioration of the cognitive abilities and increased neuronal degeneration associated with age (Lu *et al.*, 2004).

Transcription dysregulation is characteristic of HD pathology (Hodges *et al.*, 2006). cDNA microarray approaches have been used in both HD mouse models and post-mortem brain tissues from HD patients to study the gene expression profiles associated with HD (Cha *et al.*, 1998; Luthi-Carter *et al.*, 2000; Sugars and Rubinsztein, 2003; Hodges *et al.*, 2006; Moumné, Betuing and Caboche, 2013). More recently, RNA-sequencing transcriptomic analysis was used in whole blood from HD cohorts where the findings correlated with those previously found in the caudate of HD brains (Hensman Moss *et al.*, 2017). Interestingly these analyses reported downregulation of genes associated with synaptic function and plasticity, mitochondrial function, neuron survival, vesicle trafficking and DNA repair in HD. There is a clear overlap between HD transcriptional profiles and the age-associated downregulated genes described by Lu *et al.*, (2004). This suggests that HD-associated mutations predispose specifically the caudate region of the brain to neurodegeneration, whereby accumulation of DNA damage over time and the consequent ageing process trigger the onset of HD-specific cascade of events.

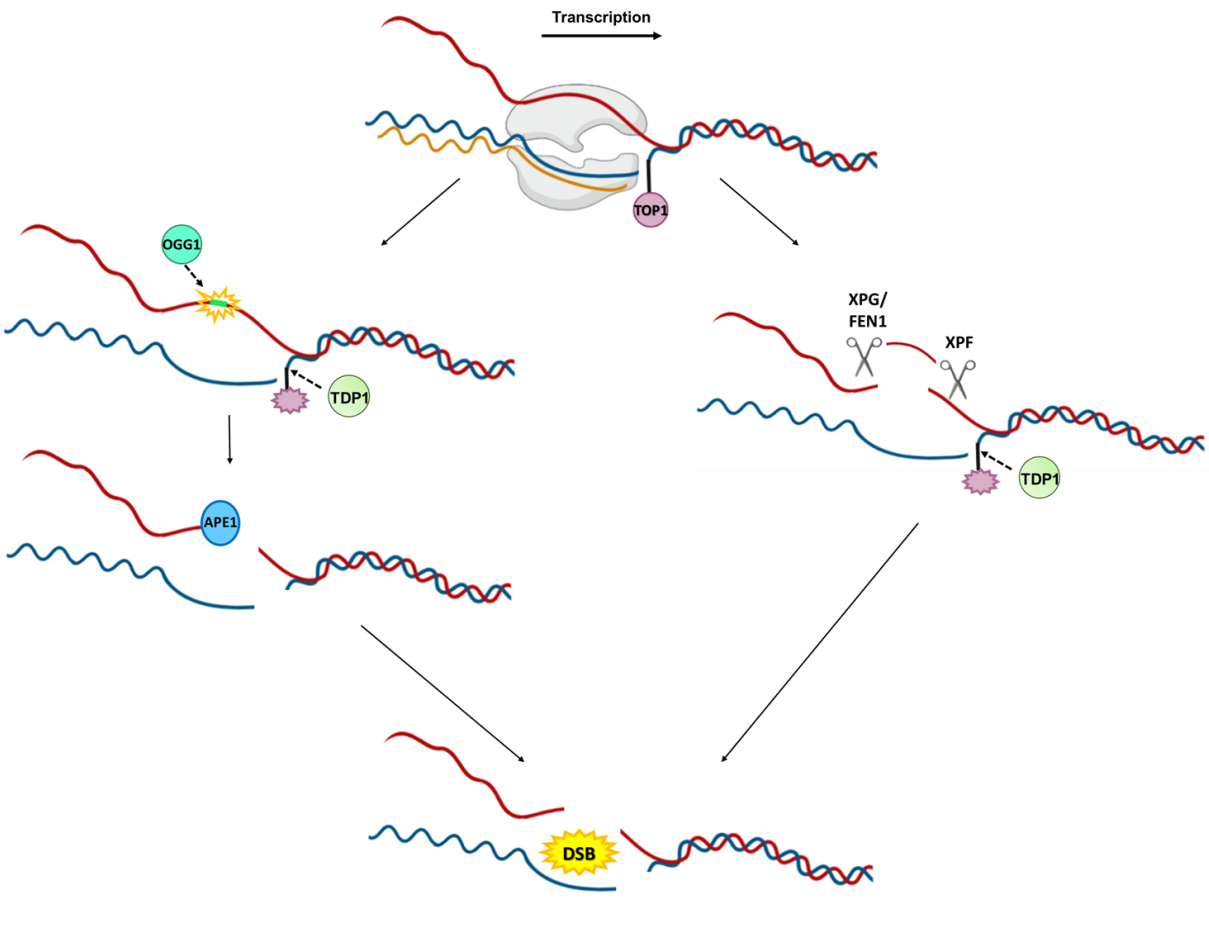

Figure 1.3.2 – Co-existent TOP1cc and R-loops promote transcription-dependent DSB formation

Transcription-dependent DSBs can arise from two SSBs on opposite strands due to the removal of co-transcriptional R-loops and TOP1ccs. Repair of the trapped TOP1cc involve the hydrolysis of the phosphotyrosyl bond between TOP1 and DNA, resulting in a SSB. Concomitantly, the presence of trapped TOP1cc promote R-loop formation. (Left) On one hand, the displaced ssDNA strand in R-loops can be a target to oxidative damage, triggering BER. This involves recognition and excision of the oxidised base by OGG1, generating an AP-site that is processed by APE1, leading to SSB formation. (Right) Additionally, R-loop formation can activate TC-NER. Here, ssDNA strand is cleaved at its 5' and 3' ends by the flap-encoducleases XPG and XPF or by FEN1 and XPF, also generating a SSB. This way, the existence of two SSBs on opposite strands generated by the co-processing of TOP1cc and by either BER or TC-NER triggered by a co-transcriptional R-loop, contribute to DSB formation. Adapted from (Cristini *et al.*, 2019). (Created with BioRender.com).

1.3.1.3. Neuronal activity-induced DNA breaks

Early clues suggesting DNA breaks promote neuronal activity come from a study showing increase of γH2AX in response to the activation of iontropic glutamate neurons (Crowe *et al.*, 2006). In agreement, another study showed that activities associated with exploratory behaviour led to an elevation of DSBs in mice neurons (Suberbielle *et al.*, 2013). A follow-up report supported the findings of Suberbielle *et al.* by demonstrating that DSBs induced by etoposide, a TOP2β poison, facilitated the expression of neuronal early-response genes (Madabhushi *et al.*, 2015). Furthermore, γH2AX ChIP-seq analysis showed that neuronal activity was accompanied by enrichment of γH2AX at the promoters of early-response genes. In addition, depletion of TOP2β resulted in synaptic dysfunction. Together, these findings demonstrated that TOP2β-induced DSBs support neuronal activity by promoting the expression of genes essential for neuron functioning (Madabhushi *et al.*, 2015). These studies indicate that neuronal functioning and activity are dependent on the induction of DNA strand breaks at specific locations of the genome. This raises the question of whether failure to repair these breaks could contribute to the development of neurological diseases.

Interestingly, Wu *et al.*, (2021) did not find a correlation between SAR-seq signal and neuronal gene activity, as EdU incorporation was detected in both transcribed and non-transcribed DNA strands. Similarly, Reid *et al.*, (2021) showed DRHs were not associated with the induction of neuronal activity. This suggests activity-induced DSBs are not privileged sites for repair in postmitotic neurons. Understanding why the DNA repair machinery prioritises these hotspots for protection over other genomic regions known to be targets of damaging events induced by neuronal activity is of paramount importance to get more insight into how neurons protect their genome and the role of these mechanisms in the development of neurodegenerative diseases.

1.3.1.4. The role of ATM in protecting against endogenous brain lesions

Accumulation of unresolved TOP1cc has been linked to neurodegeneration. In Spinocerebellar ataxia with axonal neuropathy (SCAN1), TDP1 mutations cause faulty repair of TOP1cc, leading to the deleterious accumulation of replication-independent TOP1-SSBs (El-Khamisy et al, 2005; Alagoz et al, 2013). Accumulation of endogenous TOP1cc has also been described in ataxia telangiectasia (A-T) syndrome (Katyal *et al.*, 2014). The similar phenotypes observed in both SCAN1 and A-T patients prompted the possibility that ATM was also involved in the resolution of TOP1cc (Alagoz *et al.*, 2013; Katyal *et al.*, 2014). In agreement with this hypothesis, persistent TOP1cc after CPT treatment endorsed the formation of transcription

dependent DSBs in quiescent cells, inducing both canonical and non-canonical activation of ATM (Sordet *et al.*, 2009; Alagoz *et al.*, 2013; Katyal *et al.*, 2014; Cristini *et al.*, 2016).

In non-replicating cells such as neurons, transcription-dependent DSBs can arise from two neighbouring SSBs in opposite DNA strands that are created during transcription (Cristini *et al.*, 2019). Upon CPT treatment, trapped TOP1cc are repaired by TDP1 excision pathway, generating an SSB intermediate in the transcribed DNA strand (El-Khamisy *et al.*, 2005; Cristini *et al.*, 2019). On the opposite DNA strand, CPT can induce co-transcriptional R-loops. Endonuclease-mediated cleavage during R-loop processing generates SSBs. This way, the co-occurrence of TOP1cc- and R-loop-related SSBs in proximity generates neuronal transcription blocking DSBs (Cristini *et al.*, 2019).

In response to trancriptional DSBs, the canonical ATM pathway is activated. Here ATM acts as a DSB transducer, leading to ATM-induced phosphorylation of its downstream substrates, γH2AX and 53BP1. CHK2 and p53 are also targets of ATM activity, and their activation mediated by ATM-induced phosphorylation trigger cell cycle arrest and apoptosis, respectively (Burma *et al.*, 2001; Pommier *et al.*, 2003; Cristini *et al.*, 2016; Blackford and Jackson, 2017). DNA-PK is also activated by ATM, promoting both NHEJ repair as well as H2AX and H2A monoubiquitination, which further helps sustaining ATM focal activity, through 53BP1 recruitment (Lee *et al.*, 2010; Baldock *et al.*, 2015; Cristini *et al.*, 2016).

Additionally, CPT-induced DSBs promote the non-canonical activation of ATM (Cristini *et al.*, 2016). In this scenario, ATM and TDP1 cooperate in a non-epistatic way to modulate TOP1cc turnover. ATM together with DNA-PK promote proteolysis of DNA-bound TOP1, as DNA-PK promotes ubiquitination of TOP1, allowing TDP1 excision pathway to take place (Cristini *et al.*, 2016).

Ubiquitination has also been shown to play an important role in R-loop biology. R-loop resolution depends on the activity of the helicase SETX. SETX stability was shown to be dependent on USP11, a deubiquitinating enzyme responsible for hydrolysing K48-linked polyubiquitin chains from SETX and reducing its proteasomal degradation (Jurga *et al.*, 2021). Inhibition of USP11 results in decreased SETX levels, together with increased R-loop formation that are converted into DSBs (Jurga *et al.*, 2021).

Another non-canonical role of ATM in postmitotic cells has been described by Tresini *et al.*, (2015) Transcription-blocking DNA lesions were shown to promote the displacement of the late-stage spliceosome components U2 and U5 from the chromatin. This culminated in intron

retention which further facilitated R-loop formation at the damage sites. The accumulation of R-loops then led to ATM activation independent of DSB formation. Interestingly, R-loop-mediated ATM activation initiated a feedforward loop, further enhancing intron retention and spliceosome disassembly, since inhibition of ATM promoted spliceosome activity and pre-mRNA processing after UV radiation (Tresini *et al.*, 2015). Although the biological consequences of this non-canonical ATM function remain a mystery, a tempting possibility is that ATM regulates mRNA processing in response to transcription-dependent DNA lesions to prevent genomic instability triggered by R-loop accumulation. This way, in detriment of ensuring fidelity mechanisms of pre-mRNA splicing, ATM promotes spliceosome disassembly and consequent intron retention, possibly to encourage R-loop resolution, which constitutes a threat to the cells (Tresini *et al.*, 2015, 2016).

Increased oxidation is another endogenous neuronal event that trigger ATM activation independent of its role in DSB signalling, indicating ATM acts non-canonically to protect neurons against oxidative stress (Guo *et al.*, 2010). ROS induces cytosolic ATM dimerization and activation (Guo *et al.*, 2010). In turn, ATM promotes BER by inducing nuclear translocation of huntingtin, which is essential for the assembly of the BER complexes at the sites of oxidation (Maiuri *et al.*, 2017). Loss of ATM induces mitochondrial dysfunction and ROS overproduction, hinting that ATM is crucial for mitochondrial functioning (Valentin-Vega *et al.*, 2012).

Notably, a recent report has shown that hypoxic environment triggers the formation of R-loops and enhances the expression of SETX (Ramachandran *et al.*, 2021). SETX depletion was shown to trigger ATM-dependent DDR signalling and to compromise viability of hypoxic cells. SETX protective effects were transcription-dependent, as inhibition of transcription decreased the damage induced by hypoxia (Ramachandran *et al.*, 2021).

ATM activity was also found to be important for the removal of damaged mitochondria via mitophagy by activating the PINK1–Parkin pathway, thus protecting cells against ROS induced by mitochondrial stress (Qi *et al.*, 2016). Similarly, ATM kinase activity is also responsible to defend cells against peroxisomal-induced ROS. In response to ROS, ATM is activated and phosphorylates PEX5, which initiates peroxisome degradation by pexophagy (Zhang *et al.*, 2015).

Furthermore, a recent study has demonstrated that ATM deficiency triggers protein aggregation, a hallmark of neurodegeneration, via PARP1 hyperactivation (Lee *et al.*, 2021).

ATM-deficient cells showed elevated levels of ROS and subsequent formation of transcription-dependent lesions, including SSBs and R-loops, which induced excessive PARylation. This attracts aggregation-prone proteins to associate with PAR polymers and to form toxic insoluble aggregates (Lee *et al.*, 2021). This mechanism has been associated with neurodegeneration. Hyperactivation of PARP1 was found to cause degeneration of dopaminergic neurons in Parkinson's disease. Pathological aggregates of α-synuclein promote activation of PARP1 and the generation of a hypertoxic PAR-α-synuclein strain (Kam *et al.*, 2018). In ALS, increased PARylation was also found to induce aggregation of RNA-binding proteins, such as TDP-43 into stress granules (Duan *et al.*, 2019). Since augmented PARP1 expression was also reported in HD brains (Vis *et al.*, 2005), increased PARylation could potentially be involved in toxic protein aggregation in HD. In support of this hypothesis, inhibiting PARP1 in R6/2 HD models reduced striatal intranuclear inclusions (Paldino *et al.*, 2017).

The mentioned studies unveil that transcription-dependent DNA damage, common in postmitotic neurons and a driver of neurodegeneration, instigates reciprocal regulation between DDR, protein homeostasis and pre-mRNA processing, all centred around ATM activity (Figure 1.3.3).

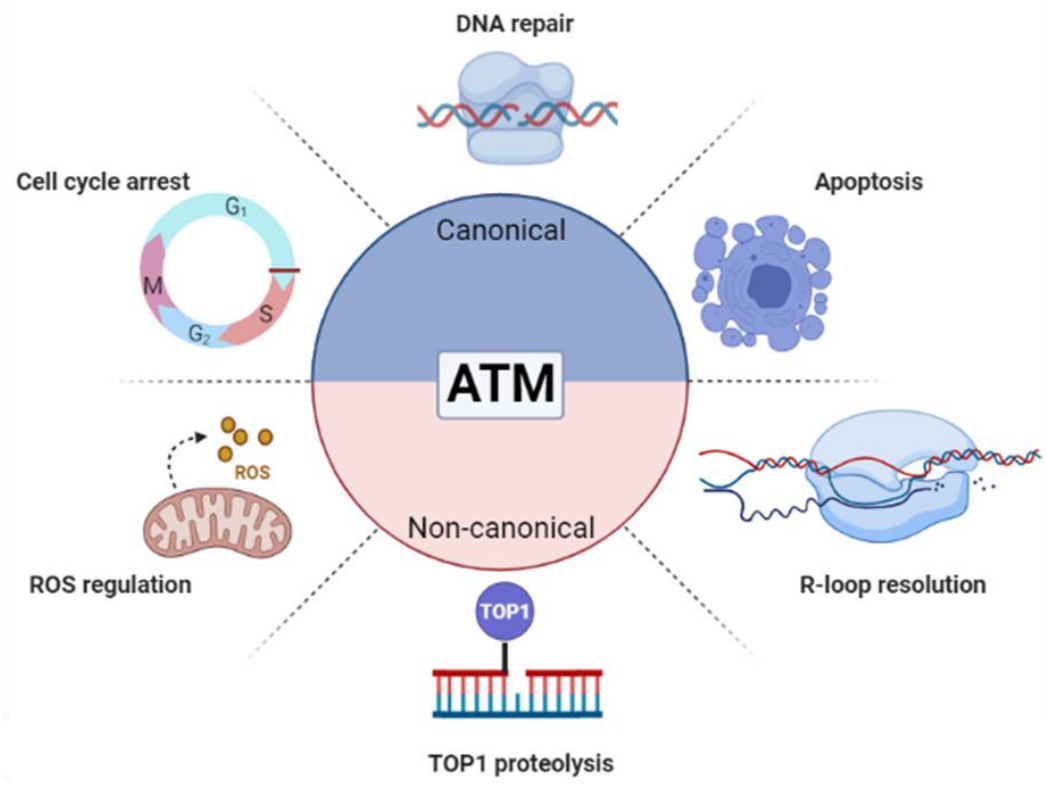

Figure 1.3.3 – The canonical and non-canonical functions of ATM contribute for maintenance of neuronal homeostasis.

ATM is mostly known as a master kinase involved in the orchestration of DDR. The canonical activities of ATM involve the checkpoint activation and consequent cell cycle arrest, as well as activation of DNA repair pathways and apoptosis, by phosphorylating numerous substrates. ATM is also engaged in additional roles independent of its kinase activity. These non-canonical activities include protection against reactive oxidative species (ROS), proteolysis of TOP1 covalently bound to DNA and spliceosome displacement to help resolution of R-loops. Both canonical and non-canonical functions of ATM have proven to be beneficial for brain health, as demonstrated by the fact that ATM depletion or inactivation results in serious neuronal impairment. (Created with BioRender.com).

1.3.2. Defects in DNA repair and neurodegeneration

Neurons are equipped with a diverse array of DNA damage response and repair mechanisms that safeguard the genome. The existence of neurological disorders deriving from mutations in DNA repair genes proves the relationship between neuronal health and maintenance of genomic stability (Table 1.3.1). One of the earlier clues showing that impaired DNA repair underpins neurological disturbances comes from studies of A-T syndrome. A-T is caused by mutations in the serine/threonine kinase, ATM (Lavin, 2008). Cells from A-T patients show marked accumulation of DSB, sensitivity to DNA damage inducing agents and premature cellular senescence (Katyal *et al.*, 2014). The hallmark neurological features of this disease include ataxia, severe cerebellar degeneration, oculomotor apraxia (absence of eye movements) and dysarthria (slurred speech) (Frappart and McKinnon, 2006; Madabhushi, Pan and Tsai, 2014). The symptomatology of A-T is not restricted to the CNS. Additional clinical features include increased radiosensitivity, telangiectasia, cancer predisposition and immunodeficiency (Frappart and McKinnon, 2006). Yet, these studies demonstrate the importance of DNA repair in maintaining genome integrity of the nervous system. Another disorder called ataxia telangiectasia-like disease (ATLD) is caused by mutations in MRE11 (Uziel *et al.*, 2003; Blackford and Jackson, 2017). ATLD is also a multisystemic disorder and the neurological features are similar to those of the A-T patients (Taylor, Groom and Byrd, 2004; Frappart and McKinnon, 2006). Since MRN regulates ATM function, ATLD cells also exhibit defective ATM signalling. (Blackford and Jackson, 2017).

Neurons have to endure a high oxidative load that quickly becomes lethal if the proper genome maintenance factors are not in place (Chow and Herrup, 2015). This makes the CNS particularly vulnerable to defects in DNA repair proteins that are involved in SSBR (El-Khamisy *et al.*, 2005; Hoch *et al.*, 2017). SCAN1 is a neurodegenerative disease caused by defective TDP1, essential for the repair of TOP1-linked SSBs. As a result, SCAN1 cells accumulate unrepaired DNA breaks, leading to increased neuronal cell death (El-Khamisy *et al.*, 2005; Katyal *et al.*, 2007). Ataxia with oculomotor apraxia type-1 (AOA1) is a result of mutations in the aprataxin (*APTX*) gene, that codifies to the SSBR protein APTX (Gueven *et al.*, 2004). Although patients with SCAN1 and AOA1 can present extra neurological symptoms (hypercholesterolaemia and hypalbuminaemia), the almost exclusive neuropathological phenotype of these disorders demonstrate the importance of SSBR in neuronal health (Date *et al.*, 2001; Scott *et al.*, 2019). This is not surprising as SSBs occur frequently in the brain as a result of high ROS. The lack of antioxidants also makes the brain more susceptible to the

genotoxic effects generated by the free oxygen radicals than other organs (McKinnon, 2013; Madabhushi, Pan and Tsai, 2014).

The neurodegenerative phenotypes of A-T, ATLD, AOA1 and SCAN1 are very similar, suggesting the same endogenous lesions might drive neurodegeneration. In fact, accumulation of TOP1cc underpins the neurological phenotypes of all these disorders (Katyal *et al.*, 2014).

Remarkably, all mentioned disorders affect mainly the cerebellum. The cerebellum continues to develop after birth, until the age of 1-2 years, which coincides with the typical childhood onset of A-T (Lavin, 2008; McKinnon, 2009; Marzban *et al.*, 2015). This suggests that defects in ATM-mediated DSB repair tend to affect proliferating tissue, which explains the multisystemic phenotypic nature of this disorder. Conversely, the later onsets and tissue specificity of SCAN1 and AOA1 suggest that during the developing stages, the cerebellum can still cope with the damage being inflicted, since cells benefit from a wider array of repair pathways (Madabhushi, Pan and Tsai, 2014). As neurons mature and become postmitotic, the backup DNA repair mechanisms, such as HR, are no longer available and the increasing genotoxic load cannot be tolerated by the brain (McKinnon, 2013). This suggests that neuropathology in SCAN1 and AOA1 reflect an age-dependent accumulation DNA damage caused by constant internal insults in the CNS that later result in gradual neuronal degeneration since cells cannot repair the damage.

Other neurodegenerative disorders have also been linked to defective DNA repair (Hou *et al.*, 2019). In contrast with the congenital syndromes, the onset occurs during adulthood and the cerebrum is primarily affected (Fu, Hardy and Duff, 2018). The differences in developmental and degenerative neurological phenotypes, the onset of the neurological symptoms, and the specific CNS regions that are affected might reflect that: (i) different brain regions/ types of neurons have unique thresholds for the build-up of DNA lesions; (ii) the time and place that specific DNA repair factors are needed differ during proliferation, differentiation, maturation and ageing stages of the CNS; (iii) the different types of neurons that constitute the CNS have specific metabolic and respiratory needs, as well as different transcriptional activities, resulting in a regional elevation of endogenous DNA lesions, explaining why certain CNS regions are more susceptible to genomic instability than others.

A prime example of that is illustrated by familial ALS, which can be caused by mutations in genes directly or indirectly involved in DNA repair (Kok *et al.*, 2021). The first gene to be associated with ALS was SOD1. Mutations in SOD1 are the second most prevalent cause of

familial ALS (Zou *et al.*, 2017). SOD1 functions as a ROS scavenger, thus playing an important role in preventing age-associated oxidative stress (Mercado-Uribe *et al.*, 2020). As expected, the presence of SOD1 mutations causes an elevation of DNA damage markers and activation of DDR factors (Aguirre *et al.*, 2005; Li *et al.*, 2019). Apart from mutations in SOD1, ALS can also be caused by mutations in RNA-binding proteins with direct roles in DDR and DNA repair (Mastrocola *et al.*, 2013; Wang *et al.*, 2013; Mitra *et al.*, 2019). Mutations in TDP-43 and FUS cause cytoplasmic mislocalisation into insoluble aggregates (Higelin *et al.*, 2016; Suk and Rousseaux, 2020). Cells from patients carrying TDP-43 and FUS mutations experience defective DDR signalling and increased DNA damage, thus indicating a role of defective DNA repair in the pathogenesis of ALS (Qiu *et al.*, 2014; Higelin *et al.*, 2016; Guerrero *et al.*, 2019; Konopka *et al.*, 2020).

Likewise, mutations in DNA repair genes are also observed in other late-onset neurodegenerative diseases, including in HD (Table 1.3.1). Mutations in MMR factors have been identified in HD genome-wide association studies (GWAS) and are believed to drive CAG repeat instability (GeM-HD, 2015). Moreover, mutant huntingtin (mtHTT) is thought to directly influence DDR by interacting abnormally with ATM and to cause defective DNA repair and increased DNA damage (Maiuri *et al.*, 2017). More details about these topics will be discussed later.

Table 1.3.1 – Neurological disorders associated with defective DNA repair.

Adapted from (McKinnon, 2009; Abugable *et al.*, 2019)

Disorder	DNA repair gene	Affected repair pathway	Tissue specificity	Neurological deficits	Onset
Cockayne syndrome	*CSA, CSB, XPB, XPD and XPG*	TC-NER	Multisystemic	Developmental (microcephaly; demyelination)	All ages
Fanconi anaemia	*FANCA-FANCP*	HR	Multisystemic	Developmental (microcephaly)	Childhood
Spinocerebellar ataxia with axonal neuropathy (SCAN1)	*TDP1*	SSBR	Mainly CNS	Degenerative (ataxia; neurodegeneration; motor and sensorial neuropathy; muscle weakness)	Adolescent
Ataxia with oculomotor apraxia-1 (AOA1)	*APTX*		Mainly CNS	Degenerative (ataxia; neurodegeneration; oculomotor apraxia)	Childhood
AOA2	*SETX*	R-loop resolution	CNS	Degenerative (ataxia; neurodegeneration; oculomotor apraxia)	Adolescent/ Adult
Ataxia telangiectasia (A-T)	*ATM*	DSBR	Multisystemic	Degenerative (ataxia; neurodegeneration; and dysarthria)	Childhood
Ataxia telangiectasia-like disease (ATLD)	*MRE11*		Multisystemic	Degenerative (ataxia; neurodegeneration; oculomotor apraxia and dysarthria)	Neonaltal/ Infancy
Nijmegen breakage syndrome (NBS)	*NBS1*		Multisystemic	Developmental (microcephaly)	Neonaltal/ Infancy
RIDDLE syndrome	*RNF168*		Multisystemic	Developmental/ degenerative (ataxia; learning disabilities)	Childhood
LIG4 Syndrome	*LIG4*	DSBR (NHEJ)	Multisystemic	Developmental (microcephaly)	Neonaltal/ Infancy
Seckel syndrome	*ATR*	Replication-coupled repair	Multisystemic	Developmental (microcephaly; intellectual disabilities)	Prenatal
Amyotrophic lateral sclerosis (ALS)	*SOD1, FUS, TARBP, SETX*	SSBR, NHEJ, R-loop resolution	CNS	Neurodegenerative	Adult
Huntington's disease (HD)	*MSH3, MLH1, PMS1, MLH3, FAN1*	MMR	CNS	Neurodegenerative	Adult
Alzheimer's disease	*Polβ, APE1, NEIL1, UNG*	BER	CNS	Neurodegenerative	Adult
Parkinson's disease	*XRCC1, APE1*	BER	CNS	Neurodegenerative	Adult

1.4. Introduction to Huntington's disease

HD is an autosomal dominant neurodegenerative disorder that affects 1 in 7300 people in Western countries (Bates *et al.*, 2015). Currently there are no treatments available to reverse the disease. HD is a monogenic disease caused by mutations in the exon 1 of huntingtin gene (*HTT*, also called *IT15*), on chromosome 4p16.3, that produce elongation of cytosine-adenine-guanine (CAG) trinucleotide repeats, resulting in extended polyglutamine (polyQ) tracts in the N-terminus of the HTT protein (Bhat *et al.*, 2014). HD belongs to a group of polyQ disorders that comprises nine other autosomal dominant (except for one) neurodegenerative diseases, all caused by expanded CAG repeats. These include spinocerebellar ataxias (SCA) 1, 2, 3, 6, 7, 12 and 17, dentatorubral-pallidoluysian atrophy (DRPLA) and spinal and bulbar muscular atrophy (SBMA), an X-linked recessive disorder (Abugable *et al.*, 2019).

At the molecular level, mtHTT contributes to the specific degeneration of MSNs, inhibitory gamma-aminobutyric acid (GABA)ergic neurons that comprise the majority of the striatum (Paraskevopoulou, Herman and Rosenmund, 2019; Tabrizi *et al.*, 2020).

The molecular pathogenesis of HD result from the combination of several factors, including direct effects from the CAG expansions within the *HTT* gene, and toxicity from the mtHTT protein (Tabrizi *et al.*, 2020). The polyQ expansions at the protein level cause mtHTT to misfold, which interferes with the functioning of essential cellular processes through mechanisms of gain of toxicity and loss of normal HTT function (Tabrizi *et al.*, 2020). MtHTT interferes with transcription, mitochondrial functioning, axonal transportation, proteostasis, synaptic plasticity and DNA repair mechanisms, all culminating in loss of neuronal homeostasis and death of striatal cells (Bates *et al.*, 2015).

1.4.1. Clinical features of Huntington's disease

Macroscopically, HD is characterized by profound degeneration of the cerebral striatum, characterized by gradual atrophy of the caudate and putamen. As the disease progresses, the brain cortex also deteriorates (McColgan and Tabrizi, 2018). HD patients experience a triad of distinctive symptoms, including motor dysfunction, which manifests as chorea during the early stages and evolves into motor rigidity in later stages; behavioural and cognitive disturbances are also typical clinical presentations of the disease (Table 1.4.1) (Roos, 2010; Jimenez-Sanchez *et al.*, 2017; McColgan and Tabrizi, 2018).

The onset of HD is clinically defined when the individual shows undeniable motor symptomatology, especially involuntary choreiform movements. This criterion is defined according to the Unified HD Rating Scale total motor score and assesses not only chorea, but also gait, dystonia, oculomotor function and speech abilities (McColgan and Tabrizi, 2018). However, cognitive, behavioural and subtle motor changes (clumsiness and fidgeting) are the first signs in pre-symptomatic/ prodromal patients (Roos, 2010). As the disease progresses the motor functions become more aggravated, completely incapacitating the patient. The diagnosis of HD combines the settlement of the HD motor features, brain imaging and the confirmation of a detailed family history (Roos, 2010).

Table 1.4.1 - Clinical features of Huntington's disease

Stages	Motor features	Cognitive features	Behavioural features
Prodromal stage (Roos, 2010; Stout *et al.*, 2012; Schiefer, Werner and Reetz, 2015)	- Clumsiness - Fidgeting - Involuntary movements of fingers and toes - Facial muscles twitches	- Multitasking and concentration problems - Executive functions such as planning and initiation of new tasks become hard to preform - Less efficient thinking	- Irritability (usually the first symptom) - Depression - Anxiety - Agitation - Suicide risk (At-risk positive-tested individuals) - Obsessive compulsive behaviour - Personality changes
Clinically symptomatic:			
Early (stage i) (Kirkwood *et al.*, 2001; Roos, 2010; Schiefer, Werner and Reetz, 2015)	- Chorea (unwanted, involuntary movements) - Unstable walking - Hyperkinesia - Tics - Akathisia (unable to stay still) - Loss of coordination -Physically independent	-Progressive decline of cognitive features - Impulsivity - Impaired decision making - Attention deficit	- Worsening of irritability and depression - Apathy - Obsessive compulsive behaviour - Suicide risk - Disinhibition - Personality changes
Middle/ progressive (stage ii) (Kirkwood *et al.*, 2001; Roos, 2010; Novak and Tabrizi, 2011)	- Progressive loss of voluntary movements - Aggravation of chorea - Difficulties in walking - Balance problems - Frequent falls - Starts to be physically dependent - Weight loss - Swallowing problems	- Progressive executive dysfunction - Trouble in organization skills - Impaired thinking process - Difficulties in communication - Memory loss - Deficit in visuospatial perception - Progressive loss of mental judgement	- Aggravation of behavioural signs - Irritability and frustration - Aggressive behaviour - Increased apathy - Maniac-depressive behaviour - Suicide risk - Sexual disturbances - Sleep disturbances
Late/ terminal (stage iii) (Roos, 2010; Novak and Tabrizi, 2011)	- Severely incapacitating motor features - Declining of chorea - Rigidity - Bradykinesia - Hypokinesia - Dystonia - Severe weight loss - Swallowing problems -Completely dependent on care	- Muteness - Unable to perform daily tasks - Dementia (less frequent)	- Sleep deprivation - Increased apathy - Psychosis - Agitation - Irritability - Behavioural features difficult to assess due to communication problems

1.4.2. Huntingtin function

HTT is one of the largest proteins that compose the proteome of both invertebrates and vertebrates, with 3144 amino acids. HTT is ubiquitously expressed, with highest expression in the CNS and testes (Liu and Zeitlin, 2017). HTT is composed by a 17 amino acid-long amphipathic helix at the N-terminal (N17), followed by the polyQ region known to cause HD when expanded, and a poly-proline rich stretch. Distributed along the HTT protein are multiple clusters of Huntingtin, Elongation Factor 3, PR65A scaffolding subunit of protein phosphatase 2A, and Target of rapamycin (TOR) kinase (HEAT) repeats, that mediate the protein:protein interactions between its multiple partners. The HEAT repeats are composed of paired α-helix motifs, that confer to HTT protein its flexible elongated superhelical solenoid structure (Liu and Zeitlin, 2017). A nuclear export signal (NES) located at the C-terminal and a nuclear localization signal (NLS) at the N-terminal have also been identified, suggesting HTT has the capacity for nucleocytoplasmic trafficking (Bessert *et al.*, 1995; Xia *et al.*, 2003).

The subcellular localization of HTT is quite complex and dynamic. HTT adopts multiple conformations depending on the cellular compartment it is located. This feature of HTT was demonstrated in an early study showing that different anti-HTT monoclonal antibodies could distinguish different HTT conformations and that these conformations changed depending on the subcellular location (Ko, Ou and Patterson, 2001). This characteristic of HTT together with its ubiquitous presence throughout the body, makes it difficult to assign a specific role to this protein.

To get some hints regarding the function of HTT, several biochemical approaches have been used to search for the proteomic interactome of HTT. Using yeast two-hybrid screens, immunoprecipitation (IP) and affinity-purification mass spectrometry assays, researchers have identified a multitude of proteins that are complexed with HTT (Harjes and Wanker, 2003; Shirasaki *et al.*, 2012). Such intricate network of HTT-interacting partners implicates HTT in many cellular processes and suggests HTT acts as a scaffold protein.

HTT facilitates organelle trafficking, including axonal transport of synaptic vesicles and transport of endosomes and autophagosomes (Saudou and Humbert, 2016). Particularly, HTT mediates the transport of brain-derived neurotrophic factor (BDNF) vesicles, an important prosurvival factor for striatal projection neurons (Gauthier *et al.*, 2004). HTT has revealed to be an essential protein during embryonic development, given that germline inactivation of the mouse HD gene homolog (*Hdh*) is lethal in mouse embryos (Duyao *et al.*, 1995; Nasir *et al.*,

1995). 50% reduction of HTT expression during the development of mice embryos produces serious defects in neurogenesis and causes malformations in the cerebral cortex and striatum, demonstrating the importance of HTT during brain development (White *et al.*, 1997). In particular, HTT is involved in cell fate determination of cortical progenitor cells during embryonal corticogenesis by regulating mitosis through interaction with dynein and NuMA/LGN complex, promoting their accumulation at the spindle poles for proper spindle orientation. (Godin *et al.*, 2010; Elias *et al.*, 2014).

Additionally, HTT is a regulator of transcription, as its interaction with numerous factors promotes or represses the transcription of several genes. For example, HTT is a positive regulator of *BDNF* transcription, by binding to its inhibitor, the repressor element-1 transcription factor/neuron restrictive silencer factor (REST/NRSF) in the cytoplasm and preventing its nuclear translocation (Zuccato *et al.*, 2003). HTT also modulates transcription by influencing chromatin remodelling. For instance, HTT associates with cAMP-response element (CREB)-binding protein (CBP), a transcription co-activator that possesses histone acetyltransferase activity, allowing a more permissive chromatin for transcription (Steffan *et al.*, 2000; Roy, George and Palli, 2017).

Furthermore, HTT was shown to regulate selective autophagy through interaction of autophagy factors, promoting autophagosome formation and loading of the cargos to be degraded (Rui *et al.*, 2015). A role of HTT in DDR has also been described. In response to oxidative stress, the N17 domain of HTT is phosphorylated at serine 13 and 16, promoting the HTT translocation from the cytoplasm to the nucleus (DiGiovanni *et al.*, 2016). Once in the nucleus, ATM kinase activity regulates accumulation of HTT at the DNA damage sites where it interacts with several repair proteins involved in oxidative-induced damage, including XRCC1 (Maiuri *et al.*, 2017).

Given the properties of wild-type HTT (wtHTT), it is not surprising the increased cytotoxicity instigated by mtHTT as it disrupts crucial cellular functions. (Rui *et al.*, 2015; Lopes *et al.*, 2016; Maiuri *et al.*, 2017). Expansion of the polyQ tracts causes mtHTT to fold abnormally, accumulating into soluble oligomers that tend to aggregate and form large insoluble inclusions (Hoffner and Djian, 2014). Therefore, HD is considered a proteinopathy (Golde *et al.*, 2013). Evidence indicates that soluble N-terminal oligomers have increased toxicity, due to their highly interactive nature and propensity for nuclear accumulation, engaging in toxic interactions that interfere with key cellular processes (Havel *et al.*, 2011; Nucifora *et al.*, 2012; Kim *et al.*, 2016). Neurons developed a protective mechanism that attempt to mitigate the

toxicity employed by the oligomers and involves mtHTT sequestration into larger and less interactive insoluble inclusion bodies (Arrasate *et al.*, 2004; Sahl *et al.*, 2012; Kim *et al.*, 2016). In line with this, it is thought that HD arises from both a toxic gain-of-function (GoF) and a loss of the normal functioning of HTT (Cattaneo *et al.*, 2001; Paine, 2015).

GoF mechanisms in HD are supported by the fact that HD is an autosomal dominant disorder caused by CAG expansions, which are able to confer toxicity on their own (Paine, 2015). Also, the fact that caspase-mediated cleavage of mtHTT generates N-terminal mtHTT fragments with acquired toxicity, favours a GoF mechanism (Wellington *et al.*, 2002). Moreover, mtHTT develops the ability for new interactions or increases its affinity for its existing interacting partners, resulting in deleterious novel functions. An example of GoF involved in the pathogenesis of HD results from the increased affinity of mtHTT with huntingtin-associated protein 1 (HAP1), which results in defective axonal transport of BDNF (Gauthier *et al.*, 2004).

On the other hand, the fact that reduced levels of wtHTT mimic some HD phenotypes supports the notion that loss-of-function (LoF) of the HTT protein also contributes to HD (Cattaneo, Zuccato and Tartari, 2005). An example of LoF in HD is illustrated by the fact that HD mouse models and patients exhibit decreased levels of BDNF in the brain (Zuccato *et al.*, 2001; Yu *et al.*, 2018; Gutierrez *et al.*, 2020). The reduced *BDNF* gene expression is caused by the loss of mtHTT affinity to REST/NRSF, failing to retain it in the cytoplasm and eventually leading to the silencing of *BDNF* gene expression (Zuccato *et al.*, 2003). In addition, the fact that overexpression of wtHTT protects against the increased cell death triggered by mtHTT, is also suggestive of reduced HTT activity in HD (Zhang *et al.*, 2006).

The table below summarises the functions and mechanisms of HTT, how they become disrupted in HD and whether it reflects a GoF and/or LoF of wtHTT (Table 1.4.2).

Table 1.4.2 – Functions of huntingtin in physiology and disease

Function	*Mechanism*	*HD phenotype*	*GoF/LoF*	*References*
Organelle and vesicle transport	• Through direct interaction with dynein motor complex or indirectly through association with HAP1 and p150^{Glued} subunit of dynactin, HTT regulates microtubule-based trafficking. • HTT mediates the anterograde and retrograde axonal trafficking of a plethora of synaptic vesicles, including: BDNF- APP- and GABA-containing vesicles; as well as organelles: mitochondria, autophagosomes, endosomes and lysosomes.	• Axonal transportation is disrupted by mtHTT • mtHTT has increased affinity to HAP1. This disrupts HAP1 association with the motor machinery, reducing the capacity for axonal transportation of BDNF. • N-terminal of mtHTT interferes with mitochondrial axonal transportation.	GoF	(Gauthier *et al.*, 2004; Trushina *et al.*, 2004; Caviston *et al.*, 2007, 2011; Colin *et al.*, 2008; Orr *et al.*, 2008)
Transcription	• HTT associates with multiple transcription factors, including: NeuroD, p53, SP1, NFκB. • HTT interacts with transcription activators and repressors, including the transcription activator CBP and the repressor of neuronal gene expression REST/NRSF. • HTT potentiates the transcription of the REST/NRSF-target gene, *BDNF*. • HTT associates and promotes PRC2 tri-methyltransferase activity, increasing the levels of the chromatin repressor, H3K27me3.	• mtHTT causes CBP mislocalisation, leading to decreased CBP-mediated transcription. • mtHTT shows decreased affinity to REST/NRSF, leading to its nuclear translocation and consequent silencing its target genes, including *BDNF*. • mtHTT represses PGC-1α transcription in the striatum of HD mice. • mtHTT associates with ATXN3, which inactivates its activity as a deubiquitinating enzyme, increasing ubiquitination and degradation of CBP. • mtHTT compromises the integrity of the TCR complex and promotes accumulation of DNA breaks at actively transcribing genes, promoting transcription dysregulation.	GoF and LoF	(Steffan *et al.*, 2000; Li *et al.*, 2002; Bito and Takemoto-Kimura, 2003; Zuccato *et al.*, 2003; Cui *et al.*, 2006; Seong *et al.*, 2009; Gao *et al.*, 2019)
Ciliogenesis	• HTT regulates cilia biogenesis by associating with HAP1 and PCM1 at the centrosomes. • HTT is necessary to maintain PCM1 centrosome localization	• mtHTT increases PCM1 localization at the centrosomes and PCM1 accumulation in ependymal cells. • HD mice and HD patient cells show increased ciliogenesis, with longer and disoriented cilia, causing abnormal CSF flow	GoF	(Keryer *et al.*, 2011)
Neurogenesis	• HTT controls cell fate of cortical progenitors by ensuring proper spindle orientation.	• PolyQ expansions in mtHTT impairs RAB11 activity, leading to impaired radial migration of the embryonic cortical neurons	LoF	(Godin *et al.*, 2010; Barnat *et al.*, 2017)

Function	*Mechanism*	*HD phenotype*	*GoF/LoF*	*References*
	• HTT is necessary for the development of the cerebral cortex and is enriched in polarizing neurons in the neocortex. • By regulating RAB11, HTT controls multipolar-bipolar transition of projection neurons and maintenance of neuronal polarization during during cortex development			
Cell division	• HTT locates at the mitotic spindles. • Regulates spindle orientation by promoting cortical localization of the dynein/dynactin/NuMA/LGN complex during neurogenesis.	• Developmental malformations in HD brains	LoF	(Godin *et al.*, 2010; Nopoulos *et al.*, 2011; Hickman *et al.*, 2021)
Synaptic plasticity	• HTT is required for a balanced establishment of the cortico-striatal excitatory synapses. • HTT regulates cortical and striatal connectivity and function.	• mtHTT promotes disproportionate formation of cortical and striatal excitatory synapses, followed by rapid synaptic deterioration	LoF	(McKinstry *et al.*, 2014; Burrus *et al.*, 2020)
Selective autophagy	• HTT binds to p62 to promote p62-mediated cargo recognition and p62 binding to LC3. • HTT mediates axonal transport of autophagosome in neurons.	• Presence of empty autophagosomes in HD cells due to faulty cargo recognition. • Expanded polyQ in mtHTT disturbs autophagosome trafficking, causing defective cargo degradation and accumulation of mtHTT aggregates	LoF	(Martinez-Vicente *et al.*, 2010; Wong and Holzbaur, 2014; Rui *et al.*, 2015)
Macrophage function	• HTT controls the release of proinflammatory cytokine from macrophages. • HTT regulates macrophage phagocytic ability and response to stress	• Increased expression of NFκB-target proinflammatory genes through interaction with IKK. • Elevated macrophagic phagocytosis in HD.	GoF and LoF	(Kwan *et al.*, 2012; Träger *et al.*, 2014; O'Regan *et al.*, 2020)
Cell survival and stress response	• HTT protects neurons against cell death triggered by several stressors, including mtHTT itself. • HTT is required for the survival of striatal projection neurons during ageing. • HTT binds and prevents activation of caspase-3 and -9. • HTT binds to HIP-1 and Hippi, preventing the formation of the pro-apoptotic complex HIP-1/Hippi/procaspase-8.	• Expression of exon1 of mtHTT promotes cells death. • MtHTT has lower affinity to caspase-3 and loses its inhibitory effect towards caspase-3 activation of apoptosis. • PolyQ expansions decrease mtHTT affinity to HIP-1 and Hippi. HIP-1 and Hippi are free to form a pro-apoptotic complex that activates caspase-3.	GoF and LoF	(Rigamonti *et al.*, 2000, 2001; Ho *et al.*, 2001; Gervais *et al.*, 2002; Wellington *et al.*, 2002; Gauthier *et al.*, 2004; Leavitt *et al.*, 2006; Zhang *et*

Function	*Mechanism*	*HD phenotype*	*GoF/LoF*	*References*
	• HTT promotes transcription and trafficking of BDNF to the cortico-striatal synapses, necessary for activation of the striatal survival signalling.	• mtHTT is target for caspase-3, -6 and -9-mediated cleavage, generating toxic poly-Q containing N-terminal fragments. • mtHTT disrupts axonal transportation of BDNF, leading to neuronal death.		*al.*, 2006; Burrus *et al.*, 2020)
DNA damage repair	• Phosphorylation of HTT at N17 domain in response to oxidative stress triggers its nuclear translocation. • ATM regulates HTT recruitment and retention at the sites of damage. • Cdk5 phosphorylates HTT at S1181 and S1201 in response to DNA damage • Participates in BER by interacting with DNA repair proteins – pATM, XRCC1, APE1 – in response to oxidative damage. • HTT is involved in TCR and forms a TCR complex with ATXN3, POL2, PNPK and LIG3	• Increased levels of DNA damage from prodromal to clinically manifesting stages. • mtHTT preserves its ability to locate at the sites of damage. • Cdk5 is reduced during the later stages of HD, leading to decreased mtHTT phosphorylation. This confers toxicity to polyQ expansions and triggers p53-mediated cell death. • mtHTT inactivates PNPK, induces breaks at active transcribed genomic regions and triggers ATM-p53 pathway. • mtHTT sequesters Ku70 into inclusion bodies, impairing NHEJ	GoF and LoF	(Anne, Saudou and Humbert, 2007; Enokido *et al.*, 2010; DiGiovanni *et al.*, 2016; Maiuri *et al.*, 2017; Yehuda *et al.*, 2017; Gao *et al.*, 2019)

1.4.3. CAG repeat length and age of onset in Huntington's disease

The age of motor onset is tightly correlated with the length of the CAG tracts as longer expansions are associated with earlier onsets (Bates *et al.*, 2015; Keum *et al.*, 2016; Lopes *et al.*, 2016). Individuals carrying up to 35 CAG nucleotide repeats do not manifest the disease. Reduced penetrance is observed in carriers with 36-39 CAG repeats. Mutations in *HTT* gene are fully penetrant when CAG repeats go beyond a threshold of 40, where the age of onset is dependent on the allele with longer expansions within the *HTT* gene (Bates *et al.*, 2015; Keum *et al.*, 2016; Tabrizi *et al.*, 2020). Patients carrying 40-50 CAG repeats often exhibit the first clinical symptoms around the age of 40. Juvenile forms of HD have been reported to occur in almost 10% of HD cases. These patients are characterized by carrying more than 60 CAG repeats and the age of motor onset occurs typically before the age of 21 (Quigley, 2017).

Since the discovery of the CAG expansions within the *HTT* gene as a cause for HD in 1993 (MacDonald *et al.*, 1993), researchers have been faced with the conundrum of whether the size of CAG expansions in the *HTT* gene or the length of the glutamine tracts at the protein level dictates the progression and severity of the disease. On one hand, the age of onset of HD is defined by the length of the CAG repeats (Keum *et al.*, 2016). Still, studies exploring the pathogenesis of HD mainly focus on how the expanded glutamine stretches affect the HTT protein function and its consequences on the various biological processes (Hoffner, Souès and Djian, 2007; Arrasate and Finkbeiner, 2012; Xi *et al.*, 2016; Bäuerlein *et al.*, 2017; Sun *et al.*, 2017; Tabrizi *et al.*, 2020).

Nonetheless, the length of trinucleotide repeats only explains around 50-70% of the variability in the age of motor onset and severity of the symptoms, as additional heritable genetic modifiers and environmental factors have been found to contribute to the phenotypic variances observed in HD patients. (Gusella, Macdonald and Lee, 2014; GeM-HD, 2015, 2019; Arning, 2016; Keum *et al.*, 2016; Tabrizi *et al.*, 2020; Wheeler and Dion, 2021).

1.4.3.1. Instability of expanded CAG repeats

The aberrant CAG expansions within *HTT* gene are highly prone to germline and somatic instability, meaning they are susceptible to either contract or expand (Mirkin, 2007; Dion, 2014; Usdin, House and Freudenreich, 2015). Regarding somatic *HTT* CAG instability, extensive expansions occur preferentially in the striatum, where the CAG repeats can reach more than 1,000 units, which explains partially the tissue selectivity of HD (Kennedy *et al.*, 2003; Goula *et al.*, 2009).

Cellular processes that require DNA unwinding such as DNA repair, replication, transcription, and recombination can lead to the formation of non-B structures, such as hairpins or slipped strands due to incorrect annealing of DNA at the repeats (Mirkin, 2007). These structures are susceptible to error-prone repair or can even escape repair, causing expansions of the repeat tract (Panigrahi *et al.*, 2005; Guo *et al.*, 2016).

Components of the MMR pathway have been shown to drive CAG repeat instability. Insights regarding the role of MMR machinery in repeat instability were demonstrated in an early study by Manley *et al.*, (1999). Deletion of *Msh2* in transgenic mice carrying the exon 1 of human *HTT* abrogated CAG expansions in somatic tissues, particularly in the striatum (Manley *et al.*, 1999). Lin, Dion and Wilson, (2006) also showed that decreasing the levels of MSH2 and MSH3 using small interfering (siRNA) induced CAG repeat contractions in a transcription-dependent manner (Lin, Dion and Wilson, 2006). In agreement, another study demonstrated that depletion of *Msh3* was beneficial in *Hdh*^{Q111} knock-in mice as it significantly reduced CAG instability and decreased mtHTT aggregates in mice striatum (Dragileva *et al.*, 2009). These studies implicate MutSβ (MSH2-MSH3) complex as an important mediator of CAG instability. In concordance, MutSβ binds to short CAG/CTG slipped structures and hairpins, leading to the recruitment of MutL endonucleases (Owen *et al.*, 2005; Panigrahi *et al.*, 2010; Pluciennik *et al.*, 2013; Nakatani *et al.*, 2015; Kadyrova *et al.*, 2020). The MutL complexes introduce nicks into the DNA. In the presence of pre-existing nicks, MutL has a preference towards the nick-containing strand. If pre-existing nicks are absent, MutL can cleave either strand in an unbiased way (Pluciennik *et al.*, 2013). The subsequent processing of MutL-induced nicks can produce repeat expansions (Pluciennik *et al.*, 2013; Usdin, House and Freudenreich, 2015; Kadyrova *et al.*, 2020; Wheeler and Dion, 2021).

Remarkably, both MutLα (MLH1-PMS2) and MutLγ (MLH1-MLH3) have been shown to promote CAG/CTG repeat expansions (Gomes-Pereira *et al.*, 2004; Pluciennik *et al.*, 2013; Kadyrova *et al.*, 2020). In the context of HD, loss of *Mlh1* and *Mlh3* reduced significantly *HTT* CAG expansion in the striatum of *Hdh*^{Q111} mice (Pinto et al., 2013). A recent study has also revealed that *HTT* CAG expansions depend on the endonuclease activity of MLH3, as mutations in the endonuclease domain of MLH3 and abrogation of this domain through splicing redirection eliminated CAG expansions in *Hdh*^{Q111} mice and in primary fibroblasts from HD patients (Roy *et al.*, 2021).

FAN1 has also been implicated in CAG repeat instability. FAN1 is an endonuclease and exonuclease involved in ICL DNA repair and in the restart of stalled replication forks (Liu *et al.*, 2010; MacKay *et al.*, 2010; Lachaud *et al.*, 2016). A functional study demonstrated that FAN1 depletion using siRNA resulted in somatic instability of the CAG repeats in U2OS cells ectopically expressing HTT expansions, and in iPSCs and differentiated neurons from HD patients. Accordingly, overexpression of FAN1 reduced *HTT* CAG repeats, pointing FAN1 as a modulator of HD pathogenesis responsible for stabilizing CAG expansions (Goold *et al.*, 2019). The mechanism by which FAN1 prevents CAG repeat instability was recently discovered (Goold *et al.*, 2021; Porro *et al.*, 2021). Goold *et al.*, (2021) identified an SPYF motif at the N-terminal of FAN1. This highly conserved region mediates FAN1 interaction with MLH1. By binding to MLH1, FAN1 prevents MSH3-MLH1 interaction and inhibits MMR-driven CAG expansion. Moreover, FAN1-MLH1 interaction was also shown to be important for the repair of CAG slip-outs (Porro *et al.*, 2021).

Oxidative damage has also been implicated as a trigger for repeat instability. Age-dependent accumulation of 8-oxoG correlated with increased CAG repeat expansions in the brains of R6/1 mice, further providing evidence about how ageing contribute to neurodegeneration (Kovtun *et al.*, 2007). Repeat instability was found to be dependent on OGG1 excision activity, as deletion of Ogg1 from R6/1 mice decreased somatic CAG expansions (Kovtun *et al.*, 2007). Similarly, abrogation of Neil1 also protected against somatic repeat expansions in the brains of R6/1 mice (Møllersen *et al.*, 2012). NEIL1 is another DNA glycosylase responsible for the excision of oxidised bases involved in BER (Møllersen *et al.*, 2012).

Mechanistically, a study proposed that CAG repeat expansions are promoted by long-patch BER pathway (Liu *et al.*, 2009). This sub-pathway involves DNA synthesis by Polymerase β (Polβ) to fill in the gap left by the excision of the oxidised base, leaving a 5'-flap as a result. This flap is then removed by FEN1. When this mechanism occurs within CAG repeats, the formation of hairpins interferes with FEN1 cleavage activity, while Polβ continues gap-filling DNA synthesis. This induces FEN1 alternate cleavage activity to remove the 5'-flaps generated by Polβ at the base of the CAG hairpins, resulting the incorporation of the hairpin into the DNA and consequent CAG expansion (Liu *et al.*, 2009). Another study demonstrated that MutSβ promotes CAG repeat expansion through recruitment of Polβ, which uses CAG hairpin as template during DNA synthesis (Guo *et al.*, 2016). This suggests repeat instability might involve the coordination between different repair pathways.

Further studies trying to understand the role of transcription in repeat instability have demonstrated that the SSBR machinery prevents repeat instability, as chemical inhibition as well as siRNA knockdown of individual elements of this repair pathway – TOP1, TDP1, PARP1 and XRCC1 – increased repeat contractions during transcription of CAG tracts (Hubert *et al.*, 2011; Lin and Wilson, 2012; Nakatani *et al.*, 2015). Repeat contractions induced by dysfunctional SSBR pathway were mediated by TC-NER (Hubert *et al.*, 2011). Destabilization of large trinucleotide repeats were later shown to be dependent on MMR, TC-NER and SSBR pathways, as well as on R-loops, since depletion of SETX increased repeat instability (Nakatani *et al.*, 2015). Together, these studies implicate DNA repair pathways as mediators of CAG repeat instability.

1.4.3.2. Genetic modifiers of the age of onset in Huntington's disease

In 2015, the Genetic Modifiers of HD (GeM-HD) Consortium performed GWAS on a cohort of 4082 individuals with HD with the goal of identifying genetic factors that explain the variability of the age of HD onset (GeM-HD, 2015). Three modifiers located at two distinct loci were identified. On chromosome 15 two independent signals, likely corresponding to *FAN1* gene, were found to have opposite effects on HD onset. The rs146353869 single nucleotide polymorphism (SNP) hastened the disease in 6.1 years and the rs2140734 SNP delayed the HD onset in 1.4 years (GeM-HD, 2015).

Another variant responsible for delaying the HD onset in 0.7 years was identified in the locus corresponding to *MLH1* gene in chromosome 3 (J.-M. Lee *et al.*, 2017). Furthermore, a follow-up GWAS that counted with 216 participants from the TRACL-HD study and 1773 individuals from the European HD Network REGISTRY cohort, detected a polymorphism in chromosome 5 that was associated with slower disease progression, corresponding to *MSH3* or *DHFR* genes, as both share the same promoter (Moss *et al.*, 2017). In agreement, a transcriptome-wide association study (TWAS) in a cohort of HD patients demonstrated that increased cortical expression of MSH3 was associated with an early HD onset and faster disease progression (Flower *et al.*, 2019).

In 2019, the GeM-HD extended the GWAS to include 9064 HD subjects (GeM-HD, 2019). The study confirmed the abovementioned loci and detected another two independent SNPs corresponding to *MSH3/DHRF* loci. One delayed the HD onset by 6.1 years and the other accelerated the onset in 0.8 years. The latter was concomitant with increased MSH3 expression and elevated CAG expansion in the blood of HD individuals. Three additional loci containing

genes associated with DNA repair have also emerged as HD modifiers. These loci corresponded to genes encoding for PMS1, PMS2 and LIG1 proteins. Complementary TWAS analysis discovered that later HD onset was associated with increased MSH1 and PMS1 expression and decreased MSH3 levels, which agrees with the studies performed by Flower *et al.*, (2019) and Goold *et al.*, (2019). A variant in *LIG1* locus associated with an earlier onset was linked to increased LIG1 levels in the cerebral cortex (GeM-HD, 2019). These studies provide evidence of the involvement of DNA repair genes as modifiers of the HD age of onset by influencing *HTT* CAG somatic expansion.

1.4.3.3. Interruption of the CAG expansions and the age of onset in Huntington's disease

Variations of the CAG repeat sequence within the *HTT* gene were also shown to impact the HD onset. Several genetic studies have used complementary approaches to understand the effect of uninterrupted CAG repeats on the age of onset (Ciosi *et al.*, 2019; GeM-HD, 2019; Wright *et al.*, 2019; Findlay Black *et al.*, 2020). 95% of HD patients carry an uninterrupted CAG tract followed by a CAA-CAG interrupting sequence. Although CAA and CAG encode both for glutamine, loss of this interrupting sequence to CAG-CAG led to an earlier onset of the motor symptoms, even though the resultant HTT protein contained the same polyglutamine length (GeM-HD, 2019). Conversely, duplication of the interruption delayed the onset. Additionally, differences in these interrupting sequences also explain in part variations in the age of onset in individuals carrying reduced penetrant alleles (36-39 CAG), where one third of the individuals that developed HD symptoms, carried loss of CAG interruption (Wright *et al.*, 2019).

These observations show the importance that uninterrupted CAG expansions have as drivers of the pathogenesis of HD and in influencing the age of onset. However, it is yet to understand how the different CAG interrupting variants drive genomic instability. Loss of CAG tract interruption might exert its deleterious effects by influencing the somatic expansion of the HTT CAG repeats. Longer CAG repeats are highly unstable, especially in the striatum and cortex, and tend to adopt aberrant structures (Shelbourne *et al.*, 2007; Dion, 2014; Wright *et al.*, 2020).

It has been long established the importance of the expanded CAG tracts in determining the HD onset, as opposed to the glutamine length at the protein level. Nonetheless, whether there are different toxicity levels employed by the expanded polyQ tracts encoded by interrupted CAA-CAG sequences, in comparison with the ones encoded by uninterrupted CAG sequences is

unknown. Moreover, it is still uncertain which one – CAG repeats or the polyQ expansions – drive neuronal damage in HD, as it is unclear if the CAG toxicity precedes and/or triggers polyQ poisonous effects.

Additional mechanisms involved in the pathogenesis of HD, regarding HTT RNA toxicity, aberrant splicing, and unconventional translation mechanisms, might help shed a light on this subject (Sobczak *et al.*, 2010; Sathasivam *et al.*, 2013; Bañez-Coronel *et al.*, 2015). At the RNA level, CAG expansions promote the formation of toxic hairpin structures, while RNAs composed of CAA repeats or CAA-CAG sequences form unstructured transcripts (Sobczak *et al.*, 2010). Furthermore, expanded CAG RNAs perturb the function of RNA-binding proteins, leading to disruptions in several cellular processes, including alternative splicing, RNA transport and translation (Martí, 2016). In addition, expanded CAG transcripts in R6/2 HD mice were found to induce nucleolar stress by sequestering nucleolin and promoting ribosomal RNA (rRNA) degradation, which triggered p53-dependent cell death (Tsoi and Chan, 2013). Another study demonstrated that the striatum of human HD brains accumulate toxic aggregates of polyalanine, polyserine, polyleucine and polycysteine peptides, which are products of repeat-associated non-ATG (RAN) translation (Bañez-Coronel *et al.*, 2015). Hence, these studies provide evidence that *HTT* CAG repeats drive toxicity independently of the polyQ tracts at the protein level. It is possible that expanded CAG repeats within *HTT* gene are the main driver of cellular toxicity until the onset of the motor symptoms. Once the disease is settled, polyQ toxicity takes place. This is consistent with the fact that the disease duration in HD, i.e., the time between onset and death, is independent of the CAG repeat length (Keum *et al.*, 2016).

1.4.4. DNA damage response signalling in Huntington's disease

The genetic studies mentioned above demonstrate how DNA repair mechanisms regulate CAG repeat instability and establish a direct role in the pathogenesis of HD. Furthermore, the involvement of wtHTT in DNA repair processes and consequent disruption of these mechanisms by mtHTT also provide extra hints regarding the involvement of DDR and repair in HD pathology.

The HTT act as a sensor for ROS stress (DiGiovanni *et al.*, 2016). HTT possesses a highly conserved methionine at position 8 of its N17 domain, found to be sensitive to redox conditions. In response to oxidation, this methionine is subjected to sulphoxidation, which promotes structural changes to N17 α-helix. This contributes to N17 detachment from the endoplasmic reticulum membrane and consequent solubilization, making it a good target for

phosphorylation. Indeed, HTT is phosphorylated at S13 and S16 after oxidative DNA damage, which promotes HTT nuclear translocation (DiGiovanni *et al.*, 2016). Once at the nucleus, HTT locates at the sites of DNA damage in an ATM-dependent manner, where it acts as a scaffold for BER proteins, including XRCC1 (Maiuri *et al.*, 2017). MtHTT lacks S13 and S16 phosphorylation, however, it still retains the ability for nuclear retention and focal localization at the damage sites after oxidative stress (Maiuri *et al.*, 2017). One possibility is that nuclear mtHTT in its hypophosphorylated form harmful interactions with ATM, preventing its activity in DDR signalling.

This is consistent with the findings demonstrated by Ferlazzo *et al.*, (2014). They described that HD fibroblasts yield slower clearance of γH2AX foci in comparison with control fibroblasts after irradiation. As such, irradiated HD cells show decreased γH2AX foci formation at earlier time points and accumulation of γH2AX foci at later times. These findings indicate that HD cells lack competent signalling of DSBs response, resulting in deficient DNA repair. Additionally, irradiated HD cells have shown impaired 53BP1 recruitment. (Ferlazzo *et al.*, 2014). In parallel, as DNA damage accumulates, HD cells might try to compensate by hyperactivating ATM to levels beyond the threshold of which mtHTT can affect ATM. This prolonged activation of ATM would then lead to elevated p53 activation and consequent apoptotic cell death.

In agreement, reduction of ATM levels and inhibition of its kinase activity were shown to improve HD phenotype in patient cells and HD *Drosophila* models (Lu *et al.*, 2014). *Atm*$^{+/-}$ heterozygous crosses with BACHD mice also reduced HD neuropathology, decreased mtHTT brain aggregates and improved behavioural phenotypes (Lu *et al.*, 2014). Inhibition of ATM also prevented mtHTT nuclear retention, suggesting the detrimental effects of mtHTT in the nucleus goes beyond its impact on ATM activity (Maiuri *et al.*, 2017). Indeed, transcription dysregulation is a mark of HD caused by mtHTT aberrant protein interactions in the nucleus.

Transcription-coupled repair (TCR) is also part of the repertoire of HTT functions (Gao *et al.*, 2019). During transcription elongation, HTT scaffolds the formation of TCR complex, by associating with PNKP, ATXN3, RNA polymerase II, DNA ligase 3 and transcription factors. The HTT-TCR complex secures the preservation of genome integrity in actively transcribed genome in postmitotic neurons. In HD neurons, however, mtHTT diminishes the 3'-phosphatase activity of PNKP, leading to a preferential accumulation of DNA breaks in the

active genome. The persistent DNA breaks further trigger ATM-mediated activation of p53 and consequent induction of apoptosis (Gao *et al.*, 2019).

Another report described a mechanism in which mtHTT perturbs DSB repair by sequestering key repair proteins involved in NHEJ repair. mtHTT was shown to interact with Ku70. Binding of mtHTT prevented Ku70/Ku80 heterodimer formation and Ku70-DNA interaction, thus impairing DNA-PK complex activity (Enokido *et al.*, 2010).

In agreement with the notion that mtHTT contributes to NHEJ defects, another study demonstrated that inclusion bodies formed by aggregated polyQ impact proper histone PTM in response to DNA damage. U2OS cells expressing HTT-polyQ expansions exhibited deficient ubiquitination, fundamental for recruitment of repair factors (Yehuda *et al.*, 2017). In fact, these cells have also shown diminished 53BP1 recruitment to the damaged chromatin. Inclusion bodies formed by aggregated HTT attract 53BP1, which might contribute in part to the defects in 53BP1 recruitment to the damage sites (Yehuda *et al.*, 2017). Although it is apparent that mtHTT perturbs DSB repair signalling by disturbing histone modification and consequent recruitment of DNA repair factors, the underlying mechanisms are yet to be identified.

Despite an evident involvement of defective DDR signalling in the pathogenesis of HD, it is uncertain whether accumulation of DNA damage causes striatal neuron degeneration or is rather an effect from other impaired mechanisms implicated in HD. For example, disfunctions in mitochondrial metabolism, structure, biogenesis and axonal trafficking are involved in HD pathology (Choo *et al.*, 2004; Cui *et al.*, 2006; Shirendeb *et al.*, 2011). These result in increased ROS generation and consequent augmented oxidative DNA damage, further triggering apoptotic cell death. Moreover, mtHTT aberrantly interacts with mitochondria outer membrane, causing the release of cytochrome *c*, resulting in apoptosis initiation (Orr *et al.*, 2008). MSN survival in HD is also impacted by mtHTT-mediated abnormal expression and cortical-striatal transport of BDNF (Yu *et al.*, 2018). Thus, the cerebral striatum of HD patients has a scarce supply of this vital factor for neuronal survival. These examples might suggest that mtHTT trigger neuron degeneration by mechanisms independent of DNA damage and cumulative DNA damage is itself a secondary effect of other cellular processes. Nonetheless, a recent report has found increased presence the DSB marker, γH2AX, in the peripheral blood of pre-symptomatic HD individuals (Castaldo *et al.*, 2019). In addition, the levels of γH2AX seemed to increase with age in the pre-symptomatic stage but not after the HD onset, indicating

that accumulation of DNA damage precedes striatal neuron degeneration. Most likely, accumulation of DNA damage is both a cause for neurodegeneration and an effect from other mechanisms involved in the pathogenesis of HD.

Moreover, it remains unclear what the exact causes for DNA damage in HD are and how mtHTT causes DNA breaks. As explained before, the neuronal genome is regularly threatened by endogenous sources of DNA damage, including oxidative DNA damage and TOP1-linked DNA breaks (McKinnon, 2017). Remarkably, increased DNA oxidation is itself a source for the formation of chromosomal DNA breaks (Sordet *et al.*, 2008). Still, if these lesions are implicated in HD, how mtHTT impairs their repair and whether HD cells are hypersensitive to this type of damage is unknown.

1.4.5. Defects in protein clearance in Huntington's disease

MtHTT protein is highly prone to misfolding and consequent aggregation, forming polyQ aggregates within the cytoplasm and nucleus of cells (Labbadia and Morimoto, 2013). In fact, the presence of intracellular insoluble inclusions caused by aggregation of misfolded proteins is a histological hallmark of HD and a common feature of several polynucleotide expansion neurological disorders, including SCAs and ALS. (Moily *et al.*, 2017).

Cells utilize two main mechanisms to degrade misfolded proteins and maintain proteostasis: the ubiquitin proteasome system (UPS) and the autophagy-lysosome system. Autophagy can be distinguished between a non-selective degradation system, in which starvation induces degradation in bulk of long-lived proteins and organelles for energy production (Yang and Klionsky, 2010); and between selective autophagy, in which cargos to be degraded are ubiquitinated for a selective recognition by cargo adaptors, such as p62 (Johansen and Lamark, 2011). This thesis will focus on selective autophagy (alternatively referred to as autophagy).

P62 or sequestosome 1 (SQSTM1) is a cargo adaptor and receptor involved in autophagy and UPS (Liu *et al.*, 2016). Via its ubiquitin-associated (UBA) domain, p62 binds preferentially to K63-polyubiquitin positive proteins and loads the cargo inside the autophagosome, by interacting with LC3-II protein at autophagosome membrane, where p62 is also degraded (Johansen and Lamark, 2011). Alternatively, p62 delivers ubiquitinated cargos for proteasomal degradation by interacting through its N-terminal PB1 domain with 26S proteasome (Myeku and Figueiredo-Pereira, 2011).

Protein aggregation in HD is associated with insufficient protein degradation due to defects in the UPS and selective autophagy mechanisms in an age-dependent manner (Waelter *et al.*, 2001; Mitra, Tsvetkov and Finkbeiner, 2009; Martinez-Vicente *et al.*, 2010; Bhat *et al.*, 2014). Aggregated mtHTT is highly ubiquitinated, which was first regarded as a preferential substrate for UPS degradation. However, ubiquitination also targets cargos for selective autophagy, indicating mtHTT is degraded by both UPS and autophagy mechanisms (Mitra, Tsvetkov and Finkbeiner, 2009; Arrasate and Finkbeiner, 2012; Martin *et al.*, 2015).

The first evidence of UPS impairment in HD comes from a study that demonstrated the formation of nuclear and cytoplasmic aggregates of mtHTT and other polyQ expanded proteins severely impaired UPS function (Bennett *et al.*, 2005). HTT aggregates can be ubiquitinated via K48 or K63 polyubiquitin chains. K48-mediated ubiquitination promotes protein degradation via UPS. On the other hand, K63-linked ubiquitin chains stimulate protein stability and aggregation (Bhat *et al.*, 2014). Ube3a is an E3 K48-ubiquitin ligase involved in proteasome degradation that decreases with age. A study showed that in HD, as Ube3a decreases in an age-dependent manner, mtHTT loses K48-polyubiquitination and accumulates K63-linked polyubiquitin chains, which promotes mtHTT aggregation (Bhat *et al.*, 2014). These two studies suggest a mechanism in which ageing contributes to a feedforward process by decreasing cellular UPS capacity in degrading mtHTT and promoting its aggregation (Bhat *et al.*, 2014) . In turn, augmented mtHTT aggregation would further contribute to UPS impairment (Bennett *et al.*, 2005).

Under physiological conditions, wtHTT was shown to be a mediator of selective autophagy by interacting with autophagy-related proteins, including p62, thus promoting recognition and its interaction with K63-linked ubiquitinated cargos (Rui *et al.*, 2015). Defects in selective autophagy in HD models have also been described. Although autophagosome formation occur at normal or even higher rates than normal cells, HD cells often exhibit empty autophagic vacuoles indicating deficient cargo recognition (Martinez-Vicente *et al.*, 2010). This might signify a compensatory mechanism in which HD cells upregulate autophagosome formation to balance the disruptive effects mtHTT inflicts upon autophagy. Interestingly, others have proposed that defects in clearance of polyQ aggregates are, at least in part, conformation dependent. MtHTT can adopt different conformations which can be recognised by different anti-polyQ antibodies. By measuring the degradation rates of mtHTT in fibroblasts derived from patients with HD, Fu *et al.*, (2017) identified that 3B5H10-recognised mtHTT species

were degraded at lower rates. These mtHTT species lacked efficient recognition by p62 due to impaired K63-ubiquitination. These findings indicate that different conformations adopted by aggregated mtHTT have different levels of toxicity, since some species are resistant to autophagic degradation (Fu *et al.*, 2017; Sun *et al.*, 2017). Through an siRNA screening, the same group has also identified HIPK3 as a negative modulator of selective autophagy in HD (Yu *et al.*, 2017). HIPK3 was found to interfere with the mtHTT degradation by decreasing autophagic flux in HD patient fibroblasts and iPSC-derived neurons, further increasing mtHTT protein levels. In turn, mtHTT upregulated *HIPK3* mRNA levels. This shows a positive feedback mechanism in which mtHTT promotes its own accumulation by upregulating *HIPK3* expression, which decreases mtHTT autophagic degradation (Yu *et al.*, 2017).

An additional mechanism by which mtHTT disrupts autophagy is through interaction with the striatal protein, Rhes. Rhes is selectively expressed in the striatum, where it acts as a positive regulator of autophagy by competing against Bcl-2 for the binding to the autophagy regulator, Beclin 1. Beclin 1 act as an autophagy inducer, by promoting autophagosome formation and is inhibited by interaction with Bcl-2 (Kang *et al.*, 2011). In the striatum, Rhes liberates Beclin 1 from the inhibitory effects of Bcl-2, promoting autophagy induction. However, mtHTT sequesters Rhes, leading to Beclin 1 inactivation (Mealer *et al.*, 2014). During initiation of autophagy, autophagosome assembly depends on the recruitment of the PI3K-III complex composed by Beclin 1, ATG14, VPS34 and VPS15, and activation via ULK1-mediated phosphorylation of Beclin 1 at its S15 and ATG14 at S29 (Menon and Dhamija, 2018). Remarkably, phosphorylation levels were decreased in HD cells and in Q175 HD mouse models, due to p62-mediated sequestration of ULK1, consequently increasing proteotoxic stress (Wold *et al.*, 2016).

Parallel to the direct influence of mtHTT in autophagy, mtHTT also indirectly interferes with autophagy by hindering microtubule trafficking of autophagosomes, an important step for autophagosome-lysosome fusion, due to aberrant association with HAP1 (Wong and Holzbaur, 2014). Additionally, mtHTT has reduced association with the Golgi apparatus, concomitant with decreased presence of the optineurin and Rab8. Optineurin and Rab8 form a complex important for post-Golgi vesicle trafficking to lysosomes and for lysosomal dynamics. This way, mtHTT contributes to defective lysosome function and consequently interferes with autophagolysosomal formation (Toro *et al.*, 2009).

1.5. Research rationale

Several lines of evidence support a relationship between defects in autophagy and impaired DDR and their role in neurodegeneration. P62 plays a central role in this crosstalk. Cells defective of autophagy mechanisms accumulate p62 in their nuclei, which has been related to disruptions in the DSB repair pathways, NHEJ and HR (B. L. Lee *et al.*, 2017; Lee, Kim and Ryu, 2017). Regarding NHEJ, as p62 accumulates it binds and inhibits the DNA damage-induced E3 ubiquitin ligase RNF168, resulting in deficient H2A ubiquitination and inadequate recruitment of 53BP1, thus perturbing NHEJ signalling (Y. Wang *et al.*, 2016). On the other hand, p62 was also shown to inhibit HR by promoting proteasomal degradation of filamin A (FLNA), necessary for the recruitment of RAD51, and degradation of RAD51 itself (Hewitt *et al.*, 2016).

Recent approaches have put effort into dismantling the role of the crosstalk between DNA repair and autophagy in neurodegeneration. A report has described that in ALS, *C9orf72* repeat expansions disturb ATM-mediated chromosomal-break repair due to accumulation of p62 and concomitant defective H2A ubiquitination. Consequently, motor neurons exhibit increased unrepaired DSBs, which trigger premature cell death and promote motor neuron degeneration (Walker *et al.*, 2017).

HD share some similarities with ALS, including the fact that both are neurodegenerative disorders caused by polynucleotide repeat expansions and the clear involvement of DNA repair and autophagy in the pathogenesis of both disorders. In line with this, the following research question has emerged:

Are Huntington's disease cells deficient of chromatin ubiquitination due to toxic accumulation of autophagy-related proteins, leading to inadequate DNA repair and elevated cell death?

Chapter 2: Materials and Methods

2.1. Mammalian cell culture

2.1.1. Reagents and materials

Table 2.1.1 - List of reagents, materials and equipment used in cell culture.
Details about reagents, supplier, materials and equipment are provided.

Reagents	**Supplier**
Minimum Essential Medium Eagle (MEM)	Sigma-Aldrich, Cat.: M2279
Dulbecco's Modified Eagle's Medium (DMEM)	Sigma-Aldrich, Cat: D6546
Opti-MEM™	ThermoFisher, Cat.: 10592693
KnockOut™ DMEM/F-12	ThermoFisher, Cat.: 12660012
Neurobasal™ Medium	ThermoFisher, Cat.: 21103049
Penicillin-Streptomycin	Gibco™, Cat.: 15140122
L-Glutamine	Gibco™, Cat.: 25030149
Sigma Foetal Bovine Serum (FBS)	Sigma-Aldrich, Cat.: F7524
Biosera FBS	Biosera Cat.: FB-1001/500B
Non-essential amino acids (NEAA)	Sigma-Aldrich, Cat.: M7145
GlutaMAX™ Supplement	ThermoFisher, Cat.: 35050061
B-27™ Supplement (50X), serum free	ThermoFisher, Cat.: 17504001
N-2 Supplement (100X)	ThermoFisher, Cat.: 17502001
Recombinant Human Dickkopf-1 (DKK-1)	PeproTech, Cat.: 120-30
Recombinant Human Sonic Hedgehog (SHH)	PeproTech, Cat.: 100-45
BDNF Recombinant Human Protein	ThermoFisher, Cat.: PHC7074
Rock inhibitor Y-27632	Tocris, Cat.: 1254
Trypsin	Gibco, Cat.: 27250-018
StemPro™ Accutase™ Cell Dissociation Reagent	ThermoFisher, Cat.: A1110501
Phosphate Buffered Saline (PBS) - tablets	Gibco, Cat.: 11510546
Dimethyl sulfoxide (DMSO)	Sigma-Aldrich, Cat.: D2650
Polyethylenimine (PEI)	Polysciences, Cat.: 23966
Ethylenediaminetetraacetic Acid (EDTA).	Fisher, Cat.: 10618973
Lipofectamine-2000	Invitrogen, Cat.: 11668019
DharmaFECT	Dharmacon™, Cat.: 11591731
RNAiMAX	Invitrogen, Cat.: 13778150
Camptothecin (CPT)	Sigma-Aldrich, Cat.: C9911
MIU1-Rhodamine B peptide (> 90% purity)	ThermoFisher (Costum made)
Materials	**Equipment**
T75/T175 flasks	Beckman GP Centrifuge
Pipettes (P2; P20; P200; P1000)	Vertical laminar flow hood
Tips	Vortex
Stripettes (5 mL; 10 mL)	Mettler AE 163 Scales
15 mL/ 50 mL tubes	Microwave
96-/24-/6-well plates	CO_2 incubator HERAcell®
Microcentrifuge tubes (1.5 mL; 2 mL)	FLUOstar Omega, BMG Labtech
10 cm^3 / 15 cm^3 dishes	
Cryovials	
Sterile syringe filter; 25 mm; 0.2 µm	
Syringes	

2.1.2. Cell lines

2.1.2.1.MRC5

Medical Research Council strain 5 or MRC5 cells are constituted by fibroblasts obtained from normal human lung tissue from a 14-week-old male foetus.

2.1.2.2. HEK293

Human embryonic kidney 293 is an adherent epithelial kidney cell line obtained from a female foetus.

2.2.2.3.GM08402

GM08402 is a human primary skin fibroblast retrieved from an apparently healthy male at the age of 32-year-old. These cells were obtained from Coriell Institute Repositories.

2.2.2.4.GM04799

GM04799 are adherent primary cells purchased from Coriell Institute Repositories. GM04799 is composed of skin fibroblasts retrieved from a male with Huntington's disease, with onset at the age of 47-year-old. This individual is heterozygous for CAG repeat expansions in the *HTT* gene. The mutated allele contains 42 CAG repeats.

2.2.2.5.GM04869

GM04869 are primary cells derived from skin fibroblasts retrieved from a female unrelated to GM04799, also clinically affected with Huntington's disease (onset at age of 31 years). This individual is heterozygous for CAG trinucleotide repeat expansions in the *HTT* genes. The wild type allele contains 15 repeats and the mutated allele carries 47 repeats. These cells were purchased from Coriell Institute Repositories.

2.2.2.6.GM23225

GM23225 are induced pluripotent stem cells (iPSCs) reprogrammed from human skin fibroblasts obtained from a 20-year-old female diagnosed with Huntington's disease (age of onset: 14-year-old). The individual carries 17 and 68 CAG repeats within the wild-type and mutant alleles, respectively.

2.2.2.7.CS14

iPSCs from an apparently healthy female with 30 years old, reprogrammed from human skin fibroblasts.

All cell lines used in this project were routinely tested negative for mycoplasma.

Table 2.1.2 – Cell lines used in this project

Details about type of cell line, HD diagnosis, number of CAG repeats, age at collection, gender, source, identifier, and purpose of use are provided. All cells were tested for mycoplasma and confirmed to be negative.

Cell line	Diagnosis	(CAG)n	Age at collection (yr)	Gender	Source	Identifier	Purpose of use
Established cell lines							
MRC5	--	--	Foetal	Male	ATCC	RRID:CVCL_0440	Overexpression of CAG constructs for IFs
HEK293	--	--	Foetal	Female	ATCC	RRID:CVCL_0045	Overexpression of CAG constructs for Co-IP. Used for experiments that required large amounts of cells
Fibroblast							
GM08402	Non-HD	--	32	Male	Coriell	RRID:CVCL_7485	Cell line derived from healthy individual. Used for experiments that did not require large amounts of cells.
GM04869	HD	47	32	Female	Coriell	RRID:CVCL_1I73	HD patient-derived cell line: clinically relevant. Used for experiments that did not require large amounts of cells
GM04799	HD	42	47	Male	Coriell	RRID:CVCL_Y887	HD patient-derived cell line: clinically relevant. Used for experiments that did not require large amounts of cells
iPSCs							
CS14iCTR	Non-HD	--	30	Female	Cedars-Sinai	RRID:CVCL_JK54	Differentiation into GABAergic neurons: HD-specific cell type. Clinically and physiologically relevant model.
GM23225	HD	68	20	Female	Coriell	RRID:CVCL_F169	Differentiation into GABAergic neurons: HD-specific cell type. Clinically and physiologically relevant model.

2.1.3. Preparation of solutions

2.1.3.1.Media preparation

MRC5 cells were grown in MEM supplemented with 10% FCS (Sigma-Aldritch), 1% penicillin/streptomycin and 1% L-Glutamine. HEK293 cells were grown DMEM, supplemented with 10% FBS, 1% penicillin/streptomycin and 1% L-Glutamine.

GM08402, GM04799 and GM04869 were grown in DMEM supplemented with 10% FBS (Biosera), 1% penicillin/streptomycin, 1% L-Glutamine and NEAA.

Neural progenitor cells (NPCs) were maintained in neural medium: 50% of KnockOut™ DMEM/F-12 medium; 50% of Neurobasal medium; 0.5x N2 supplement; 1x Gibco® GlutaMAX™ Supplement; 0.5x B-27, 50 U/mL penicillin and 50 mg/mL and streptomycin.

For differentiation into GABAergic neurons, the media used were:

- GABAergic 1-10 medium: Neural medium (as before) supplemented with 200ng/mL of recombinant human SHH, 100ng/mL of recombinant human DKK1 and 30ng/mL of recombinant human BDNF.
- GABAergic 11-60 medium: Neurobasal™ medium supplemented with 1x B27, 50ng/mL BDNF and 1% penicillin/streptomycin.

2.1.3.2.Standard solutions

PBS (working solution)

One PBS tablet dissolved into 500 mL of distilled water (dH_2O). The solution was autoclaved at 121ºC for 20 minutes (min) and kept at room temperature (RT)

0.25% (w/v) Trypsin (Stock solution)

1 g of Trypsin powder dissolved in 20 mL of autoclaved PBS. The solution was filter-sterilised into a sterile 500 mL bottle and 380 mL of autoclaved PBS was added. Kept at 4ºC.

4% (w/v) EDTA

4 g of EDTA dissolved in 100 mL dH_2O. pH was adjusted to 8 and the solution was autoclaved. Kept at 4ºC.

Trypsin-EDTA (Working solution)

37.5 mL of autoclaved PBS; 30 mL of 0.25% Trypsin; 7.5 of 4% EDTA. Kept at 4ºC

PEI

50 mg of PEI powder were dissolved in 50 mL dH_2O. To help dissolving the powder, the solution was heated at 60-80ºC. The pH was adjusted to 7.4. The solution was aliquoted and kept at -80ºC.

10 mM CPT (stock solution)

100 mg of CPT powder were dissolved in 28 mL DMSO. The solution was aliquoted into 1.5 mL centrifuge tubes and stored at -20ºC.

1 mM Recombinant MIU 1 peptide (stock solution)

MIU1 peptide (sequence: EEQLKSDEELARKLSIDINNF), tagged at the C-terminal with rhodamine B was custom made by the Thermo Scientific Peptide Synthesis Service.

1 mg of lyophilised powder were dissolved in 284.4 µL of DMSO. 31.6 µL of dH_2O were added to the solution for a final concentration of 1 mM. The solution was aliquoted into 0.5 mL centrifuge tubes and stored at -20ºC.

2.1.4. Cell passage

MRC5, HEK293 and primary patient fibroblasts were all grown in T75 or T175 flasks and sub-cultured when 70%-80% confluent. All cells were cultured at 20% O_2, 5% CO_2 and at 37ºC. After removing the media, the flasks were washed once with PBS. The flasks were then incubated with 2 mL of trypsin at 37ºC for 5 min. To inactivate the trypsin, the cells were re-suspended in 8 mL of growing media and the suspensions were transferred into 15 mL tubes. The cells were then spun at 1000 rpm for 5 min. After spinning the supernatant was discarded and the pelleted cells were re-suspended in fresh media. The cells were counted by aliquoting 10 µL of the suspension into a haemocytometer. The cell suspension was then aliquoted into T75 or T175 flasks containing fresh complete medium, depending on the split ratio intended. MRC5 and HEK293 were normally split in a ratio between 1:4-1:10, while primary cells were usually split in a ratio of 1:2-1:4.

2.1.5. Induced pluripotent cell (iPSC) culture (performed by Cleide Souza, SITraN)

Human iPSCs were maintained in Matrigel-coated plates according to the manufacturer's recommendations in complete mTeSR™-Plus™ Medium. Cells were passaged every 6 days

as clumps using ReLeSR™, an enzyme-free reagent for dissociation according to the manufacturer's recommendations. For all the experiments in this study, iPSCs were used between passage 20 and 30, all iPSCs were cultured in 5% O_2, 5% CO_2 at 37°C.

2.1.6. Differentiation of iPSCs into NPCs (performed by Cleide Souza, SITraN)

Neural differentiation of iPSCs was performed using the modified version dual SMAD inhibition protocol (Du *et al.*, 2015). iPSCs were plated in Matrigel-coated plate. After the cells have reached ~100% confluence, they were washed once with PBS and grown in neural medium (50% of KnockOut™ DMEM/F-12; 50 % of Neurobasal; 0.5× N2 supplement; 1x Gibco® GlutaMAX™ Supplement; 0.5x B-27, 50 U/mL penicillin and 50 mg/mL and streptomycin). The medium was additionally supplemented with SMAD inhibitors (2 μM DMH-1; 10 μM SB431542 and 3 μM CHIR99021). The medium was replaced every day for 6 days. On day 7, the medium was replaced for neural medium supplemented with 2 μM DMH-1, 10 μM SB431542 and 1 μM CHIR; 0.1 μM All-Trans Retinoic Acid (RA) and 0.5 μM Purmorphamine (PMN). The cells were kept in this medium until day 12 when is possible to see a uniform neuroepithelial sheet. The cells were then split 1:3 with Accutase onto Matrigel substrate in the presence of 10 μM of rock inhibitor (Y-27632 dihydrochloride), originating a sheet of neural progenitor cells (NPC). In this stage the NPC were expanded in the same medium containing 3μM CHIR99021; 2 μM SB431542; 0.1 μM RA; 0.5 μM PMN and 0.5 μM Valproic acid (expansion medium) and split 1:3 once a week with Accutase. NPCs were frozen in 10% DMSO in expansion medium, in liquid nitrogen and cultured again in expansion medium after thawing.

2.1.7. Differentiation of striatal neurons from NPCs

On day 0 NPCs were plated in Matrigel-coated 6-well plates at a minimum density of $1x10^6$ cells/well. When cells reached 80% confluency the NPC cells incubated for 10 days in GABAergic 1-10 medium. The media was changed every 2 days. At day 11 the cells were subjected to final passage. For the final passage, the GABAergic progenitors were incubated with Rock inhibitor (1:1000) for 1 hour (h) at 37ºC. The media was aspirated, and the cells were rinsed with PBS. The cells were then incubated with 1 mL Accutase™ for 5-7 min at 37ºC. The cells were collected into a 15 mL tube containing twice the volume of GABAergic 1-10 medium. The cells were centrifuged at 200 rpm for 4 min, the supernatant was discarded, and the cell pellet resuspended in 1 mL GABAergic 1-10 medium containing 10 μM Rock

inhibitor. The cells were then seeded in Matrigel-coated 96-well plates at a density of $2x10^4$ cells/well and incubated at 37ºC. After 24h the medium was replaced with GABAergic 11-60 medium. The medium was replaced every 2 days until day 60.

2.1.8. Thawing and freezing cell vials

Cell vials stored in liquid nitrogen were thawed in water bath at 37 ºC for 2 min. The suspended cells were then pipetted into T75 flasks containing 20 mL of the corresponding growing medium.

To freeze cells, after trypsinisation, the suspended cells were aliquoted into cryotubes and 10% DMSO was added. The tubes were maintained for 24h in a freezing genie at -80ºC and moved to liquid nitrogen the following day.

2.1.9. Seeding cells, transfection conditions and treatments

2.1.9.1.List of DNA plasmids and siRNA used

Table 2.1.3 - List of DNA plasmids and siRNA
Details about plasmids, siRNA and corresponding suppliers.

Plasmids	**Supplier**
pEGFP-Q23	Addgene, Cat.: 40261
pEGFP-Q74	Addgene, Cat.: 40262
pCDNA3.1-Flag-H2A K5-9-118-119-125-127-129R	Addgene, Cat.: 63565
siRNA	**Supplier**
Sip62	Santa-Cruz Biotechnology, Cat.: sc-29679

2.1.9.2.MRC5 and HEK293

For immunofluorescence purposes, MRC5 cells were seeded in 24-well plates on coverslips at a cell density of $1x10^5$ cells/well and incubated overnight at 37ºC. Cells were transiently transfected with 0.5 µg of GFP-tagged plasmids containing the exon 1 of HTT with either 23 CAG repeats (GFP-Q23: wtHTT) or 74 CAG repeats (GFP-Q74: mtHTT). Since the presence of serum can interfere with transfection efficiency, transfection complexes were prepared in serum-free medium (Opti-MEM™) and Lipofectamine-2000 as transfection reagent at a molar ratio of 2.5:1 (Lipofectamine:DNA). After incubation for 48h at 37ºC, MRC5 cells were treated with 10 µM CPT or DMSO for 1h.

For the experiments using recombinant MIU1 peptide, 24h after transfection with GFP-Q23/-Q74 plasmids, the cells were treated with either DMSO (no peptide) or with 5 µM MIU1 overnight. The following day (48h after transfection), the cells were treated with 10 µM CPT for 53BP1 immunofluorescence assay.

For western blotting, MRC5 cells were plated in 10 cm^3 at a density of $1x10^6$ cells/plate and transfected with 5 µg of GFP-Q23 or GFP-Q74. Transient transfection was obtained by using PEI at a concentration of 2:1 (PEI:DNA). After transfection, the cells were incubated for 48 h at 37ºC prior to harvesting.

For p62 siRNA experiments, MRC5 cells were seeded on coverslips in 6-well plates at a cell density of $4.5x10^5$ cells/well. The following day, the cells were co-transfected with 2 µg of GFP-tagged plasmids (Q23 or Q74) using PEI as described above, along with 25 nM of either p62 siRNA or scramble particles using DharmaFECT at a ratio of 1:1 (v/v). Cells were grown at 37ºC for 48 h after transfection and treated with 10 µM of CPT for 1 h.

For RNF168 co-immunoprecipitation (Co-IP) assay, HEK293 cells were plated in 10 cm^3 dishes. When around 80% confluent, the cells were transiently transfected with 5 µg of GFP-Q23 or GFP-Q74 plasmids. Complexes were prepared in Opti-MEM™ using PEI as a transfection reagent at a ratio of 2:1 (PEI:DNA). Cells were incubated for 48h at 37ºC before being harvested for cell fractionation. For RNF168 co-IP experiments in the presence of recombinant MIU1 peptide, 24h after transfection with GFP-Q23/-Q74 plasmids, the cells were treated with either DMSO or with 5 µM MIU1 overnight at 37ºC. Next day the cells harvested and fractionated.

For Flag IP, HEK293 cells were seeded in 15 cm^3 plates until 80% confluent. The cells were co-transfected with 7.5 µg of pCDNA3.1-Flag-H2A K5-9-118-119-125-127-129R plasmid (Flag-H2A K13/K15) and 7.5 µg of GFP-Q23 or GFP-Q74. Alternatively, cells were transfected with 15 µg of Empty-GFP. For both, the transfection complexes were prepared in Opti-MEM™ and PEI at a ratio of 2:1 (PEI:DNA). The cells were incubated for 48 h at 37ºC and treated with 10 µM CPT for 1h at 37ºC. Cells were then harvested for cell fractionation.

For GFP Co-IP assay, HEK293 cells were plated in 15 cm^3 plates until. 80% confluent. The cells were transiently transfected with 15 µg of either Empty-GFP, GFP-Q23 or GFP-Q74 plasmids. PEI was used as a transfection reagent at a ratio of 2:1 (PEI:DNA) and the complexes

were prepared in Opti-MEM™. After 48h, the cells were treated with 10 μM CPT for 1h at 37ºC and harvested for cell fractionation.

2.1.9.3.Patient fibroblasts

For all immunofluorescence assays, human primary fibroblasts were seeded in 24-well plates at a cell density of $3x10^4$ cells/well and incubated overnight at 37ºC. For 53BP1 immunofluorescence analysis, the cells were treated with 0.5 μM CPT or DMSO for 1 h before immunostaining with anti-53BP1 antibody. To analyse γH2AX kinetics, primary human fibroblasts were treated with 2 μM CPT for 1 h, followed by CPT removal and incubation at 37ºC with CPT-free media for 1 h, 2 h, 4 h and 24 h. For TOP1cc immunofluorescence, primary fibroblasts were treated with 10 μM CPT for 10 min.

For western blotting, primary fibroblasts were seeded in $10cm^3$ plates at a cell density of $5x10^5$ cells/plate and incubated at 37ºC until 80-90% confluent. The cells were then harvested and subjected to whole-cell extraction or cell fractionation (see below).

For cleaved caspase-3 analysis, fibroblasts were seeded in were seeded in 6-well plates at a cell density of $2.5x10^5$ cells/well and incubated overnight at 37ºC Next the cells were treated with 10 μM CPT or DMSO for 72 h prior harvesting for whole-cell lysis.

For sip62 knockdown, primary fibroblasts were seeded in 6-well plates, on coverslips, at a cell density of $2.5x10^5$ cells/well. Next day, the cells were transfected with 15 nM of p62 or control siRNA particles using Lipofectamine RNAiMAX at a ratio of 1:3 (siRNA:RNAiMAX; v/v). The cells were then incubated for 48 h at 37ºC, followed by treatment with 0.5 μM CPT for 1 h before immunostaining with anti-53BP1 antibody.

For viability assay, fibroblasts were seeded at a density of 5000 cells/well on a 96-well plate (black with clear bottom) and incubated at 37ºC overnight. Next day the cells were treated with increasing concentrations of CPT (0-10 μM) and left for 96 h at 37ºC (final volume in the wells: 100 μL).

2.1.9.4.GABAergic neuron treatments

For 53BP1 immunofluorescence analysis, the cells were treated with 0.5 μM CPT or DMSO for 1 h. For γH2AX, neurons were treated with 2 μM CPT for 1 h, followed by CPT removal and incubation at 37ºC with CPT-free media for 1 h, 2 h, 4 h and 24 h. For cleaved caspase-3 analysis, neurons were treated with 10 μM CPT or DMSO for 72 h.

2.1.10. CellTiter® Blue viability assay

20 µL of CellTiter® blue reagent were added to each well and incubated overnight at 37ºC. The fluorescence was recorded at 540/590nm using a microplate reader (FLUOstar Omega, BMG Labtech).

2.2. DNA plasmids

2.2.1. Materials and reagents

Table 2.2.1 - List of reagents, materials and equipment used

Details about reagents, supplier, materials and equipment are provided.

Reagents	**Supplier**
QIAprep® Spin Mini-prep kit	Qiagen, Cat.: 101674Z
QIAGEN® Plasmid Plus Midi-prep kit	Qiagen, Cat.: 12243
LB broth	Sigma-Aldrich, Cat: L3022
LB agar	Sigma-Aldrich, Cat: L2897
Ampicillin	Sigma-Aldrich, Cat.: 10835242001
Kanamycin	Sigma-Aldrich, Cat.: 10106801001
Glycerol	Sigma-Aldrich, Cat.: G5516
Materials	**Equipment**
Pipettes (P2; P20; P200; P1000)	Bunsen burner
Tips	Microwave
Stripettes (5 mL; 10 mL)	Mettler AE 163 Scales
Glass bottles (500 mL)	Incubator
Erlenmeyer flask (250 mL; 500 mL)	Thermo Scientific Heraeus Pico 17 Microcentrifuge
10 cm^3 dishes	Sanyo Falcon 6/300 Refrigerated Centrifuge
Cryovials	New Brunswick Scientific U57085-85ºC Ultra Low Freezer
	Thermo Scientific ND-1000 Nanodrop Spectrophotometer

2.2.2. Preparation of solutions

LB broth

8 g of LB broth were dissolved in 400 mL dH_2O. The solution was autoclaved at 121ºC for 20 min and kept at RT.

LB-agar

14 g of LB agar were dissolved in 400 mL dH_2O. The solution was autoclaved at 121ºC for 20 min and kept at RT.

Ampicillin (1 mg/mL stock solution)

10 mg of ampicillin powder were dissolved in 10 mL dH_2O.The solution was aliquoted and stored at -20ºC.

Kanamycin (0.5 mg/mL stock solution)

5 mg of kanamycin powder were dissolved in 10 mL dH_2O.The solution was aliquoted and stored at -20ºC.

Ampicillin agar plates

First the agar was melted in the microwave. The solution was left to cool down for about 20 min at RT. Next, near a Bunsen burner, ampicillin stock solution was added to a final concentration of 100 µg/mL. The agar+ampicillin was then poured into $10cm^3$ dishes and left to solidify at RT. The plates were stored at 4ºC.

Kanamycin agar plates

As before, the agar was melted in the microwave. The solution was left to cool down for about 20 min at RT. Near a Bunsen burner, kanamycin stock solution was added to a final concentration of 50 µg/mL. The agar+kanamycin was poured into $10cm^3$ dishes and left to solidify at RT. The plates were stored at 4ºC.

80% (v/v) Glycerol

80 mL of 100% glycerol was mixed with 20 mL dH_2O. Autoclaved and stored at RT.

2.2.3. Handling bacterial stabs

After receiving, the bacterial stabs were streaked using a plastic loop into an agar plate containing the appropriate antibiotic (pEGFP plasmids: kanamycin; pCDNA3.1 plasmid:

ampicillin). The plates were incubated overnight at 37ºC. The next day single colonies were picked and inoculated in LB containing the appropriate antibiotic and grown at 37ºC with shaking (200 rpm) overnight. Next day glycerol stocks were created for long-term storage.

2.2.4. Glycerol stocks

750 µL of liquid bacterial culture was mixed with 250 µL of 80% glycerol. Kept at -80ºC.

2.2.5. DNA plasmid purification

2.2.5.1.Miniprep

Using a pipette tip, a portion of the glycerol stock was inoculated into 5 mL LB broth containing the appropriate antibiotic and grown overnight at 37ºC with shaking (200 rpm). Next day the culture was centrifuged at 8000 rpm at RT for 3 min and the DNA plasmid was isolated by carrying out, step-by-step, the quick-start protocol provided in the QIAprep® Spin Mini-prep kit. Plasmid DNA was eluted in 30 µL elution buffer and quantified using a nanodrop spectrophotometer, by following the instructions on the screen.

2.5.2.2.Midiprep

Using a pipette tip, a portion of the glycerol stock was inoculated into 50 mL LB broth containing the appropriate antibiotic and grown overnight at 37ºC with shaking (200 rpm). Next day the culture was centrifuged at 6000 g at 4ºC for 15 min and the DNA plasmid was isolated by carrying out, step-by-step, the Quick-Start Protocol provided in the QIAGEN® Plasmid Plus Midi-prep kit. Plasmid DNA was eluted in 200 µL elution buffer and quantified using a nanodrop spectrophotometer, by following the instructions on the screen.

2.6. Immunofluorescence assay

2.6.1. Materials and reagents

Table 2.6.1 - Reagents and materials used during immunofluorescence assay
Details about reagents, supplier, materials and equipment are provided.

Reagents	**Supplier**
Formalin solution, neutral buffered, 10%	Sigma-Aldrich, Cat.: HT501128
Triton-X-100	Sigma-Aldrich, Cat.: X100
PBS	
Bovine serum albumin (BSA)	Sigma-Aldrich, Cat.: A3803
NaCl	Fisher, Cat.: S/3160/60
Tris-Base	Fisher, Cat.: 10376743
Sodium dodecyl sulfate (SDS)	Sigma-Aldrich, Cat.: L5750
Skimmed milk powder	
Donkey serum (DS)	Sigma-Aldrich, Cat.: D9663
4,6-diamidino-2-phenylindole (DAPI)	Sigma-Aldrich, Cat.: D9542
VECTASHIELD® with DAPI	VECTOR Laboratories, Cat.: H-1200
Goat serum	SLS, Cat.: G9023
Materials	**Equipment**
Pipettes (P2; P20; P200; P1000)	Leica FW4000 Fluorescent Microscope
Tips	Nikon confocal microscope system A1
Stripettes (5 mL; 10 mL)	Opera Phenix™ High Content Screening System
Microcentrifuge tubes (1.5 mL; 2 mL)	
Forceps	
Glass slides	
Coverslips	

2.6.2. Preparation of solutions

2% BSA

0.4 g of BSA powder was dissolved in 20 mL of PBS. The solution was filter-sterilised. Always made fresh.

Wash buffer (TOP1cc IF protocol)

0.1% (w/v) BSA; 0.1% (v/v) Triton X-100 in PBS. Always made fresh.

TSM buffer (TOP1cc IF protocol)

10% (w/v) skimmed milk; 150mM NaCl; 10mM Tris-HCl pH 7.4, in dH_2O. Always made fresh.

2.6.3. Protocol for immunofluorescence

Following the appropriate treatment, cells were washed twice with cold PBS. The cells were fixed in 10% formalin for 10 min at RT. The cells were washed twice with PBS and permeabilized for 5 min with 0.5% (v/v) Triton X-100 in PBS followed by two washes with PBS. Prior to incubation with primary antibody, the cells were blocked with 2% BSA for 30 min at RT. Next, the cells were incubated with primary antibody in 2% BSA for 1h at RT. Cells were washed three times with PBS (5 min each) and incubated with Alexa Fluor® 488 or 594 goat anti-rabbit IgG secondary antibody (Life Technologies, 1:500 in 2% BSA) for 1 h at RT. Finally, cells were washed three times with PBS for 5 min each and mounted in glass slides using VECTASHIELD® with DAPI (Hard-set). The slides were stored at 4ºC.

For TOP1cc immunofluorescence, the cells were washed twice with PBS and fixed in 10% formalin for 15 min at 4ºC. After fixation, the cells were washed three times and permeabilized in 0.2% (v/v) Triton X-100 diluted in PBS for 2 min on ice, followed by incubation with 0.1% SDS in PBS for 5 min at RT. Blocking was carried out by incubating cells with TSM buffer for 1h. Next the cells were incubated with primary antibody (diluted in 5% goat serum) overnight at 4ºC. Next day, the cells were washed 5 times with wash buffer for 4 min each wash and incubated with Alexa Fluor® 488 or 594 secondary antibody (Life Technologies, 1:1000 in 5% goat serum) for 1h at RT. Finally, cells were washed five times with wash buffer and mounted in glass slides as mentioned before.

For the striatal GABAergic neurons, immunofluorescence assays were performed in 96-well plates. The cells were washed with PBS and fixed with 4% PFA for 10 min at RT. After

fixation, samples were washed three times with PBS (5 min each wash) and permeabilized with 0.3% Triton X-100 diluted in PBS for 5 min. The cells were subsequently blocked in 5% DS for 1 h. After blocking, cell cultures were incubated with the appropriate primary antibodies diluted in PBS containing 1% of DS overnight. Cells were then washed with PBS three times. Fluorescent secondary antibodies (Alexa Fluor 488, 555, 594 or 647, diluted 1:400 with DS) were subsequently added to the cells and incubated for 1h. The samples were washed with PBS three more times and incubated with DAPI (1.0 mg/mL) for nuclear staining. All experiments included cultures where the primary antibodies were not added. In these negative controls, non-specific staining was not observed.

The details for the primary antibodies used in this study are provided in Table 2.6.2.

2.6.4. Image acquisition and analysis

Immunofluorescence images from MRC5 and primary fibroblasts were obtained on a Leica FW4000 Fluorescent Microscope (Leica Microsystems) using the 63x lens or Nikon confocal microscope system A1 (Nikon Instruments, Tokyo, Japan), using the 60x lens. 53BP1 and γH2AX foci quantification in MRC5 and primary fibroblasts was done manually. For 53BP1 analysis, cells were considered positive if containing > 5 foci. For γH2AX, cells with > 10 foci were considered positive. TOP1cc foci quantification was conducted using ImageJ software.

Images from GABAergic neurons were acquired by Cleide Souza using Opera Phenix™ High Content Screening System at 40x magnification. The Harmony™ Image analysis software was used to analyse the images.

2.6.5. Statistical analysis

All graphs and statistical analysis were generated using GraphPad Prim (GraphPad Software Inc.). Shapiro-Wilk test was used to verify if data followed a normal distribution. A Gaussian distribution was considered when $P \geq 0.05$, whereby parametric tests were used to test for statistical significance.

All data is presented as means ± standard errors of the mean (s.e.m.). Student's *t*-test was used to compare the means between two groups. Alternatively, the nonparametric test Mann-Whitney was used. One-way ANOVA was used to compare three or more groups, followed by Tukey's *post-hoc* test for multiple comparisons. The nonparametric Kruskal-Whallis test was used in alternative to compare three or more groups, followed by the *post-hoc* Dunn test for multiple comparisons. Area under the curve (A.U.C.) was calculated using the Prism 9

integrated formula, considering baseline as Y=0 (GraphPad Statistics Guide/AUC). Statistical significance was considered when $P < 0.05$. Asterisks denote statistical significance, whereby * = $P < 0.05$; ** = $P < 0.01$; *** = $P < 0.001$; and **** = $P < 0.0001$. ns states for nonsignificant ($P \geq 0.05$). The actual *P*-values are stated in each figure legend.

Table 2.6.2 – List of primary antibodies used in this project

Details about host species, supplier, working concentration and application are provided. IF, immunofluorescence; WB, western blot; Co-IP, co-immunoprecipitation

Antibody	Host Species	Supplier (Cat.:)	Concentration	Application
53BP1	Rabbit	Bethyl (A300-272A)	1:1000	IF
TOP1cc	Mouse	Millipore (MABE1084)	1:1000	IF
γH2AX	Mouse	Merk (JBW301)	1:1000	IF
p62/SQSTM1	Rabbit	Merk (P0067)	1:1000	IF/WB
Beta III Tubulin (TUJ1)	Chicken	Merk (AB9354)	1:1000	IF
MAP2	Guinea pig	Synaptic Systems (188004)	1:1000	IF
Caspase 3, active (cleaved) form	Rabbit	Merk (AB3623)	1:200	IF
GABA	Rabbit	Sigma-Aldrich (A2052)	1:1000	IF
DARPP32	Rabbit	Abcam (ab40801)	1:100	IF
H2A	Rabbit	Abcam (ab18255)	1:1000	WB
RNF168	Mouse	Santa-Cruz Biotechnology (sc-101125)	1:1000	WB/Co-IP
Flag	Mouse	Sigma-Aldrich (F1804)	1:1000	WB/Co-IP
Fk2	Mouse	Enzo Life Sciences (BML-PW8810-0100)	1:1000	WB
Cleaved caspase-3 (Asp175, clone 5A1E)	Rabbit	Cell Signaling Technology (9664)	1:1000	WB
GFP	Rabbit	Abcam (ab290)	1:2500	WB
ATM (phospho S1981)	Rabbit	Abcam (ab81292)	1:1000	WB
β actin	Mouse	Abcam (ab8224)	1:1000	WB

2.7. Cell lysis

2.7.1. Materials and reagents

Table 2.7.1 - List of reagents, materials and equipment used to lyse cells
Details about reagents, supplier, materials and equipment are provided.

Reagents	**Supplier**
SDS	Sigma-Aldrich, Cat.: L5750
BaseMuncher	Expedeon, Cat.: BM0025
Hepes	Fisher, Cat.: 17257
KCl,	Sigma-Aldrich, Cat.: BPE366-500
$MgCl_2$,	Fisher, Cat.: AA12315A1
Glycerol	Sigma-Aldrich, Cat.: G5516
Triton-X-100	Sigma-Aldrich, Cat.: X100
EDTA	Fisher, Cat.: 10618973
NaCl	Fisher, Cat.: S/3160/60
IGEPAL® CA-630 (NP-40)	Sigma-Aldrich, Cat.: I8896
Iodoacetamide	Sigma-Aldrich, Cat.: I6125
cOMPLETE™, Mini, EDTA-free Protease inhibitor cocktail	Sigma-Aldrich, Cat.: 4693159001
Materials	**Equipment**
Pipettes (P2; P20; P200; P1000)	ThermoMixer® C Eppendorf
Tips	Vortex
Stripettes (5 mL; 10 mL)	Cooling Microcentrifuge
Centriguge tubes (1.5 mL; 2 mL)	
Scraper	

2.7.2. Preparation of solutions

50x Protease inhibitor cocktail

1 tablet of cOMPLETE^{TM}, Mini, EDTA-free Protease inhibitor cocktail was dissolved in 1 mL dH_2O

1% NP-40 lysis buffer

50mM Tris-HCL pH 8, 150mM NaCl and 1% (v/v) NP-40 in dH_2O. 1x protease inhibitors and 1 mM DTT were added prior to use.

Hypotonic buffer

20mM Hepes pH 8.0, 10mM KCl, 1mM $MgCl_2$, 20% (v/v) glycerol and 0.1% Triton-X-100 in dH_2O. Supplemented with 1x protease inhibitor prior to use.

Hypertonic buffer

20mM Hepes pH 8.0, 1mM EDTA, 20% (v/v) glycerol, 400mM NaCl and 0.1% Triton-X-100 in dH_2O. Supplemented with 1x protease inhibitor prior to use.

Insoluble buffer

20 mM Hepes pH 8.0, 150 mM NaCl, 1% (w/v) SDS, 1% (v/v) NP-40 and 10 mM iodoacetamide in dH_2O. Supplemented with 1x protease inhibitor prior to use.

2.7.3. Obtaining whole-cell and fractionated extracts

After the corresponding treatments, the cells were washed twice with ice-cold PBS and subjected to whole-cell extraction or to cell fractionation. For whole-cell lysate extraction, cells were first scraped from the wells/plates into a microcentrifuge tube previously labelled. The cells were pelleted by centrifugation (1000 rpm for 5 min at 4ºC). Supernatant was removed and the cell pellets were washed twice with ice-cold PBS and centrifuged as before. Then, the cells were lysed for 30 min on ice with 1% NP-40 lysis buffer supplemented with 1x protease inhibitor, 1 mM DTT and 250 units BaseMuncher, with periodical vortexing (every 5 min). The lysates were centrifuged at 13200 rpm for 20 min and the supernatant was collected into a new microcentrifuge tube. The lysates were stored at -20ºC,

To fractionate the cells, they were first incubated with hypotonic buffer for 10 min on ice. The cells were scraped into microcentrifuge tubes and centrifuged at 6400 rpm for 4 min. The supernatant corresponds to the cytoplasmic fraction and was collected into a separate

microcentrifuge tube if needed. Subsequently, to separate the soluble nuclear fractions, the remaining cell pellets were resuspended in hypertonic buffer and incubated for 20 min on ice with periodical agitation (every 5 min). The cells were centrifuged at 13200 rpm for 5 min and the supernatant (soluble nuclear fraction) was collected into a new microcentrifuge tube. To collect the chromatin-bound fractions, the pellets were incubated with insoluble buffer for 50 min at 4ºC in the thermomixer (1000 rpm). The lysates were further incubated with 0.5 µL BaseMuncher at 25ºC for 15 min in the thermomixer (1000 rpm) and centrifuged at 13200 rpm for 5 min. The supernatant (insoluble nuclear fraction) was collected into a new microcentrifuge tube.

For Flag IP experiments, all buffers used for cell fractionation were further supplemented with 20 µM N-Ethylmaleimide (NEM) to prevent ubiquitin degradation.

2.8. SDS-PAGE and western blotting

2.8.1. Materials and reagents needed

Table 2.8.1 – List of reagents, materials and equipment used for SDS-PAGE and western blotting.
Details about reagents, supplier, materials and equipment are provided.

Reagents	**Supplier**
Coomassie Plus (Bradford) Assay Reagent	ThermoFisher Scientific, Cat.: 23238
SDS	Sigma-Aldrich, Cat.: L5750
2-Mercaptoethanol	Fisher, Cat.: 125472500
Bromophenol blue	Sigma-Aldrich, Cat.: B5525
Glycine	Fisher, Cat.: 101401
NaCl	Fisher, Cat.: S/3160/60
Tris Base	Fisher, Cat.: 10376743
Tween-20	Sigma-Aldrich.: P7949
Trans-Blot® Turbo™ 5x transfer buffer	BioRad, Cat.: 10026938
Clarity Western ECL substrate	BioRad, Cat.: 705061
Skimmed milk powder	
Goat Anti-Mouse IgG (H + L)-HRP Conjugate	BioRad, Cat.: 170-6516
Goat Anti-Rabbit IgG (H + L)-HRP Conjugate	BioRad, Cat.: 170-6515
Materials	**Supplier**
Pipettes (P2; P20; P200; P1000)	
Tips	
Stripettes (5 mL; 10 mL)	
4-15% precast gel	BioRad, Cat.: 4561093
Trans-Blot® Turbo™ Nitrocellulose membranes	BioRad, Cat.: 1704271
Trans-Blot® Turbo™ Transfer stacks	BioRad, Cat.: 1704271
Cuvettes	
Equipment	
BioRad ChemiDoc™ MP Imaging System	
BioRad Trans-Blot® Turbo™ Transfer System	
BioRad PowerPac™ HC	
BioRad Gel Electrophoresis Tanks	
Jenway Genova Spectrophotometer	
Stuart Block Heater SBH130	

2.8.2. Preparation of solutions

5x SDS loading buffer

2 g of SDS was mixed with 5 mL of 1M Tris pH6.8 in 4 mL of dH_2O until SDS was dissolved. Then 1 mL of 2-Mercaptoethanol, 10 mL of 100% glycerol and 5 mg of bromophenol blue were added under a fume hood and mixed thoroughly. Stored at RT.

10x TBS

24 g of Tris base and 88 g of NaCl were dissolved in 900 mL dH_2O. pH was adjusted to 6.8 using HCl. dH_2O was added to a final volume of 1000 mL with dH_2O. Kept at RT.

1x TBS/Tween-20 (TBST)

100 mL of 10x TBS were diluted in 900 mL dH_2O. 1 mL of Tween-20 was added. Kept at RT.

10x Running buffer

144 g of glycine, 30.3 g of Tris base and 10 g of SDS were dissolved in 1000 mL dH_2O.

5% milk

1 g of skimmed milk powder was dissolved in 20 mL of TBST. Made fresh for each use.

2.8.3. Bradford assay

The protein concentration from whole-cell lysates and chromatin-bound fractions were quantified by Bradford assay by adding 1 µL of cell lysate to 999 µL Coomassie blue reagent. The absorbance for each lysate was measured in a spectrophotometer at 595 nm. The values obtained were standardised against BSA.

2.8.4. Sodium dodecyl sulphate polyacrylamide gel electrophoresis (SDS-PAGE) and Western blotting

20 µg of lysates were mixed with 5x SDS loading buffer, boiled at 95ºC for 5 min and run in 4-15% precast gel for 40 min-1 h at 180 V. The gel was semi-dry transferred onto a nitrocellulose membrane for 15 min at 1.3 A and 25 V. The membrane was then blocked in 5% milk for 30 min and incubated overnight at 4ºC with primary antibodies diluted in 5% milk. The primary antibodies used for western blotting and corresponding dilutions are displayed in Table 2.6.2. Next day the membranes were washed thrice with 1x TBST for 5 min each and incubated with goat anti-rabbit or anti-mouse IgG (H+L) HRP conjugated antibodies (1:4000

in 5% milk) for 1h. After 3 washes with 1x TBST (5 min each), the membranes were incubated with an enhanced ChemiLuminescence (ECL) substrate and revealed by exposure at a ChemiDoc™ imaging system. The images obtained were processed using Image Lab 4.1 software.

2.9. Co-immunoprecipitation (Co-IP)

2.9.1. Materials and reagents used

Table 2.9.1 – List of reagents, materials and equipment used for Co-IP assay
Details about reagents, supplier, materials and equipment are provided.

Reagents	**Supplier**
Dynabeads™ protein G	Invitrogen, Cat.: 10765583
BS_3 crosslinking agent	Thermofisher, Cat.: 21580
GFP-Trap beads (Chromotek)	Chromotek, Cat.: gtma
PBS	
NaCl	Fisher, Cat.: S/3160/60
Tris Base	Fisher, Cat.: 10376743
Tween-20	Sigma-Aldrich.: P7949
IGEPAL® CA-630 (NP-40)	Sigma-Aldrich, Cat.: I8896
Citric acid	Sigma-Aldrich, Cat.: C0759
EDTA	Fisher, Cat.: 10618973
5x SDS loading buffer	
Materials	**Equipment**
Pipettes (P2; P20; P200; P1000)	DynaMag™ magnet (ThermoFisher, 12320D
Tips	Mettler AE 163 Scales
Stripettes (5 mL; 10 mL)	Rotator
15 mL/50mL tubes	
Microcentrifuge tubes (1.5 mL; 2mL)	
Eppendorf® Protein LoBind tubes	
Cuvette	

2.9.2. Preparation of solutions

Conjugation buffer

20 mM Sodium Phosphate and 150mM NaCl in dH_2O. Made freshly prior to use.

100 mM BS_3 (stock solution)

Since the powder is moisture sensitive, it was first allowed to reach to RT before opening the bottle. Then 5.72 mg powder were dissolved in 100 µL of conjugation buffer. Made freshly prior to use.

5 mM BS_3 (working solution)

50 µL of 100 mM BS_3 were diluted in 950 µL of conjugation buffer. Always made fresh.

1 M Tris pH 7.5

131.14g Tris base were dissolved in 900ml dH_2O. pH was adjuster to 7.5 and dH_2O was added to a final volume of 1000 mL

2M Tris pH 8

131.14g Tris base were dissolved in 400ml dH_2O. pH was adjuster to 8 and dH_2O was added to a final volume of 500 mL

PBS/ 0.01% (v/v) Tween-20 (PBST)

500 µL of 1% (v/v) Tween-20 were diluted in 49.5 mL of PBS. Kept at RT

0.2% NP-40 lysis buffer

50mM Tris-HCL pH 8, 150mM NaCl and 0.2% (v/v) NP-40 in dH_2O.

Dilution buffer

50mM Tris pH 8 and 150mM NaCl in dH_2O. Kept at RT.

0.1M citric acid

192.12 mg of citric acid were dissolved in 10 mL of dH_2O. pH adjusted to 2.6. Kept at RT.

GFP-dilution buffer

10mM Tris pH 7.5; 150mM NaCl and 0.5mM EDTA in dH_2O. Kept at RT.

2.9.3. RNF168 Co-IP and Flag-IP

An overview of the RNF168 Co-IP and Flag-IP protocol is represented in Figure 2.9.1. In both cases a direct capture method was used, in which the bait antibody (or IgG control) was immobilised onto magnetic beads. Prior to incubation with the cell lysates, the antibody-conjugated beads were crosslinked by using BS_3 as a crosslinking agent. The reason why the antibody-conjugated beads were crosslinked was to avoid denaturation of the heavy and light IgG chains, which would later interfere with the Western blotting analysis. For the same reason, I avoided using SDS-containing buffer and boiling the beads to elute the samples. Instead, elution of the immunoprecipitated proteins and complexes was performed by using a low-pH buffer (0.1 M citric acid pH 2.6).

2.9.3.1.Preparation of beads for RNF168 Co-IP and Flag-IP

Magnetic Dynabeads^{TM} protein G were first washed with 200 µL PBST twice in 1.5 mL LoBind tubed (30 µL beads/condition). The beads were separated from the supernatant using a magnetic stand and the beads were incubated with the corresponding antibodies, as follows: For RNF168 Co-IP, the beads were incubated for 1h at RT with 2 µg RNF168 or mouse IgG antibody in 200 µL PBST in a rotator, with tilting. For Flag-IP, the beads were incubated for 1h at RT with 5 µg Flag or mouse IgG antibody in 200 µL PBST in a rotator, with tilting.

2.9.3.2.Crosslink antibody-conjugated beads

After incubating the beads with the corresponding antibodies, the antibody-coupled beads were washed twice with 200 µL conjugation buffer and incubated with 5 mM BS_3 crosslinking reagent (250 µL/ tube) for 30 min at RT, in the rotator (with tilting). The reaction was then quenched with 12.5 µL of 1 M Tris-HCl pH 7.5 for 15 min at RT in the rotator (with tilting).

2.9.3.3.RNF168 Co-IP

After crosslinking the antibody-coupled beads, the beads were then washed three times with PBST and equilibrated in 4 volumes/lysate of 1% NP-40 lysis buffer. 150-200µg of nuclear extracts (combined soluble and insoluble nuclear fractions) were incubated with the crosslinked beads for 2 h at 4ºC with rotation. The beads were then washed by vortexing, once in 1% NP-40 lysis buffer, followed by three washes in 0.2% NP-40 lysis buffer. Each time, the beads and supernatant were separated using a magnetic stand. Prior to elution, the beads were mildly centrifuged (300 rpm for 5 seconds) to remove the excess buffer. The beads were eluted twice in 20µL 0.1M citric acid pH 2.6 for 2 min each, at RT with rotation/ tilting. The eluates were

collected in the magnetic stand into a new microcentrifuge tube, previously containing 5µL of 2 M Tris pH 8 to neutralise the eluate. The eluates were analysed by Western blotting after probing for anti-RNF168 and anti-p62 antibodies (Table 2.6.2).

2.9.3.4.Flag-IP

After crosslinking the antibody-coupled beads, the beads were then washed three times with PBST and equilibrated in 2 volumes/ diluted lysate of 1% NP-40 lysis buffer. 100 µg of chromatin extracts were diluted 10 times in dilution buffer and incubated with the crosslinked beads for 1.5 h at 4ºC. The beads were then washed by vortexing, twice in 1% NP-40 lysis buffer followed by two more washes in 0.2% NP-40 lysis buffer. Washing buffer and beads were separated with a magnetic stand after each wash and the supernatant was discarded. Prior to elution, the beads were mildly centrifuged (300 rpm for 5 seconds) to remove the excess buffer. The beads were eluted twice in 20 µL 0.1 M citric acid pH 2.6 for 5 min each, at RT with rotation/ tilting. The eluates were collected in a magnetic stand into a new microcentrifuge tube and neutralized in 5µL of 2 M Tris pH 8. The eluates were analysed by Western blotting after probing for anti-Flag and anti-Fk2 antibodies (Table 2.6.2).

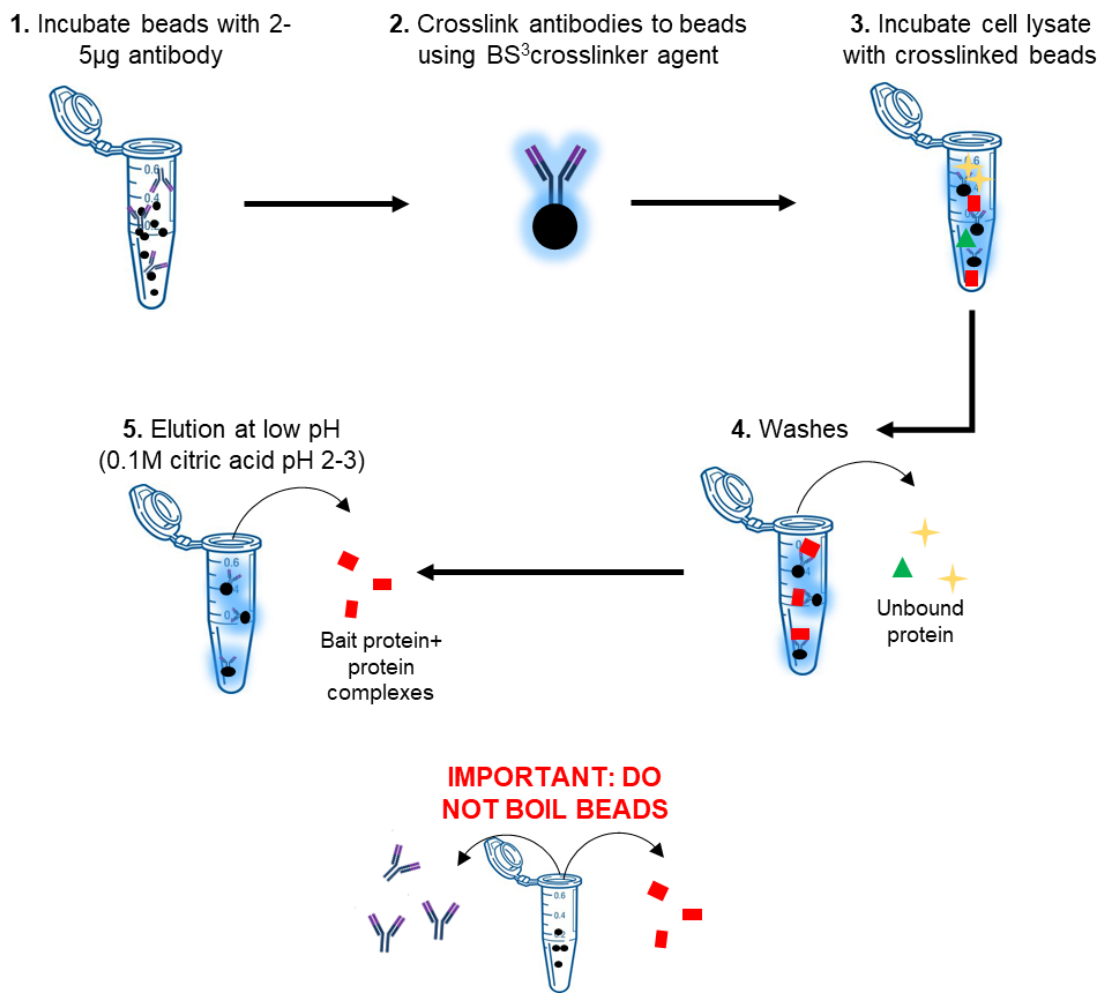

Figure 2.9.1 – Summary of RNF 168 Co-IP and Flag-IP protocol

Schematic representation showing an overview of the RNF168 Co-IP and Flag-IP protocols. **1.** The magnetic beads are first incubated with the bait antibodies/ IgG control (RNF168: 2 µg; Flag: 5 µg). **2.** The antibody-conjugated beads are crosslinked using bis(sulfosuccinimidyl)suberate (BS_3) crosslinking agent. **3.** The crosslinked antibody-conjugated beads are then incubated with the cell lysates to immunoprecipitate the antibody-target proteins and complexes onto the beads. **4.** To remove the unbound proteins, the beads are washed several times. **5.** Finally, the target proteins are eluted from the beads using a low pH buffer (0.1 M citric acid pH 2-3). To avoid antibody heavy and light chains denaturation it is important to avoid boiling the beads and to not use SDS-containing buffers.

2.9.4. GFP Co-IP

Magnetic GFP-Trap beads were first washed twice in dilution buffer. The buffer and beads were separated using a magnetic stand and the supernatant discarded. The nuclear lysates were added to the beads previously resuspended in 4 volumes of NP-40 lysis buffer. The cytoplasmic lysates were directly added to the beads. In both cases, the lysates were incubated with the beads for 2 h at 4ºC in a rotator. Next, the beads were washed three times with 1% NP-40 lysis buffer. Elution of the protein complexes was achieved by boiling the beads at 95ºC for 5 min, with vortexing every minute, in 30 µL of 1x SDS loading buffer. The eluates were analysed by Western blotting after probing for anti- ATM (phospho S1981) and anti-GFP antibodies (Table 2.3.3.1).

Chapter 3: Mutant huntingtin impairs the repair of topoisomerase I-linked DNA breaks

3.1. Introduction

Transient TOP1cc occur naturally in the brain (Berger *et al.*, 2017). However, TOP1 can become trapped in the DNA causing TOP1-linked DNA breaks, which can be deleterious to neuronal cell survival, especially if turned into DSBs (Pommier, 2006; Sordet *et al.*, 2009; Meisenberg *et al.*, 2015). Indeed, TOP1cc can be turned into lethal transcription-dependent DSBs (Cristini *et al.*, 2016, 2019). These can occur due to endogenous processes, including the presence of another TOP1cc or an R-loop in the opposite strand, the existence of another ROS-generated SSB in proximity, or by collision with transcription machinery (Sordet *et al.*, 2010; Berger *et al.*, 2017; Cristini *et al.*, 2019). Treatment with CPT can also induce DSB by promoting the accumulation of TOP1cc (Pommier, 2006). TOP1cc-induced DSBs favour the activation of the master kinase ATM, which mediates the DDR signalling through phosphorylation of γH2AX to amplify the signal and recruit DNA repair proteins (Sordet *et al.*, 2009; Katyal *et al.*, 2014).

Accumulation of TOP1cc is a feature of several neurodegenerative disorders, such as A-T, ALS and SCAN1, due to ATM or TDP1 deficiencies, respectively (El-Khamisy *et al.*, 2005; Katyal *et al.*, 2014; Walker *et al.*, 2017). In these disorders, the increased TOP1cc formation and consequent excessive DSBs impact genome stability and promote neuronal death, thus showing the importance of proper DNA repair mechanisms in preventing neurodegeneration. (El-Khamisy *et al.*, 2005; Alagoz *et al.*, 2013; Katyal *et al.*, 2014; Walker *et al.*, 2017; Prasad Tharanga Jayasooriya *et al.*, 2018).

Although TOP1-linked DNA breaks are known to drive neurodegeneration, it is unclear whether HD cells can effectively signal and repair this type of damage.

The implication of DNA damage and repair in the pathogenesis of HD has long been studied. Several GWAS revealed genes involved in DNA repair as genetic modifiers of both the age of onset and severity (GeM-HD, 2015, 2019). In addition, several studies reported accumulation of DNA damage since the prodromal stages until more advanced phases of HD (Castaldo *et al.*, 2019; Maiuri *et al.*, 2019). Moreover, the fact that HTT is itself involved in DDR, by acting as a scaffold protein during oxidative damage together with ATM and during TCR with PNKP

and ataxin-3, provides extra clues that DNA damage is involved in HD (Maiuri *et al.*, 2017; Gao *et al.*, 2019).

Defective DSB repair signalling and repair has also been reported in HD. Impaired γH2AX, 53BP1 and ATM signalling were described different HD models, including primary human fibroblasts (Ferlazzo *et al.*, 2014), cells ectopically expressing HTT polyQ expansions (Yehuda *et al.*, 2017) and in HD mice models (Jeon *et al.*, 2012). However, it has not been explored whether these mechanisms are also impaired in striatal neurons derived from HD patients after induction of TOP1 DNA damage.

3.2. Hypothesis and Aims

In line with the abovementioned studies, I hypothesise that HD cells exhibit insufficient DDR signalling, leading to accumulation of unrepaired DNA breaks and consequent cell death in response to TOP1-induced DNA damage.

To test this hypothesis, the aim of this chapter is to investigate the repair of TOP1-linked DNA breaks in HD models. The specific objectives are:

- To examine NHEJ repair by analysing 53BP1 foci formation in HD cell models after TOP1-induced breaks, by immunofluorescence assay.
- To assess pATM levels at the chromatin in patient-derived HD skin fibroblasts.
- To study the interaction between HTT and pATM by co-immunoprecipitation assays.
- To examine the levels of TOP1cc in HD primary fibroblasts after CPT treatment.
- To monitor the repair kinetics of DSBs, by analysing the clearance of the DSB marker γH2AX after recovery from CPT treatment.
- To assess sensitivity to CPT of HD cells.

3.3. Results

3.3.1. Mutant huntingtin disrupts deficient 53BP1 recruitment in response to topoisomerase-induced DNA damage

In neurons, TOP1-induced transcription-dependent DSBs are mainly repaired via NHEJ repair pathway. In addition, neurons can only rely on NHEJ for DSB repair, indicating the importance of NHEJ for neuronal survival (Sordet *et al.*, 2009; Cristini *et al.*, 2020). Previous work have shown that mtHTT prevented the formation of DNA-PK complex, resulting in defective NHEJ repair in response to ionizing radiation (IR) (Enokido *et al.*, 2010). However, the mechanisms by which mtHTT interferes with TOP1-linked DNA breaks is unknown. Because 53BP1 promotes the choice of NHEJ pathway, I first sought to investigate whether the recruitment of the 53BP1 in response to TOP1-linked DNA breaks is altered in HD models. Since the main goal was to study the response of HD cell models specifically to TOP1-associated DNA breaks, DNA damage was induced using a specific TOP1 poison, CPT.

It has been established that the exon 1 of the *HTT* gene with expanded CAG repeats is sufficient to mimic the phenotype seen in HD cells (Mangiarini *et al.*, 1996). To investigate 53BP1 foci formation after TOP1-mediated DNA damage, MRC5 cells transiently expressing a GFP fusion plasmid containing the exon 1 of *HTT* with either 23 CAG repeats (GFP-Q23, wtHTT) or 74 CAG repeats (GFP-Q74, mtHTT) were treated with CPT for 1h and analysed by immunofluorescence assay (Figure 3.3.1 a). During the immunostaining protocol, transfected MRC5 cells were initially fixed in methanol acetone, which resulted in weak GFP signal when the slides were imaged at the fluorescence microscope. This technical problem could have been caused by the fact that acetone and methanol can quench GFP fluorescence signal (Nybo, 2012). Therefore, the cells were fixed in 10% formalin, which helped preserving the GFP signal and solved the problem.

After I solved the technical issue, I performed immunostaining with an anti-53BP1 antibody which revealed that cells overexpressing GFP-Q23 responded to CPT treatment by significantly increasing the percentage (%) of 53BP1 positive cells (more than five 53BP1 foci) in comparison with mock (DMSO) treated cells. Whereas GFP-Q74 expressing cells showed no significant differences in the % of 53BP1 positive cells when compared with the mock treated GFP-Q74, indicating these cells failed to form 53BP1 foci after CPT treatment (Figure 3.3.1 b).

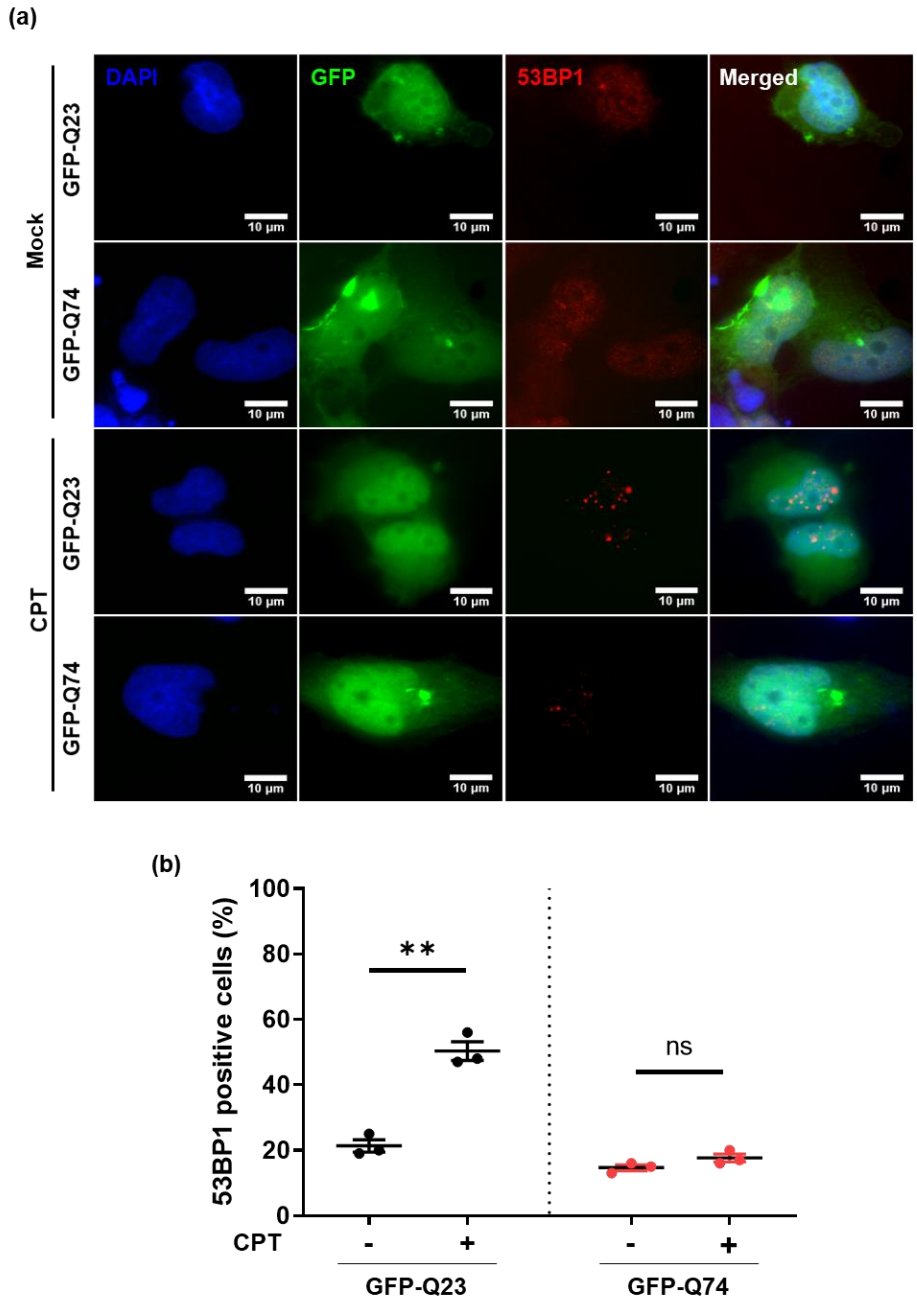

Figure 3.3.1 – Cells ectopically expressing mtHTT exhibit deficient 53BP1 recruitment in response to DNA damage.

MRC5 cells transiently transfected with HTT GFP-tagged plasmids containing either 23 CAG repeats (GFP-Q23: wtHTT) or 74 CAG repeats (GFP-Q74: mtHTT). Cells were treated with either DMSO (Mock) or 10 µM CPT for 1 hour. **(a)** Representative images of MRC5 immunostained with 53BP1 are shown (scale bar: 10µm). DAPI shows nuclei. **(b)** The percentage of transfected cells 53BP1 positive (more than 5 foci) was quantified manually and analysed using paired Student's *t*-test (n=3, 50 GFP transfected cells were counted per replicate). Error bars represent ± s.e.m. ***P* = 0.0012; ns: nonsignificant

Since patient-derived primary cells represent a more clinically relevant cell model, 53BP1 foci formation was next investigated in primary skin fibroblasts from a healthy individual (GM08402; non-HD) and from two patients with HD (GM04799 and GM04869) each harbouring 42 and 47 CAG repeats, respectively (Hu *et al.*, 2014; Marchina *et al.*, 2014).

First, to address the optimal CPT concentration for the treatment of primary fibroblasts, a CPT dose-response was performed, where the non-HD cells were treated with increasing CPT concentrations for 1h (0 µM – 10 µM), followed by staining with anti-53BP1 antibody. Analysis of the slides by immunofluorescence microscopy indicated that treatment with 0.5 µM CPT was the optimal concentration for these fibroblasts, since the number of foci per cell was in average between 5 to 10, which facilitated manual counting.

Similar to MRC5 cells ectopically expressing CAG expansions, immunofluorescence analysis of primary human fibroblasts, which endogenously harbour CAG expansions showed that both HD patient cells did not increase significantly the % of 53BP1 positive cells after treatment with CPT. On the other hand, the healthy non-HD GM08402 cells responded to CPT by significantly increasing the % of 53BP1 positive (Figure 3.3.2 a and b). Comparing the number of foci per cell, in mock treated cells, GM08422 showed an average of 1.784 ± 0.2 foci per cell, while the GM04799 HD cells displayed an average of 1.196 ± 0.155 foci per cell and the GM04869 cells, an average of 1.218 ± 0.157 foci per cell. After CPT, GM04799 and GM04869 HD cells exhibited significantly fewer of 53BP1 foci per cell (GM04799, 2.471 ± 0.25 foci per cell; GM04869, 2.279 ± 0.23 foci per cell) in comparison with GM08402 cell line (8.539 ± 0.56 foci per cell) (Figure 3.3.2 c). Together these results suggest that the CAG repeat expansions in mtHTT cause defective 53BP1 foci formation in response to TOP1-induced DNA damage.

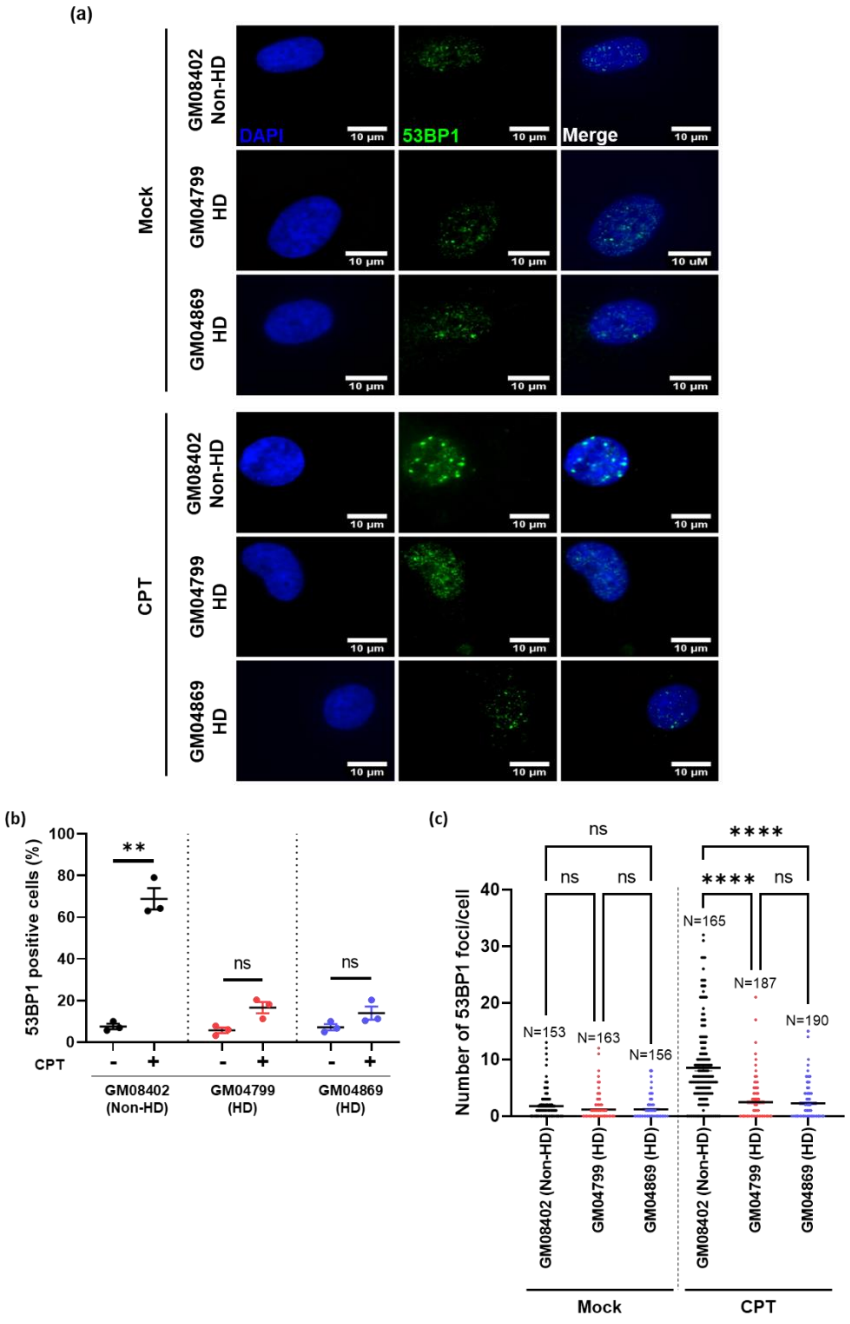

Figure 3.3.2 - HD patient-derived primary cells exhibit deficient 53BP1 recruitment in response to DNA damage.

Primary skin fibroblasts were treated with either mock (DMSO) or 0.5 µM CPT for 1 hour. GM08402 represents the healthy non-HD individual. GM04799 and GM04869 are fibroblasts retrieved from patients clinically affected with HD. All cells were purchased from Coriell Institute. **(a)** Representative image showing patient fibroblasts immunostained with 53BP1 after treatment with 0.5µM of CPT/mock for 1h (scale bar: 10 µm). DAPI shows nuclei. **(b)** The percentage average of cells 53BP1 positive (more than 5 foci) was quantified and analysed using paired Student's *t*-test. Error bars represent ± s.e.m. (n=3, 10 fields per replicate). $^{**}P = 0.0080$; ns: nonsignificant. **(c)** Scatter dot plot showing the number of 53BP1 foci per cell quantified from 3 biological experiments and analysed using Kruskal–Wallis test, followed by Dunn's multiple comparisons test (10 fields per replicate). Error bars represent ± s.e.m. N= number of cells counted; $^{****}P<0.0001$; ns: nonsignificant.

3.3.2. Chromatin levels of pATM are not altered in fibroblasts from patients with Huntington's disease

Since 53BP1 recruitment during DDR depends on the activity of ATM, I next examined the level of pATM in HD fibroblasts. ATM is mostly known for its activity in DSB repair (Shiloh and Ziv, 2013). In response to DSBs, ATM is recruited to the sites of damage by the MRN complex and becomes activated by autophosphorylation at its S1981 residue (pATM). Activated ATM then phosphorylates histone variant H2AX at S139, which acts as a signal for the recruitment of downstream DSB repair effectors, resulting in the activation of NHEJ or HR repair pathways (Podhorecka, Skladanowski and Bozko, 2010).

ATM mediates 53BP1 recruitment to the chromatin through induction of RNF8-RNF168 pathway (Mattiroli *et al.*, 2012). In addition 53BP1 itself is necessary for the tethering of pATM at the damaged chromatin, suggesting a positive feedback loop, where 53BP1 and ATM sustain each other signalling activities (Lee *et al.*, 2010; Baldock *et al.*, 2015).

To test whether the defects in 53BP1 recruitment after damage observed in HD models caused deficient retention of activated pATM at the chromatin, patient-derived skin fibroblasts were treated with 10 μM CPT for 1 h and subjected to chromatin fractionation.

Western blotting analysis of the chromatin fractions of the non-HD GM08402 fibroblasts and the GM04869 HD cells showed no significant differences in the levels of pATM. The results suggest that although 53BP1 recruitment is deficient in HD cells, pATM is still present at the chromatin (Figure 3.3.3 a and b).

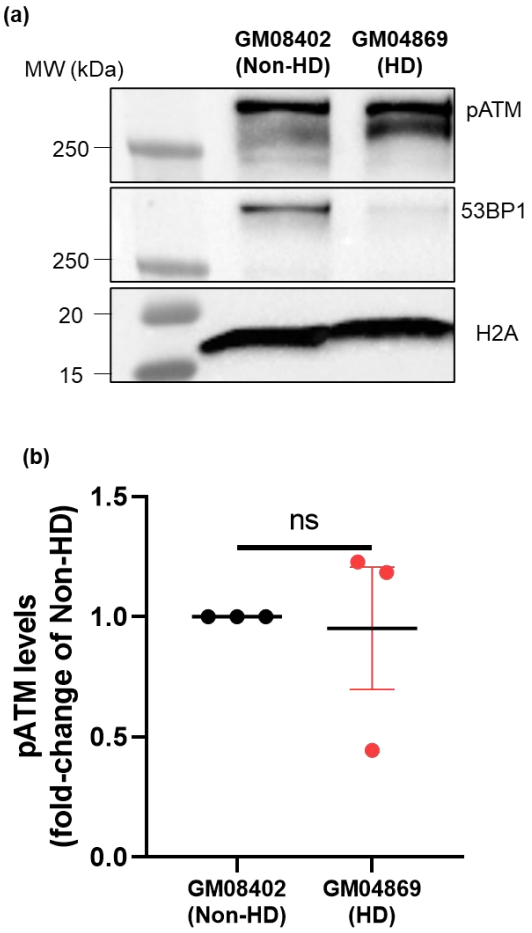

Figure 3.3.3 - Chromatin levels of pATM are unaltered in HD patient fibroblasts

(a) Chromatin-fractions of primary skin fibroblasts from a healthy non-HD individual (GM08402) and a HD patient (GM04869) were obtained after treatment with 10 μM CPT for 1 h and analysed by western blotting. The blot was incubated with an antibody specific for phosphorylated ATM at S1981 (pATM) and with an anti-53BP1 antibody. H2A signal shows equal loading.

(b) pATM signalling was quantified and normalised against H2A signal. Data is shown as average of the fold-enrichment levels of pATM, in comparison with the non-HD cells. Error bars represent ± s.e.m.; n=3. The data was analysed by unpaired Student's *t*-test. ns, nonsignificant.

3.3.3. Mutant huntingtin sequesters pATM to the cytoplasm

A previous report has demonstrated that HTT specifically binds to ATM in HD cells, while in wild-type cells this interaction does not occur (Ferlazzo *et al.*, 2014). The interaction with mtHTT potentially prevents ATM activity during DNA damage (Ferlazzo *et al.*, 2014; Ferlazzo and Foray, 2016). In fact, they showed deficits in the nuclear translocation of pATM after irradiating HD cells. Moreover, the group suggested that this interaction causes cytoplasmic retention of ATM, given that HTT is mainly present at the cytoplasm (Ferlazzo *et al.*, 2014).

In line with this study and since after CPT treatment the chromatin levels of pATM in HD patient cells did not differ from those of the healthy cells, the next aim was to study the interaction between wild-type or mtHTT and pATM. In addition, it was also of interest to analyse in which subcellular compartment this interaction occurs. For that, HEK293 cells were overexpressed with either GFP-Q23 or GFP-Q74 plasmids and treated with 10 μM CPT or mock treated for 1 h. Cells were also overexpressed with GFP-empty plasmids as a negative control. To analyse whether HTT:pATM interaction happened in the cytoplasm and/or in the nucleus, the cells were fractionated and the cytoplasmic and nuclear (soluble and chromatin) fractions were kept separated. The fractions were subjected to a GFP co-immunoprecipitation (Co-IP) assay, using magnetic GFP-trap beads. The eluates were then analysed by Western blot.

GFP co-IP analysis showed that only mtHTT binds to pATM at the cytoplasmic fraction, while wtHTT does not (Figure 3.3.4; lave 4 vs lane 5). This interaction was induced by CPT, since mock treated cells do not show mtHTT:pATM interaction (lane 3 vs lane 5). pATM binding appears to be specific to mtHTT since the negative control lane (lane 1) showed no pATM signal. To note, the inputs blot showed pATM was only present at the nuclear fractions, indicating the results observed are not an artifact caused by nuclear contamination of the cytoplasmic fractionation. Moreover, pATM levels increased after CPT-induced damage, which agrees with the fact that ATM is activated after TOP1-induced DNA damage (Sordet *et al.*, 2009; Blackford and Jackson, 2017). Also, the levels of nuclear pATM after CPT were similar in both Q23 and Q74 expressing cells, which is in agreement with the results observed in Figure 3.3.3. Moreover, analysis of the nuclear fractions of the GFP Co-IP blot indicated that, opposite to what happened in the cytoplasmic fractions, both wild-type and mtHTT bind to pATM (Figure 3.3.4; lane 9 vs lane 10). Furthermore, although the levels of the bait-GFP were similar in both Q23 and Q74 expressing cells, the amount of pATM pull-down levels in

Q23 expressing cells was higher than those of Q74 expressing cells. Again, this interaction was triggered by CPT, possibly due to CPT-mediated pATM activation (Figure 3.3.4; inputs blot, lanes 9 and 10).

These results suggest a possible cytoplasmic sequestration of pATM by mtHTT, as suggested by Ferlazzo et al, 2014. Interestingly, the interaction observed between wtHTT and pATM reinstates the notion that HTT might be involved in the ATM-mediated in DDR after TOP1-linked DNA breaks. A previous study has shown that HTT interacts with ATM via its N17 domain, to help ATM localising at the sites of damage in response to oxidative damage (Maiuri *et al.*, 2017). It is therefore possible that the same layer of regulation occurs after other genotoxins. Furthermore, mtHTT also binds the nuclear pATM, however it is still unclear whether this interaction interferes with ATM function.

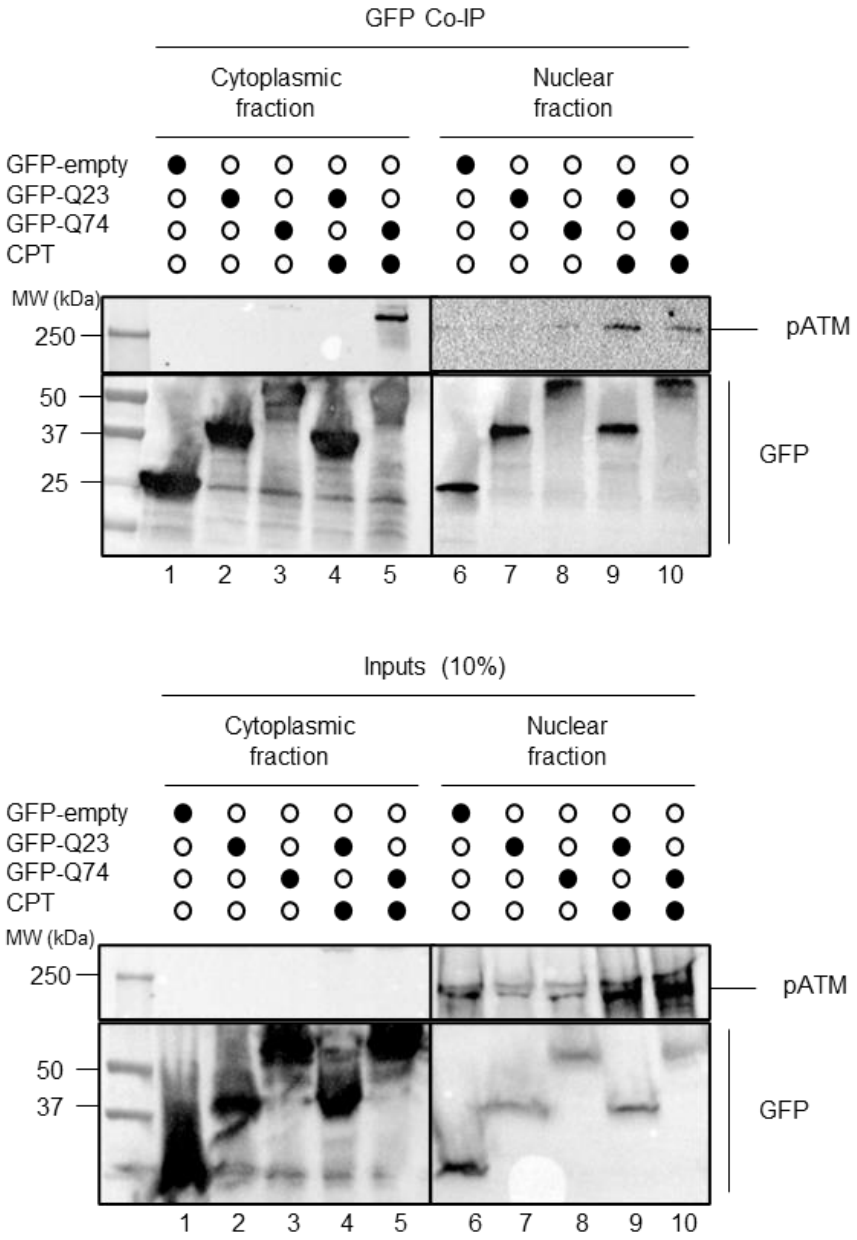

Figure 3.3.4 – Interaction between HTT and pATM

GFP co-immunoprecipitation (GFP co-IP) was performed in cytoplasmic and nuclear fractions of HEK293 co-transfected with either GFP-Q23 or GFP-74. Cells were transfected with GFP-empty plasmid as a negative control. The cells were treated with 10 μM CPT/DMSO for 1 h. Top: Western blotting analysis show the interaction between mtHTT (GFP-Q74) and pATM in the cytoplasmic fraction (lane 5). Lanes 9 and 10 show that both wtHTT (GFP-Q23) and mtHTT interact with pATM in the nuclear fraction Bottom: 10% of the nuclear lysates were analysed by western blotting after incubation with anti-pATM and anti-GFP antibodies.

3.3.4. Cells from patients with Huntington's disease show increased TOP1cc levels

Previous studies have shown ATM participates in the repair of TOP1cc in two ways: through a kinetic-dependent manner, by inducing the canonical function of ATM in signalling the DDR; and through a pathway independent of kinase activity, by promoting TOP1 degradation (Sordet *et al.*, 2009, 2010; Katyal *et al.*, 2014). Not surprisingly, neurodegenerative diseases characterised by faulty ATM-mediated repair accumulate TOP1cc, as described in A-T, SCAN1 and C9orf72-ALS models (Katyal *et al.*, 2007; Alagoz *et al.*, 2013; Walker *et al.*, 2017).

The results on Figure 3.3.4 suggest mtHTT sequesters pATM to the cytoplasm, possibly interfering with ATM-related functions. Given that ATM deficiency leads to accumulation of TOP1cc, if mtHTT prevents proper ATM activity, it is expected that HD cells accumulate TOP1cc. Therefore, I intended to look at the levels of TOP1cc in HD cells to gain further evidence about defective ATM signalling.

To examine the levels of TOP1cc, healthy (GM08402) and HD patient derived (GM04799) primary skin fibroblasts were treated with 10 μM CPT for 10 min and analysed by immunofluorescence assay, using an antibody specific for TOP1cc (Chiang *et al.*, 2017; Fielden *et al.*, 2020) (Figure 3.3.5 a).

The quantification of the number of TOP1cc foci per cell showed that GM04799 HD patient cells exhibited a greater number of TOP1cc foci, with an average of 42.1 ± 2.2 foci per cell, in comparison with the GM08402 cells (26.21 ± 1.4 foci/cell) (Figure 3.3.5 b). These results suggest HD cells accumulate TOP1cc, which is consistent with defective ATM signalling.

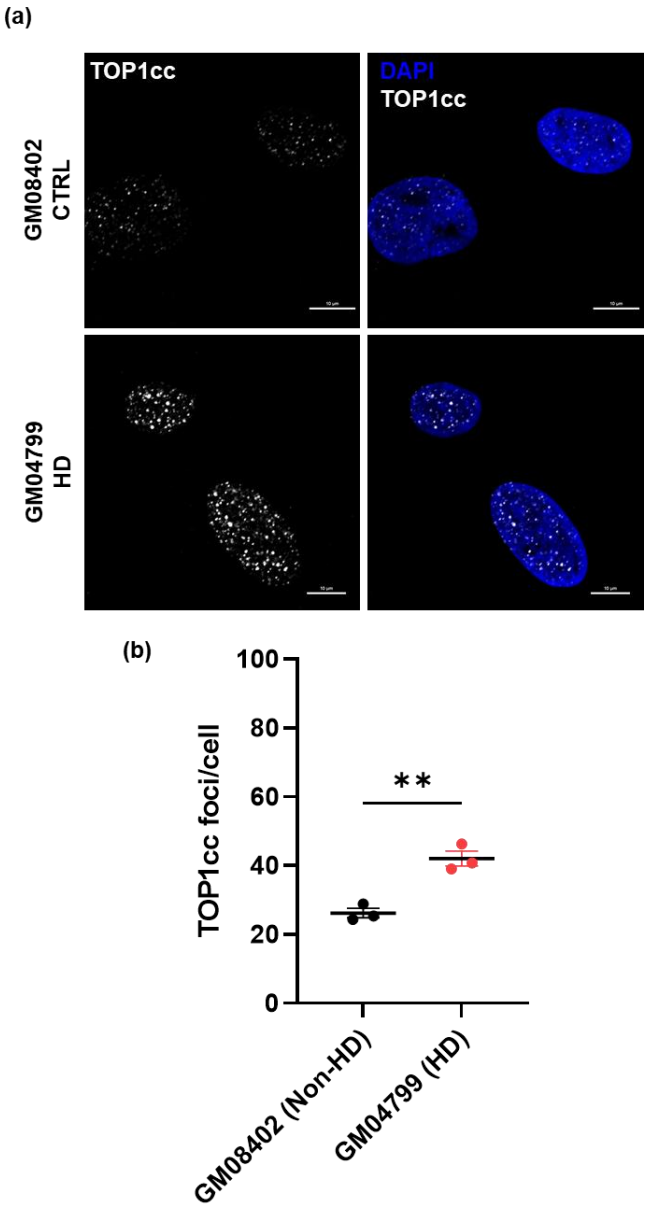

Figure 3.3.5 – HD patient-derived fibroblasts show increased TOP1cc levels after CPT treatment

(a) Representative images of primary skin fibroblasts from a healthy individual (GM08402) and a HD patient (GM04799) after treatment with 10 μM CPT for 10 min and immunostained with a specific antibody against TOP1cc. DAPI shows nuclei. Scale bar: 10 μm.

(b) The number of TOP1cc foci per cell was quantified and analysed by unpaired Student's t-test. Data is presented as average of 3 independent experiments. $^{**}P = 0.0036$.

3.3.5. Huntington's disease patient cells exhibit slower DSB repair rates

Persistent TOP1cc increases genomic instability by favouring the generation of transcription-dependent DSB (Cristini *et al.*, 2020). Moreover, defects in NHEJ, sustained by the deficient 53BP1 focal recruitment might result in an inadequate repair of the damage induced by trapped TOP1cc, ultimately leading to accumulation of DSBs. Indeed, adequate recruitment of 53BP1, consistent with proper NHEJ activity, was shown to promote the removal of the DSB marker γH2AX, indicating efficient DSB repair (Anglada, Genescà and Martín, 2020).

In line with this, the hypothesis was that the defective DDR signalling as indicated by lack of 53BP1 observed in HD models culminated in defective repair of the TOP1-induced damage, ultimately leading to the formation of DSB. Therefore, I intended to study the DSB repair kinetics of the HD patient cell line GM04799 and non-HD fibroblasts (GM08402) after CPT treatment. The goal was to understand whether HD cells experience accumulation of unrepaired DSBs after treatment with CPT and if these cells can efficiently repair the damage. To do that, the cells were treated for 1 h with 2 μM CPT, followed by removal of CPT and recovery in complete media for 1-24 h. Since it was established that each DSB corresponds to one γH2AX focus, quantification of γH2AX foci has been often used as a measure for the detection of DSB (Mah, El-Osta and Karagiannis, 2010; Sharma *et al.*, 2015). Therefore, the cells were then subjected to immunofluorescence analysis of the DSB marker, γH2AX (Figure 3.3.6 a). For this experiment, cells with more than 10 γH2AX foci were considered positive.

GM08402 cells and GM04799 HD fibroblasts exhibited nonsignificant differences in basal levels of γH2AX, with 25.929 % ± 8.4 and 31.735 % ± 2.8 positive cells, respectively. After CPT-induced damage, the average percentage of γH2AX positive cells reached the maximum after 1 h post treatment time in both cell lines. In GM08402 cells, about 45.762 % ± 3.8 cells stained positive for γH2AX, while for the HD GM04799 cells, 48.510 % ± 8.8 of the cells were γH2AX positive (Figure 3.3.6 b). In the subsequent post-CPT treatment time points, the non-HD fibroblasts showed a reduction in the percentage of γH2AX positive cells, to levels close to those of the mock treated cells. At 2 h post CPT treatment, only 21.661% ± 1.4 of the cells were positive for γH2AX. After 24 h recovery, the percentage of GM08402 cells positive for γH2AX was lower than the mock treated cells (19.615 % ± 1.6 vs 25.929 % ± 8.4, respectively), suggesting that the healthy GM08402 cells can efficiently repair the damaged induced by CPT (Figure 3.3.6 b).

In HD cells, the percentage of γH2AX positive cells at 2 h, 4 h and 24 h post CPT treatment also decreased in comparison to the 1 h time-point but remained significantly higher than the non-HD cell lines: 2 h (HD: 40.029 % ± 5.5; Non-HD: 21.661 % ± 1.4), 4 h (HD: 38.002 % ± 2.7; Non-HD: 21.311 % ± 1.8) and 24 h (HD: 37.220 % ± 3.0; Non-HD: 19.615 % ± 1.6) (Figure 3.3.6 b). Hence, I conclude from these experiments that HD primary fibroblasts exhibit slower DSB repair rates in comparison with the non-HD fibroblasts, which is consistent with the previous work by (Ferlazzo *et al.*, 2014).

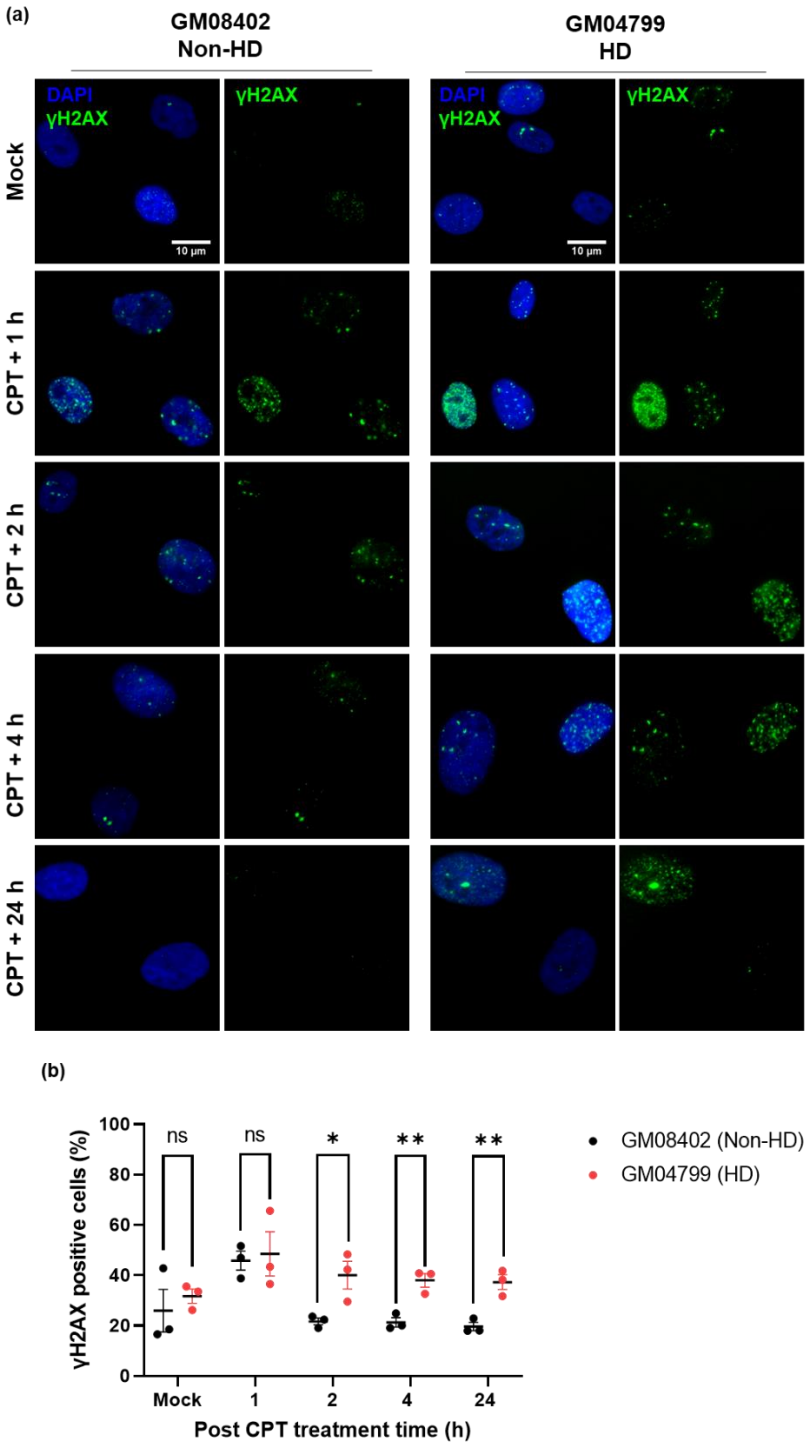

Figure 3.3.6 - Accumulation of unrepaired DNA damage in fibroblasts from patients with HD after CPT treatment

(a) Representative images of GM08402 non-HD and GM04799 HD patient-derived fibroblasts immunostained with an anti-γH2AX antibody after treatment with 2 µM CPT for 1 h and recovery in complete medium for different time points: 1 h; 2 h; 4 h and 24 h (scale bar: 10µm). DAPI shows nuclei **(b)** The percentage (%) of γH2AX positive cells (> 10 foci) were quantified for each time point using ImageJ software and analysed by unpaired Student's *t*-test. Data is shown as average of 3 independent experiments (10 fields each). Error bars represent ± s.e.m. **P* = 0.032; ***P* = 0.0069 (4h); ***P* = 0.0065 (24h); ns, nonsignificant.

3.3.6. Primary cells from Huntington's disease patients are hypersensitive to topoisomerase I poisons.

Stabilized TOP1cc can lead to the production of DSBs (Pommier, 2006; Sordet *et al.*, 2009; Cristini *et al.*, 2019; Mei *et al.*, 2020). Accumulation of unrepaired DSBs is extremely harmful to the cells, since it promotes loss of genome stability, ultimately leading to cell death (McKinnon, 2013). Defects in the repair of TOP1cc contributes to the aetiology of several neurodegenerative diseases, including A-T, SCAN1 and ALS. In these disorders, defects in TOP1cc repair and concomitant accumulation of DNA strand breaks over time increases neuronal death (El-Khamisy *et al.*, 2005; Alagoz *et al.*, 2013; Katyal *et al.*, 2014; Walker *et al.*, 2017).

Considering the accumulation of TOP1cc and the decreased DSB repair rates in HD cells, as shown by the slower disappearance of γH2AX foci, it was speculated that the continued exposure to TOP1 poisons would consequently be more cytotoxic to HD cells than non-HD cells. Hence, the objective was to test if the defective damage repair observed in HD cells in response to CPT causes sensitivity to this drug. Given that CPT was shown to induce apoptosis, I sought to investigate the presence of markers of active execution of apoptosis, such as the cleavage of caspase-3 following CPT treatment.

As cells undergo apoptosis, they tend to detach from the surface. Therefore, to access the optimal time point to harvest the cells, I first monitored the time at which CPT caused primary skin fibroblasts to detach. Exposing the cells to 10 μM CPT for 72h, increased HD patient cells detachment, while most of the non-HD fibroblasts remained attached to the well.

Investigation of cleaved caspase-3 levels by western blotting confirmed activation of apoptosis induced by CPT in both GM04799 and GM04869 HD fibroblasts. The respective levels of cleaved caspase-3 in GM04799 and GM04869 HD cells were 1.2- and 1.4-fold higher when comparing with the non-HD fibroblasts (Figure 3.3.7 a and b). Mock treated cells failed to show cleavage of capase-3. Hence, elevated cleavage of caspase-3 in HD cells following CPT treatment indicates TOP1-induced damage effectively kills HD cells by inducing apoptosis, further suggesting HD sensitivity to this genotoxin.

To confirm these findings, I also performed a CellTiter® Blue assay to monitor cell viability after CPT treatment. In comparison with non-HD cells, both patient-derived HD cells displayed

decreased percent survival (% survival) in response to increasing CPT concentrations (Figure 3.3.8 a and b). Together, these findings show that HD cells are hypersensitive to CPT.

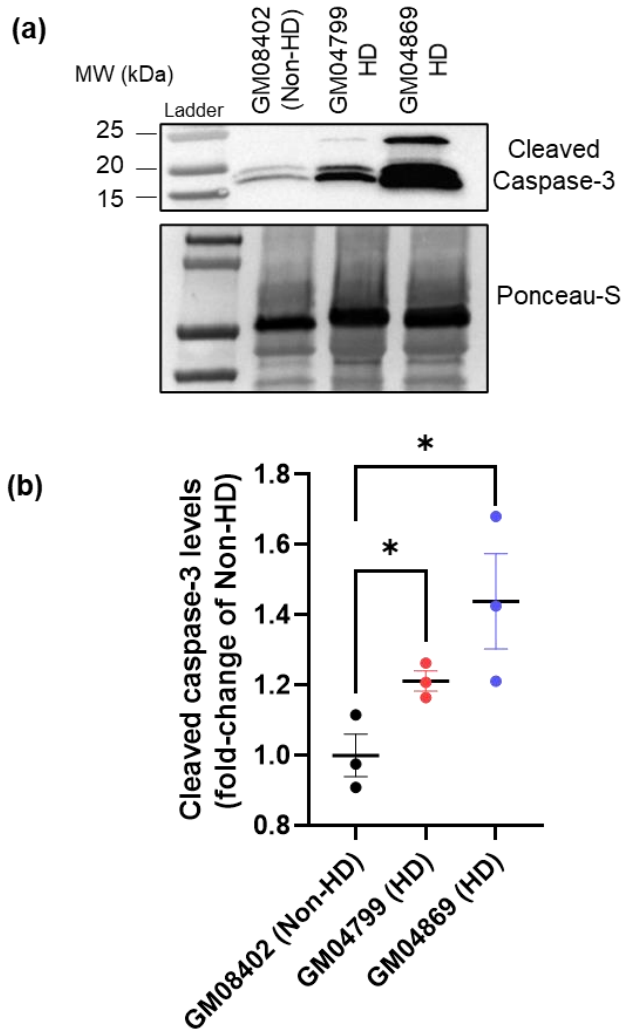

Figure 3.3.7 – CPT treatment induces caspase-3 activation in fibroblasts from patients with HD

(a) Western blotting analysis of healthy and HD patient fibroblasts after treatment with 10 μM CPT for 72 hours and incubation with a cleaved caspase-3 specific antibody. Ponceau-S staining of total protein shows loading.

(b) Quantification of the densitometry levels of cleaved caspase-3 normalised against the loading (Ponceau-S). Fold-change of cleaved caspase-3 levels relative to non-HD cells was calculated and analysed by unpaired Student *t*-test. Error bars represent s.e.m. from 3 biological experiments, as presented by the scatter dot plot. **P* = 0.0344 (GM04799); **P* = 0.0419 (GM04869).

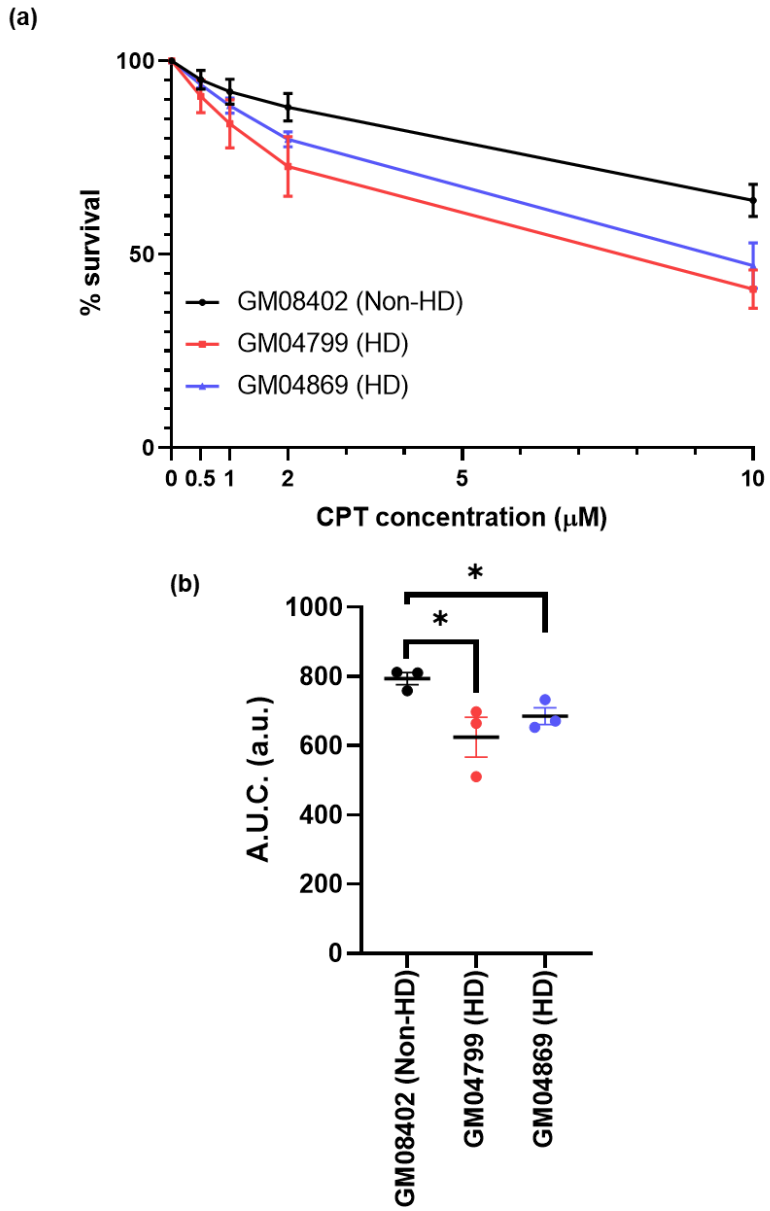

Figure 3.3.8** - **Primary skin fibroblasts from patients with HD show increased sensitivity to CPT treatment

(a) Sensitivity to CPT treatment of non-HD and HD patient fibroblasts was monitored by CellTiter-Blue® assay after 96 hours treatment with increasing concentrations of CPT (0 -10 μM). Y-axis represent the mean percentage survival (% survival) of 3 biological experiments plotted against CPT concentration. Percent (%) survival in treated fibroblasts was assessed by normalising against the corresponding untreated condition (0 μM). Error bars represent ± s.e.m.

(b) The area under the curve (A.U.C.) was calculated for each condition and plotted as average of 3 biological replicates. The data was analysed by unpaired Student *t*-test (error bars: ± s.e.m.). **P* = 0.0270 (GM04799); **P* = 0.0101 (GM04869)

3.3.7. GABAergic striatal neurons generated from HD patients also exhibit deficient 53BP1 recruitment

The data presented so far was obtained in replicating cells, which poses a problem, since CPT is mostly known to induce replication-related DSBs, when the replication machinery encounters a trapped TOP1cc. However, in neurons, which are non-replicating postmitotic cells, CPT causes transcriptional SSBs and DSBs.

In addition, HD is characterised by the progressive degeneration of the striatum (Bates *et al.*, 2015; Jimenez-Sanchez *et al.*, 2017). The gamma-aminobutyric acid (GABA)ergic MSNs, which comprise around 95% of the striatal neuron population, are particularly vulnerable to the toxic effects of mtHTT, where loss of MSNs is observed during the progression of HD (Ehrlich, 2012; Zheng and Kozloski, 2017).

Given that HD is characterized as a striatal pathology and to mitigate the replicative damage caused by CPT, I next aimed to test whether the findings previously observed in non-neuronal cells are also featured in primary GABAergic striatal neurons. To do this, induced neural progenitor cells (iNPCs) from a patient with HD (GM23225) and a healthy individual (CS14) were differentiated into striatal GABAergic neurons based on a three-step differentiation protocol developed by Lin *et al.*, 2015 (Figure 3.3.9).

The first stage of the differentiation protocol consisted of the neural induction of the NPCs for 10 days. The neural induction was obtained by supplementing the medium with the developmental factors sonic hedgehog (SHH) and Dickkopf-1 (DKK-1), together with brain-derived neurotrophic factor (BDNF) that pushes the cells into a striatal pathway (Lin *et al.*, 2015). After 10 days, the cells were subjected to a final passage and fed with a neurobasal medium supplemented with an increased concentration of BDNF, important for neuronal cell survival, which promotes neural maturation. The protocol optimisation was conducted by my colleague in the El-Khamisy and Ferraiuolo labs, Cleide dos Santos Souza, who harvested the cells at each of the 3 steps demonstrated in Figure 3.3.9, for characterization. NPCs exhibited a rosette-like shape and stained positive for Nestin and PAX6. GABAergic progenitors and the mature GABAergic neurons showed long neurite projections and expressed neuronal markers, such as DARPP32, GABA, MAP2.

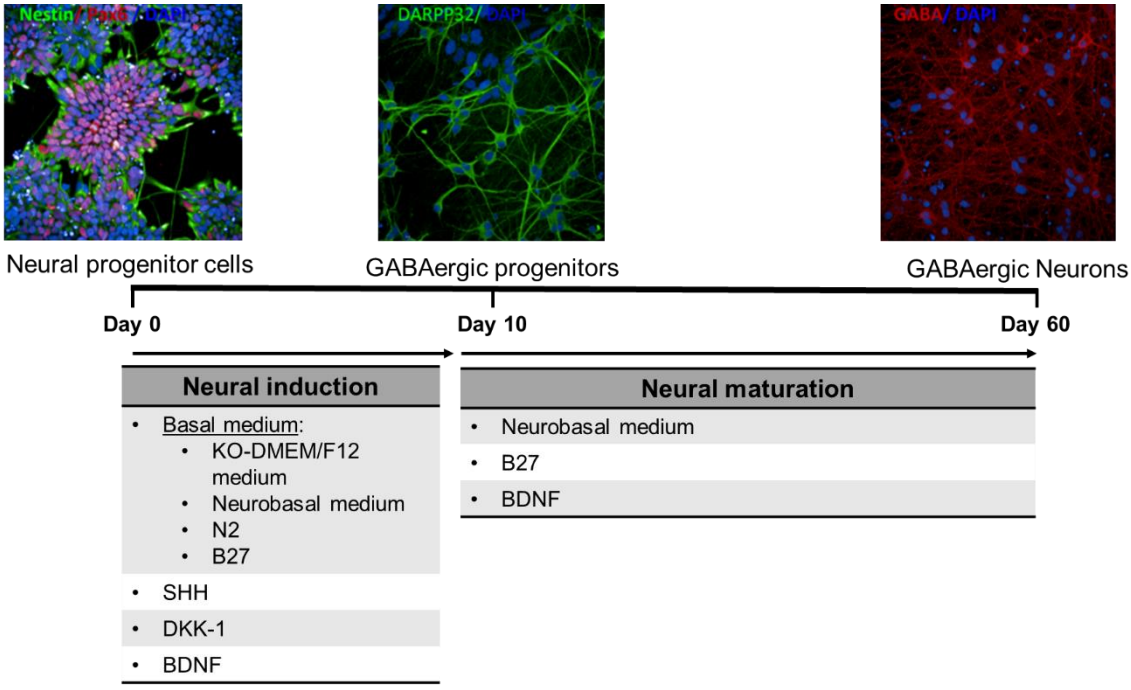

Figure 3.3.9 – Differentiation of neural progenitor cells into GABAergic neurons

Schematic representation showing the outline of three-step differentiation protocol of neural progenitor cells (NPCs) into GABAergic neurons. On day 0 NPCs are plated onto matrigel-coated 6-well plates. These cells are positive for the NPC markers Nestin and PAX6. NPCs first follow neural induction by feeding the cells with basal medium supplemented with sonic hedgehog (SHH) and Dickkopf-1 (DKK-1), which promotes specific striatal differentiation, and brain-derived neurotrophic factor (BDNF), important for striatal neuron survival. After ten days it is possible to observe GABAergic progenitors, staining positive for dopamine and cyclic AMP-regulated phosphoprotein of 32 kDa (DARPP32), a specific striatal neuronal marker. At day 10 the GABAergic progenitors are subjected to a final passage and plated onto Matrigel-coated 96-well plates, to proceed to neural maturation, which involves feeding the neurons with a neurobasal medium supplemented with B27 and BDNF. At day 60 it is possible to observe fully matured striatal neurons, staining positive for GABA

After the 60-day differentiation protocol, the GABAergic neurons were treated with 0.5 μM CPT for 1 h. 53BP1 foci formation in response to CPT was assessed by immunofluorescence (Figure 3.3.10 a). While CS14 non-HD neurons showed a significant increase in the percentage of cells positive for 53BP1 staining after CPT treatment (Mock: 18.244 % ± 7.2 vs CPT: 35.362 % ± 6.6), striatal neurons from the GM23225 HD patient exhibited no CPT-driven 53BP1 response (Mock: 9.939 % ± 1.6 vs CPT: 15.799% ± 7.7) (Figure 3.3.10 b). Analysis of the number of foci per cell revealed that HD neurons exhibited fewer 53BP1 foci than the healthy non-HD neurons before CPT treatment. This difference became statistically significant after CPT treatment (Non-HD: 3.4 ± 0.36 foci/cell vs HD: 1.8 ± 0.78 foci/cell) (Figure 3.3.10 c). These results were in line with the previous observations in non-neuronal patient derived fibroblasts and in cells transiently expressing the HTT expansions.

Together, these findings described showed that 53BP1 foci recruitment or retention is compromised in HD cells after DNA damage induced by CPT treatment. Importantly, this was true in multiple HD cell models including ectopic expression of CAG expansions, HD patient-derived cells expressing endogenous expansions and in GABAergic neurons.

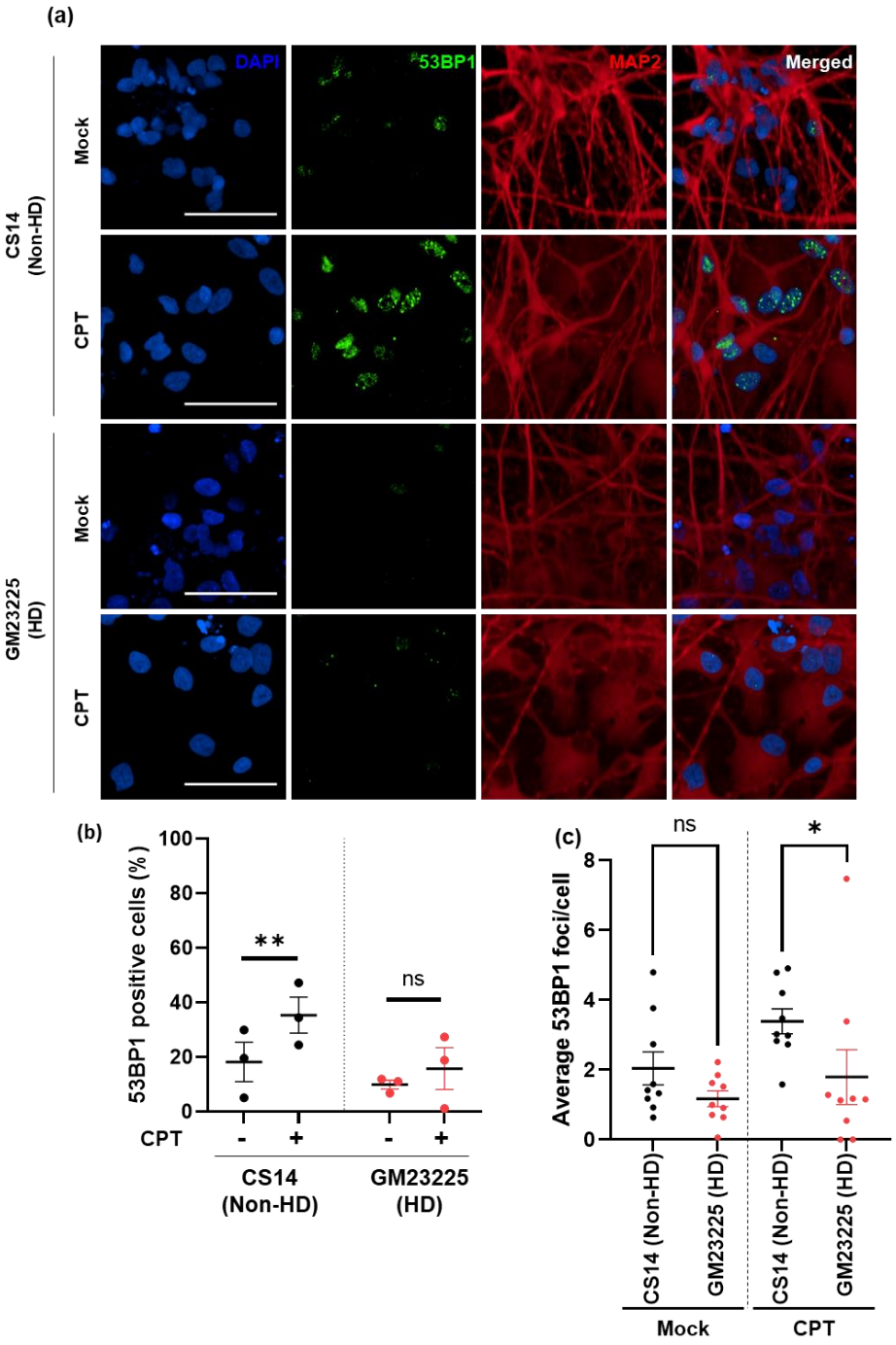

***Figure 3.3.10* – GABAergic neurons from HD patients exhibit decreased 53BP1 signalling**

(a) Representative images showing CS14 non-HD and GM23225 HD iPSC-derived GABAergic neurons immunostained with an anti-53BP1 antibody after treatment with 0.5 µM CPT or DMSO for 1 hour (scale bar: 50µm). DAPI shows nuclei. MAP2: Neuronal marker.

(b) The percentage 53BP1 positive cells (> 2 foci) was quantified and analysed by paired Student *t*-test. Data is shown as average of 3 independent experiments. Error bars represent ± s.e.m. ***P* = 0.0057; ns: nonsignificant.

(c) Scatter dot plot showing the average number of 53BP1 foci per cell quantified from 9 technical replicates across 3 biological experiments and analysed using Mann-Whitney test. Error bars: ± s.e.m. **P* = 0.0188; ns

3.3.8. The Kinetics of DSB repair in GABAergic neurons from Huntington's disease patients is different from primary fibroblasts

To assess whether 53BP1 defects lead to faulty repair of TOP1-induced breaks, the repair kinetics of striatal GABAergic neurons was studied following CPT treatment. As before, the clearance of γH2AX foci was monitored by immunofluorescence assay after inducing DNA damage by treating the cells with 2 μM CPT for 1 h, followed by CPT washout and recovery in complete media for 1-24 h (Figure 3.3.11 a). For this analysis, cells were considered positive when harbouring more than 2 foci. The reasoning behind changing the cut off from 10 to 2 foci in neurons was because neurons harboured an average of 3.8 γH2AX foci/cell, while fibroblasts an average of 10.6 foci/cell.

Immunofluorescence analysis of mock treated cells showed the percentage of neurons γH2AX positive showed a tendency to be lower than non-HD neurons, despite showing statistical non significance (Non-HD: 23.392 % ± 7.7; HD: 3.170 ± 1.1). After 1 h post CPT treatment, there was a sharp increase in the percentage of HD neurons positive for γH2AX staining, reaching an average of 50.710 %. The average of healthy neurons also positive for γH2AX also increased at 1 h time point, with an average of 40.043 % positive cells. Remarkably, the levels of non-HD neurons positive for γH2AX continued to increase, reaching a maximum at 2 h post CPT treatment (54.033 % ± 4.6). In the following recovery time points, the percentage of non-HD neurons γH2AX positive decreased, reaching an average of 33.811 % after 24 h recovery.

Unexpectedly, the average percentage of HD neurons γH2AX positive were consistently lower than non-HD neurons at later recovery time points, especially after 24 h post CPT treatment (Non-HD: 33.811 % ± 2.4 vs HD: 10.090 % ± 4.6) (Figure 3.3.11 b). These results indicate that HD iPSC-derived striatal neurons have altered γH2AX signalling in response to CPT. This is consistent with previous work showing deficient DNA damage-induced γH2AX levels in striatal cells of HD knock in mice (Jeon *et al.*, 2012). Whether these altered γH2AX responses translate to altered sensitivity of the striatal neurons to apoptotic cell death is what I examined in the following section.

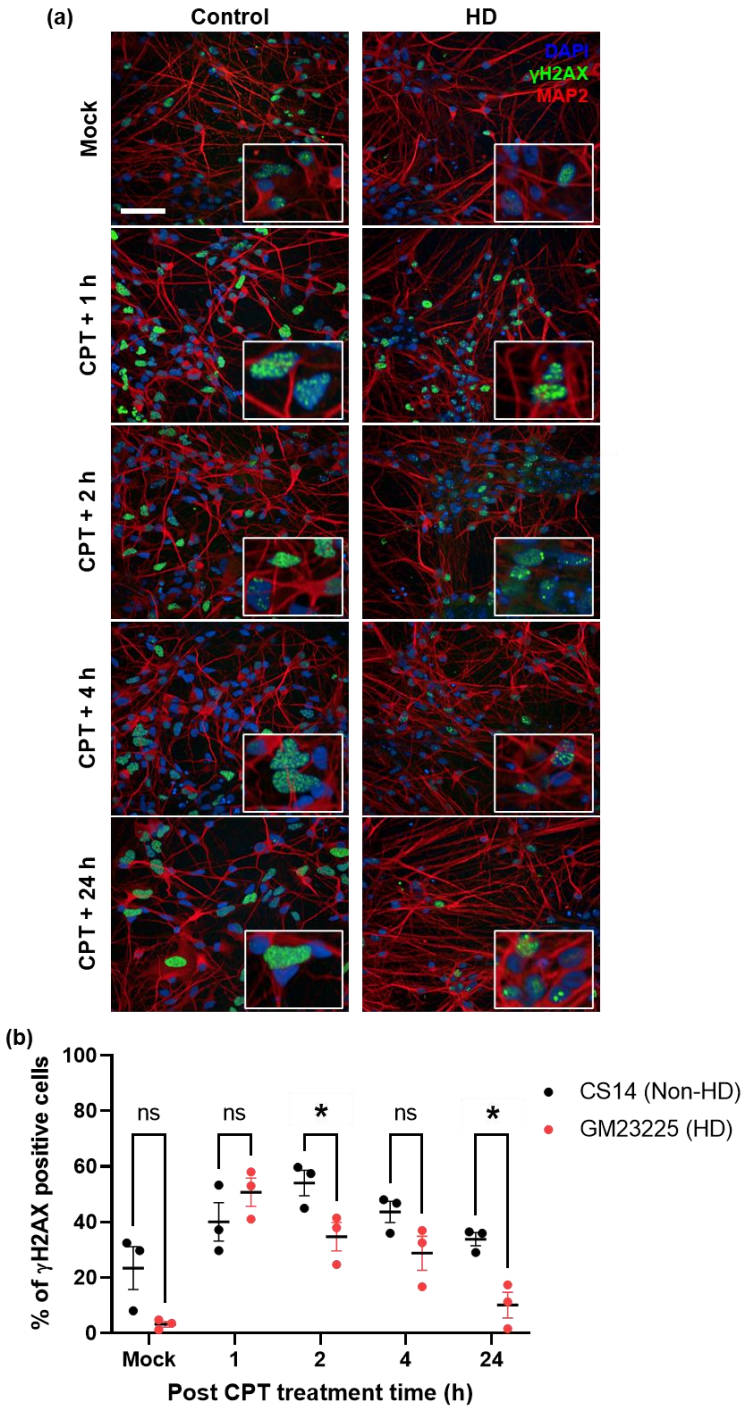

Figure 3.3.11 – Kinetics of γH2AX after treatment with CPT in GABAergic neurons

(a) Representative images of GABAergic neurons differentiated from NPCs from a non-HD individual (CS14) and a patient with HD (GM22325) immunostained with a specific γH2AX antibody after treatment with 2 µM CPT or DMSO for 1 hour and recovery in complete medium for 1-24 hours (scale bar: 50µm). DAPI shows nuclear staining. MAP2 is a specific marker for neuronal cytoskeleton.

(b) %γH2AX positive cells (> 2 foci) were quantified for each time point and presented as fold-change of mock (DMSO) and analysed by unpaired Student *t*-test for each time point. Data is shown as average of 3 independent experiments. Error bars represent ± s.e.m. **P* = 0.0482 (2h); **P* = 0.102 (24h); ns, nonsignificant.

3.3.9. Topoisomerase I-induced damage causes activation of apoptotic markers in striatal neurons from patients with Huntington's disease

The previous results showed altered 53BP1 and γH2AX foci formation in response to TOP1-induced damage caused by CPT treatment in HD GABAergic neurons. In line with the notion that unrepaired TOP1-linked DNA breaks causes premature neuronal death, I questioned whether HD GABAergic neurons were hypersensitive to CPT treatment. Therefore, I next tested whether treatment with CPT also induced the activation of the apoptotic marker, cleaved caspase-3, in HD GABAergic neurons.

Immunofluorescence analysis revealed that after treatment with 10 μM CPT for 48h, HD neurons exhibit a ~2.6-fold increase in the levels of cleaved caspase 3, compared with the ~1.4-fold increase in the healthy neurons (Figure 3.3.12 a and b). Thus, these results demonstrate that HD neurons exhibit an increased sensitivity to CPT as illustrated by the increased levels of apoptotic markers in these cells, similar to what was observed in HD fibroblasts.

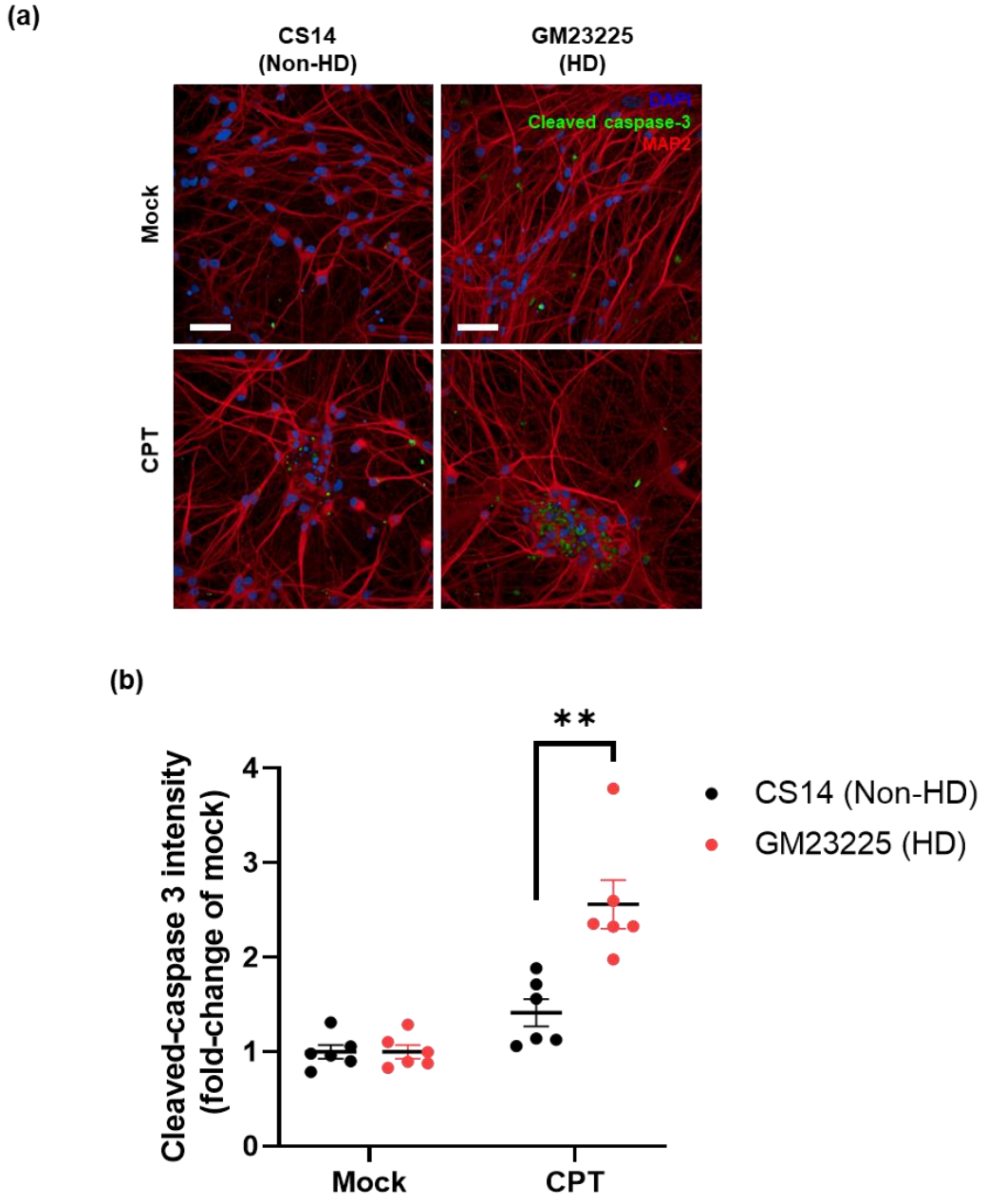

Figure 3.3.12 – GABAergic neurons from HD patients exhibit increased activation of the apoptotic marker cleaved caspase-3 after treatment with CPT

(a) Representative images of GABAergic neurons differentiated from iPCS-derived NPCs from a healthy individual (CS14) and a patient with HD (GM23225) immunostained with a specific cleaved caspase-3 antibody after treatment with 10 µM CPT or mock (DMSO) for 48 h (scale bar: 50 µm). DAPI: nuclear staining. MAP2: neuronal marker

(b) The intensity of cleaved caspase-3 signal was quantified. Data is shown as average of 6 technical replicates across 2 biological experiments and plotted as fold-change of the corresponding mock (DMSO treated cells). Analysis by unpaired Student *t*-test. Error bars represent ± s.e.m. ***P* = 0.0030.

3.4. Discussion

The main aim of this chapter was to study the effects of mtHTT in the repair of TOP1-induced breaks. The interest in investigating these lesions in the context of HD result from the fact that DNA strand breakage caused by irreversible TOP1cc occurs endogenously and are common DNA alterations in the brain (Sordet *et al.*, 2008). This results from normal neuronal activity, as neurons exhibit increased oxygen consumption and high transcriptional activity (Pourquier, Ueng, *et al.*, 1997; Sordet *et al.*, 2010; McKinnon, 2016; Berger *et al.*, 2017). In fact, others have reported the presence of endogenous TOP1cc in the brains of different model organisms, including mice and zebrafish (Katyal *et al.*, 2014; Zaksauskaite *et al.*, 2021).

Different types of DNA lesions compose the aetiology of neurodegenerative disorders. Accumulation of TOP1cc is present in many neurodegenerative disorders. This includes SCAN1, due to defects in the excision repair of TOP1cc caused by mutations in TDP1 (El-Khamisy *et al.*, 2005). TOP1cc also cause DNA damage in both A-T and C9orf72-ALS due to defects in ATM activity (Alagoz *et al.*, 2013; Katyal *et al.*, 2014; Walker *et al.*, 2017). This indicates that TOP1cc and related DNA breaks are common causes of DNA damage in neurodegeneration.

In line with the fact that TOP1-mediated DNA lesions are common events in the brain, one would wonder whether these lesions are also part of the aetiology of HD. Moreover, since mtHTT was shown to interfere with multiple DDR mechanisms, a plausible question would be whether the repair of TOP1 DNA breaks is influenced by mtHTT in HD. To answer these questions, CPT was used to induce damage to the cells, since it is a specific TOP1 poison, known to cause TOP1cc (Pommier, 2006).

To summarize, in this chapter I first identified that mtHTT caused deficient 53BP1 recruitment to the nucleus of cells after TOP1-induced damage in different cellular models, including striatal neurons from HD patients. Simultaneously, I observed mtHTT sequesters pATM to the cytosolic fractions, possibly causing defects in ATM signalling. Accordingly, increased levels of CPT-induced TOP1cc in HD fibroblasts were detected, which could be related to ATM defects.

HD fibroblasts repaired the damage induced by CPT at a slower rate than healthy cells, as shown by the increased percentage of γH2AX positive cells at later recovery time points. These results indicate that HD cells struggle to repair TOP1-induced DNA lesions and accumulate unrepaired DSBs. Interestingly, HD GABAergic neurons showed different rates of γH2AX

appearance/ disappearance than those observed in HD fibroblasts. A previous work showed that HD knock-in striatal mice cells exhibited decreased levels of γH2AX in comparison with non-HD cells after induction of DNA damage, which agrees with the findings observed in the iPSC-derived HD GABAergic neurons used here (Jeon *et al.*, 2012). In contrast, Ferlazzo *et al*. also described a delayed γH2AX disappearance rate in HD fibroblasts, which is in line with what was observed in the HD fibroblasts used in this study (Ferlazzo *et al.*, 2014). Albeit these differences, both patient-derived HD fibroblasts and GABAergic neurons exhibited augmented activation of apoptotic markers in response to CPT treatment, indicating HD cells are hypersensitive to CPT, which triggers apoptotic cell death.

Together, these observations suggest that in HD cells, the DDR signalling triggered by TOP1-mediated DNA lesions is compromised, contributing to increased TOP1cc-triggered DNA damage and consequent cell death. Thus, the hypothesis stated at the beginning of this chapter is supported by these findings.

3.4.1. Defects in 53BP1 foci formation, cytoplasmic sequestration of pATM and accumulation of TOP1cc in HD cells

Different scenarios explain the generation of transcription related DSBs mediated by TOP1 stalling. Firstly, these DSBs can arise by the presence of two TOP1cc on opposite strands, creating two proximal SSBs during TOP1cc processing (Pommier *et al.*, 2014). A similar mechanism happens when a TOP1cc and an R-loop are present at neighbouring DNA strands repaired, given that the processing of both DNA conformations generates SSBs (Katyal *et al.*, 2007; Das *et al.*, 2014; Cristini *et al.*, 2019). Finally, transcriptional-DSBs can also arise when a TOP1cc is opposite to DNA nicks, generated for example during the repair of oxidative damage by BER (Wilson and Bohr, 2007; Iyama and Wilson, 2013; Yang *et al.*, 2020). In all these scenarios, DSBs are generated by the presence of SSBs in close proximity, which favour the repair by NHEJ (Balmus *et al.*, 2019). In addition, HD affects striatal neurons, which are postmitotic cells and thus depend on NHEJ for the repair of DSBs (Madabhushi, Pan and Tsai, 2014; Zheng and Kozloski, 2017). Therefore, I focused on analysing NHEJ repair, by studying 53BP1 foci formation.

The results presented in this chapter demonstrate that the presence of mtHTT interferes with NHEJ by preventing 53BP1 recruitment to the sites of TOP1-mediated DNA lesions. In agreement with these findings other studies have also described NHEJ defects in HD models. A study described a mechanism by which mtHTT sequesters Ku70, a component of the NHEJ

machinery (Enokido *et al.*, 2010). Ku70, in complex with Ku80 is responsible for the downstream recruitment of DNA-PK. Binding of mtHTT prevented Ku70-Ku80 and Ku70-DNA interactions, thus impairing DNA-PK activity (Enokido *et al.*, 2010). In addition, inclusion bodies formed by aggregated HTT were shown to attract 53BP1, which also contributes to deficient 53BP1 recruitment to the damaged sites (Yehuda *et al.*, 2017). To note, sequestration of 53BP1 by mtHTT was beyond the scope of the present study. A study conducted by the Foray group showed HD fibroblasts yield fewer 53BP1 foci in comparison with non-HD fibroblasts after irradiation, indicating a deficient recruitment of 53BP1 to irradiation-induced DSBs, which is consistent with the findings shown here (Ferlazzo *et al.*, 2014).

Growing evidence suggests 53BP1 occupancy at DNA damage sites is controlled by the interaction of 53BP1-$BRCT_2$ domain with γH2AX, which is necessary for the retention of ATM at the chromatin and to sustain and propagate ATM-dependent signalling (Baldock *et al.*, 2015). In fact, 53BP1 was shown to promote ATM signalling and to rescue ATM kinase activity in the absence of MRN (Lee *et al.*, 2010).

Indeed, 53BP1 signalling in HD fibroblasts was found to be associated with the lack of pATM signalling after irradiation (Ferlazzo *et al.*, 2014). Similarly, defective 53BP1 and pATM foci formation in response to TOP1-mediated DNA lesions was observed in both RNA repeat expansion (RRE) and dipeptide repeats (DPR) models of *C9orf72* ALS/FTD, another polynucleotide expansion neurodegenerative disorder (Walker et al., 2017). Interestingly, the analysis of pATM retention at the chromatin following CPT treatment observed here revealed that the levels of pATM were similar in both HD and healthy fibroblasts. Nonetheless, the similarities in the defective 53BP1 signalling suggests common mechanisms might be involved in the pathogenesis of both neurodegenerative disorders.

The same study conducted by Foray group showed that mtHTT could bind to ATM, while wtHTT did not. The group suggested that since mtHTT is mainly found in the cytoplasm, it sequesters ATM to the cytoplasm, thus explaining the deficient nuclear-cytoplasmic translocation of ATM after irradiating HD cells (Ferlazzo *et al.*, 2014). In concordance, the co-IP data showed in this chapter confirms cytoplasmic sequestration of pATM by mtHTT. Interestingly, the interaction observed between wtHTT and pATM suggest HTT might be involved in the ATM-mediated in DDR after TOP1-linked DNA breaks. A previous study has shown that HTT interacts with ATM via its N17 domain, to help ATM localising at the sites

of damage in response to oxidative damage (Maiuri *et al.*, 2017). It is possible the same mode of regulation occurs after other genotoxins. Furthermore, mtHTT also binds the nuclear pATM, however it is still unclear whether this interaction interferes with ATM function. Similar to what was described in this chapter, Nihei *et al.*, (2019) also demonstrated that poly-glycine–alanine (poly-GA), DPRs frequently observed in *C9orf72* ALS/FTD patients, induced cytoplasmic sequestration of pATM. This suggests that sequestration of DDR elements by aggregation-prone proteins might be a common mechanism involved in the pathogenesis of different neurodegenerative disorders.

Accumulation of TOP1cc is observed in brains and cells with defects in ATM signalling (Katyal *et al.*, 2014; Walker *et al.*, 2017). Besides the canonical role of ATM in acting as a major DDR kinase upon TOP1cc-triggered DNA damage, ATM also plays a role in mediating TOP1 proteasomal degradation, by regulating SUMOylation and DNA-PK-induced ubiquitination of TOP1 (Katyal *et al.*, 2014; Cristini *et al.*, 2016). Accordingly, I demonstrated in Figure 3.3.5 that HD fibroblasts showed increased TOP1cc in comparison with healthy fibroblasts after CPT treatment. Although it would have been interesting to investigate the endogenous levels of TOP1cc in HD cells, these results imply impaired TOP1cc processing in HD cells. This impairment could be related to ATM deficiencies, possibly due to mtHTT-mediated cytoplasmic sequestration of ATM, together with faulty DNA-PK activity as described by Enokido *et al.*, (2010).

3.4.2. Differences in γH2AX signalling in HD models

Analysis of γH2AX foci formation is commonly used as a mechanism to assess the presence of DSBs, since it was previously demonstrated a correlation between the two, in which one γH2AX foci corresponds to one DSB (Löbrich *et al.*, 2010). For that reason, I decided to study γH2AX foci formation to infer about the ability of HD cells to repair DSBs generated by TOP1 lesions. The data showed in section 3.3.5 revealed that in HD fibroblasts, the rate of γH2AX foci disappearance following CPT washout is slower than in non-HD fibroblasts. These results suggest that in HD fibroblasts the repair of CPT induced DSBs is defective. These findings are consistent with other studies showing increased H2AX phosphorylation in response to DNA damage in HD models. For example, an early study demonstrated that oxidative damage induced exaggerated activation of ATM signalling, concomitant with the increased presence of γH2AX in HD patient fibroblasts (Giuliano, 2003). Similarly, increased γH2AX levels were also found in post-mortem brain tissues of HD patients and in cells from BACHD mice after

oxidative stress (Lu *et al.*, 2014). Elevated levels of γH2AX were also found in peripheral blood of HD patients (Castaldo *et al.*, 2019). Together, these studies and the results demonstrated in this chapter indicate abnormal activation of DDR mechanisms in HD cells and brains with concomitant accumulation of unrepaired DNA damage.

On the other hand, analysis of γH2AX signalling after recovery from CPT treatment in GABAergic neurons revealed that HD neurons harboured defective γH2AX foci formation, except at 1 h post CPT removal, where the levels of γH2AX were similar of those of healthy GABAergic neurons. A study described similar results in HD knock-in striatal cell models (Jeon *et al.*, 2012). After CPT treatment Q111 knock-in cells showed decreased levels of γH2AX, together with deficient distribution of γH2AX foci. These defects were explained by defects in ATM activation and BRCA1 phosphorylation. The study revealed that in HD, γH2AX lost the ability to bind to BRCA1 (Jeon *et al.*, 2012). This is suggestive of a mechanism by which nuclear distribution of γH2AX is modulated via BRCA1-BRCT interaction with γH2AX. 53BP1 also contains two tandem BRCT domains, that were shown to interact with γH2AX in response to DNA damage (Baldock *et al.*, 2015). Although this interaction is dispensable for 53BP1 localization at DNA breaks, it was shown to be important in maintaining ATM activity (Celeste *et al.*, 2003; Baldock *et al.*, 2015; Salguero *et al.*, 2019). Similarly, it is possible γH2AX interaction with BRCT domain of 53BP1 could also regulate γH2AX focal distribution.

Therefore, the defects in γH2AX signalling described in HD GABAergic neurons could be explained in two ways: (i) the faulty 53BP1 foci formation in HD results in deficient γH2AX focal distribution, similar to what was described in the study conducted by the Ryu group (Jeon *et al.*, 2012); (ii) Deficient H2AX phosphorylation is a consequence of defective ATM signalling. This can also be explained by the deficit in 53BP1 recruitment (Baldock *et al.*, 2015; Blackford and Jackson, 2017; Lanz, Dibitetto and Smolka, 2019). Additionally, impaired ATM activity and consequent γH2AX foci formation, can also be caused by mtHTT cytoplasmic sequestration of pATM, as observed in Figure 3.3.4.

Nonetheless, these speculations do not explain the disparities in γH2AX signalling observed between neuronal and non-neuronal HD cells. Others have voiced concerns about the use of γH2AX as a way of detecting DSBs, since γH2AX can be formed in other types of damage, such as breaks created during replication in S-phase (Löbrich *et al.*, 2010). Since the primary fibroblasts used in this experiment were not arrested, it could be possible that γH2AX did not

correspond solely to DSBs. However, lesions occurring during S-phase present a pan-nuclear staining in contrast to the discrete foci observed in Figure 3.3.6 (Löbrich *et al.*, 2010). In addition, H2AX can also be phosphorylated by the other two PIKK, DNA-PK and ATR (Blackford and Jackson, 2017). Consequently, the presence of γH2AX foci in HD fibroblasts might not be solely related to ATM activity. Hence, arresting the primary fibroblasts by serum starvation or the use of replication inhibitors, such as aphidicolin, as well as DNA-PK and ATR inhibitors could have been suitable solutions to this problem.

3.4.3. Topoisomerase I poisons are toxic to Huntington's disease cells

Despite the differences in γH2AX signalling in non-neuronal and neuronal HD cells it was hypothesised that the accumulation of TOP1cc, together with defective TOP1-mediated DNA damage signalling observed in the HD cell models, would ultimately lead to increased unrepaired DNA damage and consequent cell death. Indeed, the results presented in Figure 3.3.7 and Figure 3.3.12 showed that both patient fibroblasts and GABAergic neurons from HD patients showed increased activation of apoptotic markers triggered by exposure to CPT. Furthermore, these findings were complemented by viability assays in HD patient fibroblasts, confirming hypersensitivity to CPT treatment. Thus, these results demonstrate that HD cells exhibit increased TOP1-mediated DNA lesions, which promote apoptotic cell death.

3.4.4. Final observations

The results showed in this chapter indicate mtHTT interferes with DDR signalling in response to TOP1cc-mediated DNA damage in several ways, including: (i) mtHTT mediates cytoplasmic sequestration of pATM; (ii) mtHTT hinders 53BP1 focal recruitment. Similar defects were shown in other polynucleotide disorder, such as *C9orf72*-ALS (Walker *et al.*, 2017; Nihei *et al.*, 2019). This provides an attractive possibility in which neurodegeneration in polynucleotide expansion disorders might be triggered by similar mechanisms. In addition, the increased cell death observed in HD cells after exposure to CPT suggests increased sensitivity of HD cells to TOP1 DNA lesions. Given that these lesions occur regularly in the brain, there is a possibility that accumulation of TOP1 mediated DNA damage together with defective DNA repair might contribute to neurodegeneration in HD.

For the next chapter I will focus on understanding the mechanisms by which 53BP1 signalling is disrupted in HD cells in response to TOP1-induced DNA damage.

Chapter 4: Crosslink between autophagy and dysregulated DNA damage response in Huntington's disease

4.1. Introduction

Histone PTM synchronise the response and repair of DSBs (Bai *et al.*, 2020). Ubiquitination is one of such PTM that orchestrate the strict hierarchy of events that culminate in the repair of DSBs (Singh *et al.*, 2019; Aquila and Atanassov, 2020) Two E3 ubiquitin ligases are involved in chromatin ubiquitination during DSB repair: RNF8 and RNF168 (Doil *et al.*, 2009; Bartocci and Denchi, 2013; Thorslund *et al.*, 2015; Schmid *et al.*, 2018).

Neuronal genome stability can be affected by impaired chromatin ubiquitination, leading to accumulation of DNA damage and resultant neuronal degeneration. Examples of that are seen when DNA damage related proteins involved in the cascade of histone ubiquitination are missing, or their activity is hindered. For instance, suppression of RNF8 was shown to harbour a negative impact on DSB repair in mice brains, by decreasing chromatin ubiquitination and the subsequent recruitment of 53BP1 and BRCA1, thus increasing neuronal degeneration (Ouyang *et al.*, 2015). Another example is shown in patients with radiosensitivity, immunodeficiency, dysmorphic features, and learning difficulties (RIDDLE) syndrome, associated with abortive RNF168 activity and concomitant with defective H2A ubiquitination and 53BP1 signalling (Stewart et al, 2009). Patients with RIDDLE syndrome manifest neurological symptoms, including ataxia (Devgan *et al.*, 2011). Also, in ALS-*C9orf72* models, limited RNF168 activity together with decreased H2A ubiquitination and lack of 53BP1 signalling has been reported (Walker *et al.*, 2017). Mice brains lacking RAD6B/UBE2B, the E2 conjugating for the E3 ubiquitin ligase RAD18, exhibited decreased H2B ubiquitination and reduced 53BP1 and BRCA1 signalling. As a consequence, RAD6B-deficient mice brains presented with increased genomic instability and neurodegeneration (Guo *et al.*, 2019). These reports document the importance of proper DNA damage-dependent histone ubiquitination in the maintenance of neuronal genomic stability, whereby disruption of the enzymes involved in the ubiquitination cascade results in impaired chromatin ubiquitination. Lack of histone ubiquitination then causes defects in the recruitment of DNA repair factors, which culminates in accumulation of unrepaired DNA damage and progressive neuron loss.

Growing evidence supports a link between protein degradation mechanisms, such as autophagy, and DDR. The first observation of a crosstalk between DNA repair and autophagy

was identified in autophagy deficient cells, where decreased Beclin1 levels, a central player in the regulation of autophagy, resulted in increased genomic instability (Karantza-Wadsworth *et al.*, 2007). Further proof demonstrating a strong connection between DDR and autophagy is evidenced by the fact that DNA damage activates autophagy. (Czarny *et al.*, 2015; Stagni *et al.*, 2021). The master kinase and DNA damage sensor, ATM, modulates autophagy in several ways. In response to DNA damage, ATM phosphorylates PTEN, triggering its nuclear translocation and further promoting autophagy induction (Chen *et al.*, 2015). Another way of ATM-mediated activation of autophagy is through inhibition of mTORC1 in response to elevated ROS levels (Alexander *et al.*, 2010). P53, a downstream substrate of ATM activity also plays a role in modulating autophagy (Mrakovcic and Fröhlich, 2018). Depending on its subcellular localization, p53 can act as both promotor and repressor of autophagy (Mrakovcic and Fröhlich, 2018; Stagni *et al.*, 2021). Nuclear p53 upregulates the expression of several autophagy related genes, including AMPK and PTEN (Feng *et al.*, 2005). On the other hand, cytoplasmic p53 induces activation of the autophagy repressor mTORC1, thus inhibiting autophagy (Tasdemir *et al.*, 2008).

Interestingly, the connection between autophagy and DDR is a two-way street: not only the DDR directly modulates autophagy, as exemplified before, but autophagy directly regulates the DDR (Hewitt *et al.*, 2016; Y. Wang *et al.*, 2016; Feng and Klionsky, 2017; Hewitt and Korolchuk, 2017). Orchestration of DDR by autophagy can occur through regulation of histone ubiquitination (Y. Wang *et al.*, 2016; Singh *et al.*, 2019).

Although both 53BP1 (NHEJ promotor) and BRCA1 (HR) depend on the activity of RNF8 to be recruited to the damage sites, the persistent presence of RNF8 at the chromatin was shown to favour HR by preventing RNF168 binding to ubiquitinated H1 (Singh *et al.*, 2019). At the same time, RNF168 recruitment and consequent NHEJ induction depends on RNF8-mediated ubiquitination of H1 (Thorslund *et al.*, 2015). This suggests that for RNF168 activity to happen, RNF8 needs to ubiquitinate H1 and to be rapidly removed from the chromatin, leading to the repair by NHEJ. Thus, the choice between NHEJ and HR repair pathways depends on the tight regulation of the presence of RNF8 at the chromatin. This regulation is orchestrated by a complex formed by ataxin-3 and p97, which promotes RNF8 extraction from the chromatin and its proteasomal degradation (Singh *et al.*, 2019).

Another regulatory mechanism employed by protein degradation upon chromatin ubiquitination during DDR is mediated by p62/SQSTM1 (Y. Wang *et al.*, 2016). P62 is an

ubiquitin-binding protein that recognises cargos carrying K63-polyubiquitin chains and recruits them to autophagosomes or for proteasomal degradation (B. L. Lee *et al.*, 2017; Lee, Kim and Ryu, 2017). P62 was found to negatively regulate histone ubiquitination through inhibition of RNF168 activity, thus preventing H2A K13/K15 ubiquitination and leading to defective 53BP1 and BRCA1 recruitment (Y. Wang *et al.*, 2016).

The association between p62 and defective histone ubiquitination is of great interest in the context HD since p62 accumulation and aggregation is often present in neurodegenerative diseases, as a consequence of dysregulated autophagic degradation (Gal *et al.*, 2007; Pircs *et al.*, 2018; Ma, Attarwala and Xie, 2019; Vicencio *et al.*, 2020). In fact, p62 accumulates into inclusion bodies and associates with ubiquitin-containing aggregates of proteins involved in various neurodegenerative diseases, including mtHTT aggregates in HD and in all inclusions found in ALS (Gal *et al.*, 2007; Ramesh and Pandey, 2017; Noguchi *et al.*, 2018). Interestingly, accumulation of p62 driven by ALS-*C9orf72* repeat expansions was found to disrupt ATM-mediated chromosomal-break repair due to defective H2A ubiquitination and concomitant impaired 53BP1 recruitment (Walker *et al.*, 2017).

Both expression of the mtHTT expansions and HD cell lines exhibited defects in 53BP1 signalling upon induction of chromosomal DNA damage, which is reminiscent to the findings observed in *C9orf72*-ALS models (Walker *et al.*, 2017). Moreover, both HD and ALS display similarities regarding impaired autophagy mechanisms. Given that, the following questions emerged: (i) Is H2A ubiquitination, specifically at K15, impaired in HD cells? (ii) If so, is p62 accumulation the perpetrator of such defects that result in the disruption of 53BP1 signalling observed in HD cells?

4.2. Hypothesis and Aims

In this chapter the hypothesis is that the defects in 53BP1 signalling observed are, in part, caused by defective chromatin ubiquitination due to p62 accumulation.

The aim of this chapter was to investigate the mechanisms that contribute to 53BP1 deficiency in HD cells in response to TOP1-mediated chromosomal DNA breaks. The specific objectives were:

- To analyse histone H2A ubiquitination levels is HD models.
- To verify p62 levels in HD cells.
- To test the effects of p62 depletion in 53BP1 signalling and cell viability in HD cells

4.3. Results

4.3.1. Mutant huntingtin impairs DNA damage induced H2A ubiquitination.

53BP1 uses its UDR motif to recognise the damaged-induced H2AK15ub, a ubiquitination event catalysed by the E3 ubiquitin ligase RNF168 (Zimmermann and De Lange, 2014; Uckelmann and Sixma, 2017; Walser *et al.*, 2020). Recognition of ubiquitinated H2A by 53BP1 triggers its localization to the damaged chromatin, promoting NHEJ repair (Kashiwagi *et al.*, 2018). Therefore, the first aim of the current chapter was to understand whether the reduced 53BP1 signalling observed in HD cells was due to lack of H2A ubiquitination.

Chromatin-bound fractions from MRC5 cells expressing GFP-Q23 and GFP-Q74 were analysed by Western blotting using an antibody against H2A. The use of this antibody is advantageous since it recognises not only unmodified H2A, with a molecular weight of 17KDa, but also ubiquitinated forms of H2A ($H2A^{ub}$), which can be observed as band-shifts at a higher molecular weight (Figure 4.3.1 a and c). Other studies have also demonstrated this antibody is able to recognize ubiquitinated H2A (Walker *et al.*, 2017; Becker *et al.*, 2021).

Notably, expression of mtHTT (GFP-Q74) caused a decrease in H2A ubiquitination by ~3-fold in comparison with expression of wild-type HTT (GFP-Q23) (Figure 4.3.1 a and b). Next, to confirm these results in primary human cells, primary skin fibroblasts were subjected to chromatin fractionation and analysed by Western blotting after probing with an anti-H2A antibody. Similarly, Western blotting analysis of primary fibroblasts from the HD patient GM04869 showed a ~6-fold reduction in H2A ubiquitinated species in comparison with GM08402 fibroblasts (Figure 4.3.1 c and d). These results suggest HD cells have defective H2A ubiquitination.

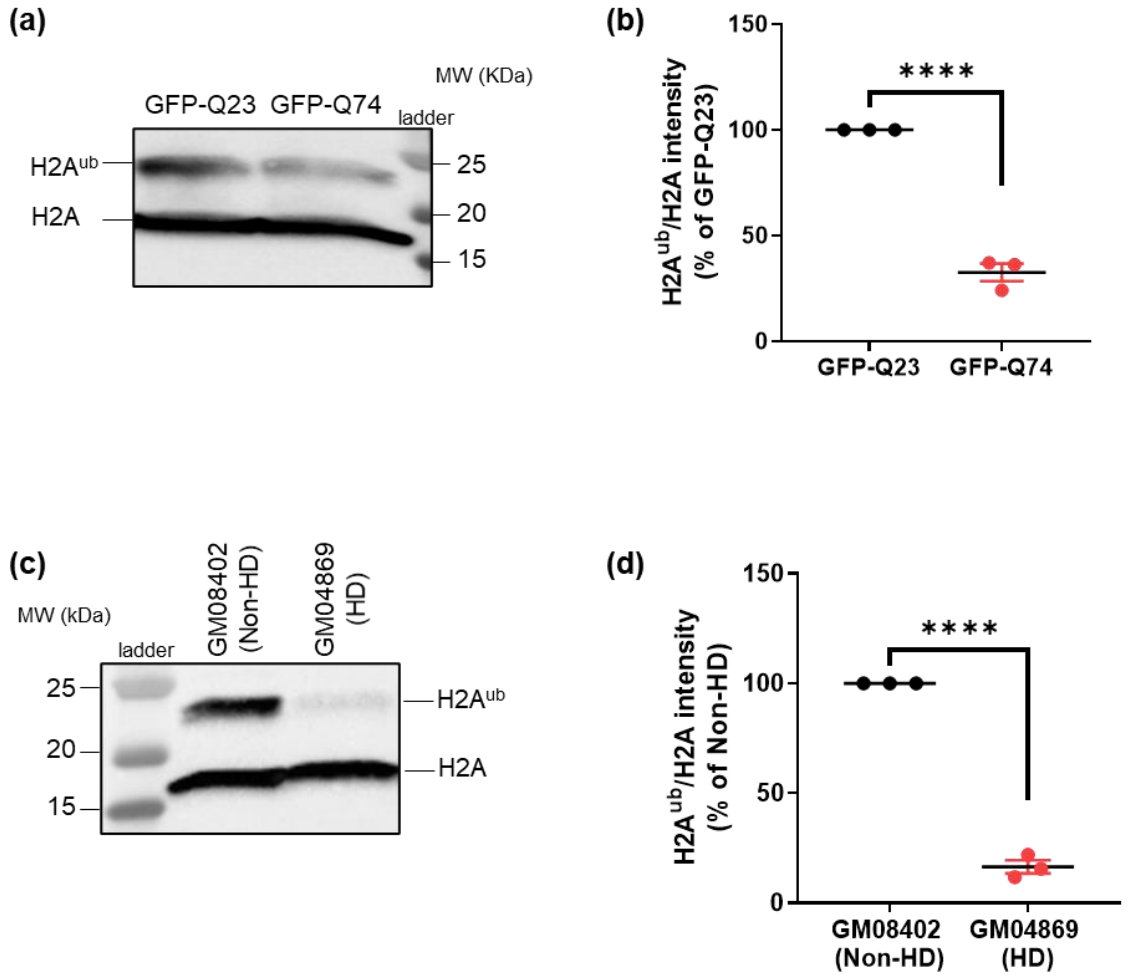

Figure 4.3.1 – Mutant huntingtin impairs H2A ubiquitination.

(a) Western blotting analysis of chromatin-bound fractions from MRC5 ectopically expressed with GFP-Q23 or GFP-Q74 plasmids after probing with an antibody against H2A. Bottom band at ~ 17KDa represents unmodified H2A, showing equal loading. Top band represents ubiquitinated H2A ($H2A^{ub}$). **(b)** Quantification of the relative band intensity of $H2A^{ub}$, normalised against the loading control (H2A) and presented as percentage of non-HD (% of non-HD) and analysed by unpaired Student's *t*-test. Error bars represent ± s.e.m. from 3 biological experiments. ****p<0.0001 **(c)**: Chromatin-bound fractions from GM08402 non-HD fibroblasts and fibroblasts from a patient with HD (GM04869) were analysed by western blotting using an antibody specific to H2A. Bottom band represents unmodified H2A, showing equal loading. Top band represents $H2A^{ub}$. **(d)** Densitometry analysis of $H2A^{ub}$, normalised against H2A (loading control) and presented as % of non-HD. The data was analysed by unpaired Student's *t*-test and is shown as means ± s.e.m (n=3). ****p<0.0001

H2A ubiquitination is a DNA damage-dependent post-translation modification. Different E3 ubiquitin ligases ubiquitinate H2A at specific sites, resulting in different cellular effects. RNF168 is responsible for ubiquitinating H2A on K13/K15, which triggers NHEJ by promoting the anchoring and stabilization of 53BP1 at the chromatin during DSB repair (Horn *et al.*, 2019). The polycomb repressive complex 1 (PRC1) ubiquitinates K118/K119 of H2A, responsible for transcriptional silencing. Lastly, the BRCA1/BARD1 dimer targets K127/129 for ubiquitination, which promotes end resection and, subsequently, triggers HR (Uckelmann and Sixma, 2017).

Although the Western blotting analysis using H2A antibody suggests defective H2A ubiquitination, this analysis does not show which specific H2A lysine lacks this modification. Since 53BP1 recruitment depends specifically on RNF168-mediated ubiquitination of H2A at K13/K15, the next step was to investigate the ubiquitination levels of histone H2A, specifically at K13 and K15. To do this, HEK293 cells were co-overexpressed with either GFP-Q23 or GFP-Q74, together with a Flag-H2A plasmid in which all known lysine residues (K5; K9; K118; K119; K125; K127 and K129) were mutated to arginine except K13 and K15 (Flag-H2A K13/K15). This way, performing a Flag co-immunoprecipitation (co-IP) assay would allow to specifically analyse the modifications occurring at K13/K15 of H2A. Other groups have, in fact, resorted to this approach to study H2A ubiquitination (Z. Wang *et al.*, 2016; Velimezi *et al.*, 2018).

To test which beads provided the best results, chromatin fractions from CPT-treated HEK293 cells, overexpressing the CAG expansions and the Flag-H2A K13/K15 plasmids were subjected to Flag co-IP assays, using either Anti-Flag M2 magnetic beads or by conjugating Flag antibody onto protein G Dynabeads.

Western blotting analysis of the eluates showed that when using the Anti-Flag M2 beads, it is possible to observe two bands at 25kDa and 50kDa after probing with and a specific Flag antibody (Figure 4.3.2 a). Given that both bands were present in the lane that corresponds to the empty-GFP transfected cells (Figure 4.3.2 a, first lane), which were not overexpressed with a Flag-containing plasmid, the results indicate that IgG heavy and light chains were denatured from the beads and recognised by the anti-mouse secondary antibody. The second and third lanes show stronger bands at the 25 kDa mark, when compared with the first lane. Since-Flag H2A has a molecular weight of around 20 kDa it is possible that Flag-H2A and IgG light chain bands are masking each other (Figure 4.3.2 a). On the other hand, when using magnetic protein

G Dynabeads, only one band was visualized at 20 kDa, in the second and third lanes, which corresponds to cells overexpressing Flag-H2A plasmids (Figure 4.3.2 b). Opposite to what was observed when using Anti-Flag M2 beads, no bands were detected on the empty-GFP lane (Figure 4.3.2 b, first lane). These results indicate that using protein G Dynabeads is a better option for the purpose of this experiment.

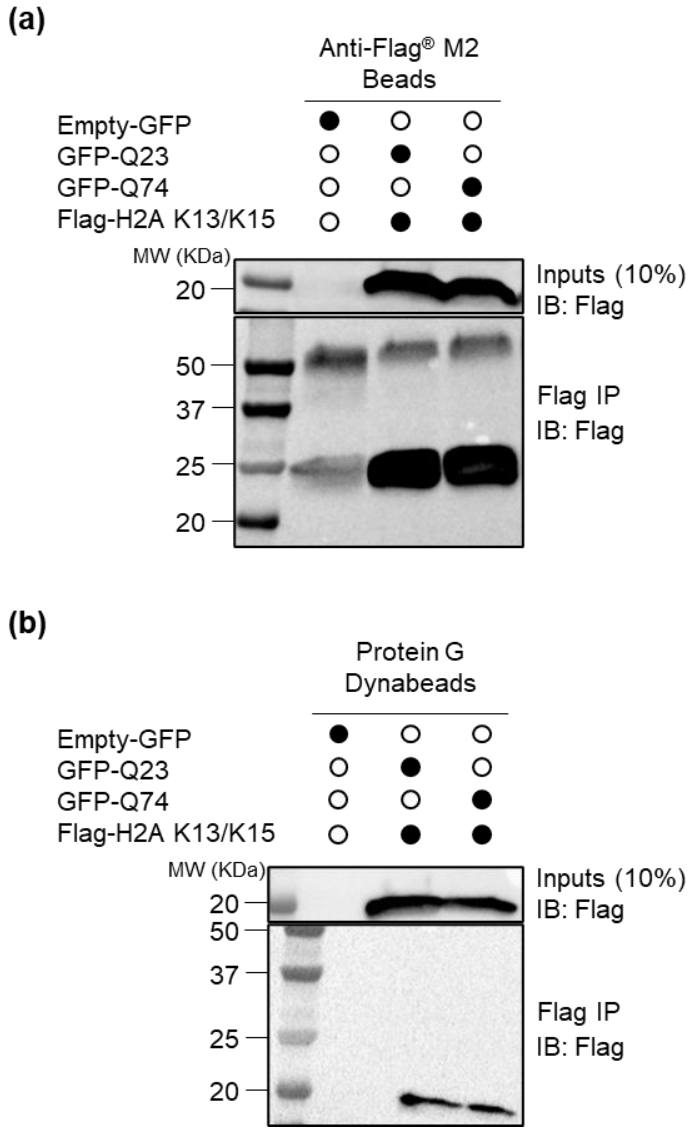

Figure 4.3.2 – Comparison of Flag immunoprecipitation assays using Anti-Flag® M2 beads and Protein G Dynabeads

Chromatin-fractions of HEK293 cells co-transfected with GFP-Q23 or GFP-Q74 together with a Flag-H2A-K5; K9; K118; K119; K125; K127; K129R mutant plasmid (Flag-H2A K13/K15) were incubated with either Anti-Flag® M2 magnetic beads or magnetic protein G Dynabeads after treatment with 10 µM CPT for 1h. Empty-GFP transfected cells were used as negative control **(a)**. 10% of the lysates (inputs) and the eluates from the Anti-Flag® M2 beads were analysed by western blotting after probing with an anti-Flag antibody. **(b)** 10% of the lysates (inputs) and the eluates from the protein G Dynabeads coated with a Flag antibody, were analysed by western blotting after incubation with a Flag antibody. Co-IP: co-immunoprecipitation; IB: immunoblotting. GFP-Q23: wtHTT; GFP-Q74: mtHTT.

To test whether mtHTT impacts H2A ubiquitination at K13 and K15, in response to TOP1-mediated chromosomal DNA damage, HEK293 cells transfected with GFP-Q23/Q74 and Flag-H2A K13/K15 were treated with 10 µM CPT for 1 h. After treatment, the chromatin fraction was extracted from the cells and incubated with magnetic protein G Dynabeads coated with a Flag antibody. Following co-IP the samples were eluted from the beads and subjected to Western blotting analysis, using a pan-ubiquitin antibody (FK2).

The cells that express wtHTT (GFP-Q23, second lane) possessed more ubiquitin bound to H2AK13/K15 in comparison to mtHTT cells (GFP Q74, third lane) (Figure 4.3.3 a and b). To note, although ubiquitin seems to stick non-specifically to the magnetic beads, as observed in the first lane, the strong Fk2 signal in the second lane indicates most of the ubiquitination analysed is specific to Flag-H2A K13/K15 (Figure 4.3.3 a). Thus, these results suggest faulty H2A ubiquitination in HD models, specifically at K13 and K15, which might explain the defective 53BP1 recruitment.

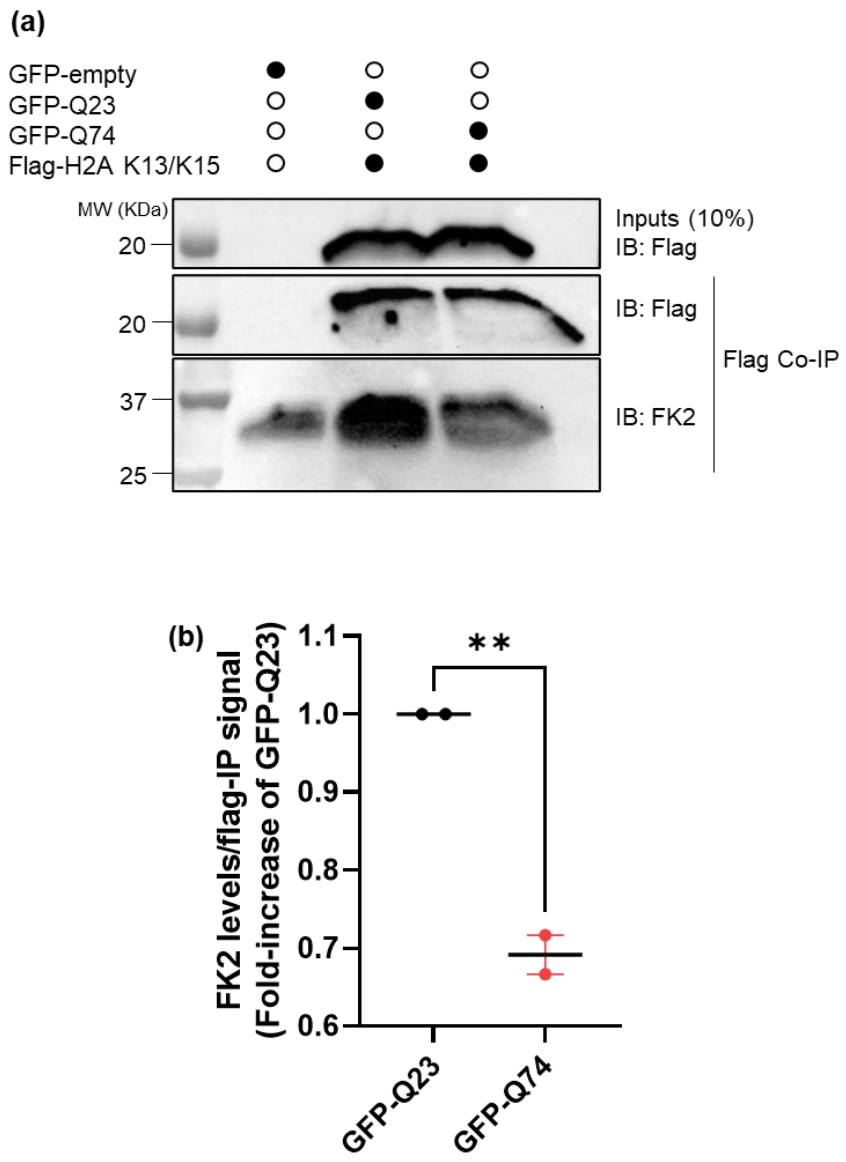

Figure 4.3.3 – Mutant huntingtin expression leads to defective DNA damage induced H2A ubiquitination at lysins 13 and 15

(a) Chromatin-fractions of HEK293 cells co-transfected with GFP-Q23 or GFP-Q74 and a Flag-H2A K5-9-118-119-125-127-129R mutant plasmid (Flag-H2A K13/K15) were subjected to Flag co-immunoprecipitation (Flag co-IP) after treatment with 10 μM CPT for 1h. Cells transfected with empty-GFP plasmid were used as negative control. H2A K13/K15 ubiquitination was detected using a pan-ubiquitin antibody (Fk2). 10% of the lysates were analysed by Western blotting after incubation with anti-Flag antibody, where GFP-Q23 and GFP-Q74 express similar levels of Flag-H2A K13/K15 (Inputs). **(b)** The levels of FK2 were quantified and normalised against the corresponding Flag-IP signal. Data is shown as means ± s.e.m. (n=2) and was analysed by unpaired Student's *t*-test. ***P* = 0.0065. Co-IP: co-immunoprecipitation; IB: immunoblotting; GFP-Q23: wtHTT; GFP-Q74: mtHTT.

4.3.2. Huntington's disease cells show increased p62 levels

Defects in selective autophagy is a common feature of neurodegenerative diseases (Martinez-Vicente *et al.*, 2010; Bhat *et al.*, 2014; Walker *et al.*, 2017; Abugable *et al.*, 2019). p62 is an autophagy receptor that accumulates in autophagy-defective cells (Y. J. Lee *et al.*, 2017). Overexpression of p62 was shown to negatively impact H2A ubiquitination by Wang *et al.*, (2016). Consequently, p62-induced loss of H2A ubiquitination results in defective recruitment of DNA repair factors, including 53BP1 (Y. Wang *et al.*, 2016; Walker *et al.*, 2017)

In line with these studies, the levels of p62 were verified in HD patient-derived fibroblasts and GABAergic neurons. Western blotting analysis of patient-derived skin fibroblasts showed that both HD GM04799 and GM04869 cells exhibit significantly increased p62 levels in comparison with the healthy GM08402 cells (Figure 4.3.4 a and b). Similarly, analysis of the p62 levels in GABAergic neurons by immunofluorescence, after probing with a specific p62 antibody, also showed a significant accrual in p62 levels in HD neurons, when compared to the CS14 non-HD neurons (Figure 4.3.4 c and d). These results suggest that HD cells tend to accumulate p62.

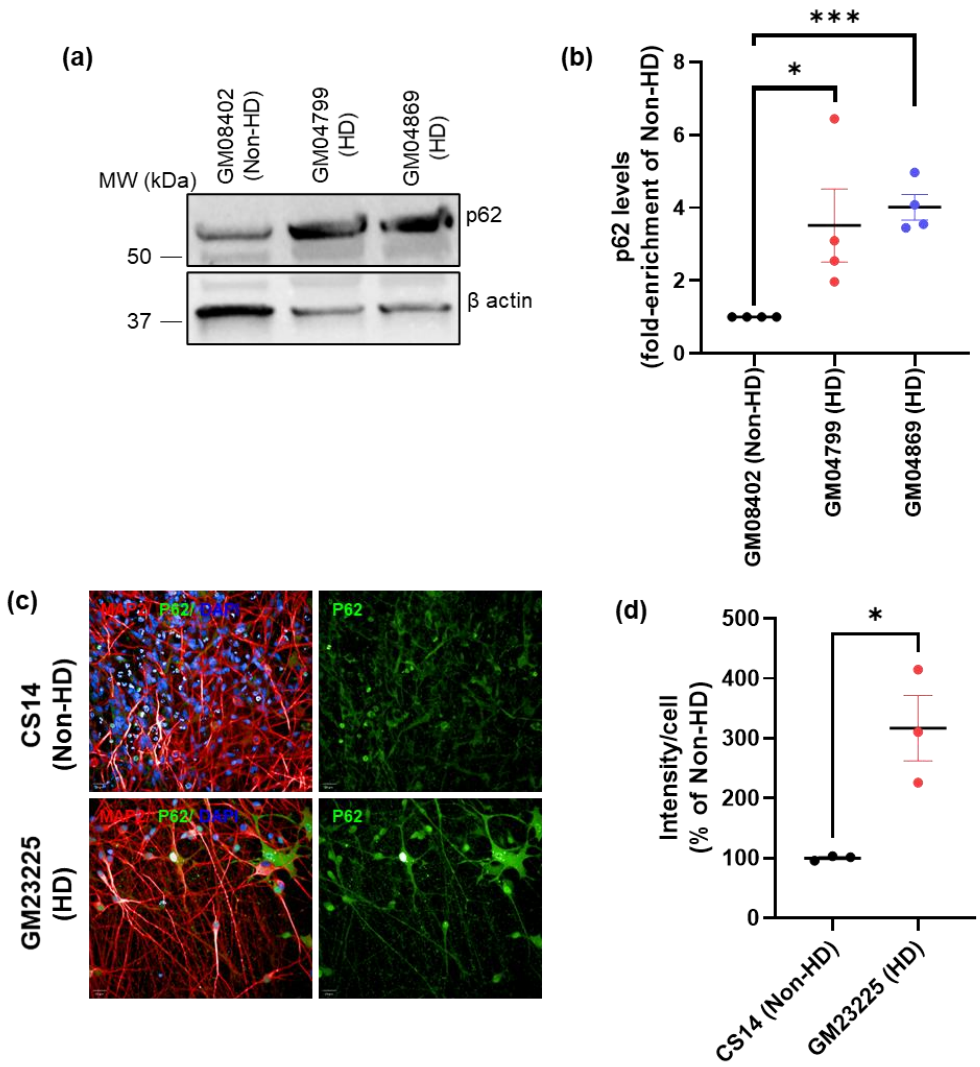

Figure 4.3.4 – Huntington's disease patient fibroblasts and GABAergic neurons show increased p62 levels

(a) Whole cell extracts from healthy non-HD primary cells (GM08402) and HD patient fibroblasts (GM04799 and GM04869) were analysed by western blotting using a p62 antibody. β actin corresponds to the loading control. **(b)** p62 levels were normalised against the corresponding actin levels and presented as fold-enrichment of non-HD cells (ratio between normalised-p62 values of each cell line against the normalised-p62 values of the non-HD cell line). The data was analysed by unpaired Student's *t*-test. Error bars: ± s.e.m. from 4 biological experiments. **P* = 0.0462; ****P* = 0.0001 **(c)** Immunofluorescence images of CS14 non-HD and GM23225 HD GABAergic striatal neurons differentiated from iPSC-derived iNPC and stained for p62. DAPI shows nuclear staining and MAP2 represents a neuronal marker (scale bar: 50μm). **(d)** Intensity of p62 per cell was quantified and is represented as percentage (%) of non-HD. Data was analysed by unpaired Student's *t*-test (error bars: ± s.e.m. from 3 technical repeats). *P = 0.0165

4.3.3. Depletion of p62 restores 53BP1 signalling and reduces sensitivity to topoisomerase I poisons in Huntington's disease cells

Since accumulation of p62 is associated to defects in DNA damage induced H2A ubiquitination and consequent impairment in the recruitment of DNA repair factors, it is possible that the 53BP1 defects observed in the HD cell models resulted from the negative effects exerted from the build-up of p62. Therefore, it was speculated that depletion of p62 would be sufficient to restore 53BP1 signalling in these cells.

To test this hypothesis, MRC5 cells were transfected with either GFP-Q23 or GFP-Q74. To knockdown p62, the cells were also transfected with siRNA particles that targeted either p62 (sip62) or a random sequence (siCTRL). After 48 h transfection, the cells were treated with 10 μM CPT for 1 h and analysed by immunofluorescence after staining with an anti-53BP1 antibody.

Firstly, p62 depletion was analysed by western blotting analysis (Figure 4.3.5 a). Next, the immunofluorescence analysis revealed that comparing the cells transfected with siCTRL after TOP1 DNA damage, GFP-Q23 cells showed a significant increase in the percentage of 53BP1 positive cells, with an average of 46.667% of the cells staining positive for 53BP1, while in the GFP-Q74 expressing cells, only an average of 16.00% of the cells were positive for 53BP1 signalling (Figure 4.3.5 b and c). Conversely, when p62 was depleted from the GFP-Q74 expressing cells, the percentage of 53BP1 positive cells increased to levels close to those of the GFP-Q23 cells (36.667% ± 2.9 vs 50.00% ± 5.8, respectively) (Figure 4.3.5 b and c).

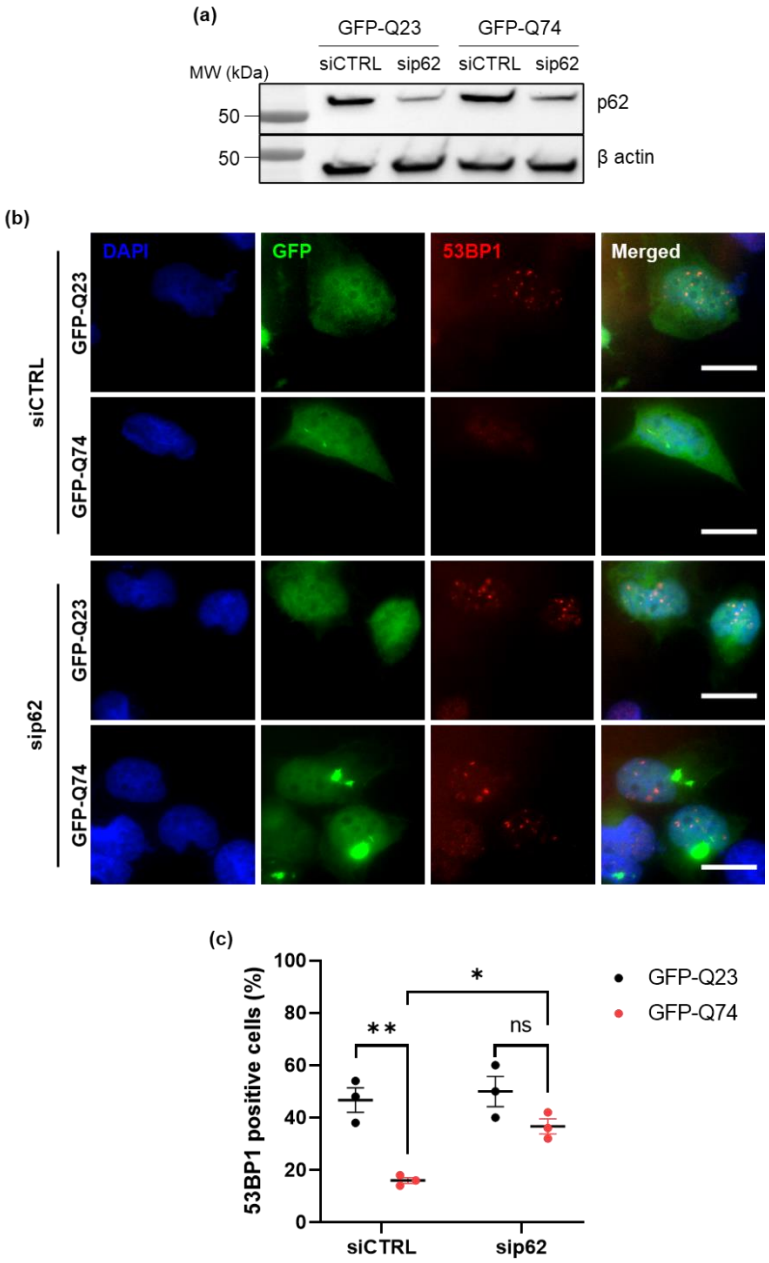

***Figure 4.3.5* – Depletion of p62 rescues 53BP1 recruitment.in cells overexpressing mutant huntingtin.**

MRC5 cells were co-transfected with either GFP-Q23 or GFP-Q74 alongside with siRNA against p62 or scramble (siCTRL) sequences. **(a)**. Whole-cell extracts were analysed by western blotting using an antibody specific to p62. β-actin shows equal loading **(b)** Immunofluorescence images of MRC5 cells ectopically expressing GFP-Q23 or GFP-Q74 and transfected with either control siRNA particles (siCTRL) or targeting p62 (sip62) after treatment with 10 µM of CPT for 1 h (scale bar: 10µm). DAPI: nuclei. **c)** The percentage 53BP1 positive cells (> 5 foci) was quantified and analysed by One-way ANOVA. The *post-hoc* Tukey's test was used for multiple comparisons. Data is presented as average of 3 biological replicates (50 GFP-transfected cells/ replicate) ± s.e.m. ***P* = 0.0029; **P* = 0.0276; ns, nonsignificant. GFP-Q23: wtHTT; GFP-Q74: mtHTT.

The next aim was to analyse whether p62 depletion also restores 53BP1 signalling in primary HD patient cells. For that, non-HD cells (GM08402) and GM04869 HD cells were transiently transfected with either siCTRL or sip62 particles, followed by treatment with 0.5 µM CPT for 1 h and stained for 53BP1.

Western blotting analysis confirmed depletion of p62 in both GM08402 and GM04869 cells (Figure 4.3.6 a). Immunofluorescence analysis showed that in cells transfected with siCTRL, the healthy GM08402 exhibited an average of 46.67% 53BP1 positive cells. In comparison, the GM04869 HD siCTRL cells showed a significantly lower percentage of 53BP1 positive cells, with 33.82% of the cells staining positive for 53BP1 (Figure 4.3.6 b and c). When p62 was depleted from the cells (sip62), CPT treatment induced an average of 51.27% of the GM08402 cells to stain positive for 53BP1, while the HD GM04869 cells showed a similar result, with an average of 53.40% 53BP1 positive cells (Figure 4.3.6 b and c). Together these results indicate that depletion of p62 is sufficient to reinstate 53BP1 signalling in HD cells.

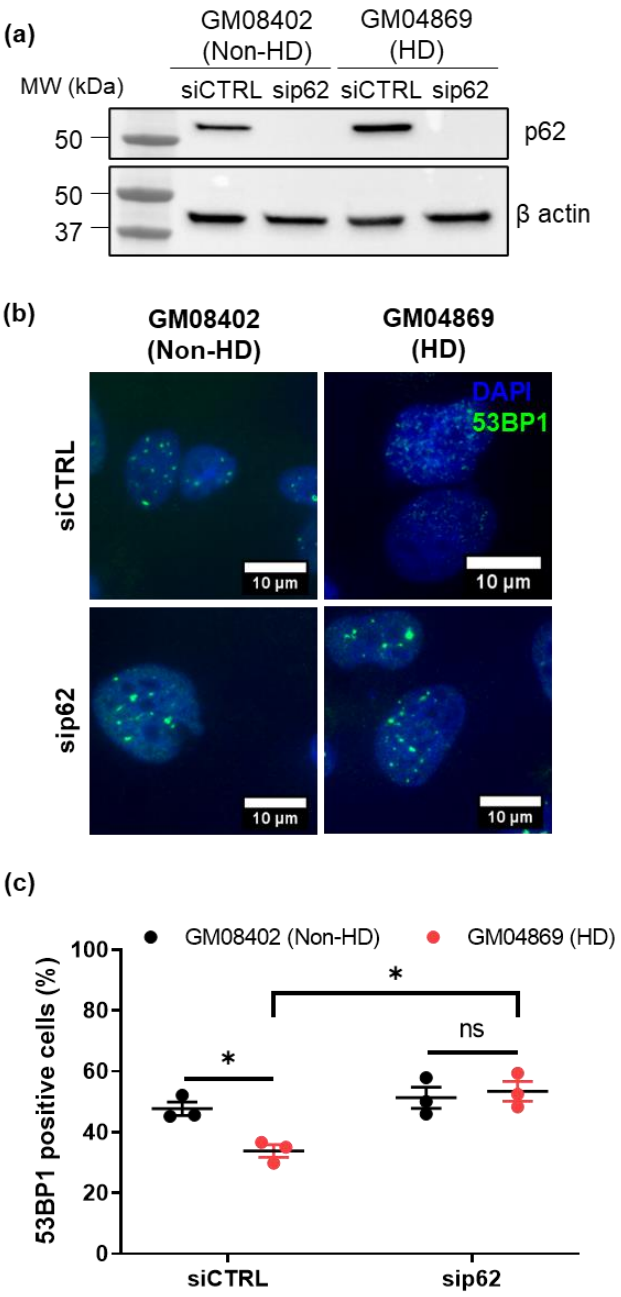

Figure 4.3.6 – p62 depletion restores 53BP1 signalling in HD primary skin fibroblasts.

(a) Non-HD (GM08402) and HD fibroblasts (GM04869) were transfected with either control siRNA particles (siCTRL) or targeting p62 (sip62) and analysed by western blotting using an antibody specific to p62. Actin staining shows loading. **(b)** Immunofluorescence images of non-HD GM08402 fibroblasts and fibroblasts from a patient with HD (GM04869) transfected sip62 or siCTRL after treatment with 0.5 µM of CPT for 1 h and stained for 53BP1 (scale bar: 10 µm). DAPI shows nuclear staining. **(c)** The percentage of cells showing more than five 53BP1 foci (53BP1 positive cells) was quantified. Data is presented as average of 3 biological replicates (10 fields/ replicate) ± s.e.m. The data was analysed by One-way ANOVA, followed by Tukey's multiple comparisons test. *P = 0.0349; ** P = 0.0053; ns, nonsignificant. CTRL: control.

Since effective 53BP1 signalling is crucial for proper NHEJ DNA repair and given that p62 depletion was able to restore the 53BP1 signalling defects in HD cells, one emerging question is whether depletion of p62 is enough to improve the ability of HD cells to sustain TOP1-mediated DNA damage. To answer this question, the goal was to test whether p62 knockdown results in reduced hypersensitivity to CPT treatment in primary HD cells.

As before, p62 was depleted by siRNA in both GM08402 cells and in two HD cell lines (GM04799 and GM04869), as confirmed by Western blotting (Figure 4.3.7 a). After siRNA transfection the cells were exposed to increasing concentrations of CPT (0 – 10 μM) for 96 h and the cell viability was monitored by CellTiter® blue assay (Figure 4.3.3).

By analysing the survival graph, it was possible to observe that, in the presence of p62 (in siCTRL transfected cells), both HD cells showed a more accentuated decrease in the percent survival with increasing CPT concentrations, where an average of 12.48% (GM04799) and 18.27% (GM04869) of the cells survived following exposure to 10 μM CPT. In comparison, the GM08402 siCTRL cells did not experience such decrease in the percent survival, with nearly half of the cells (51.14%) resisted treatment with 10 μM CPT (Figure 4.3.7 b). On the other hand, p62 depletion ameliorated the decrease in the percent survival of both HD cell lines, displaying a percentage of surviving cells at 10 μM CPT close to those of the GM08402 sip62 cells (GM08402: 57.988% ± 6.1; GM04799: 46.481% ± 3.6; GM04869: 55.015% ± 3.9) (Figure 4.3.7 b).

For a more accurate comparison of the dose-response curves between the different conditions, the area under the dose response data, or area under de curve (A.U.C.) was computed. GM04799 and GM04869 HD cells transfected with siCTRL exhibited a highly significant lower A.U.C, in comparison with the GM08402 siCTRL cells, which is consistent with increased cell death (Figure 4.3.7 c). Conversely, after depletion of p62, the A.U.C. of both HD cells were similar to the A.U.C. from GM08402 cells, which suggests sip62 improved HD cell survival after CPT exposure (Figure 4.3.7 c). These results thus demonstrated that p62 depletion is beneficial to HD cells, ameliorating the hypersensitivity of HD cells to TOP1-induced DNA lesions, as observed by the reduced cell death in HD cells upon p62 depletion.

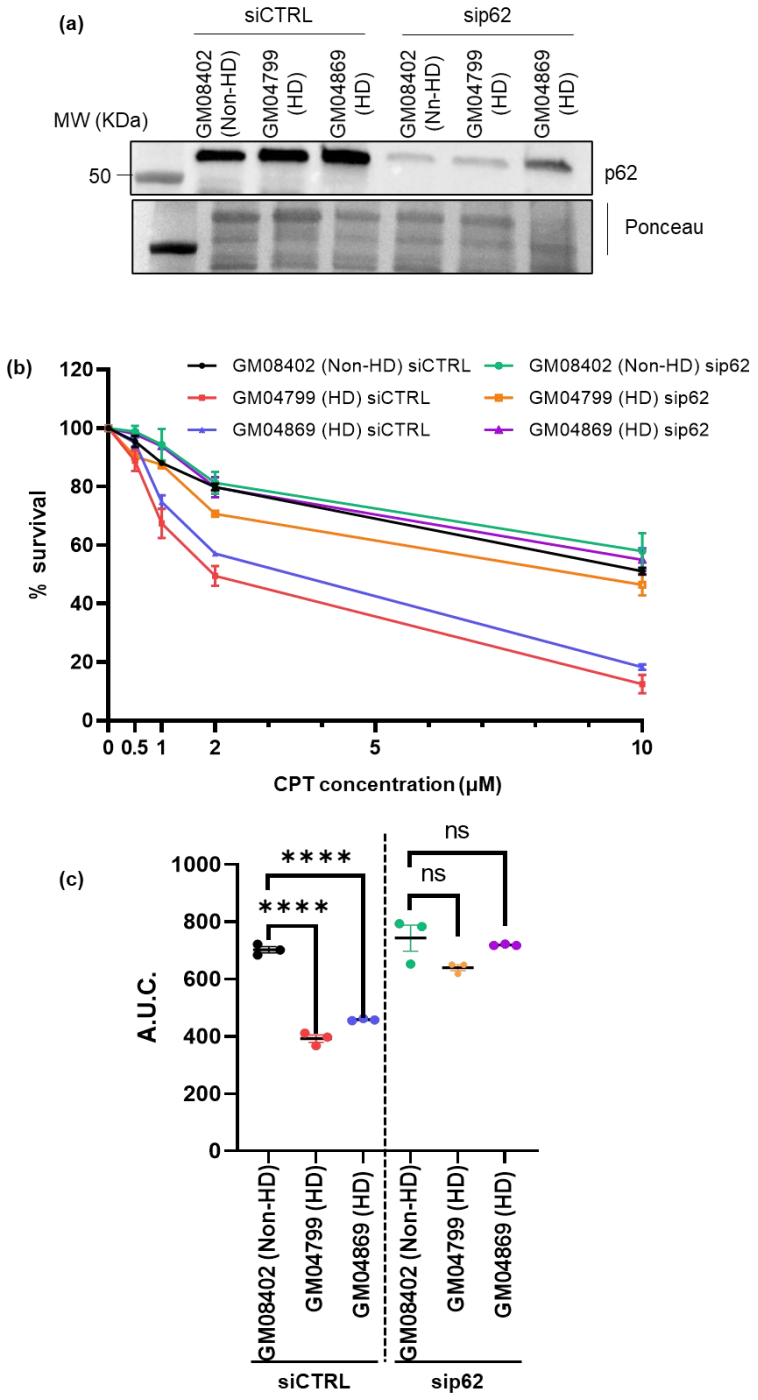

Figure 4.3.7 – p62 depletion ameliorates hypersensitivity of HD cells to TOP1 DNA damage

(a) Western blotting analysis of healthy (GM08402) and HD patient-derived fibroblasts GM04799 and GM04869 after siCTRL or sip62 transfection, using an anti-p62 antibody. Ponceau staining indicates loading. **(b)** Sensitivity to CPT treatment of non-HD and HD patient fibroblasts transfected with either siCTRL or sip62 was monitored by CellTiter-Blue® assay after 96 hours treatment with increasing concentrations of CPT (0-10 µM). Y-axis: mean percentage survival (% survival) of 3 biological experiments plotted against CPT concentration. % survival was assessed by normalizing against the corresponding untreated condition (0 µM). **(c)** The area under the curve (A.U.C.) was calculated for each condition and plotted as average of 3 biological replicates as in. (Balmus *et al.*, 2019) The data was analysed by unpaired Student's *t*-test (error bars: ± s.e.m.). ****p<0.0001; ns, nonsignificant.

4.4. Discussion

The central goal of this chapter was to investigate the mechanisms by which mtHTT elicits the 53BP1 signalling defects during the repair to TOP1-mediated chromosomal DNA damage. The fine tuning of DNA signalling is crucial for the repair of these genomic threats. Impaired 53BP1 signalling is a pathophysiological characteristic of neurological and neurodegenerative disorders (Stewart *et al.*, 2007; Walker *et al.*, 2017; Abugable *et al.*, 2019). An example of that is shown in ALS driven by the hexanucleotide expansions in the *C9orf72* gene, where defects in 53BP1 signalling are linked to another hallmark of neurodegenerative disorders: defective autophagy (Walker *et al.*, 2017; Walker and El-Khamisy, 2018). The main player responsible for these DNA repair defects is p62, which accumulates into aggregates in *C9orf72*-ALS cells.

Autophagy and the UPS are the two key pathways for clearance of misfolded proteins. When disrupted, misfolded proteins tend to aggregate and form toxic inclusions within the nucleus of cells (Kurosawa *et al.*, 2015). Defects in autophagy are common features of neurodegenerative diseases, including HD, thus explaining the tendency for protein aggregation characteristic of these disorders. Central to these mechanisms is p62, a key component for selective autophagy of ubiquitinated substrates. p62 accumulates in the nucleus of autophagy deficient cells as itself is a cargo for degradation (Kurosawa *et al.*, 2015; Hewitt *et al.*, 2016; Y. Wang *et al.*, 2016). Cumulative nuclear p62 is related with decreased efficiency in DSB repair processes by negatively regulating DNA damage-induced histone H2A ubiquitination (Y. Wang *et al.*, 2016; Feng and Klionsky, 2017). Consequently, cells with an abnormal accrual of p62 experience defects in the signalling of DNA repair factors such as 53BP1 and BRCA1.

Given these facts, I hypothesised that the weak 53BP1 signalling followed chromosomal DNA damage, in HD cells, is a consequence of defective chromatin ubiquitination caused by abnormal p62 build-up. To test this hypothesis, the levels of H2A ubiquitination and p62 in HD cells were investigated. Secondly, it was explored whether depletion of p62 re-established 53BP1 signalling and what consequences it had in the cell viability of HD cells after exposure to TOP1 DNA lesions.

In summary, HD cells exhibited weak histone H2A ubiquitination, more specifically in K13/K15 residues of H2A, thus hinting a causal mechanism for the 53BP1 defective signalling detected in HD cells. This was accompanied by increased p62 expression in both fibroblast and GABAergic neurons from HD patients. Excitingly, depletion of p62 from HD cell models resulted in the reinforcement of 53BP1 foci formation upon chromosomal DNA damage. P62

attenuation also ameliorated the adverse effects of CPT treatment in HD cells, as these cells were able to sustain TOP1-induced DNA damage as well as the heathy cells. The data presented here demonstrated that, in HD cells, the compromised NHEJ signalling results from defective chromatin ubiquitination, in part due to atypical p62 accrual. Together, these results support previously mentioned hypothesis.

4.4.1. Decreased histone DNA damage-induced H2A ubiquitination in HD models

The study of histone ubiquitination is of particular interest for the context of HD for the following reasons: (i) 53BP1 recruitment, which was shown to be defective in HD cells after TOP1-mediated DNA damage, depends on the presence of H2AK15ub; (ii) defects in histone ubiquitination have been reported to affect neuronal genome stability and are implicated in neurological syndromes and neurodegenerative disorders.

For example, absent H2A ubiquitination is observed in RIDDLE syndrome, a disease caused by mutations in RNF168 (Stewart *et al.*, 2009). Cells from RIDDLE patients also display defects in 53BP1 signalling consistent with lack RNF168-mediated H2A ubiquitination (Stewart *et al.*, 2007, 2009; Pietrucha *et al.*, 2017). The clinical manifestations of this disorder include ataxia and learning difficulties, showing that neurological impairment is triggered by faulty H2A ubiquitination and defective 53BP1 signalling (Devgan *et al.*, 2011). Similarly, depletion of RNF8, an E3 ubiquitin ligase upstream of RNF168, caused defects in H2A ubiquitination together with deficient 53BP1 signalling in mice neurons. This prompted accumulation of DNA damage, leading to neuronal degeneration. Consistently, mice depleted of RNF8 exhibited memory impairment (Ouyang *et al.*, 2015). Insufficient H2A ubiquitination is also observed in *C9orf72*-ALS models, resulting in accumulation of DNA damage and neurodegeneration (Walker *et al.*, 2017).

Likewise, the results presented in this chapter revealed that both ectopic expression of mtHTT and HD patient fibroblasts exhibited attenuated H2A ubiquitination. Further analysis was performed to test whether the H2A specifically lacked ubiquitination at K15, which mediates 53BP1 binding.

H2AK15ub was detected by taking advantage of IP techniques. Histone H2A harbours a total of eleven lysine residues. The site at which this modification occurs determines what signalling cascade is modulated, depending on its downstream reader (Uckelmann and Sixma, 2017). Given that, a Flag-H2A plasmid where all lysine sites were mutated to arginine, apart from K13/K15, was used as a bait for IP. Sequential Western blotting analysis of the eluates using a

specific antibody against ubiquitin (Ub), such as the Fk2 antibody, would then allow to investigate the ubiquitination status of Flag-H2A K13/K15. Others have used this technique to examine this same H2A modification. Works performed by Z. Wang *et al.*, (2016) and Velimezi *et al.*, (2018) used the commercially available Anti-Flag® M2 beads to immunoprecipitate Flag-tagged H2A. Another method is to manually conjugate the Flag antibody onto beads. In line with this, firstly it was assessed which of these methods served the best results.

Since the aim was to analyse ubiquitination of H2A and not to study whether H2A binds to ubiquitinated proteins, the IP was performed under denaturing conditions by adding SDS to the chromatin lysis buffer. The presence of SDS in the lysis buffer not only allows a better extraction of histones from the chromatin, but also denatures any non-covalent bond when performing a IP, thus ensuring that the data analysed refers specifically to any modification occurring at the residues under examination. The caveat of using SDS in an IP is that it denatures the antibody heavy and light chains, which can interfere with the results after Western blotting analysis of the eluates, since it will be picked up by the secondary antibody. In this scenario, since Flag H2A and IgG light chains have similar molecular weights (~20 kDa vs ~25 kDa, respectively) it was of upmost importance to avoid antibody denaturation from the beads. To achieve this, several measures were taken: (i) the Flag-antibody was crosslinked to the protein G Dynabeads; (ii) the lysates were diluted 10 times in dilution buffer (refer to materials and methods section) before being incubated with the beads; (iii) the elution was carried out by incubating the beads with 0.1 M citric acid pH 2.6 when using Dynabeads, or with 0.1 M glycine pH 3.0 when using Anti-Flag® M2 beads, instead of boiling the beads in the presence of SDS sample buffer.

Using the same conditions with both types of beads, it was possible to observe that when using magnetic protein G beads manually conjugated with a Flag antibody there was no antibody denaturation. Therefore, this was the best methodology for the aim of this experiment.

Analysis of the ubiquitination status of the K13/K15 residues of H2A after chromosomal DNA damage demonstrated that cells expressing mtHTT displayed weak H2AK13/K15 ubiquitination after CPT, thus supporting the hypothesis that impaired 53BP1 recruitment is caused by defects in H2A ubiquitination. These results reminisce to the defects observed in RIDDLE syndrome (Stewart *et al.*, 2009). In addition, ALS models also present similar

observations, thus supporting a link between defective H2A ubiquitination and neurodegeneration (Walker *et al.*, 2017).

The results showed in Figure 4.3.1 and Figure 4.3.3 demonstrate that inadequate H2A ubiquitination and subsequent defective 53BP1 signalling after TOP1-induced DNA damage underpins the cellular phenotypes observed in HD models and is possibly, in part, causative of the neurodegenerative phenotypes. These findings are not unprecedented since imbalanced histone ubiquitination has been reported in the context of HD. A study conducted by Yehuda *et al.*, (2017), demonstrated that aggregation of the expanded polyQ into ubiquitin-containing inclusion bodies accompanies histone H2B deubiquitination. Excitingly, the results demonstrated in this chapter provide an additional insight into the link between abnormal histone ubiquitination and defective DDR and its role in the pathogenesis of HD.

4.4.2. p62 accumulates in HD cells and interferes with 53BP1 signalling

p62 is a scaffold multifunctional protein (Ma, Attarwala and Xie, 2019). Through its multiple protein interaction domains, p62 participates in a plethora of cellular signalling pathways and is a major player in the maintenance of protein homeostasis via selective autophagy and UPS (Noguchi *et al.*, 2018; Sánchez-Martın and Komatsu, 2018; Jakobi *et al.*, 2020). Regarding its function in autophagy, p62 is an autophagic adapter and a cargo receptor, responsible for delivering ubiquitinated substrates for autophagosomal degradation. The UBA domain of p62 binds preferentially to K63-linked Ub chains, forming p62 bodies or sequestosomes. These bodies are then transported to the autophagosome, where LC3 protein continues autophagosome elongation. Cytosolic LC3 (LC3-I) is cleaved by Atg4 and its C-terminal is then lipidated on the inner surface of the nascent autophagosome, forming LC3-II (Runwal *et al.*, 2019). Through its LIR domain, p62 binds to LC3-II, enclosing the ubiquitinated cargos inside the autophagosome. This way both ubiquitinated cargos and p62 are degraded once the autophagolysome has matured. Thus, p62 is also a cargo for autophagic degradation and is frequently used as a biomarker for autophagic flux, as it accumulates when autophagy is compromised.

The involvement of p62 in neurodegenerative diseases, in particular those regarded as proteinopathies, has been widely studied. The hallmark of proteinopathies is the presence of deposits of aggregated misfolded proteins into ubiquitin-positive inclusion bodies (Ma, Attarwala and Xie, 2019). Alzheimer's disease is characterized by the deposition of β-amyloid protein into amyloid plaques and the formation of neurofibrils consisting of

hyperphosphorylated Tau (Lee, Lee and Rubinsztein, 2013). In Parkinson's disease, α-synuclein accumulates into ubiquitin-positive aggregates, forming the Lewis bodies (Engelender, 2008). In ALS, TDP-43-positive ubiquitinated inclusions are commonly found in the cytoplasm and nucleus of motor neurons (Junttila *et al.*, 2016). In HD, the presence expanded polyQ prompts mtHTT to misfold and aggregate into ubiquitin-positive insoluble inclusion bodies (Bhat *et al.*, 2014; Juenemann *et al.*, 2018; Sap and Reits, 2020). Similarly, in another polyQ disease, Machado Joseph Disease (or SCA3), formation of deposits of aggregated mutant ataxin-3 can also be found (Nóbrega *et al.*, 2013). Remarkably, p62 associates with all the protein aggregates mentioned, suggesting an effort to clear the neurons from the toxicity of these inclusions (Nagaoka *et al.*, 2004; Seidel *et al.*, 2010; Mori *et al.*, 2012; Drummond *et al.*, 2020; Trinkaus *et al.*, 2021). Unfortunately, another common characteristic shared by these proteinopathies is the absence of functional autophagic mechanisms (Menzies *et al.*, 2017). Consistently, in HD, the presence of mtHTT was shown to drive defects in selective autophagy by perturbing autophagosome-mediated cargo recognition. Although mtHTT increased initiation of autophagy and autophagosome formation, HD cells exhibited empty autophagic vacuoles, indication defective cargo clearance (Martinez-Vicente et al., 2010). Interestingly, under physiological conditions wtHTT physically interacts with p62 to facilitate the recognition of the K63-linked Ub cargos by p62 (Rui *et al.*, 2015). These studies demonstrate that the perturbation of autophagy in HD is a direct consequence of the loss of a native function of HTT, resulting in an impediment of p62 activity as an autophagic cargo receptor.

Besides the direct influence mtHTT displays on p62 function, another detail that is particularly interesting in the context of the present work is the fact that p62 directly controls efficiency of DDR by controlling histone ubiquitination. The Zhao group has demonstrated that when autophagy is impaired, p62 accumulates and counteracts chromatin ubiquitination (Y. Wang *et al.*, 2016).

In line with this I examined whether p62 accumulates in HD cells. As described in Figure 4.3.4, it was noticeable that p62 levels were increased in HD cells, indicating a predisposition for p62 accumulation in fibroblasts and striatal neurons from HD patients. In agreement with these findings, increased p62 levels have been reported in several HD models, including mouse Neuro2a cells expressing 150Q (Nagaoka *et al.*, 2004) and striatal neurons of HdhQ200 mice (Heng *et al.*, 2010). A recent report also described increased p62 expression in both HEK293 cells transduced with mtHTT (66Q) and in striatal neurons expressing mtHTT (Pircs *et al.*,

2018). Another study in R6/1 HD mice models, has shown reduced p62 levels in the mice brain in the early stages of the disease (Rué *et al.*, 2013). In the later stages, however, p62 accumulation was detected in the nuclei of striatal neurons, suggesting an age-dependent accumulation of p62 as the disease progresses, which is modulated by p62 aberrant interaction with mtHTT (Rué *et al.*, 2013).

Given the multifunctional properties of p62, one limiting factor is the fact that the analysis performed in this chapter does not reassure that the accrual of p62 observed is due to defective autophagy mechanisms. Measuring correlated autophagy biomarkers is a useful approach to complement the analysis of p62 levels. For instance, detection of LC3-II levels or calculation of the ratio between LC3-II and LC3-I is a commonly used method to monitor autophagy, since increased levels of LC3-II and elevated LC3-II/LC3-I ratio are indicative of dysregulation of the final stages of autophagy (Mizushima and Yoshimori, 2007; Yoshii and Mizushima, 2017). Excitingly, Pircs *et al.*, (2018) demonstrated that mtHTT hampers autophagy, concomitant with p62 accumulation and high levels of LC3-II and LC3-II/LC3-I ratio. Thus, the increased levels of p62 observed in HD cells are likely to be related to autophagy deficiency.

Given the negative impact p62 has on DNA damage dependent H2A ubiquitination, the hypothesis was that if HD cells were depleted of p62, then chromatin ubiquitination would be restored and 53BP1 signalling would be re-established. In support of this hypothesis, p62 depletion using siRNA ameliorated the adverse effects of p62 in DDR induced by chromosomal DNA damage. In both cells ectopically expressing mtHTT and in primary HD fibroblasts, sip62 reinstalled 53BP1 foci. These results are in agreement with another report showing that in *C9orf72*-ALS cells, depletion of p62 restores ATM signalling and NHEJ repair as it re-establishes RNF168-mediated H2A ubiquitination and 53BP1 recruitment (Walker *et al.*, 2017).

4.4.3. p62 as a therapeutic target in Huntington's disease

Since HD cells benefited from p62 depletion by restoring 53BP1 signalling in response to TOP1-mediated DNA damage, the next step was to determine whether depriving HD cells from p62 would also be advantageous for cell survival, ameliorating HD cell sensitivity to chromosomal DNA lesions.

As shown in Figure 4.3.7, depletion of p62 enhanced the survival of HD fibroblasts after exposure to CPT, while no perceptible changes were observed in the survival of non-HD

fibroblasts. Notably, these findings are reminiscent of a previous study showing that ablation of p62 reduced nuclear inclusions in the striatum and extended the life span of HD mice (Kurosawa *et al.*, 2015). The reduced nuclear polyQ inclusions and increased cytoplasmic aggregates followed by p62 depletion further indicates p62 is involved in the autophagic clearance of cytosolic polyQ inclusions (Kurosawa *et al.*, 2015). Defects in clearing toxic aggregates is a risk factor for neurodegenerative diseases such as HD (Martin *et al.*, 2015). Moreover, p62 is involved in multiple cellular pathways, many of them involved in the pathogenesis of HD. Therefore, although decreasing p62 levels restored 53BP1 response and led to better survival in HD cells after TOP1-induced DNA damage, the possible negative impact of p62 depletion require further investigation.

Nevertheless, the results suggest that increased p62 is, in part, responsible for increased sensitivity of HD cells to chromosomal DNA damage by preventing effective DDR signalling, possibly by negatively modulating DNA damage dependent H2A ubiquitination.

4.4.4. Final observations

The results shown in this chapter identified a novel mechanism dysregulated in HD. The central culprit of such disruptions is p62, whose accumulation is likely to be due to defective autophagy mechanisms, consequence of the polyQ repeat expansions in mtHTT. P62 negatively impacts HD cell response to chromosomal DNA damage by interfering with 53BP1 signalling, contributing to increased cell death. The regulation imposed by accumulative p62 in HD cells is likely to be through prevention of RNF168-mediated H2A ubiquitination, as suggested by the decreased ubiquitination levels at H2A K13/K15 in HD cells, the substates for RNF168 activity. However, it is not clear whether RNF168 is involved in this mechanism.

P62 accumulation and defects in chromatin ubiquitination and DNA repair are frequent pathological events that occur in other neurodegenerative disorders (Nagaoka *et al.*, 2004; Nóbrega *et al.*, 2013; Ouyang *et al.*, 2015; Walker *et al.*, 2017; Pircs *et al.*, 2018). Thus, this work further builds up on the possibility that similar molecular mechanisms underlie neuronal death in neurodegenerative diseases.

Since it remains elusive whether p62 toxic effects in the regulation of the DDR signalling in response to chromosomal DNA damage in HD cells are exercised through direct RNF168 inhibition, in the next chapter the involvement of RNF168 in HD pathogenesis will be explored.

Chapter 5: Mutant huntingtin drive RNF168 impairment via p62 aberrant interaction

5.1. Introduction

In response to DSBs, the E3 ubiquitin ligase RNF168 catalyses the ubiquitination of histone H2A. RNF168 not only monoubiquitinates but is also responsible for polyubiquitinating H2A with K63-, K48- and K27-linked chains (Pinato *et al.*, 2009; Mattiroli *et al.*, 2012; Gatti *et al.*, 2015). The substrates of all these ubiquitination events are K13 and K15 residues of H2A (Mattiroli *et al.*, 2012). Though to date the role for H2AK13ub has not been recognised, studies identified H2AK15ub as a docking site for the binding of several DSB repair related proteins: 53BP1, BARD1, RAD18, RNF169 and RNF168 itself, all bind to this ubiquitin mark, indicating RNF168-mediated ubiquitination of H2AK15 is crucial to initiate DSB repair (Fradet-Turcotte *et al.*, 2013; Hu *et al.*, 2017; An *et al.*, 2018).

Mechanistically, 53BP1 specifically reads RNF168-catalysed monoubiquitinated H2AK15, favouring the choice of NHEJ repair pathway (Fradet-Turcotte *et al.*, 2013). RAP80 also binds to the RNF168-produced K63-linked polyubiquitin chains on K15 of H2A via its ubiquitin-interacting motif (UIM) (Sobhian *et al.*, 2007). RAP80 counteracts HR by sequestering BRCA1-BARD1 into the BRCA1-A complex, thus limiting excessive DNA end processing (Sobhian *et al.*, 2007; Lombardi, Matunis and Wolberger, 2017). This way, BRCA1 cannot bind to PALB2 and restrict the loading of RAD51 onto the DSB, favouring NHEJ (Typas *et al.*, 2015).

RNF168 has also been described to promote the HR pathway by recruiting PALB2 to the chromatin in G2/S phase (Luijsterburg *et al.*, 2017). PALB2 was found to associate with K63-linked ubiquitin chains on H2AK15, only in the presence of RNF168, which facilitated the recruitment of BRCA1 and RAD51 (Luijsterburg *et al.*, 2017). In addition, monoubiquitination of H2AK15 by RNF168 recruits BARD1 to the damage sites, followed by accumulation of BRCA1, PALB2 and RAD51(Becker *et al.*, 2021; Krais *et al.*, 2021).

Deubiquitinating (DUB) enzymes are the off-switch of every ubiquitination signal (Hutchins *et al.*, 2013). Several DUBs have been found to specifically counteract the activity of RNF168 by cleaving ubiquitin from H2A (Nakada, 2016). USP3 was found to remove ubiquitin conjugates from the K13 and K15 residues of H2A, causing diminished recruitment of specific H2AK15ub interacting partners when overexpressed, including 53BP1, BRCA1 and RAP80

(Sharma *et al.*, 2014). Similar results were observed upon overexpression of USP44, another DUB that targets H2A K13/K15 (Mosbech *et al.*, 2013). USP51 is also a regulator of H2A K13/K15 ubiquitination in response to DNA damage (Z. Wang *et al.*, 2016).

Factors other than DUBs have been described to interfere with the activity of RNF168. In the absence of functional autophagy, p62 was reported to accumulate in the nuclei of cells and to physically bind RNF168, diminishing its E3 ligase activity (Y. Wang *et al.*, 2016). Consequently, autophagy deficient cells exhibit less RNF168-induced H2A ubiquitination and deficient recruitment of DDR factors, including 53BP1 (Y. Wang *et al.*, 2016). The physiological reasoning behind this interaction is unknown, but the toxic effects of p62-mediated inhibition of RNF168 and its consequences on the efficiency of DNA repair have been depicted in disease (Walker *et al.*, 2017; Walker and El-Khamisy, 2018).

The data described in the earlier chapters demonstrated the involvement of p62 in driving NHEJ defects in HD cells, as suggested by the reestablishment of 53BP1 foci upon p62 depletion. Further analysis showed that HD cells lack H2A ubiquitination specifically on K13/K15 residues, suggesting insufficient RNF168 activity. In line with these findings and given the documented influence of p62 in RNF168-mediated H2A ubiquitination, the following question has surfaced: Does p62 negatively regulate RNF168 activity through aberrant interaction and is this interaction responsible for the NHEJ defects observed in HD cells?

5.2. Hypothesis and Aims

In this chapter I hypothesised that in mtHTT expressing cells, p62 binds and inactivates RNF168 activity and disruption of this interaction restores 53BP1 signalling.

The aim of this chapter was to explore whether p62 interferes with RNF168 activity in HD. To achieve that, the specific goals were:

- To examine the interaction between p62 and RNF168 by co-IP in cells expressing the CAG expansion plasmids
- To test whether inhibition of RNF168:p62 interaction rescues 53BP1 signalling in cells expressing mtHTT

5.3. Results

5.3.1. Cells expressing mutant huntingtin exhibit increased p62 binding to RNF168

The data demonstrated in the previous chapters indicated that HD cells exhibit reduced 53BP1 foci formation and low levels of H2A K13/K15ub. Thus, there is a likelihood these defects are in part due to faulty RNF168 activity. Since p62 can physically bind to RNF168, resulting in inhibition of its E3 ubiquitin ligase activity, the first goal was to explore whether expression of mtHTT incites p62 binding to RNF168 (Y. Wang *et al.*, 2016).

To address this, RNF168 antibody was immobilised to magnetic beads and incubated with nuclear extracts of HEK293 cells expressing either GFP-Q23 or GFP-Q74. Western blotting analysis of the eluates showed that p62 strongly co-immunoprecipitated with RNF168 in nuclear extracts from cells expressing GFP-Q74 (lane 4), with a ~2.6-fold increase, whereas cells expressing GFP-Q23 (lane 3) showed less p62 pulled-down by RNF168 (Figure 5.3.1 a and b). The absence of bands in the first and second lanes of the co-IP blot (lanes 1 and 2) further proved the specificity of the RNF168 pull-down, demonstrating that p62 does not bind to the beads non-specifically (Figure 5.3.1 a, left blot).

10% of the nuclear extracts used for the RNF168 co-IP were also analysed by Western blotting. Interestingly this analysis revealed that cells overexpressing GFP-Q74 seemed to display decreased RNF168 expression (Figure 5.3.1 a, right blot). Nevertheless, the co-IP blot showed that similar amounts of the bait RNF168 was bound to the beads of both GFP-Q23 and GFP-Q74, indicating similar levels of RNF168 pulled-down different amounts of p62.

These results suggest that mtHTT expression promotes p62 interaction with RNF168. Therefore, the defective 53BP1 response to CPT observed might be explained by reduced RNF168 activity due to increased p62:RNF168 interaction promoted by mtHTT.

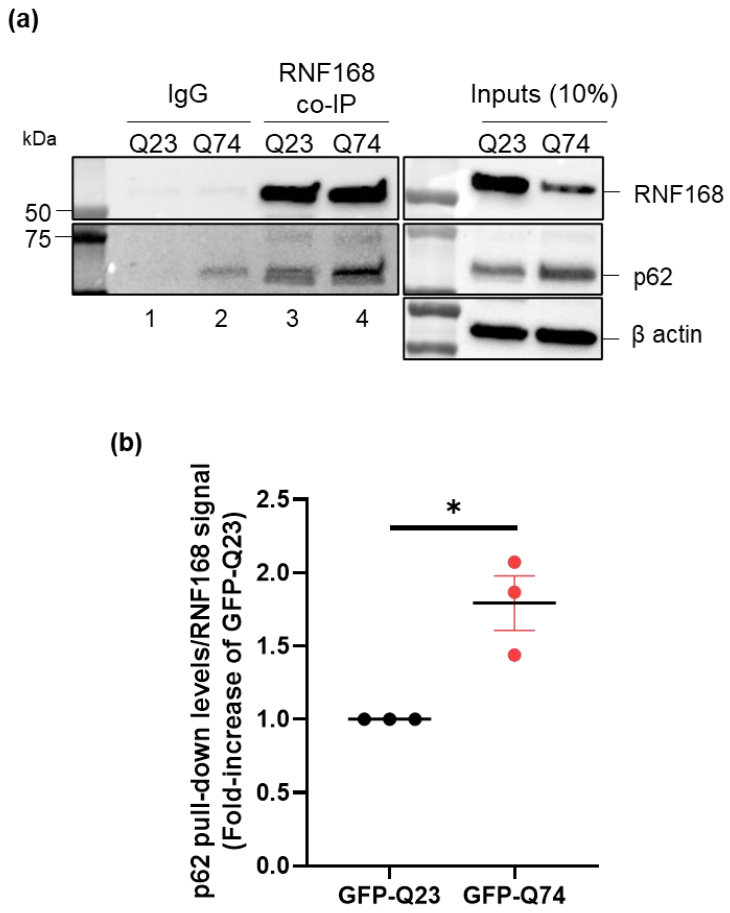

Figure 5.3.1 – Expression of mutant huntingtin incites p62 binding to RNF168

(a) RNF168 co-immunoprecipitation (RNF168 co-IP) was performed in nuclear fractions of HEK293 co-transfected with either GFP-Q23 or GFP-74. Left: Western blotting analysis show the interaction between RNF168 and p62. Right: 10% of the nuclear lysates were analysed by western blotting after incubation with anti-RNF168 and anti-p62 antibodies. Actin staining shows loading. (Q23: wild-type huntingtin. Q74: mutant huntingtin). **(b)** Pull-down levels of p62 were quantified and normalised against the levels of p62 present in the inputs. This value was further normalised against the bait RNF168. The data is shown as fold-increase of GFP-Q23. The data was analysed by unpaired Student's *t*-test. (± s.e.m., n=3). **P* = 0.0131.

5.3.2. Pharmacological inhibition of p62 binding to RNF168 restores 53BP1 signalling in cells expressing mutant huntingtin

The interaction between RNF168 and p62 was previously mapped: the LIN-11, Isl1 and MEC-3 (LIM) protein-binding (LB) domain of p62 interacts with the motif interacting with ubiquitin 1 (MIU1) of RNF168 (Y. Wang *et al.*, 2016). Given that the interaction between p62 and RNF168 is enough to abolish RNF168 activity, it was hypothesised that the disruption of this interaction would be sufficient to restore RNF168 ability to ubiquitinate H2A and therefore re-establish 53BP1 signalling in mtHTT cells.

Others have resorted to the use of oligopeptides to supress the interaction between two proteins (Nishitoh *et al.*, 2008). This is particularly exciting, since the mapping of the p62:RNF168 interaction supplied by Wang *et al.*, (2016) provide the opportunity to design a recombinant peptide that mimics the MIU1 domain and competes with RNF168 for the binding to the LB domain of p62, thus freeing RNF168 to execute its activity (Figure 5.3.2 a). In line with this, a RNF168-MIU1 oligopeptide tagged with rhodamine was designed using the amino acid sequence of the MIU1 domain of RNF168.

First, to test whether expressing cells with this recombinant peptide was sufficient to prevent p62 binding to RNF168, an RNF168 co-IP was performed. HEK293 cells were transfected with GFP-Q23 or GFP-Q74 plasmids and treated with either 5 μM MIU1 or DMSO (Mock) overnight. Consistent with previous data, increased levels of p62 were pulled by RN168 in the nuclear extracts from cells expressing GFP-Q74 in comparison with GFP-Q23 cells (Figure 5.3.2 b, lanes 3 and 4). This interaction was shown to be specific since the negative control IgG lanes do not show any bands (Figure 5.3.2 b, lanes 1 and 2). Notably, treatment with MIU1 was able to suppress the RNF168:p62 interaction in both GFP-Q23 and GFP-Q74 expressing cells (Figure 5.3.2 b, lanes 5 and 6). This was confirmed by the fact that although similar levels of the bait RNF168 can be visualized in lanes 3-6, in the lanes corresponding to the cells treated with MIU1 peptide (lanes 5 and 6), no p62 signal was detected (Figure 5.3.2 b).

.

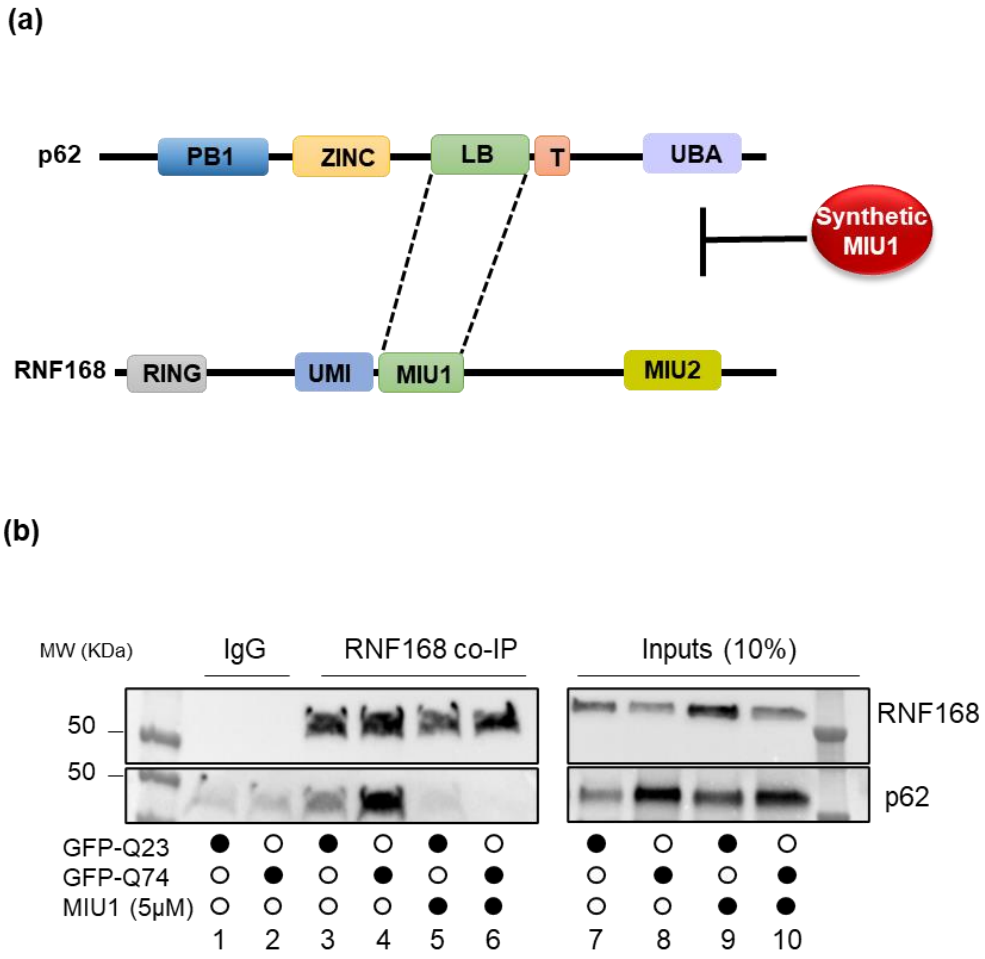

Figure 5.3.2 – Recombinant MIU1 peptide disrupts RNF168:p62 interaction

(a) Schematic representation of the interaction between p62 and RNF168. LB domain of p62 interacts with motif interacting with ubiquitin 1 (MIU1) of RNF168. The interaction between p62 and RNF168 is interrupted after treatment with a recombinant rhodamine-tagged peptide that mimics MIU1 domain of RNF168. **(b)** RNF168-CoIP was performed in nuclear fractions of HEK293 co-transfected with either GFP-Q23 or GFP-74. Left: Western blotting analysis show the interaction between RNF168 and p62 (lanes 3 and 4). The interaction is perturbed after incubation with 5μM recombinant MIU1 peptide for 24h (lanes 5 and 6). Right: 10% of the nuclear lysates were analysed by western blotting after incubation with anti-RNF168 and anti-p62 antibodies. (Q23: wild-type huntingtin. Q74: mutant huntingtin).

Next, I examined whether disrupting p62 binding to RNF168 with synthetic MIU1 rescues the defective 53BP1 phenotype in HD models. MRC5 cells expressing either GFP-Q23 or GFP-Q74 were exposed to 5μM recombinant MIU1 peptide overnight. To induce chromosomal DNA damage, the cells were then treated with 10 μM CPT for 1 h and stained with an anti-53BP1 antibody (Figure 5.3.3 a). After 53BP1 immunostaining, the analysis revealed that in both no peptide- and MIU1-treated GFP-Q23, cells responded to CPT treatment by forming 53BP1 foci, with a respective average of 58.0% and 51.3% of the cells staining positive for 53BP1 (Figure 5.3.3 b). In contrast, comparing with the no peptide-GFPQ23, the GFP-Q74 cells not exposed to MIU1 peptide (no peptide) exhibited significantly less cells staining positive for 53BP1 in response to CPT, with an average of 22.0%. After exposure to MIU1 peptide, cells expressing GFP-Q74 re-established 53BP1 response to CPT treatment, showing an average of 53BP1 positive cells resembling those of the MIU1-treated GFP-Q23 (53.3% vs 51.3%, respectively) (Figure 5.3.3 b).

These results suggest that in HD, RNF168 activity is reduced due to increased p62 binding, leading to defects in 53BP1 recruitment during DNA repair signalling. Treatment with a synthetic peptide that mimics RNF168 binding site to p62, liberated RNF168 and rescued 53BP1 foci formation during DDR signalling.

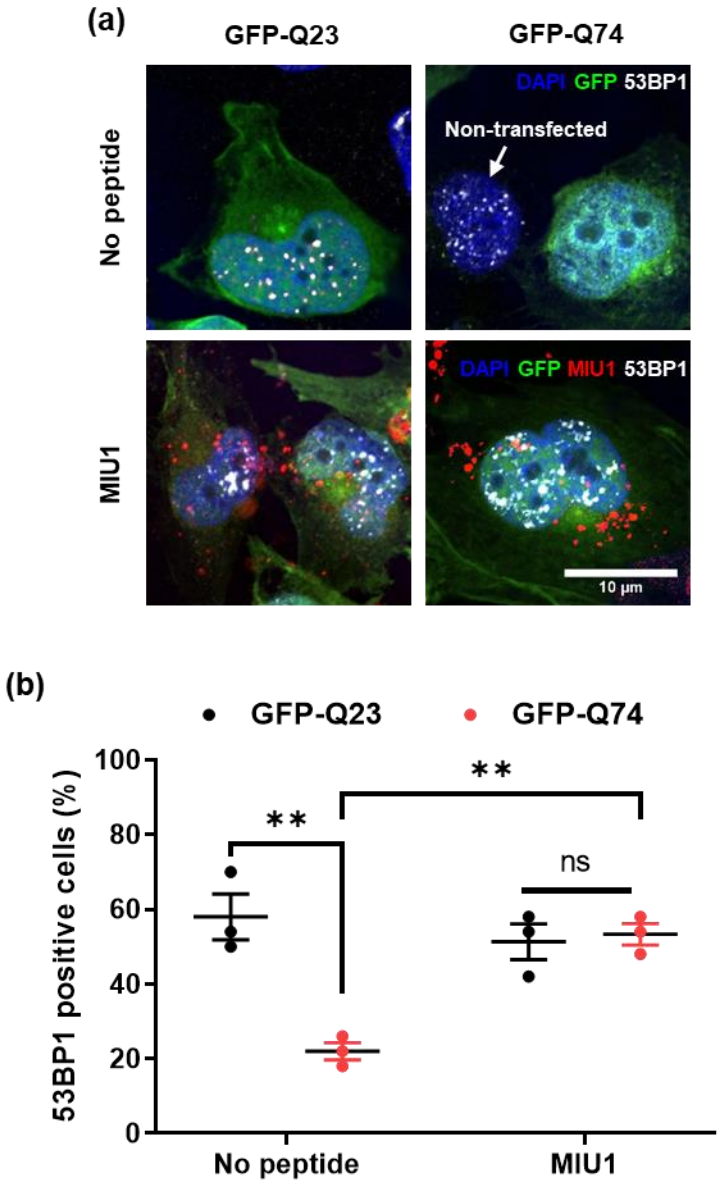

Figure 5.3.3 – Treatment with recombinant MIU1 re-establish 53BP1 foci formation in mutant huntingtin expressing cells.

(a) MRC5 cells were transfected with GFP-Q23 or GFP-Q74 plasmids and exposed to DMSO (no peptide) or 5 µM rhodamine-tagged synthetic MIU1 peptide. The cells were treated with 10 µM CPT for 1 h in all conditions and analysed by immunofluorescence (scale bar: 10 µm). DAPI shows nuclei. **(b)** The percentage of transfected cells showing more than five 53BP1 foci were quantified and analysed by One-way ANOVA- Multiple comparisons analysed by the *post-hoc* Tukey's test. Data is shown as average of 3 independent experiments (50 transfected cells each) ± s.e.m. ***P*<0.01; ns, nonsignificant.

The effect of MIU1 treatment on 53BP1 signalling was also explored in primary skin fibroblasts from healthy (GM08402) and HD (GM04799 and GM04869) individuals. The cells were treated with 5 µM MIU1 or mock for 24 h, followed by treatment with 0.5 µM CPT for 1h.

53BP1 immunofluorescence analysis showed that in the absence of recombinant-MIU1 (mock-treated cells), the GM08402 cells exhibited a significantly higher percentage of cells 53BP1 positive after induction of chromosomal DNA damage, in comparison with both HD patient fibroblasts (GM08402: 58.78%; GM04799: 31.78%; GM04869: 25.48%) (Figure 5.3.4 a and b). When cells were exposed to synthetic MIU1 peptide, 53BP1 phenotype was not altered: the percentage of cells positive for 53BP1 staining remained significantly higher in the GM08402 fibroblasts, with an average of 60.15% positive cells, while the HD GM04799 and GM04869 cells showed an average of 31.66% and 23.87% 53BP1 positive cells, respectively (Figure 5.3.4 a and b). These results indicate that as opposed to what was observed in MRC5 cells overexpressed with the HTT CAG expansions, the primary skin fibroblasts from HD patients failed to respond to treatment with the RNF168-MIU1 oligopeptide.

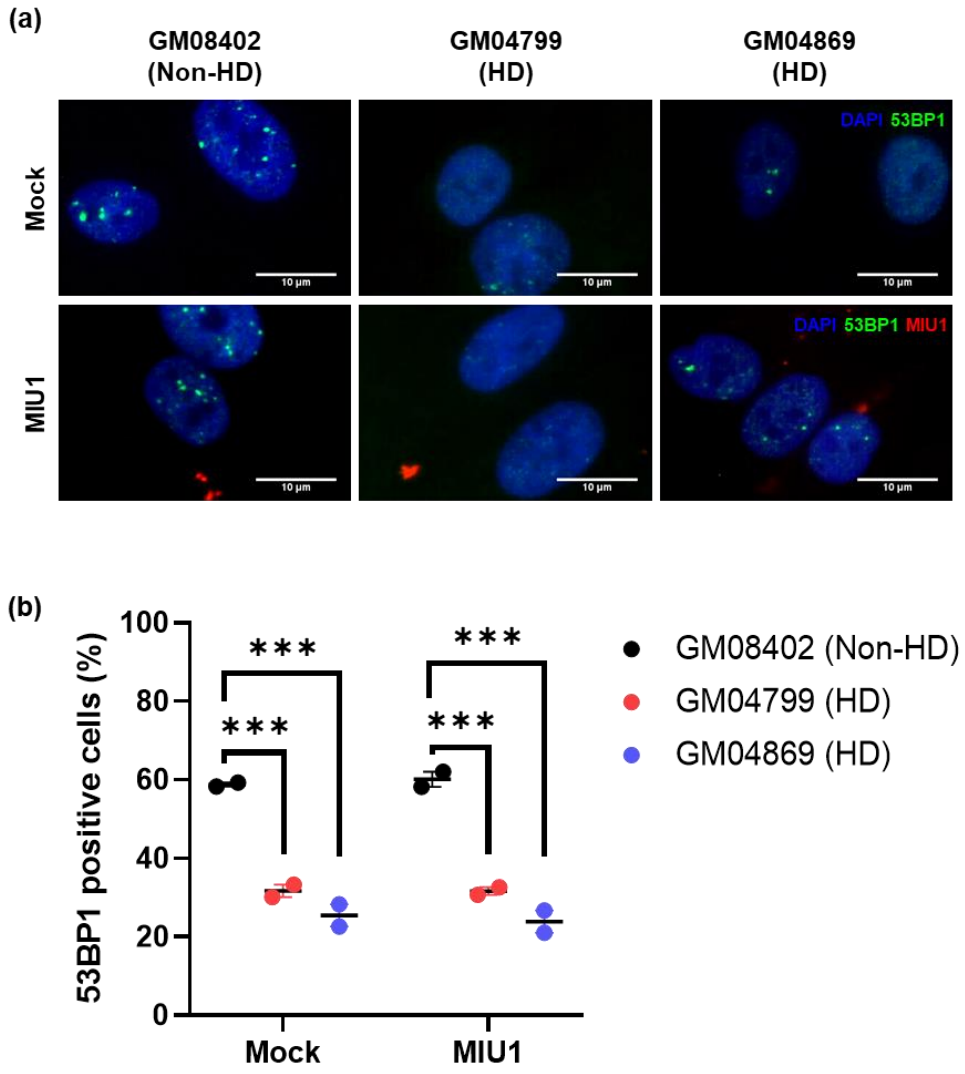

Figure 5.3.4 – Fibroblasts from patients with Huntington's disease failed to respond to treatment with recombinant MIU1.

(a) Non-HD GM08402 and HD GM04799 and GM04869 fibroblasts were exposed to either DMSO (no peptide) or 5 µM rhodamine-tagged synthetic MIU1. The cells were treated with 0.5 µM CPT for 1 h, followed by immunostaining with a 53BP1 antibody (scale bar: 10 µm). DAPI shows nuclei. **(b)** The percentage of showing more than five 53BP1 foci were quantified and analysed by One-way ANOVA, followed by Tukey's test for multiple comparisons. Data is shown as average of 2 independent experiments (10 fields each) ± s.e.m. ***$P < 0.001$.

5.4. Discussion

Based on the results of the previous chapters, it was hypothesised that p62 negatively affects the response and repair of chromosomal DNA damage in HD cells through inactivation of RNF168. Therefore, the aim of this chapter was to investigate the involvement of RNF168 in the pathogenesis of HD.

To test this hypothesis, first it was explored whether expression of mtHTT promoted the binding of p62 to RNF168. If this interaction impacted the response to TOP1-mediated DNA damage observed previously in HD cells, then interrupting this interaction would be sufficient to restore the DDR defects previously seen. By taking advantage of the information resulting from the mapping of the p62:RNF168 interaction (Y. Wang *et al.*, 2016), a recombinant MIU1 peptide was designed to perturb the aberrant interaction between p62 and RNF168.

In summary, mtHTT expressing cells exhibited an increased binding of p62 to RNF168. As expected, this interaction was responsible for the defects observed in 53BP1 signalling, since treating mtHTT cells with MIU1 oligopeptide resulted in re-establishment of 53BP1 foci in response to chromosomal DNA damage. Together, these results demonstrated that mtHTT instigates defects in DDR signalling and repair of TOP1-induced chromosomal DNA damage through p62-mediated inactivation of RNF168.

5.4.1. P62 interferes with 53BP1 signalling through inhibition of RNF168-mediated chromatin ubiquitination in HD cells

Neurological symptoms, manifested as learning disabilities and ataxia, are part of the phenotypic spectrum of RIDDLE syndrome (Devgan *et al.*, 2011). This suggests a neuroprotective role for RNF168 activity. According to Walker *et al.*, (2017), insufficient RNF168 activity is also involved in neurodegeneration observed in *C9orf72*-ALS, further contributing to this notion that RNF168 activity is crucial for neuronal homeostasis. Moreover, the fact that both RIDDLE and HD cells are characterized by increased radiosensitivity further suggests RNF168 contribution to the pathogenesis of HD (Stewart *et al.*, 2009; Ferlazzo *et al.*, 2014).

In the previous chapters it was demonstrated that HD cells exhibited defective DDR signalling in response to chromosomal DNA damage, resembling those observed in ALS models, namely: insufficient 53BP1 foci formation and lack of H2AK15ub, the specific marker for 53BP1 recruitment (Fradet-Turcotte *et al.*, 2013). H2AK15 is the substrate for the activity of the DSB-

related E3 ubiquitin ligase RNF168 (Mattiroli *et al.*, 2012). These results indicate that, like what happens in ALS cells, HD cells experience defective RNF168 activity. Another resemblance between ALS and HD cells is the tendency for accumulating p62 due to defective autophagy mechanisms (Gal *et al.*, 2007; Pircs *et al.*, 2018). The interest in p62 comes from the previous seminal report stating that p62 accumulates in autophagy deficient cells and directly binds to RNF168, perturbing its activity (Y. Wang *et al.*, 2016). Thus, this discovery provides a crosslink between two hallmarks of neurodegenerative diseases, including HD: deficient DDR signalling and repair, and insufficient autophagy mechanisms. In accordance, biochemical assays showed in

Figure 5.3.**1** indicate that the presence of mtHTT promotes the interaction of p62 to RNF168 in the nucleus of cells expressing the expanded HTT-CAG repeats.

This increased p62:RNF168 interaction could have two explanations in the context of HD: (i) mtHTT causes defects in autophagy mechanisms, leading to an abnormal accumulation of the cargo receptor p62, which then interferes with RNF168 activity; (ii) mtHTT directly influences the ability of p62 to bind to RNF168. The first point is an attractive explanation since defects in protein degradation concomitant with p62 accrual were described in HD models (Pircs *et al.*, 2018). The Zhao group also demonstrated that defects in DSB repair were more pronounced in autophagy-depleted cells, due to accumulation of p62 and consequent lack of RNF168-mediated H2A ubiquitination (Y. Wang *et al.*, 2016). In further agreement with this point, both the data presented in Chapter 4 and by Walker *et al.*, (2017) indicate accumulation of p62 is behind the defects in DDR signalling related to neurodegenerative diseases, since depletion of p62 restored 53BP1 signalling in both HD and ALS cells. However, explaining these observations solely on the increased p62 levels, can also be limiting in the context of HD.

Relative to the second point, a previous discovery pointed out a role of HTT in the activation of selective autophagy mechanisms through direct interaction with p62 (Rui *et al.*, 2015). In HD, impaired autophagy is related to deficient cargo recognition, a step that under physiological conditions involves both p62 and HTT (Martinez-Vicente *et al.*, 2010; Rui *et al.*, 2015). As confirmed by the Zhang group, the aberrant association between mtHTT and p62 in HD cells confer a loss-of-function to the ability of p62 to recognise and sequester K63-linked polyubiquitinated cargos, leading to the accumulation of empty autophagosomes (Rui *et al.*, 2015). Since the central player in both autophagic cargo recognition and autophagy-mediated inhibition of RNF168 is p62 (Rui *et al.*, 2015; Y. Wang *et al.*, 2016), one could expect that

mtHTT would also modulate the ability of p62 to bind to other of its interacting partners, including RNF168. In other words, mtHTT could simultaneously confer a toxic gain-of-function to p62, by inciting structural changes in p62 that favour an interaction with RNF168. In this scenario, the speculation is that the aberrant interaction of mtHTT would hide the UBA domain of p62, responsible for recognising K63-linked polyubiquitinated cargos, while exposing the LB domain of p62, thus facilitating RNF168 binding. However, this possibility is less likely since the RNF168 co-IP assays shown in this chapter were performed in cells expressing the exon 1 of the *HTT* gene, which corresponds to the N-terminal of HTT protein. Instead, p62 binds to the C-terminal of the HTT protein (Rui *et al.*, 2015). In fact, when probing the co-IP blots with GFP, no GFP signal was detected. This confirms that at least in the models presented here, the N-terminal of mtHTT protein, and consequently the expanded polyQ tracts, is not directly involved in the abnormal interaction of p62 to RNF168.

Nonetheless, some questions still remain unanswered: (i) What is the role of the expanded polyQ repeats in mtHTT in modulating p62:RNF168 interaction? (ii) Is there a link between full-length mtHTT and the increased binding of p62 to RNF168?

Another important factor to have in consideration is the subcellular localization on which these events are occurring. Whilst the role of HTT and p62 in selective autophagy is restricted to the cytosol (Rui *et al.*, 2015), the aberrant interaction between p62 and RNF168 occurred in the nuclear fractions of mtHTT expressing cells. This may suggest that in the cytosol, mtHTT directly interferes with p62 role in selective autophagy, leading to a build-up of p62 due to inefficient degradation. The pool of p62 that accumulates in HD cells then possibly translocates to the nucleus, leading to RNF168 inactivation. In conformity with this assumption, a recent study has demonstrated that in virus-infected cells, inhibition of autophagy promotes nuclear translocation of p62 and increased oxidative DNA damage (Wang *et al.*, 2019). Further depletion of p62 rescued RNF168-mediated histone ubiquitination, which agrees with the findings demonstrated in this thesis.

Interestingly, ROS-induced DNA damage is known to promote trapping of TOP1 onto neuronal DNA (Sordet *et al.*, 2008), implying that autophagy defects mediated by mtHTT could feed more TOP1-mediated chromosomal DNA breaks, further contributing to increasing genomic instability in HD neurons. In contrast, inhibiting autophagy in prostate cancer cells did not incite p62 interaction with RNF168, despite the observed defects in RNF168-mediated H2A ubiquitination and p62 accrual (Sharma *et al.*, 2018). Instead, p62 accumulated preferentially

in the cytoplasm and RNF168 activity was counteracted by USP14, a DUB that controls the ubiquitination on RNF168 (Sharma *et al.*, 2018). This suggests that different mechanisms operate in different disease settings. Hence, the data presented in this chapter is in line with the studies performed by Walker *et al.*, (2017) and Wang *et al.*, (2019) and suggest that the increased interaction between RNF168 and p62 in the nuclei of mtHTT expressing cells is a consequence of defective selective autophagy and subsequent build-up of nuclear p62, rather than a direct effect of polyQ expanded tracts on p62 interactome.

Despite the aforementioned uncertainties, pharmacological perturbation of the aberrant interaction between p62 and RNF168 using an RNF168-MIU1 derived oligopeptide was sufficient to restore 53BP1 signalling in cells ectopically expressing mtHTT. These results provide evidence that deficiencies in RNF168 activity are involved in the pathogenesis of HD and that these deficiencies are perpetrated by p62 increased interaction with RNF168. It is important to mention that it was decided to use MRC5 cells for the immunofluorescence assay since these cells attach to the surface more efficiently than the HEK293 cells. HEK cells were used for the RNF168 co-IP to test the ability of the peptide to interrupt the binding of p62 to RNF168, since this experiment demanded high amounts of lysate, which would require a greater number of cells and a larger volume of MIU1 peptide if the co-IP was performed in MRC5. Still, the increased levels of 53BP1 signal in mtHTT expressing cells and the MIU1-rhodamine signal detected in wtHTT and mtHTT cells (Figure 5.3.3), indicate that the peptide efficiently prevented p62:RNF168 in MRC5 cells as well. Another interesting observation was the fact that recombinant MIU1 also disrupted p62:RNF168 interaction in wtHTT cells. Even so, interrupting p62:RNF168 did not interfere with 53BP1 signalling in these cells. This data and the study conducted by the Zhao group indicates that the interaction between RNF168 and p62 also happens under physiological condition (Y. Wang *et al.*, 2016). However, the biological role of this interaction, particularly in the context of DNA repair remains elusive.

A previous study showed another p62-mediated link between protein degradation mechanisms and DDR, where p62 was shown to promote proteasomal degradation of RAD51 (Hewitt et al., 2016). An appealing possibility is that p62 could also promote RNF168 degradation. This explanation would connect the increased interaction between p62:RNF168 and the low levels of RNF168 in mtHTT expressing cells observed after Western blotting examination of the inputs in Figure 5.3.1a. However, as shown in the inputs blot of Figure 5.3.2b, disruption of p62:RNF168 interaction by recombinant MIU1 did not seem to increase the levels of RNF168

in mtHTT expressing cells, as one would expect if p62 incited RNF168 degradation. To note, the RNF168 co-IP assays after treatment with MIU1 peptide were only performed once. First, because the reasoning behind this experiment was to confirm that the peptide disrupted the interaction between p62 and RNF168, while the actual read-out was to test the effects on 53BP1 signalling. Second, due to the increased amounts of peptide this experiment requires. Inferring about the levels of RNF168 in HD cells was beyond the scope of this project, still, it would be interesting to investigate further on this matter. Nonetheless, the results presented here suggest disruption of p62:RNF168 interaction might constitute a new therapeutic strategy for HD. Further examination is necessary to assess possible toxic effects on normal cell functioning of this approach.

When examining the effects of MIU1 in primary HD patient cells, no changes in the 53BP1 phenotype were observed. The synthetic peptide was designed to harbour a rhodamine tag at the C-terminal. This way, immunofluorescence analysis would detect whether the MIU1 oligopeptide had penetrated the cells. Indeed, the rhodamine signal (labelled as MIU1) was detected in Figure 5.3.3a, which indicates the peptide was delivered into the cells. Conversely, as demonstrated in Figure 5.3.4a in patient fibroblasts, MIU1 signal could barely be detected, indicating the peptide did not enter the cells and was possibly washed off during the washing steps of the immunofluorescence assay. This could explain why no differences in 53BP1 signalling were seen in HD cells after treatment with MIU1.

Notably, primary human skin fibroblasts are considered hard-to-transfect cells, possibly due to low membrane permeability (Fountain, Lockwood and Collins, 1988; Mellott, Forrest and Detamore, 2013). Although studies usually refer to difficulties in delivering exogenous nucleic acids into the cells, these characteristics could also hamper the delivery of other macromolecules, including peptides. Cell penetrating peptides (CPPs) or protein transduction domains (PTDs) are short peptides that have the ability to transport cargos across cell membranes (Kabouridis, 2003; Ye *et al.*, 2016; Habault and Poyet, 2019). Since the discovery of the transactivator (TAT) peptide, a class of PTDs derived from the human immunodeficiency virus 1 (HIV-1), almost 2000 CPPs have been discovered (Habault and Poyet, 2019). Several studies have reported that fusing potential therapeutic peptides with PTDs, such as TAT or Antennapedia sequences, resulted in successful cellular internalization and ameliorated neurodegenerative phenotypes in HD and other polyQ disease models (Popiel *et al.*, 2007; Chen *et al.*, 2011; Zhang *et al.*, 2018). Thus, taking advantage of PTDs could be a

good strategy to enhance the delivery of MIU1 oligopeptide into the HD primary skin fibroblasts used in this study, and ultimately, into the GABAergic neurons from HD patients.

5.4.2. Final observations

In this chapter it was unveiled the involvement of a novel dysregulated molecular mechanism in the pathogenesis of HD that connects two major hallmarks of neurodegenerative diseases: defective DNA repair and dysregulated autophagy. According to the data shown here, RNF168 activity is compromised in mtHTT expressing cells due to increased binding of p62. These findings were validated by the fact that interruption of p62:RNF168 interaction rescued 53BP1 signalling in mtHTT cells. The data demonstrated here further corroborate the findings presented in the previous chapters that suggested the restricted 53BP1 signalling in HD cells in response to TOP1-induced chromosomal DNA damage is a consequence of cumulative p62, possibly due to defective autophagy, which limits H2AK15ub and consequently impairs NHEJ repair. This way, the ability of HD cells to properly defend their genome from one of the most common endogenous sources of neuronal genomic instability is hindered, leading to increased cell death. In addition, these results provide a new understanding about the mechanisms involved in HD and pave the way for the possible development of new therapeutic interventions that target p62:RNF168 interaction.

Chapter 6: General discussion

6.1. Overview

My PhD focused primarily on the study of DNA repair signalling in response to TOP1-induced chromosomal DNA breaks in HD. The interest in this topic derived firstly from the fact that chromosomal DNA breaks are physiologically relevant in the context of neuronal health, given these are common threats to neuronal genome stability (El-Khamisy *et al.*, 2005; Alagoz *et al.*, 2013; Carlessi *et al.*, 2014; Katyal *et al.*, 2014; Walker *et al.*, 2017). Secondly, accumulation of TOP1-associated DNA breaks underly the pathogenesis of several neurodegenerative diseases, including A-T (Katyal *et al.*, 2014), SCAN1 (El-Khamisy *et al.*, 2005) and *C9orf72*-ALS (Walker *et al.*, 2017). The latter is of particular interest in the context of this work given that *C9orf72*-ALS is also caused by mutations that lead to abnormal expansion of the polynucleotide repeats. However, there are some differences regarding this point: whilst HD is caused by an exonic CAG trinucleotide repeat expansion with consequent elongation of the polyQ tracts within the HTT protein, *C9orf72*-ALS is caused by an intronic G_4C_2 hexanucleotide repeat expansion within the *C9orf72* gene. Despite these differences, both HD and *C9orf72*-ALS are considered proteinopathies, meaning that defects in protein clearance and abnormal accumulation of misfolded protein aggregates underscore the pathogenesis of both disorders. Moreover, both pathologies are characterised by defects in DNA repair mechanisms (Massey and Jones, 2018; Abugable *et al.*, 2019; Kok *et al.*, 2021).

A previous report has demonstrated that a crosslink between defective DNA repair signalling, and impaired autophagy underlies *C9orf72*-ALS pathology by interfering with the repair of TOP1-induced DNA damage (Walker *et al.*, 2017). Despite the similarities between the two disorders, it is still unknown whether similar mechanisms operate in the context of HD pathology.

In Chapter 3, I demonstrated deficient 53BP1 recruitment to the nucleus of cells after TOP1-induced DNA breaks in different HD cellular models, including in cells ectopically expressing mtHTT plasmids, as well as in primary fibroblasts and iPSC-derived striatal neurons from HD patients. Simultaneously, I observed that HD fibroblasts repaired the damage induced by CPT at a slower rate than healthy cells, as suggested by the increased percentage of γH2AX positive cells at later recovery time points. In opposition, HD striatal neurons exhibited a different repair dynamic. HD neurons displayed overall decreased γH2AX positive cells in all time points in comparison with non-HD neurons, which could in part explain the deficient 53BP1 recruitment

after TOP1-induced breaks. Nonetheless, these results indicate HD cells exhibit deficient DDR signalling in response to TOP1cc-induced DNA breaks. Furthermore, HD fibroblasts seemed to accumulate more TOP1cc when compared to non-HD fibroblasts after CPT treatment. This is suggestive of defective repair of TOP1cc, which could lead to the gradual accumulation of cytotoxic DSBs and ultimately causing neuronal death in HD. In agreement with this hypothesis, both patient-derived HD fibroblasts and HD GABAergic neurons exhibited augmented activation of apoptotic markers and decreased cell survival in response to CPT treatment, indicating HD cells are hypersensitive to TOP1-induced DNA damage and die by apoptosis. This agrees with previous works showing CPT induces neuronal cell death by apoptosis (Morris and Geller, 1996; Keramaris *et al.*, 2000). Together, these observations suggest that in HD cells, the DDR signalling triggered by TOP1-related DSBs is compromised, which contributes to increased cell death.

In Chapter 4, the defects in 53BP1 signalling were traced back to insufficient DNA damage-induced H2A ubiquitination. Biochemical analyses by Flag-H2A IP demonstrated that cells expressing mtHTT displayed weak H2AK13/K15ub. Given 53BP1 retention at the chromatin is dependent on the specific binding of its UDR motif to H2AK15ub, these results support the hypothesis that impaired 53BP1 recruitment is caused by defects in H2A ubiquitination. H2AK13/15 is a specific substrate for the activity of the ubiquitin E3 ligase RNF168 (Mattiroli *et al.*, 2012). Since p62 is a proposed interactor and inhibitor of RNF168 (Y. Wang *et al.*, 2016), next I explored the hypothesis that p62 is the responsible for the decreased 53BP1. Consistent with this hypothesis, depletion of p62 using siRNA restored 53BP1 signalling in HD cells. In addition, decreasing p62 seemed to improve the survival of HD fibroblasts after CPT treatment, indicating that accumulation of p62 interferes with DDR signalling in response to chromosomal DNA breaks.

The mechanistic insights of how p62 interferes with 53BP1 signalling in HD models were explored in Chapter 5. I demonstrated that overexpression of mtHTT promoted the interaction between p62 and RNF168. Interruption of this interaction was found to be sufficient to restore 53BP1 signalling in cells expressing mtHTT, thus showing the defective 53BP1 signalling in HD cells is partially caused by the abnormal p62:RNF168 interaction, potentially due to p62-mediated abrogation of RNF168 activity.

6.2. Future perspectives

6.2.1. Cell models used in this study

In this study three types of cell models were used. Firstly, I used cells transiently expressing GFP-tagged CAG expansion plasmids, either with 23 CAG repeats, mimicking wtHTT or with 74 CAG (mtHTT). The use of this cell model allowed me to directly understand the effects of overexpressing mtHTT on the repair of TOP1-related DSBs. This model has the advantage of allowing the use of cells that are relatively easy to culture, which is convenient specially for experiments that require high cell number, such as co-IP assays. Nevertheless, this model has the disadvantage of being an artificial system.

To surpass the problem of using an artificial system, primary skin fibroblasts from patients with HD were also used. Although these are slow-growing cells and have a finite number of passages, the advantage of choosing primary skin fibroblasts is the possibility to observe the effects of endogenous full-length mtHTT. Also, because these are cells derived from HD patients, they reflect the patients biological and chronological ages (Auburger *et al.*, 2012; Waaijer *et al.*, 2016), which is important in an age-dependent neurodegenerative disorder such as HD, further demonstrating the clinical and physiological relevance of this model.

Although the use of patient-derived fibroblasts is an important step forward, it is still a non-neuronal model. Also, CPT was used to induce DNA damage due to its specificity as a TOP1 poison. However, CPT mostly causes replication-induced DSBs, triggered by the collision between stalled TOP1cc and replication machinery (Pommier *et al.*, 2003). Therefore, one limitation in using the two cell models described above – HD patient fibroblasts and cells ectopically expressing the *HTT*-CAG expansions – is that the lesions observed are possibly replication-dependent. To mitigate this issue, I used a third cell model: primary GABAergic striatal neurons, differentiated from iPSC-derived NPCs. HD is a neurodegenerative disorder that affects non-replicating medium spiny neurons (Ehrlich, 2012; Lahue, 2020). These cells compose 95% of the striatum and are characterized by expression of GABA (Ehrlich, 2012; Zheng and Kozloski, 2017). Therefore, the use of GABAergic neurons can be considered not only clinically, but also physiologically relevant cell model. Furthermore, these cells are post-mitotic, so the TOP1 DNA lesions caused by CPT were possibly transcriptional strand breaks (Sordet *et al.*, 2009). Hence, in a future approach, the use of transcription inhibitors, such as 5,6-Dichloro-1-beta-Ribo-furanosyl Benzimidazole (DRB) or α-amanitin (Bensaude, 2011),

would be useful to confirm whether the findings described here were in fact caused by transcription-dependent DNA damage.

The choice of GABAergic neurons also brings some limitations. The differentiation protocol is lengthy and expensive, and the cells are extremely sensitive and difficult to handle. Therefore, experiments that require high cell density were simply not possible with these cells. Another good complement to the cell models used would be inducing quiescence, by serum starving the HTT-overexpressed cells or even the skin fibroblasts. This approach could have helped resolve the possible replication-related damage caused by CPT treatment. Nonetheless, the experiments using primary human fibroblasts were performed at near confluency and therefore largely non-dividing, to avoid replication-dependent issues.

Regardless of these limitations, the findings observed in both overexpressed and endogenous levels of mtHTT, as well as in non-neuronal cells and GABAergic neurons were mostly similar, including the defects in 53BP1 foci formation and increased expression of apoptotic markers after exposure to CPT, indicating increased cell death. This is suggestive that the non-neuronal cell models used here are enough to understand the effects of mtHTT in the repair of TOP1 mediated DNA lesions. In fact, several studies used overexpression models of CAG expansions or primary human fibroblasts as HD models to explore HD disease mechanisms (Ratovitski *et al.*, 2012; Mollica *et al.*, 2016; Rué *et al.*, 2016; Zeitler *et al.*, 2019; Fox *et al.*, 2020; Roy *et al.*, 2021). Additionally, it is important to note that factors other than the CAG expansions might contribute to HD pathology, including genetic and environmental factors (Gusella, Macdonald and Lee, 2014; GeM-HD, 2015, 2019; Arning, 2016; Keum *et al.*, 2016; Tabrizi *et al.*, 2020; Wheeler and Dion, 2021). Thus, the findings demonstrated in this thesis might not be solely result from the CAG expansions at the *HTT* gene in HD patient cells. Further studies should include a wider arrange of patient-derived fibroblasts and GABAergic neurons harbouring different sizes of CAG expansions to further ascertain about the role of the expanded *HTT* allele in the repair of TOP1-induced damage.

6.2.2. Topoisomerase I-linked DNA breaks in Huntington's disease

CPT treatment triggered TOP1cc accumulation in HD fibroblasts and induced apoptotic cell death in both HD fibroblasts and GABAergic neurons, thus showing HD cells are hypersensitive to TOP1-induced DNA damage. This is consistent with previous evidence in the literature showing that CPT induced increased apoptosis in HD ST*Hdh*$^{Q111/111}$ mouse cells (Jeon *et al.*, 2012).

These observations suggest TOP1cc repair is defective in HD cells, which can contribute to the pathogenesis of this disorder by potentially triggering the accumulation of transcriptional DSBs and consequent neuronal death (Cristini *et al.*, 2016). A-T and SCAN1 patient cells are marked by accumulation of endogenous TOP1cc over time (El-Khamisy *et al.*, 2005; Katyal *et al.*, 2014). Despite HD onset being much later than A-T and SCAN1, which could be explained by tissue-specific features of each disorder (HD affects the striatum, while A-T and SCAN1 affect the cerebellum), the neurological symptoms of A-T and SCAN1 are also considered to be late onset. This further supports the notion that accumulation of TOP1cc could underpin HD neuropathology. In further support of this hypothesis, some characteristic features of HD pathogenesis also constitute the perfect environment for the trapping TOP1, namely the elevated ROS production and consequent increased oxidative DNA damage seen in HD, as demonstrated by the high levels of 8-oxoG detected in the caudate and in the peripheral blood of HD patients (Browne *et al.*, 1997; Chen *et al.*, 2007). TOP1cc can become stabilized by oxidized DNA bases and spontaneously form DSBs (Pourquier and Pommier, 2001; Pommier *et al.*, 2006). Further studies are necessary to ascertain the role of TOP1cc in the pathogenesis of HD, for example by monitoring the accumulation of endogenous TOP1cc in GABAergic neurons derived from HD patients, as well as in neural tissues of HD mice at different stages of the disease progression.

A recent report has demonstrated that excessive PARylation of TOP1cc blocks UPS-induced proteolysis of the DNA-trapped TOP1, necessary to expose the 3'-phosphotyrosyl bond for TDP1-mediated excision (Sun *et al.*, 2021). PARP1 accumulates in the brains of HD patients and its inhibition was found to reduce intranuclear inclusions in striatal neurons and to protect against neuronal death in R6/2 HD mouse models (Vis *et al.*, 2005; Cardinale *et al.*, 2015; Paldino *et al.*, 2017). It would be interesting to investigate whether there is a link between PARP1 accumulation and decreased TOP1cc resolution in HD.

Stabilization of TOP1cc onto the DNA also promotes R-loop formation (Aguilera and García-Muse, 2012; Baranello *et al.*, 2016). This is extremely relevant for HD pathology since the expanded CAG repeats constitute a perfect platform for R-loop stabilization (Lin *et al.*, 2010; Reddy *et al.*, 2011; Su and Freudenreich, 2017). In fact, expanded CAG tracts correlate with increased R-loop formation (Lin *et al.*, 2010; Reddy *et al.*, 2011).

Remarkably, R-loops also promote CAG/CTG repeat instability (Lin *et al.*, 2010; Su and Freudenreich, 2017). While R-loops are stabilized in expanded CAG regions during

transcription, the non-template DNA strand favours the formation of secondary structures such as hairpins due to the superhelical tension caused by RNA polymerase II (Lin *et al.*, 2010; Reddy *et al.*, 2011). This promotes misaligned re-annealing of the DNA strands after the nascent RNA is released from the RNA polymerase II, generating slip-outs (Lin *et al.*, 2010; Reddy *et al.*, 2011). These abnormal DNA structures activate MMR, leading to expansions of the CAG units (Schmidt and Pearson, 2016). Notably, MMR is known to be impaired in HD and mutations of MMR components have been identified as modifiers of disease onset (Lin, Dion and Wilson, 2006; GeM-HD, 2015, 2019; Wheeler and Dion, 2021).

Given the role of R-loops and TOP1cc in enhancing CAG instability (Lin *et al.*, 2010), it would be interesting to test whether there is a preference for R-loop and TOP1cc accumulation in the striatum over other brain regions in HD mice brains.

6.2.3. Huntington's disease cells lack efficient DDR signalling

Analysis of the DDR signalling activated by TOP1-mediated DNA damage revealed HD cells exhibit deficient 53BP1 foci formation. Further examination showed that the kinetics of γH2AX foci formation is also abnormal in HD fibroblasts. The assembly of DNA repair mediators such as 53BP1 and γH2AX into repair foci at the vicinity of DSBs is a crucial step for the recruitment of effector proteins that ligate the broken DNA ends (Harper and Elledge, 2007). This indicates that HD cells harbour inadequate signalling of TOP1-induced breaks, which can potentially impact their repair and lead to the progressive accumulation of extremely deleterious DSBs that consequently induces cell death. This hypothesis was confirmed by showing increased sensitivity of HD fibroblasts and GABAergic neurons to CPT-induced damage, thus demonstrating HD cells lack efficient means to repair TOP1 induced DNA breaks. These findings build on previous work showing disruption of DSB repair signalling cascade by mtHTT (Enokido *et al.*, 2010; Jeon *et al.*, 2012; Ferlazzo *et al.*, 2014).

Others in the literature have showed CPT is highly cytotoxic to neuronal cells by causing transcription-blocking DSBs (Morris and Geller, 1996; Keramaris *et al.*, 2000; Cristini *et al.*, 2016, 2020). This is particularly relevant in the context of HD, since a recent report have discovered that mtHTT disrupts TCR by interfering with the activity of components of the TCR complex, such as PNPK, accumulating DSBs in actively transcribing regions (Gao *et al.*, 2019). An additional interesting approach would be to look at DSB formation through observation of the tail moment by neutral comet assay in the presence and absence of transcription inhibitors

after CPT treatment, as well as analysis of HD cell viability to determine the role of TOP1-induced transcriptional DSBs in HD pathology.

Transcriptional DSBs can be generated from two adjacent TOP1cc and can arise during the processing of co-occurring R-loop and TOP1cc on opposing DNA strands (Pommier *et al.*, 2014; Cristini *et al.*, 2019). To gather further understanding on the role of these lesions in HD pathology, it would be interesting to map the genomic location of TOP1cc and R-loops in HD patient cells by TOP1cc ChIP-seq and DRIP-seq respectively, as well as mapping the localization of DSBs by breaks labelling *in situ* and sequencing (BLISS) (Yan *et al.*, 2017). These methods could furnish information about the preferable regions these lesions tend to occur in the HD genome in comparison with non-HD cells and verify whether they co-locate within genes required for neuronal activity in HD cells.

6.2.4. Chromatin ubiquitination in Huntington's disease

To gain further insight about the mechanisms influencing the disrupted 53BP1 signalling in HD cells, I verified H2A ubiquitination status in HD cell models, since one of the factors that promote 53BP1 retention at the chromatin is the monoubiquitination of H2AK15 residue (Fradet-Turcotte *et al.*, 2013). Indeed, H2AK15ub was reduced in cells expressing mtHTT, which is in line with the absence of 53BP1 signalling observed in HD cells.

Alterations in chromatin ubiquitination in HD has been studied before. HTT PolyQ inclusion bodies were found to be associated with a decrease in the nuclear ubiquitin pool and were responsible for reducing H2B ubiquitination (Yehuda *et al.*, 2017). Decreased H2BK120ub was also observed in the brains of HD R6/2 mice (Kim *et al.*, 2008). In contrast, a global increase in H2AK118/K119 ubiquitination at gene promoters has been observed in the striatum of R6/2 mice (McFarland *et al.*, 2013). Functionally, these alterations translate into elevated transcriptional repression, which agrees with the fact that transcription dysregulation is a critical event of HD pathology (Kim *et al.*, 2008; McFarland *et al.*, 2013). In addition, decreased H2BK120ub is also associated with insufficient DNA repair mechanisms, as ATM-dependent H2B ubiquitination by the RNF20-RNF40 heterodimer is necessary to the recruitment of proteins involved in NHEJ and HR repair pathways (Moyal *et al.*, 2011). This is concurrent with the findings shown here, since decreased H2AK15ub also correlates with defective H2BK120 ubiquitination (Wojcik *et al.*, 2018). Thus, this work expands on the knowledge that HD is characterized by altered chromatin modification, which disrupts critical cellular mechanisms such as transcription and DNA repair.

Monoubiquitination of H2AK13/K15 is necessary to unmask two other constitutive chromatin marks also essential to the recruitment and binding of 53BP1 to the chromatin: H4K20me2 and H3K79me2 (Huyen *et al.*, 2004; Pei *et al.*, 2011; Hu *et al.*, 2017). Investigation of the methylation levels of H4K20 and H3K79 could therefore provide more clues about the mechanisms behind the defective 53BP1 foci formation in HD cells.

Several DUBs responsible for erasing H2AK15ub and negatively regulating 53BP1 chromatin retention have been identified. These include USP3 (Sharma *et al.*, 2014), USP51 (Z. Wang *et al.*, 2016), USP44 (Mosbech *et al.*, 2013), USP14 (Sharma *et al.*, 2018), among others. Performing a high throughput DUB siRNA screening in HD patient cells to investigate which DUBs could be implicated in counteracting 53BP1 signalling would be an interesting approach. This could also pave the way to novel therapeutic strategies for HD. In fact, the ubiquitin system has been exploited for the development of drugs aiming to treat numerous human diseases (Cohen and Tcherpakov, 2010). For instance targeting DUBs using small-molecule inhibitors have been subjected to intense investigation (Cohen and Tcherpakov, 2010; Harrigan *et al.*, 2017).

6.2.5. The crosslink between DNA repair and autophagy – p62 inhibits RNF168 activity in Huntington's disease

The connection between DNA repair and autophagy has long been studied in the literature, but the actual consequences of this crosstalk in human diseases have only recently been explored. Here I showed p62 negatively interferes with 53BP1 signalling in HD cells by obstructing RNF168 activity through aberrant protein-protein interaction. These results are in line with Y. Wang *et al.*, (2016) report, showing p62 physically binds to RNF168 and counteracts its E3 ubiquitin ligase ability. Moreover, these findings further expand on the knowledge of the physiological consequence of this mechanism in human diseases.

The findings presented here suggest a new molecular mechanism involved in HD and furnish additional understanding into the processes that contribute to defective DNA repair, subsequent neurodegeneration, and functional deterioration of the brain in HD patients. In *C9orf72*-ALS models, toxic p62 accumulation was also found to suppress RNF168 activity, impacting 53BP1 signalling (Walker *et al.*, 2017). Hence this work suggests a potentially common mechanism among polynucleotide repeat expansion neurodegenerative disorders.

Additional aspects of this model were intended to be investigated further, had time permitted. These included the effects of RNF168 overexpression in rescuing 53BP1, H2AK15ub and cell viability in response to TOP1-induced damage in the HD cell models used. Attempts to deplete p62 using siRNA from iPSC-derived GABAergic neurons were also made, which unfortunately failed possibly due to the low transfection rate of these cells. In addition, I attempted to scale-up sip62 transfection in cells overexpressed with GFP-Q23/Q74 plasmids to test whether depleting p62 from mtHTT expressing cells would re-establish H2AK15ub. Unfortunately, this also failed. Using short hairpin RNA (shRNA) lentiviral particles could result in a better delivery rate and solve this problem.

A recent report has implicated RNF168 in R-loop biology (Patel *et al.*, 2021). RNF168 interacts with DHX9, a helicase responsible for unwinding R-loops. RNF168-induced ubiquitination of DHX9 was found to be essential for its recruitment to genomic regions enriched for R-loops. Depletion of RNF168 resulted in deficient DHX9 recruitment and activity, causing R-loop accumulation. This was accompanied by increased DSB levels and cell death (Patel *et al.*, 2021). Given the potential implications of R-loops in HD, it would be interesting to address the role of p62-induced abrogation of RNF168 activity in R-loop formation in HD cells. This could be tested by analysing the levels of R-loops by immunofluorescence assay using an S9.6 antibody after overexpression of RN168 and upon p62 depletion in HD cells. Moreover, to monitor the canonical functions of RNF168 that may indirectly impact R-loops, these experiments could also be performed in the absence of RNF8, thus preventing RNF168 recruitment to the chromatin during DSB repair (Thorslund *et al.*, 2015); and/or in cells expressing H2A harbouring mutations in the K13 and K15 residues, the substrates for RNF168 activity (Mattiroli *et al.*, 2012). Together these experiments would allow to infer about: (i) whether p62 aberrant interaction with RNF168 in HD cells result in R-loop accumulation, and if true (ii) whether this is independent of the p62-mediated inhibition of RNF168 role as a chromatin ubiquitin modifier in the context of HD pathology.

6.2.6. The interplay between mtHTT, ATM and p62

The observations in Chapter 3 suggest that HTT might be involved in the repair of TOP1-mediated DNA damage together with ATM, as CPT treatment triggered the interaction between pATM and GFP-Q23 in the nuclear fractions. Previous works have shown that CPT induces both the canonical activation of ATM to promote the repair of TOP1-induced transcriptional DSBs through activation of the RNF168-53BP1 pathway and also the non-canonical and

kinase-independent activation of ATM, together with DNA-PK to induce the ubiquitin- and SUMO-dependent degradation of DNA-bound TOP1 (Sordet *et al.*, 2009; Katyal *et al.*, 2014; Cristini *et al.*, 2016). In line with the notion of a possible interplay between HTT and ATM in the repair of TOP1-dependent DNA damage, further investigations are necessary to clarify the molecular mechanisms behind HTT:ATM interaction in the response to TOP1-induced DNA lesions. For example, it would be interesting to ascertain whether this interaction is dependent on the kinetic activity of ATM, which can be achieved by using ATM kinase inhibitors.

Ferlazzo *et al.*, (2014) suggested a model in which mtHTT interferes with ATM signalling cascade by preventing ATM nuclear localization. That model was confirmed here by analysing the levels of the activated form of ATM (pATM) pulled-down by the GFP-Q23/74 plasmids in fractionated cells. Indeed, the co-IP data revealed that mtHTT sequesters pATM in the cytoplasm. It is, however, unclear whether and how mtHTT interferes with the ability of ATM to resolve TOP1cc and consequent DNA breaks. Depletion of ATM from HD cells could provide clues into whether ATM has any effect on the repair TOP1cc in HD. In this scenario, if decreasing ATM levels did not lead to a further increase the levels of TOP1cc previously observed in HD cells, this would mean mtHTT interferes with ATM ability to resolve TOP1cc. It would also be interesting to study the turnover of TOP1 as well as the ubiquitination and SUMOylation status of TOP1 in HD cells to gain more insight into these mechanisms in the context of HD. ATM is responsible for mediating the SUMO- and ubiquitin-mediated turnover of TOP1 (Katyal *et al.*, 2014). Given HD cells are also devoid of UPS mechanisms (Bennett *et al.*, 2005; Bhat *et al.*, 2014), the combination of MG132 and ATM depletion from HD and non-HD cells could offer additional information into whether and how mtHTT interferes with TOP1 turnover.

Both ATM and p62 are regulators of H2A ubiquitination that counteract each other: while the canonical activity of ATM promotes H2A ubiquitination by inducing a cascade of phosphorylation events that culminates in the recruitment of RNF168; p62 prevents H2A ubiquitination by directly inhibiting RNF168 activity (Y. Wang *et al.*, 2016).

Despite the direct influence of mtHTT on p62-linked autophagic activity (Rui *et al.*, 2015), the results shown here suggest the increased interaction between p62 and RNF168 is an indirect consequence of the polyQ expansions. This is possibly due to mtHTT-mediated insufficient autophagic flux, as suggested by the tendency for p62 accumulation observed in HD cells in Chapter 4 and further supported by Pircs *et al.*, (2018). This alludes to a much broader

mechanism that potentially underlies other neurodegenerative disorders, as verified in *C9orf72*-ALS models (Walker *et al.*, 2017). Furthermore, given the fact that mtHTT induces cytoplasmic retention of ATM, I cannot exclude the possibility of a more direct role of mtHTT in preventing H2AK15ub by hindering ATM-induced recruitment and activation of the RNF8-RNF168 pathway, consequently decreasing the levels of 53BP1 foci formation in HD cells. Since ATM also depends on 53BP1 to be retained at the chromatin, a feedforward mechanism is also possible, leading to a further decrease in ATM-mediated signalling transduction cascade in HD cells, which can be further exaggerated by the p62-induced inactivation of RNF168 activity (Figure 6.2.1). Because CHK2 and p53 are substrates for ATM kinase activity, assessment of the phosphorylation status of both CHK2 and p53 could be used to study ATM activity in HD cells (Lavin, Delia and Chessa, 2006). Additionally, studying RNF8 activity by analysing H1 ubiquitination status in HD cells could also be applied.

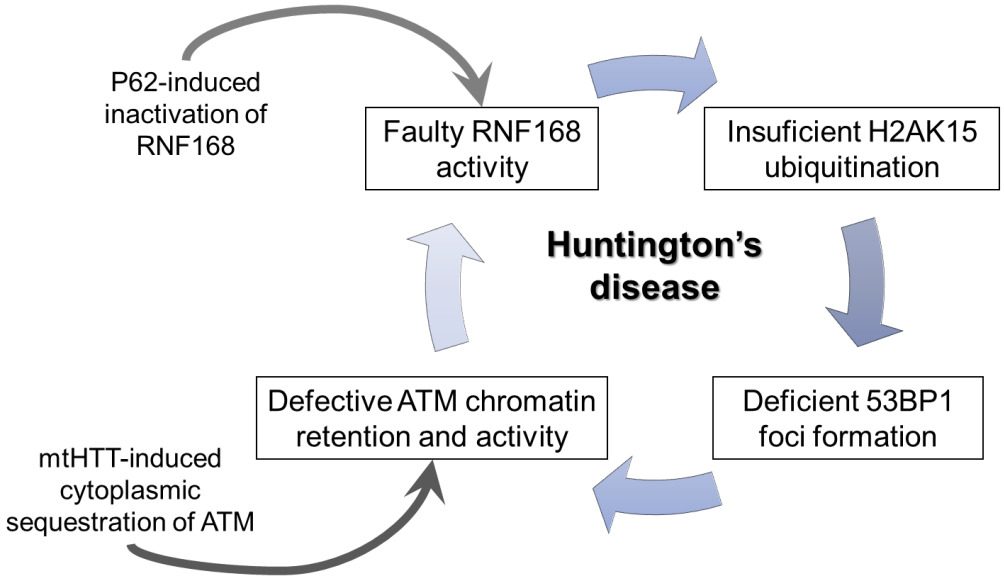

Figure 6.2.1 – Potential feedforward mechanism in Huntington's disease pathology

The work presented here suggest a feedforward mechanism might be involved in HD pathogenesis. HD cells exhibit deficits in 53BP1 recruitment into nuclear foci after TOP1-induced DNA breaks. The impaired 53BP1 foci formation is likely to be a result of the inadequate H2AK15 ubiquitination observed in mtHTT expressing cells, which is a consequence of deficient RNF168 activity as an E3 ligase. The recruitment of RNF168 to the damage sites depends on the kinase activity of ATM to induce a cascade of events that lead to the activation of RNF8-RNF168 pathway. Simultaneously, ATM retention at the chromatin depends itself on the presence of 53BP1 at the chromatin, thus creating a positive feedback loop in which each element influences the activity and recruitment of the next. In parallel, the results shown here indicate two additional factors possibly exacerbating these deficiencies: mtHTT sequesters ATM into the cytoplasm, inducing further impairment in ATM activity, and p62 interacts aberrantly with RNF168 in mtHTT expressing cells and inhibits its activity or reduces its availability.

6.2.7. Inhibition of RNF168:p62 interaction: a novel therapeutic window for HD

In Chapter 5 I demonstrated the aberrant interaction between p62 and RNF168 incited by mtHTT expression underlies, in part, the defects in NHEJ signalling experienced in HD cells. The fact that inhibiting this interaction using a synthetic peptide improved 53BP1 signalling in mtHTT expressing cells is extremely exciting, since it suggests that this aberrant interaction has the potential for being a druggable candidate for new therapeutic strategies for HD.

The use of small peptides to inhibit aberrant protein-protein interactions (PPIs) is a promising therapeutic avenue for neurodegenerative disorders (Blazer and Neubig, 2009). However, finding small molecules able to modulate PPIs, that are metabolically stable and cell/blood-brain barrier permeable is a challenging task.

A recent study described an abnormal interaction between mutant SOD1 (mtSOD1) and Derlin-1 was responsible for causing motor neuron cell death in ALS models (Tsuburaya *et al.*, 2018). By taking advantage of the time resolved fluorescence resonance energy transfer (TR-FRET) technology, the authors developed a high-throughput system to screen the efficacy of 160,000 compounds in inhibiting mtSOD1:Derlin-1 interaction. Excitingly, the screening identified one compound analogue that was able to prevent the aberrant interaction between mutant SOD1 and Derlin-1 and showed good permeability and metabolic stability. Moreover, treatment with this analogue prevented motor neuron death in ALS models (Tsuburaya *et al.*, 2018). Similar strategies could be implemented to screen for potential small molecules that inhibit p62:RNF168 interaction and test their therapeutic effects in HD models.

6.2.8. Possible implications in other polyglutamine expansion neurodegenerative disorders

HD together with eight other neurodegenerative disorders (SCA1, 2, 3, 6, 7, 12 and 17; DRPLA and SBMA) constitute a group of poly Q disorders. PolyQ disorders share some features, among which the toxic accumulation of protein aggregates in neurons, impaired DNA repair and faulty protein degradation mechanisms, that result in marked neuronal cell death (Cortes and Spada, 2015; Massey and Jones, 2018). Remarkably, p62 accumulation associated with impaired autophagic flux can also be observed in models of SCA3, SCA7 and DRPLA, which is reminiscent of HD (Mori *et al.*, 2012; Alves *et al.*, 2014; Cortes and Spada, 2015; Den Dunnen, 2018). One could ask whether the molecular mechanisms discovered here in the context of HD, regarding p62-mediated inactivation of RNF168, can also operate in other

polyQ disorders. If that is the case, these disorders could potentially all benefit from therapies that inhibit p62:RNF168 interaction.

6.3. Conclusion

The present work demonstrated that the repair of TOP1-mediated DNA damage is defective in HD cells, contributing to the apoptotic cell death. This project also unveiled an intriguing new pathway that connects faulty 53BP1-mediated DDR signalling to toxic p62 accumulation, thus linking two emerging topics in the field of neurodegeneration: insufficient DNA repair and defective autophagy mechanisms (Figure 6.3.1). This is of particular interest given the recent data provided by GWAS implicating defective DNA repair mechanisms as HD disease modifiers (GeM-HD, 2015, 2019). Therefore, the observations stated here might provide an additional insight into how dysregulated DNA damage repair and response contributes to HD pathogenesis. Finally, this work suggests that similar molecular mechanisms contribute to neurodegeneration by promoting DNA damage accumulation in both HD and *C9orf72*-ALS/FTD, thus indicating that autophagy-mediated DDR defects might be a common pathological phenotype of polynucleotide expansion neurodegenerative disorders and provide new possibilities for therapeutic intervention.

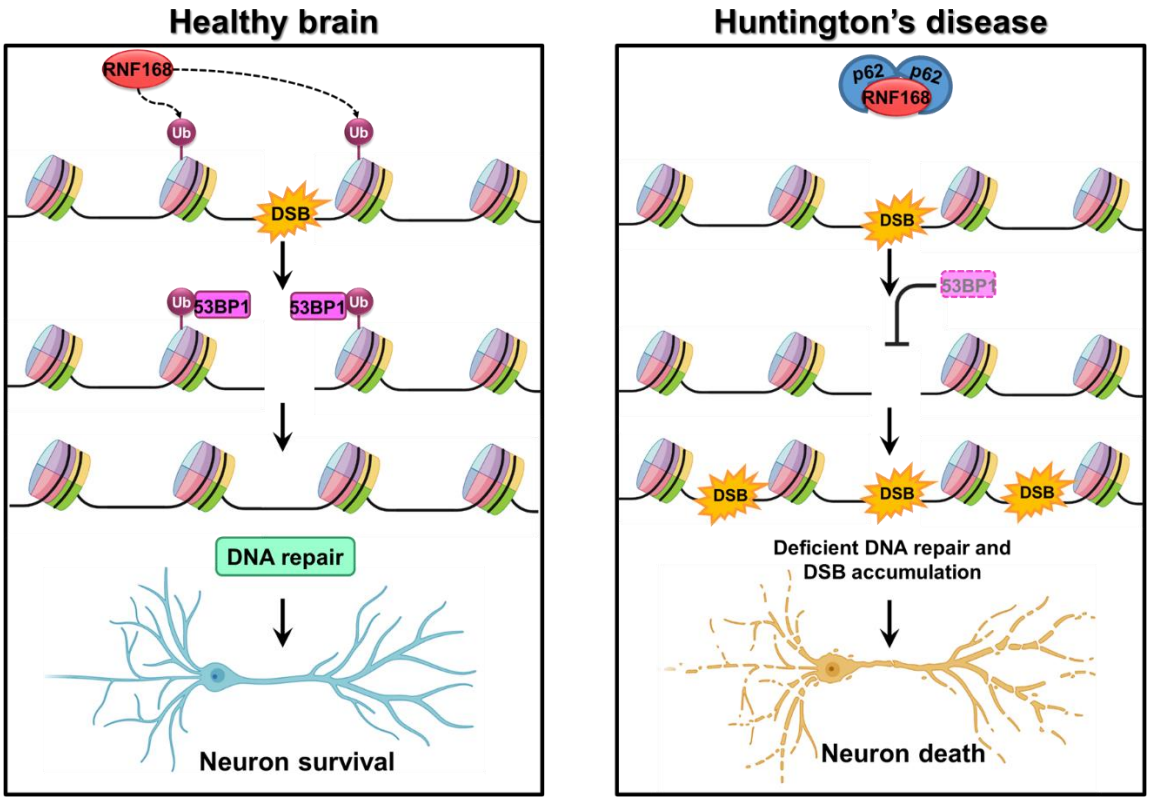

Figure 6.3.1 – Proposed model showing the crosstalk between DNA repair, chromatin modification and autophagy in Huntington's disease

Left: In the healthy brain, after a damaging event that results in the formation of DSBs, neurons activate a signalling cascade of events that lead to the recruitment of RNF168 to the damage sites. Here, RNF168 acts as an E3 ubiquitin ligase and monoubiquitinates H2A at K13 and K15 residues. Monoubiquitination of H2AK15 creates a docking site for the binding and assembling of 53BP1 into foci around the broken DNA strands. This allows 53BP1 to favour the activation of NHEJ repair pathway and consequent joining of the DNA ends. These mechanisms ensure the maintenance of neuronal genome, vital for neuron survival.
Right: In Huntington's disease, faulty autophagy mechanisms promote toxic accumulation of p62. By accumulating in the nucleus of neurons, p62 binds and inhibits the activity of RNF168, thus leading to insufficient H2AK15ub. This results in deficient 53BP1 foci formation and consequent impaired DNA repair by NHEJ. Insufficient means to repair DNA damage will promote gradual accumulation of DSBs over time, ultimately causing neuronal death and consequent decline of the brain functions.

References

Abugable, A. A. *et al.* (2019) 'DNA repair and neurological disease : From molecular understanding to the development of diagnostics and model organisms', *DNA Repair*. Elsevier, 81(July), p. 102669. doi: 10.1016/j.dnarep.2019.102669.

Achour, M. *et al.* (2015) 'Neuronal identity genes regulated by super-enhancers are preferentially down-regulated in the striatum of Huntington's disease mice', *Human Molecular Genetics*, 24(12), pp. 3481–3496. doi: 10.1093/hmg/ddv099.

Acs, K. *et al.* (2011) 'The AAA-ATPase VCP/p97 promotes 53BP1 recruitment by removing L3MBTL1 from DNA double-strand breaks', *Nature Structural and Molecular Biology*. Nature Publishing Group, 18(12), pp. 1345–1350. doi: 10.1038/nsmb.2188.

Aguilera, A. and García-Muse, T. (2012) 'R Loops: From Transcription Byproducts to Threats to Genome Stability', *Molecular Cell*, 46(2), pp. 115–124. doi: 10.1016/j.molcel.2012.04.009.

Aguirre, N. *et al.* (2005) 'Increased oxidative damage to DNA in an animal model of amyotrophic lateral sclerosis', *Free Radical Research*. Taylor & Francis, 39(4), pp. 383–388. doi: 10.1080/10715760400027979.

Alagoz, M. *et al.* (2013) 'ATM Deficiency Results in Accumulation of DNA-Topoisomerase I Covalent Intermediates in Neural Cells', *PLoS ONE*, 8(4). doi: 10.1371/journal.pone.0058239.

Alcalá-Vida, R. *et al.* (2021) 'Age-related and disease locus-specific mechanisms contribute to early remodelling of chromatin structure in Huntington's disease mice', *Nature Communications*. Springer US, 12(1), pp. 1–16. doi: 10.1038/s41467-020-20605-2.

Aleksandrov, R. *et al.* (2020) 'The Chromatin Response to Double-Strand DNA Breaks and Their Repair', *Cells*, 9(1853), pp. 1–45. doi: doi:10.3390/cells9081853.

Alexander, A. *et al.* (2010) 'ATM signals to TSC2 in the cytoplasm to regulate mTORC1 in response to ROS', *PNAS*, 107(9), pp. 4153–4158. doi: 10.1073/pnas.1206201109.

Alves, S. *et al.* (2014) 'The autophagy/lysosome pathway is impaired in SCA7 patients and SCA7 knock-in mice', *Acta Neuropathologica*, 128(5), pp. 705–722. doi: 10.1007/s00401-014-1289-8.

An, L. *et al.* (2018) 'RNF169 limits 53BP1 deposition at DSBs to stimulate single-strand annealing repair', *Proceedings of the National Academy of Sciences of the United States of America*, 115(35), pp. E8286–E8295. doi: 10.1073/pnas.1804823115.

Anglada, T., Genescà, A. and Martín, M. (2020) 'Age-associated deficient recruitment of 53BP1 in G1 cells directs DNA double-strand break repair to BRCA1/CtIP-mediated DNA-end resection', *Aging*, 12(24), pp. 24872–24893. doi: 10.18632/aging.202419.

Anne, S. L., Saudou, F. and Humbert, S. (2007) 'Phosphorylation of huntingtin by cyclin-dependent kinase 5 is induced by DNA damage and regulates wild-type and mutant huntingtin toxicity in neurons', *Journal of Neuroscience*, 27(27), pp. 7318–7328. doi: 10.1523/JNEUROSCI.1831-07.2007.

Aquila, L. and Atanassov, B. S. (2020) 'Regulation of Histone Ubiquitination in Response to DNA Double Strand Breaks', *Cells*, 9(7). doi: 10.3390/cells9071699.

Arning, L. (2016) 'The search for modifier genes in Huntington disease – Multifactorial aspects of a monogenic disorder', *Molecular and Cellular Probes*. Elsevier Ltd, 30(6), pp. 404–409. doi: 10.1016/j.mcp.2016.06.006.

Arrasate, M. *et al.* (2004) 'Inclusion body formation reduces levels of mutant huntingtin and the risk of neuronal death', *Nature*, 431(7010), pp. 805–810. doi: 10.1038/nature02998.

Arrasate, M. and Finkbeiner, S. (2012) 'Protein aggregates in Huntington's disease', *Experimental Neurology*. Elsevier Inc., 238(1), pp. 1–11. doi: 10.1016/j.expneurol.2011.12.013.

Askeland, G. *et al.* (2018) 'Increased nuclear DNA damage precedes mitochondrial dysfunction in peripheral blood mononuclear cells from Huntington's disease patients', *Scientific Reports*, 8(1), pp. 1–9. doi: 10.1038/s41598-018-27985-y.

Auburger, G. *et al.* (2012) 'Primary skin fibroblasts as a model of Parkinson's disease', *Molecular Neurobiology*, 46(1), pp. 20–27. doi: 10.1007/s12035-012-8245-1.

Ayala-Peña, S. (2013) 'Role of oxidative DNA damage in mitochondrial dysfunction and Huntington's disease pathogenesis', *Free Radical Biology and Medicine*. Elsevier, 62, pp. 102–110. doi: 10.1016/j.freeradbiomed.2013.04.017.

Bai, M. *et al.* (2020) 'The Role of Posttranslational Modifications in DNA Repair', *BioMed Research International*, 2020. doi: 10.1155/2020/7493902.

Bakkenist, C. J. and Kastan, M. B. (2003) 'DNA damage activates ATM through intermolecular autophosphorylation and dimer dissociation', *Nature*, 421(6922), pp. 499–506. doi: 10.1038/nature01368.

Baldock, R. A. *et al.* (2015) 'ATM Localization and Heterochromatin Repair Depend on Direct Interaction of the 53BP1-BRCT2 Domain with γH2AX', *Cell Reports*, 13(10), pp. 2081–2089. doi: 10.1016/j.celrep.2015.10.074.

Balmus, G. *et al.* (2019) 'ATM orchestrates the DNA-damage response to counter toxic non-homologous end-joining at broken replication forks', *Nature Communications*. Springer US, 10(1), pp. 1–18. doi: 10.1038/s41467-018-07729-2.

Bañez-Coronel, M. *et al.* (2015) 'RAN Translation in Huntington Disease', *Neuron*, 88(4), pp. 667–677. doi: 10.1016/j.neuron.2015.10.038.

Baranello, L. *et al.* (2016) 'RNA Polymerase II Regulates Topoisomerase 1 Activity to Favor Efficient Transcription', *Cell*. Elsevier Inc., 165(2), pp. 357–371. doi: 10.1016/j.cell.2016.02.036.

Barnat, M. *et al.* (2017) 'Huntingtin-Mediated Multipolar-Bipolar Transition of Newborn Cortical Neurons Is Critical for Their Postnatal Neuronal Morphology', *Neuron*. Elsevier Inc., 93(1), pp. 99–114. doi: 10.1016/j.neuron.2016.11.035.

Bartocci, C. and Denchi, E. L. (2013) 'Put a RING on it: Regulation and inhibition of RNF8

and RNF168 RING finger E3 ligases at DNA damage sites', *Frontiers in Genetics*, 4(JUL), pp. 1–12. doi: 10.3389/fgene.2013.00128.

Bates, G. P. *et al.* (2015) 'Huntington disease', *Nature Reviews Disease Primers*. Nature Publishing Group, 1(1). doi: 10.1038/nrdp.2015.5.

Bäuerlein, F. J. B. *et al.* (2017) 'In Situ Architecture and Cellular Interactions of PolyQ Inclusions', *Cell*, 171(1), pp. 179-187.e10. doi: 10.1016/j.cell.2017.08.009.

Becker, J. R. *et al.* (2021) 'BARD1 reads H2A lysine 15 ubiquitination to direct homologous recombination', *Nature*. Springer US, 596(7872), pp. 433–437. doi: 10.1038/s41586-021-03776-w.

Bennett, E. J. *et al.* (2005) 'Global impairment of the ubiquitin-proteasome system by nuclear or cytoplasmic protein aggregates precedes inclusion body formation', *Molecular Cell*, 17(3), pp. 351–365. doi: 10.1016/j.molcel.2004.12.021.

Bensaude, O. (2011) 'Inhibiting eukaryotic transcription: Which compound to choose? How to evaluate its activity?', *Transcription*, 2(3), pp. 103–108. doi: 10.4161/trns.2.3.16172.

Berger, N. D. *et al.* (2017) 'ATM-dependent pathways of chromatin remodelling and oxidative DNA damage responses', *Philosophical Transactions of the Royal Society B: Biological Sciences*, 372(1731), p. 20160283. doi: 10.1098/rstb.2016.0283.

Bessert, D. A. *et al.* (1995) 'The identification of a functional nuclear localization signal in the Huntington disease protein', *Molecular Brain Research*, 33(1), pp. 165–173. doi: 10.1016/0169-328X(95)00124-B.

Bhat, K. P. *et al.* (2014) 'Differential ubiquitination and degradation of huntingtin fragments modulated by ubiquitin-protein ligase E3A', *Proceedings of the National Academy of Sciences*, 111(15), pp. 5706–5711. doi: 10.1073/pnas.1402215111.

Bito, H. and Takemoto-Kimura, S. (2003) 'Ca2+/CREB/CBP-dependent gene regulation: A shared mechanism critical in long-term synaptic plasticity and neuronal survival', *Cell Calcium*, 34(4–5), pp. 425–430. doi: 10.1016/S0143-4160(03)00140-4.

Biton, S. *et al.* (2007) 'ATM-mediated response to DNA double strand breaks in human neurons derived from stem cells', *DNA Repair*, 6(1), pp. 128–134. doi: 10.1016/j.dnarep.2006.10.019.

Blackford, A. N. and Jackson, S. P. (2017) 'ATM, ATR, and DNA-PK: The Trinity at the Heart of the DNA Damage Response', *Molecular Cell*. Elsevier Inc., 66(6), pp. 801–817. doi: 10.1016/j.molcel.2017.05.015.

Blazer, L. L. and Neubig, R. R. (2009) 'Small Molecule Protein–Protein Interaction Inhibitors as CNS Therapeutic Agents: Current Progress and Future Hurdles', *Neuropsychopharmacology*, 34(1), pp. 126–141. doi: 10.1038/npp.2008.151.

Brouwer, I. *et al.* (2016) 'Sliding sleeves of XRCC4-XLF bridge DNA and connect fragments of broken DNA', *Nature*. Nature Publishing Group, 535(7613), pp. 566–569. doi: 10.1038/nature18643.

Browne, S. E. *et al.* (1997) 'Oxidative damage and metabolic dysfunction in huntington's disease: Selective vulnerability of the basal ganglia', *Annals of Neurology*, 41(5), pp. 646–653. doi: 10.1002/ANA.410410514.

Burgess, J. T. *et al.* (2020) 'The Therapeutic Potential of DNA Damage Repair Pathways and Genomic Stability in Lung Cancer', *Frontiers in Oncology*, 10(July), pp. 1–14. doi: 10.3389/fonc.2020.01256.

Burma, S. *et al.* (2001) 'ATM Phosphorylates Histone H2AX in Response to DNA Double-strand Breaks', *Journal of Biological Chemistry*, 276(45), pp. 42462–42467. doi: 10.1074/jbc.C100466200.

Burrus, C. J. *et al.* (2020) 'Striatal Projection Neurons Require Huntingtin for Synaptic Connectivity and Survival', *Cell Reports*. ElsevierCompany., 30(3), pp. 642-657.e6. doi: 10.1016/j.celrep.2019.12.069.

Caldecott, K. W. (2008) 'Single-strand break repair and genetic disease', *Nature reviews. Genetics*, 9(5), pp. 619–631. doi: 10.1038/nrg2380.

Callen, E. *et al.* (2013) '53BP1 mediates productive and mutagenic DNA repair through distinct phosphoprotein interactions', *Cell*, 153(6), pp. 1266–1280. doi: 10.1016/j.cell.2013.05.023.

Callen, E. *et al.* (2020) '53BP1 Enforces Distinct Pre- and Post-resection Blocks on Homologous Recombination', *Molecular Cell*, 77(1), pp. 26-38.e7. doi: 10.1016/j.molcel.2019.09.024.

Cardinale, A. *et al.* (2015) 'PARP-1 inhibition is neuroprotective in the R6/2 mouse model of huntington's disease', *PLoS ONE*, 10(8), pp. 1–22. doi: 10.1371/journal.pone.0134482.

Carlessi, L. *et al.* (2014) 'Functional and molecular defects of hiPSC-derived neurons from patients with ATM deficiency', *Cell Death and Disease*. Nature Publishing Group, 5(7), pp. 1–14. doi: 10.1038/cddis.2014.310.

Castaldo, I. *et al.* (2019) 'DNA damage signatures in peripheral blood cells as biomarkers in prodromal huntington disease', *Annals of Neurology*, 85(2), pp. 296–301. doi: 10.1002/ana.25393.

Cattaneo, E. *et al.* (2001) 'Loss of normal huntingtin function: New developments in Huntington's disease research', *Trends in Neurosciences*, 24(3), pp. 182–188. doi: 10.1016/S0166-2236(00)01721-5.

Cattaneo, E., Zuccato, C. and Tartari, M. (2005) 'Normal huntingtin function: An alternative approach to Huntington's disease', *Nature Reviews Neuroscience*, 6(12), pp. 919–930. doi: 10.1038/nrn1806.

Caviston, J. P. *et al.* (2007) 'Huntingtin facilitates dynein/dynactin-mediated vesicle transport', *Proceedings of the National Academy of Sciences of the United States of America*, 104(24), pp. 10045–10050. doi: 10.1073/pnas.0610628104.

Caviston, J. P. *et al.* (2011) 'Huntingtin coordinates the dynein-mediated dynamic positioning of endosomes and lysosomes', *Molecular Biology of the Cell*, 22(4), pp. 478–492. doi:

10.1091/mbc.E10-03-0233.

Ceccaldi, R., Rondinelli, B. and D'Andrea, A. D. (2016) 'Repair Pathway Choices and Consequences at the Double-Strand Break', *Trends in Cell Biology*. Elsevier Ltd, 26(1), pp. 52–64. doi: 10.1016/j.tcb.2015.07.009.

Celeste, A. *et al.* (2003) 'Histone H2AX phosphorylation is dispensable for the initial recognition of DNA breaks', *Nature Cell Biology*, 5(7), pp. 675–679. doi: 10.1038/ncb1004.

Cha, J. H. J. *et al.* (1998) 'Altered brain neurotransmitter receptors in transgenic mice expressing a portion of an abnormal human Huntington disease gene', *Proceedings of the National Academy of Sciences of the United States of America*, 95(11), pp. 6480–6485. doi: 10.1073/pnas.95.11.6480.

Chang, H. H. Y. *et al.* (2017) 'Non-homologous DNA end joining and alternative pathways to double-strand break repair', *Nature Reviews Molecular Cell Biology*. Nature Publishing Group, 18(8), pp. 495–506. doi: 10.1038/nrm.2017.48.

Chang, H. H. Y., Watanabe, G. and Lieber, M. R. (2015) 'Unifying the DNA end-processing roles of the artemis nuclease: Ku-dependentartemis resection atbluntdnaends', *Journal of Biological Chemistry*, 290(40), pp. 24036–24050. doi: 10.1074/jbc.M115.680900.

Chapman, J. R. *et al.* (2013) 'RIF1 Is Essential for 53BP1-Dependent Nonhomologous End Joining and Suppression of DNA Double-Strand Break Resection', *Molecular Cell*, 49(5), pp. 858–871. doi: 10.1016/j.molcel.2013.01.002.

Chapman, J. R., Taylor, M. R. G. and Boulton, S. J. (2012) 'Playing the End Game: DNA Double-Strand Break Repair Pathway Choice', *Molecular Cell*. Elsevier, 47(4), pp. 497–510. doi: 10.1016/j.molcel.2012.07.029.

Chaudhuri, A. R. and Nussenzweig, A. (2017) 'The multifaceted roles of PARP1 in DNA repair and chromatin remodelling', *Nature Reviews Molecular Cell Biology*. Nature Publishing Group, 18(10), pp. 610–621. doi: 10.1038/nrm.2017.53.

Chen, C. M. *et al.* (2007) 'Increased oxidative damage and mitochondrial abnormalities in the peripheral blood of Huntington's disease patients', *Biochemical and Biophysical Research Communications*. Academic Press, 359(2), pp. 335–340. doi: 10.1016/J.BBRC.2007.05.093.

Chen, J. H. *et al.* (2015) 'ATM-mediated PTEN phosphorylation promotes PTEN nuclear translocation and autophagy in response to DNA-damaging agents in cancer cells', *Autophagy*, 11(2), pp. 239–252. doi: 10.1080/15548627.2015.1009767.

Chen, X. *et al.* (2011) 'Expanded polyglutamine-binding peptoid as a novel therapeutic agent for treatment of Huntington's disease', *Chemistry and Biology*. Elsevier Ltd, 18(9), pp. 1113–1125. doi: 10.1016/j.chembiol.2011.06.010.

Chiang, S.-C. *et al.* (2017) 'Mitochondrial protein-linked DNA breaks perturb mitochondrial gene transcription and trigger free radical–induced DNA damage', *Science Advances*, 3(4). doi: 10.1126/sciadv.1602506.

Choo, Y. S. *et al.* (2004) 'Mutant huntingtin directly increases susceptibility of mitochondria to the calcium-induced permeability transition and cytochrome c release', *Human Molecular*

Genetics, 13(14), pp. 1407–1420. doi: 10.1093/hmg/ddh162.

Chow, H. M. and Herrup, K. (2015) 'Genomic integrity and the ageing brain', *Nature Reviews Neuroscience*. Nature Publishing Group, 16(11), pp. 672–684. doi: 10.1038/nrn4020.

Ciosi, M. *et al.* (2019) 'A genetic association study of glutamine-encoding DNA sequence structures, somatic CAG expansion, and DNA repair gene variants, with Huntington disease clinical outcomes', *EBioMedicine*. Elsevier B.V., 48, pp. 568–580. doi: 10.1016/j.ebiom.2019.09.020.

Clouaire, T. *et al.* (2018) 'Comprehensive Mapping of Histone Modifications at DNA Double-Strand Breaks Deciphers Repair Pathway Chromatin Signatures', *Molecular Cell*, 72(2), pp. 250-262.e6. doi: 10.1016/j.molcel.2018.08.020.

Cohen, P. and Tcherpakov, M. (2010) 'Leading Edge Perspective Will the Ubiquitin System Furnish as Many Drug Targets as Protein Kinases?', *Cell*, 143, pp. 686–693. doi: 10.1016/j.cell.2010.11.016.

Coleman, K. A. and Greenberg, R. A. (2011) 'The BRCA1-RAP80 complex regulates DNA repair mechanism utilization by restricting end resection', *Journal of Biological Chemistry*, 286(15), pp. 13669–13680. doi: 10.1074/jbc.M110.213728.

Colin, E. *et al.* (2008) 'Huntingtin phosphorylation acts as a molecular switch for anterograde/retrograde transport in neurons', *EMBO Journal*, 27(15), pp. 2124–2134. doi: 10.1038/emboj.2008.133.

Cortes, C. J. and Spada, A. R. La (2015) 'Autophagy in Polyglutamine Disease: Imposing Order on Disorder or Contributing to the Chaos?', *Molecular and cellular neurosciences*. NIH Public Access, 66(0 0), p. 53. doi: 10.1016/J.MCN.2015.03.010.

Crane, M. M. *et al.* (2019) 'DNA damage checkpoint activation impairs chromatin homeostasis and promotes mitotic catastrophe during aging', *eLife*, 8, pp. 1–26. doi: 10.7554/eLife.50778.

Cristini, A. *et al.* (2016) 'DNA-PK triggers histone ubiquitination and signaling in response to DNA double-strand breaks produced during the repair of transcription-blocking topoisomerase I lesions.', *Nucleic acids research*, 44(3), pp. 1161–78. doi: 10.1093/nar/gkv1196.

Cristini, A. *et al.* (2019) 'Dual Processing of R-Loops and Topoisomerase I Induces Transcription-Dependent DNA Double-Strand Breaks', *Cell Reports*, 28(12), pp. 3167-3181.e6. doi: 10.1016/j.celrep.2019.08.041.

Cristini, A. *et al.* (2020) 'Transcription-dependent DNA double-strand breaks and human disease Transcription-dependent DNA double-strand breaks and human disease', *Molecular & Cellular Oncology*. Taylor & Francis, 7(2). doi: 10.1080/23723556.2019.1691905.

Crowe, S. L. *et al.* (2006) 'Rapid phosphorylation of histone H2A.X following ionotropic glutamate receptor activation', *European Journal of Neuroscience*, 23(9), pp. 2351–2361. doi: 10.1111/j.1460-9568.2006.04768.x.

Cui, L. *et al.* (2006) 'Transcriptional Repression of PGC-1α by Mutant Huntingtin Leads to Mitochondrial Dysfunction and Neurodegeneration', *Cell*, 127(1), pp. 59–69. doi: 10.1016/j.cell.2006.09.015.

Czarny, P. *et al.* (2015) 'Autophagy in DNA damage response', *International Journal of Molecular Sciences*, 16(2), pp. 2641–2662. doi: 10.3390/ijms16022641.

Das, B. B. *et al.* (2014) 'PARP1-TDP1 coupling for the repair of topoisomerase I-induced DNA damage', *Nucleic Acids Research*, 42(7), pp. 4435–4449. doi: 10.1093/nar/gku088.

Date, H. *et al.* (2001) 'Early-onset ataxia with ocular motor apraxia and hypoalbuminemia is caused by mutations in a new HIT superfamily gene', *Nature Genetics*, 29(2), pp. 184–188. doi: 10.1038/ng1001-184.

David, S. S., O'Shea, V. L. and Kundu, S. (2007) 'Base-excision repair of oxidative DNA damage', *Nature*, 447(7147), pp. 941–950. doi: 10.1038/nature05978.

Devgan, S. S. *et al.* (2011) 'Homozygous deficiency of ubiquitin-ligase ring-finger protein RNF168 mimics the radiosensitivity syndrome of ataxia-telangiectasia', *Cell Death & Differentiation*. Nature Publishing Group, 18(9), pp. 1500–1506. doi: 10.1038/cdd.2011.18.

DiGiovanni, L. F. *et al.* (2016) 'Huntingtin N17 domain is a reactive oxygen species sensor regulating huntingtin phosphorylation and localization', *Human Molecular Genetics*, 25(18), pp. 3937–3945. doi: 10.1093/hmg/ddw234.

Dion, V. (2014) 'Tissue specificity in DNA repair: Lessons from trinucleotide repeat instability', *Trends in Genetics*. Elsevier Ltd, 30(6), pp. 220–229. doi: 10.1016/j.tig.2014.04.005.

Ditch, S. and Paull, T. T. (2012) 'The ATM protein kinase and cellular redox signaling : beyond the DNA damage response', *Trends in Biochemical Sciences*. Elsevier Ltd, 37(1), pp. 15–22. doi: 10.1016/j.tibs.2011.10.002.

Doil, C. *et al.* (2009) 'RNF168 Binds and Amplifies Ubiquitin Conjugates on Damaged Chromosomes to Allow Accumulation of Repair Proteins', *Cell*. Elsevier Ltd, 136(3), pp. 435–446. doi: 10.1016/j.cell.2008.12.041.

Dragileva, E. *et al.* (2009) 'Intergenerational and striatal CAG repeat instability in Huntington's disease knock-in mice involve different DNA repair genes', *Neurobiology of Disease*. Elsevier Inc., 33(1), pp. 37–47. doi: 10.1016/j.nbd.2008.09.014.

Drummond, E. *et al.* (2020) 'Phosphorylated tau interactome in the human Alzheimer's disease brain', *Brain*, 143(9), pp. 2803–2817. doi: 10.1093/brain/awaa223.

Du, Z. W. *et al.* (2015) 'Generation and expansion of highly pure motor neuron progenitors from human pluripotent stem cells', *Nature Communications*. Nature Publishing Group, 6, pp. 1–9. doi: 10.1038/ncomms7626.

Duan, Y. *et al.* (2019) 'PARylation regulates stress granule dynamics, phase separation, and neurotoxicity of disease-related RNA-binding proteins', *Cell Research*. Springer US, 29(3), pp. 233–247. doi: 10.1038/s41422-019-0141-z.

Den Dunnen, W. F. A. (2018) 'Trinucleotide repeat disorders', in *Handbook of Clinical Neurology*. 1st edn. Elsevier B.V., pp. 383–391. doi: 10.1016/B978-0-12-802395-2.00027-4.

Duyao, M. P. *et al.* (1995) 'Inactivation of the mouse huntington's disease gene homolog Hdh',

Science, 269(5222), pp. 407–410. doi: 10.1126/science.7618107.

Ehrlich, M. E. (2012) 'Huntington's Disease and the Striatal Medium Spiny Neuron: Cell-Autonomous and Non-Cell-Autonomous Mechanisms of Disease', *Neurotherapeutics*, 9(2), pp. 270–284. doi: 10.1007/s13311-012-0112-2.

El-Khamisy, S. F. *et al.* (2005) 'Defective DNA single-strand break repair in spinocerebellar ataxia with axonal neuropathy-1', *Nature*, 434(March), pp. 108–113. doi: 10.1038/nature03329.1.

Elias, S. *et al.* (2014) 'Huntingtin regulates mammary stem cell division and differentiation', *Stem Cell Reports*, 2(4), pp. 491–506. doi: 10.1016/j.stemcr.2014.02.011.

Engelender, S. (2008) 'Ubiquitination of α-synuclein and autophagy in Parkinson's disease', *Autophagy*, 4(3), pp. 372–374. doi: 10.4161/auto.5604.

Enokido, Y. *et al.* (2010) 'Mutant huntingtin impairs Ku70-mediated DNA repair', *Journal of Cell Biology*, 189(3), pp. 425–443. doi: 10.1083/jcb.200905138.

Esashi, F. *et al.* (2007) 'Stabilization of RAD51 nucleoprotein filaments by the C-terminal region of BRCA2', *Nature Structural and Molecular Biology*, 14(6), pp. 468–474. doi: 10.1038/nsmb1245.

Fang, E. F. *et al.* (2014) 'Defective mitophagy in XPA via PARP-1 hyperactivation and NAD +/SIRT1 reduction', *Cell*. Elsevier Inc., 157(4), pp. 882–896. doi: 10.1016/j.cell.2014.03.026.

Feng, Y. and Klionsky, D. J. (2017) 'Autophagy regulates DNA repair through SQSTM1/p62', *Autophagy*. Taylor & Francis, 13(6), pp. 995–996. doi: 10.1080/15548627.2017.1317427.

Feng, Z. *et al.* (2005) 'The coordinate regulation of the p53 and mTOR pathways in cells', *Proceedings of the National Academy of Sciences of the United States of America*, 102(23), pp. 8204–8209. doi: 10.1073/pnas.0502857102.

Ferlazzo, M. L. and Foray, N. (2016) 'Huntington Disease: A Disease of DNA Methylation or DNA Breaks?', *American Journal of Pathology*. American Society for Investigative Pathology, 186(7), pp. 1750–1753. doi: 10.1016/j.ajpath.2016.05.001.

Ferlazzo, M. L. L. *et al.* (2014) 'Mutations of the Huntington's disease protein impact on the ATM-dependent signaling and repair pathways of the radiation-induced DNA double-strand breaks: Corrective effect of statins and bisphosphonates', *Molecular Neurobiology*, 49(3), pp. 1200–1211. doi: 10.1007/s12035-013-8591-7.

Fielden, J. *et al.* (2020) 'TEX264 coordinates p97- and SPRTN-mediated resolution of topoisomerase 1-DNA adducts', *Nature Communications*. Springer US, 11(1), pp. 1–16. doi: 10.1038/s41467-020-15000-w.

Findlay Black, H. *et al.* (2020) 'Frequency of the loss of CAA interruption in the HTT CAG tract and implications for Huntington disease in the reduced penetrance range', *Genetics in Medicine*. Springer US, 22(12), pp. 2108–2113. doi: 10.1038/s41436-020-0917-z.

Fleming, A. M., Ding, Y. and Burrows, C. J. (2017) 'Oxidative DNA damage is epigenetic by regulating gene transcription via base excision repair', *Proceedings of the National Academy*

of Sciences of the United States of America, 114(10), pp. 2604–2609. doi: 10.1073/pnas.1619809114.

Flower, M. *et al.* (2019) 'MSH3 modifies somatic instability and disease severity in Huntington's and myotonic dystrophy type 1', *Brain*, 142(7), pp. 1876–1886. doi: 10.1093/brain/awz115.

Fountain, J. W., Lockwood, W. K. and Collins, F. S. (1988) 'Transfection of primary human skin fibroblasts by electroporation', *Gene*, 68(1), pp. 167–172. doi: 10.1016/0378-1119(88)90610-5.

Fox, L. M. *et al.* (2020) 'Huntington's Disease Pathogenesis Is Modified In Vivo by Alfy/Wdfy3 and Selective Macroautophagy', *Neuron*. Elsevier Inc., 105(5), pp. 813-821.e6. doi: 10.1016/j.neuron.2019.12.003.

Fradet-Turcotte, A. *et al.* (2013) '53BP1 is a reader of the DNA-damage-induced H2A Lys 15 ubiquitin mark', *Nature*, 499(7456), pp. 50–54. doi: 10.1038/nature12318.

Frappart, P. O. and McKinnon, P. J. (2006) 'Ataxia-telangiectasia and related diseases', *NeuroMolecular Medicine*, 8(4), pp. 495–511. doi: 10.1385/NMM:8:4:495.

Fu, H., Hardy, J. and Duff, K. E. (2018) 'Selective vulnerability in neurodegenerative diseases', *Nature Neuroscience*. Springer US, 21(10), pp. 1350–1358. doi: 10.1038/s41593-018-0221-2.

Fu, Y. *et al.* (2017) 'A toxic mutant huntingtin species is resistant to selective autophagy', *Nature Chemical Biology*, 13(11), pp. 1152–1154. doi: 10.1038/nchembio.2461.

Gal, J. *et al.* (2007) 'P62 Accumulates and Enhances Aggregate Formation in Model Systems of Familial Amyotrophic Lateral Sclerosis', *Journal of Biological Chemistry*, 282(15), pp. 11068–11077. doi: 10.1074/jbc.M608787200.

Gao, R. *et al.* (2019) 'Mutant huntingtin impairs PNKP and ATXN3, disrupting DNA repair and transcription', *eLife*, 8, pp. 1–31. doi: 10.7554/eLife.42988.

García-Muse, T. and Aguilera, A. (2019) 'R Loops: From Physiological to Pathological Roles', *Cell*, 179(3), pp. 604–618. doi: 10.1016/j.cell.2019.08.055.

Gatti, M. *et al.* (2015) 'RNF168 promotes noncanonical K27ubiquitination to signal DNA damage', *Cell Reports*, 10(2), pp. 226–238. doi: 10.1016/j.celrep.2014.12.021.

Gauthier, L. R. *et al.* (2004) 'Huntingtin Controls Neurotrophic Support and Survival of Neurons by Enhancing BDNF Vesicular Transport along Microtubules', *Cell*, 118, pp. 127–138.

GeM-HD (2019) 'CAG Repeat Not Polyglutamine Length Determines Timing of Huntington's Disease Onset', *Cell*, 178(4), pp. 887-900.e14. doi: 10.1016/j.cell.2019.06.036.

GeM-HD, G. M. of H. D. C. (2015) 'Identification of Genetic Factors that Modify Clinical Onset of Huntington's Disease', *Cell*, 162(3), pp. 516–526. doi: 10.1016/j.cell.2015.07.003.

Gervais, F. G. *et al.* (2002) 'Recruitment and activation of caspase-8 by the Huntingtin-interacting protein Hip-1 and a novel partner Hippi', *Nature Cell Biology*, 4(2), pp. 95–105.

doi: 10.1038/ncb735.

Giuliano, P. (2003) ‘DNA damage induced by polyglutamine-expanded proteins’, *Human Molecular Genetics*, 12(18), pp. 2301–2309. doi: 10.1093/hmg/ddg242.

Godin, J. D. *et al.* (2010) ‘Huntingtin Is Required for Mitotic Spindle Orientation and Mammalian Neurogenesis’, *Neuron*, 67(3), pp. 392–406. doi: 10.1016/j.neuron.2010.06.027.

Golde, T. E. *et al.* (2013) ‘Thinking laterally about neurodegenerative proteinopathies’, *Journal of Clinical Investigation*, 123(5), pp. 1847–1855. doi: 10.1172/JCI66029.

Gomes-Pereira, M. *et al.* (2004) ‘Pms2 is a genetic enhancer of trinucleotide CAG.CTG repeat somatic mosaicism: implications for the mechanism of triplet repeat expansion.’, *Human molecular genetics*, 13(16), pp. 1815–25. doi: 10.1093/hmg/ddh186.

Gómez-González, B. *et al.* (2011) ‘Genome-wide function of THO/TREX in active genes prevents R-loop-dependent replication obstacles’, *EMBO Journal*, 30(15), pp. 3106–3119. doi: 10.1038/emboj.2011.206.

Goold, R. *et al.* (2019) ‘FAN1 modifies Huntington’s disease progression by stabilizing the expanded HTT CAG repeat’, *Human Molecular Genetics*, 28(4), pp. 650–661. doi: 10.1093/hmg/ddy375.

Goold, R. *et al.* (2021) ‘FAN1 controls mismatch repair complex assembly via MLH1 retention to stabilize CAG repeat expansion in Huntington’s disease’, *Cell Reports*, 36(9), p. 109649. doi: 10.1016/j.celrep.2021.109649.

Goula, A.-V. *et al.* (2009) ‘Stoichiometry of Base Excision Repair Proteins Correlates with Increased Somatic CAG Instability in Striatum over Cerebellum in Huntington’s Disease Transgenic Mice’, *PLoS Genet*, 5(12), p. 1000749. doi: 10.1371/journal.pgen.1000749.

Le Gras, S. *et al.* (2017) ‘Altered enhancer transcription underlies Huntington’s disease striatal transcriptional signature’, *Scientific Reports*. Nature Publishing Group, 7(February), pp. 1–11. doi: 10.1038/srep42875.

Gregersen, L. H. and Svejstrup, J. Q. (2018) ‘The Cellular Response to Transcription-Blocking DNA Damage’, *Trends in Biochemical Sciences*. Elsevier Ltd, 43(5), pp. 327–341. doi: 10.1016/j.tibs.2018.02.010.

Guerrero, E. N. *et al.* (2019) ‘Amyotrophic lateral sclerosis-associated TDP-43 mutation Q331K prevents nuclear translocation of XRCC4-DNA ligase 4 complex and is linked to genome damage-mediated neuronal apoptosis.’, *Human molecular genetics*, 28(5), pp. 2459–2476. doi: 10.1093/hmg/ddz062.

Gueven, N. *et al.* (2004) ‘Aprataxin, a novel protein that protects against genotoxic stress’, *Human Molecular Genetics*, 13(10), pp. 1081–1093. doi: 10.1093/hmg/ddh122.

Guo, J. *et al.* (2016) ‘MutSβ promotes trinucleotide repeat expansion by recruiting DNA polymerase β to nascent (CAG) n or (CTG) n hairpins for error-prone DNA synthesis’, *Cell Research*. Nature Publishing Group, 26(7), pp. 775–786. doi: 10.1038/cr.2016.66.

Guo, Z. *et al.* (2010) ‘ATM activation by oxidative stress’, *Science*, 330(6003), pp. 517–521.

doi: 10.1126/science.1192912.

Guo, Z. *et al.* (2019) 'RAD6B Plays a Critical Role in Neuronal DNA Damage Response to Resist Neurodegeneration', *Frontiers in Cellular Neuroscience*, 13(August), pp. 1–13. doi: 10.3389/fncel.2019.00392.

Gupta, R. *et al.* (2018) 'DNA Repair Network Analysis Reveals Shieldin as a Key Regulator of NHEJ and PARP Inhibitor Sensitivity', *Cell*. Elsevier Inc., 173(4), pp. 972-988.e23. doi: 10.1016/j.cell.2018.03.050.

Gusella, J. F., Macdonald, M. E. and Lee, J. M. (2014) 'Genetic modifiers of Huntington's disease', *Movement Disorders*, 29(11), pp. 1359–1365. doi: 10.1002/mds.26001.

Gutierrez, A. *et al.* (2020) 'Evaluation of Biochemical and Epigenetic Measures of Peripheral Brain-Derived Neurotrophic Factor (BDNF) as a Biomarker in Huntington's Disease Patients', *Frontiers in Molecular Neuroscience*, 12(January), pp. 1–11. doi: 10.3389/fnmol.2019.00335.

Habault, J. and Poyet, J. L. (2019) 'Recent advances in cell penetrating peptide-based anticancer therapies', *Molecules*, 24(5), pp. 1–17. doi: 10.3390/molecules24050927.

El Hage, A. *et al.* (2010) 'Loss of Topoisomerase I leads to R-loop-mediated transcriptional blocks during ribosomal RNA synthesis', *Genes and Development*, 24(14), pp. 1546–1558. doi: 10.1101/gad.573310.

Harjes, P. and Wanker, E. E. (2003) 'The hunt for huntingtin function: Interaction partners tell many different stories', *Trends in Biochemical Sciences*, 28(8), pp. 425–433. doi: 10.1016/S0968-0004(03)00168-3.

Harper, J. W. and Elledge, S. J. (2007) 'The DNA Damage Response: Ten Years After', *Molecular Cell*, 28(5), pp. 739–745. doi: 10.1016/j.molcel.2007.11.015.

Harrigan, J. A. *et al.* (2017) 'Deubiquitylating enzymes and drug discovery: emerging opportunities', *Nature Reviews Drug Discovery 2017 17:1*. Nature Publishing Group, 17(1), pp. 57–78. doi: 10.1038/nrd.2017.152.

Havel, L. S. *et al.* (2011) 'Preferential accumulation of N-terminal mutant huntingtin in the nuclei of striatal neurons is regulated by phosphorylation', *Human Molecular Genetics*, 20(7), pp. 1424–1437. doi: 10.1093/hmg/ddr023.

Hayyan, M., Hashim, M. A. and Alnashef, I. M. (2016) 'Superoxide Ion: Generation and Chemical Implications', *Chemical Reviews*, 116(5), pp. 3029–3085. doi: 10.1021/acs.chemrev.5b00407.

Heng, M. Y. *et al.* (2010) 'Early alterations of autophagy in Huntington disease-like mice', *Autophagy*, 6(8), pp. 1206–1208. doi: 10.4161/auto.6.8.13617.

Hensman Moss, D. J. *et al.* (2017) 'Huntington's disease blood and brain show a common gene expression pattern and share an immune signature with Alzheimer's disease', *Scientific Reports*. Nature Publishing Group, 7(September 2016), pp. 1–12. doi: 10.1038/srep44849.

Her, J. *et al.* (2016) 'Factors forming the BRCA1-A complex orchestrate BRCA1 recruitment to the sites of DNA damage', *Acta Biochimica et Biophysica Sinica*, 48(7), pp. 658–664. doi:

10.1093/abbs/gmw047.

Hewitt, G. *et al.* (2016) 'SQSTM1/p62 mediates crosstalk between autophagy and the UPS in DNA repair', *Autophagy*. Taylor & Francis, 12(10), pp. 1917–1930. doi: 10.1080/15548627.2016.1210368.

Hewitt, G. and Korolchuk, V. I. (2017) 'Repair, Reuse, Recycle: The Expanding Role of Autophagy in Genome Maintenance', *Trends in Cell Biology*. Elsevier Ltd, 27(5), pp. 340–351. doi: 10.1016/j.tcb.2016.11.011.

Hickman, R. A. *et al.* (2021) 'Developmental malformations in Huntington disease: neuropathologic evidence of focal neuronal migration defects in a subset of adult brains', *Acta Neuropathologica*. Springer Berlin Heidelberg, 141(3), pp. 399–413. doi: 10.1007/s00401-021-02269-4.

Higelin, J. *et al.* (2016) 'FUS mislocalization and vulnerability to DNA damage in ALS patients derived hiPSCs and aging motoneurons', *Frontiers in Cellular Neuroscience*. Frontiers, 10, p. 290. doi: 10.3389/fncel.2016.00290.

Ho, L. W. *et al.* (2001) 'Wild type huntingtin reduces the cellular toxicity of mutant huntingtin in mammalian cell models of Huntington's disease', *Journal of Medical Genetics*, 38(7), pp. 450–452. doi: 10.1136/jmg.38.7.450.

Hoch, N. C. *et al.* (2017) 'XRCC1 mutation is associated with PARP1 hyperactivation and cerebellar ataxia', *Nature*. Nature Publishing Group, 541(7635), pp. 87–91. doi: 10.1038/nature20790.

Hodge, C. D. *et al.* (2016) 'RNF8 E3 Ubiquitin Ligase Stimulates Ubc13 E2 Conjugating Activity That Is Essential for DNA Double Strand Break Signaling and BRCA1 Tumor Suppressor Recruitment', *Journal of Biological Chemistry*, 291(18), pp. 9396–9410. doi: 10.1074/jbc.M116.715698.

Hodges, A. *et al.* (2006) 'Regional and cellular gene expression changes in human Huntington's disease brain', *Human Molecular Genetics*, 15(6), pp. 965–977. doi: 10.1093/hmg/ddl013.

Hodroj, D. *et al.* (2017) ' An ATR -dependent function for the Ddx19 RNA helicase in nuclear R-loop metabolism ', *The EMBO Journal*, 36(9), pp. 1182–1198. doi: 10.15252/embj.201695131.

Hoffner, G. and Djian, P. (2014) 'Monomeric, oligomeric and polymeric proteins in huntington disease and other diseases of polyglutamine expansion', *Brain Sciences*, 4(1), pp. 91–122. doi: 10.3390/brainsci4010091.

Hoffner, G., Souès, S. and Djian, P. (2007) 'Aggregation of expanded huntingtin in the brains of patients with Huntington disease.', *Prion*, 1(1), pp. 26–31. doi: 10.4161/pri.1.1.4056.

Horn, V. *et al.* (2019) 'Structural basis of specific H2A K13/K15 ubiquitination by RNF168', *Nature Communications*, 10(1), pp. 1–12. doi: 10.1038/s41467-019-09756-z.

Horvath, S. *et al.* (2016) 'Huntington's disease accelerates epigenetic aging of human brain and disrupts DNA methylation levels', *Aging*, 8(7), pp. 1485–1512.

Hou, Y. *et al.* (2019) 'Ageing as a risk factor for neurodegenerative disease', *Nature Reviews Neurology*. Springer US, 15(10), pp. 565–581. doi: 10.1038/s41582-019-0244-7.

Hsiao, K. Y. and Mizzen, C. A. (2013) 'Histone H4 deacetylation facilitates 53BP1 DNA damage signaling and double-strand break repair', *Journal of Molecular Cell Biology*, 5(3), pp. 157–165. doi: 10.1093/jmcb/mjs066.

Hu, J. *et al.* (2014) 'Exploring the effect of sequence length and composition on allele-selective inhibition of human huntingtin expression by single-stranded silencing RNAs', *Nucleic Acid Therapeutics*, 24(3), pp. 199–209. doi: 10.1089/nat.2013.0476.

Hu, Q. *et al.* (2017) 'Mechanisms of Ubiquitin-Nucleosome Recognition and Regulation of 53BP1 Chromatin Recruitment by RNF168/169 and RAD18', *Molecular Cell*, 66(4), pp. 473-487.e9. doi: 10.1016/j.molcel.2017.04.009.

Hubert, L. *et al.* (2011) 'Topoisomerase 1 and Single-Strand Break Repair Modulate Transcription-Induced CAG Repeat Contraction in Human Cells', *Molecular and Cellular Biology*, 31(15), pp. 3105–3112. doi: 10.1128/mcb.05158-11.

Huen, M. S. Y. *et al.* (2007) 'RNF8 Transduces the DNA-Damage Signal via Histone Ubiquitylation and Checkpoint Protein Assembly', *Cell*, 131(5), pp. 901–914. doi: 10.1016/j.cell.2007.09.041.

Huertas, P. and Aguilera, A. (2003) 'Cotranscriptionally formed DNA:RNA hybrids mediate transcription elongation impairment and transcription-associated recombination', *Molecular Cell*, 12(3), pp. 711–721. doi: 10.1016/j.molcel.2003.08.010.

Hutchins, A. P. *et al.* (2013) 'The repertoires of ubiquitinating and deubiquitinating enzymes in eukaryotic genomes', *Molecular Biology and Evolution*, 30(5), pp. 1172–1187. doi: 10.1093/molbev/mst022.

Huyen, Y. *et al.* (2004) 'Methylated lysine 79 of histone H3 targets 53BP1 to DNA double-strand breaks', *Nature*, 432(7015), pp. 406–411. doi: 10.1038/nature03114.

Iacovoni, J. S. *et al.* (2010) 'High-resolution profiling of γh2AX around DNA double strand breaks in the mammalian genome', *EMBO Journal*, 29(8), pp. 1446–1457. doi: 10.1038/emboj.2010.38.

Iyama, T. and Wilson, D. M. (2013) 'DNA repair mechanisms in dividing and non-dividing cells', *DNA Repair*. Elsevier B.V., 12(8), pp. 620–636. doi: 10.1016/j.dnarep.2013.04.015.

Jackson, S. P. and Bartek, J. (2009) 'The DNA-damage response in human biology and disease', *Nature*. Nature Publishing Group, 461(7267), pp. 1071–1078. doi: 10.1038/nature08467.

Jacquet, K. *et al.* (2016) 'The TIP60 Complex Regulates Bivalent Chromatin Recognition by 53BP1 through Direct H4K20me Binding and H2AK15 Acetylation', *Molecular Cell*, 62(3), pp. 409–421. doi: 10.1016/j.molcel.2016.03.031.

Jakobi, A. J. *et al.* (2020) 'Structural basis of p62/SQSTM1 helical filaments and their role in cellular cargo uptake', *Nature Communications*. Springer US, 11(1), pp. 1–15. doi: 10.1038/s41467-020-14343-8.

Jędrak, P. *et al.* (2018) 'Mitochondrial alterations accompanied by oxidative stress conditions in skin fibroblasts of Huntington's disease patients', *Metabolic Brain Disease*, 33(6), pp. 2005–2017. doi: 10.1007/s11011-018-0308-1.

Jeon, G. S. *et al.* (2012) 'Deregulation of BRCA1 leads to impaired spatiotemporal dynamics of γ-H2AX and DNA damage responses in Huntington's disease', *Molecular Neurobiology*, 45(3), pp. 550–563. doi: 10.1007/s12035-012-8274-9.Deregulation.

Jimenez-Sanchez, M. *et al.* (2017) 'Huntington ' s Disease : Mechanisms of Pathogenesis and Therapeutic Strategies', *Cold Spring Harb Perspect Med*. doi: 10.1101/cshperspect.a024240.

Johansen, T. and Lamark, T. (2011) 'Selective autophagy mediated by autophagic adapter proteins', *Autophagy*, 7(3), pp. 279–296. doi: 10.4161/auto.7.3.14487.

Juenemann, K. *et al.* (2018) 'Dynamic recruitment of ubiquitin to mutant huntingtin inclusion bodies', *Scientific Reports*. Springer US, 8(1), pp. 1–15. doi: 10.1038/s41598-018-19538-0.

Jungmichel, S. and Stucki, M. (2010) 'MDC1: The art of keeping things in focus', *Chromosoma*, 119(4), pp. 337–349. doi: 10.1007/s00412-010-0266-9.

Junttila, A. *et al.* (2016) 'Cerebrospinal Fluid TDP-43 in Frontotemporal Lobar Degeneration and Amyotrophic Lateral Sclerosis Patients with and without the C9ORF72 Hexanucleotide Expansion', *Dementia and Geriatric Cognitive Disorders Extra*, 6(1), pp. 142–149. doi: 10.1159/000444788.

Jurga, M. *et al.* (2021) 'USP11 controls R-loops by regulating senataxin proteostasis', *Nature Communications*. Springer US, 12(1), p. 5156. doi: 10.1038/s41467-021-25459-w.

Kabouridis, P. S. (2003) 'Biological applications of protein transduction technology', *Trends in Biotechnology*, 21(11), pp. 498–503. doi: 10.1016/j.tibtech.2003.09.008.

Kadyrova, L. Y. *et al.* (2020) 'Human MutLγ, the MLH1-MLH3 heterodimer, is an endonuclease that promotes DNA expansion.', *Proceedings of the National Academy of Sciences of the United States of America*, 117(7), pp. 3535–3542. doi: 10.1073/pnas.1914718117.

Kam, T. I. *et al.* (2018) 'Poly(ADP-ribose) drives pathologic a-synuclein neurodegeneration in Parkinson's disease', *Science*, 362(6414). doi: 10.1126/science.aat8407.

Kang, R. *et al.* (2011) 'The Beclin 1 network regulates autophagy and apoptosis', *Cell Death and Differentiation*. Nature Publishing Group, 18(4), pp. 571–580. doi: 10.1038/cdd.2010.191.

Karantza-Wadsworth, V. *et al.* (2007) 'Autophagy mitigates metabolic stress and genome damage in mammary tumorigenesis', *Genes and Development*, 21(13), pp. 1621–1635. doi: 10.1101/gad.1565707.

Kashiwagi, H. *et al.* (2018) 'Repair kinetics of DNA double-strand breaks and incidence of apoptosis in mouse neural stem/progenitor cells and their differentiated neurons exposed to ionizing radiation', *Journal of Radiation Research*, 59(3), pp. 261–271. doi: 10.1093/jrr/rrx089.

Katahira, J. (2012) 'mRNA export and the TREX complex', *Biochimica et Biophysica Acta* -

Gene Regulatory Mechanisms. Elsevier B.V., 1819(6), pp. 507–513. doi: 10.1016/j.bbagrm.2011.12.001.

Katyal, S. *et al.* (2007) 'TDP1 facilitates chromosomal single-strand break repair in neurons and is neuroprotective in vivo.', *The EMBO journal*, 26(22), pp. 4720–31. doi: 10.1038/sj.emboj.7601869.

Katyal, S. *et al.* (2014) 'Aberrant topoisomerase-1 DNA lesions are pathogenic in neurodegenerative genome instability syndromes', *Nature Neuroscience*. Nature Publishing Group, 17(6), pp. 813–821. doi: 10.1038/nn.3715.

Kennedy, L. *et al.* (2003) 'Dramatic tissue-specific mutation length increases are an early molecular event in Huntington disease pathogenesis', *Human molecular genetics*. Hum Mol Genet, 12(24), pp. 3359–3367. doi: 10.1093/HMG/DDG352.

Keramaris, E. *et al.* (2000) 'Involvement of Caspase 3 in Apoptotic Death of Cortical Neurons Evoked by DNA Damage', *Molecular and Cellular Neuroscience*. Academic Press, 15(4), pp. 368–379. doi: 10.1006/MCNE.2000.0838.

Keryer, G. *et al.* (2011) 'Ciliogenesis is regulated by a huntingtin-HAP1-PCM1 pathway and is altered in Huntington disease', *Journal of Clinical Investigation*, 121(11), pp. 4372–4382. doi: 10.1172/JCI57552.

Keum, J. W. *et al.* (2016) 'The HTT CAG-Expansion Mutation Determines Age at Death but Not Disease Duration in Huntington Disease', *American Journal of Human Genetics*. The American Society of Human Genetics, 98(2), pp. 287–298. doi: 10.1016/j.ajhg.2015.12.018.

Kim, M. O. *et al.* (2008) 'Altered histone monoubiquitylation mediated by mutant huntingtin induces transcriptional dysregulation', *Journal of Neuroscience*, 28(15), pp. 3947–3957. doi: 10.1523/JNEUROSCI.5667-07.2008.

Kim, Y. E. *et al.* (2016) 'Soluble Oligomers of PolyQ-Expanded Huntingtin Target a Multiplicity of Key Cellular Factors', *Molecular Cell*, 63(6), pp. 951–964. doi: 10.1016/j.molcel.2016.07.022.

Kirkwood, S. C. *et al.* (2001) 'Progression of symptoms in the early and middle stages of Huntington disease', *Archives of Neurology*, 58(2), pp. 273–278. doi: 10.1001/archneur.58.2.273.

Ko, J., Ou, S. and Patterson, P. H. (2001) 'New anti-huntingtin monoclonal antibodies: Implications for huntingtin conformation and its binding proteins', *Brain Research Bulletin*, 56(3–4), pp. 319–329. doi: 10.1016/S0361-9230(01)00599-8.

Kocyłowski, M. K. *et al.* (2015) 'Ubiquitin-H2AX fusions render 53BP1 recruitment to DNA damage sites independent of RNF8 or RNF168', *Cell Cycle*, 14(11), pp. 1748–1758. doi: 10.1080/15384101.2015.1010918.

Kok, J. R. *et al.* (2021) 'DNA damage as a mechanism of neurodegeneration in ALS and a contributor to astrocyte toxicity', *Cellular and Molecular Life Sciences*. Springer International Publishing, 78(15), pp. 5707–5729. doi: 10.1007/s00018-021-03872-0.

Konopka, A. *et al.* (2020) 'Impaired NHEJ repair in amyotrophic lateral sclerosis is associated

with TDP-43 mutations', *Molecular Neurodegeneration*. BioMed Central, 15(1), p. 51. doi: 10.1186/s13024-020-00386-4.

Kovtun, I. V. *et al.* (2007) 'OGG1 initiates age-dependent CAG trinucleotide expansion in somatic cells', *Nature*, 447(7143), pp. 447–452. doi: 10.1038/nature05778.

Krais, J. J. *et al.* (2021) 'RNF168-mediated localization of BARD1 recruits the BRCA1-PALB2 complex to DNA damage', *Nature Communications*. Springer US, 12(1), pp. 1–12. doi: 10.1038/s41467-021-25346-4.

Kurosawa, M. *et al.* (2015) 'Depletion of p62 reduces nuclear inclusions and paradoxically ameliorates disease phenotypes in Huntington's model mice', *Human Molecular Genetics*, 24(4), pp. 1092–1105. doi: 10.1093/hmg/ddu522.

Kwan, W. *et al.* (2012) 'Mutant huntingtin impairs immune cell migration in Huntington disease', *Journal of Clinical Investigation*, 122(12), pp. 4737–4747. doi: 10.1172/JCI64484.

Labbadia, J. and Morimoto, R. I. (2013) 'Huntington's disease: underlying molecular mechanisms and emerging concepts', *Trends Biochem Sci*, 38(8), pp. 378–385. doi: 10.1016/j.tibs.2013.05.003.Huntington.

Lachaud, C. *et al.* (2016) 'Ubiquitinated Fancd2 recruits Fan1 to stalled replication forks to prevent genome instability', *Science*, 351(6275), pp. 846–849. doi: 10.1126/science.aad5634.

Lahue, R. S. (2020) 'New developments in Huntington's disease and other triplet repeat diseases: DNA repair turns to the dark side', *Neuronal Signaling*, 4(4), pp. 1–14. doi: 10.1042/ns20200010.

Lans, H. *et al.* (2019) 'The DNA damage response to transcription stress', *Nature Reviews Molecular Cell Biology*. Springer US, 20(12), pp. 766–784. doi: 10.1038/s41580-019-0169-4.

Lanz, M. C., Dibitetto, D. and Smolka, M. B. (2019) 'DNA damage kinase signaling: checkpoint and repair at 30 years', *The EMBO Journal*, 38(18). doi: 10.15252/embj.2019101801.

Lavin, M. F. (2008) 'Ataxia-telangiectasia: From a rare disorder to a paradigm for cell signalling and cancer', *Nature Reviews Molecular Cell Biology*, 9(10), pp. 759–769. doi: 10.1038/nrm2514.

Lavin, M. F., Delia, D. and Chessa, L. (2006) 'ATM and the DNA damage response', *EMBO Reports*, 7(2), pp. 154–160. doi: 10.1038/sj.embor.7400629.

Leavitt, B. R. *et al.* (2006) 'Wild-type huntingtin protects neurons from excitotoxicity', *Journal of Neurochemistry*, 96(4), pp. 1121–1129. doi: 10.1111/j.1471-4159.2005.03605.x.

Lee, B. L. *et al.* (2017) 'Molecular Basis for K63-Linked Ubiquitination Processes in Double-Strand DNA Break Repair: A Focus on Kinetics and Dynamics', *Journal of Molecular Biology*. Elsevier Ltd, 429(22), pp. 3409–3429. doi: 10.1016/j.jmb.2017.05.029.

Lee, H., Kim, M. N. and Ryu, K. Y. (2017) 'Effect of p62/SQSTM1 polyubiquitination on its autophagic adaptor function and cellular survival under oxidative stress induced by arsenite', *Biochemical and Biophysical Research Communications*. Elsevier Ltd, 486(3), pp. 839–844.

doi: 10.1016/j.bbrc.2017.03.146.

Lee, J.-M. *et al.* (2017) 'A modifier of Huntington's disease onset at the MLH1 locus.', *Human molecular genetics*, 26(19), pp. 3859–3867. doi: 10.1093/hmg/ddx286.

Lee, J. H. *et al.* (2010) '53BP1 promotes ATM activity through direct interactions with the MRN complex', *EMBO Journal*, 29(3), pp. 574–585. doi: 10.1038/emboj.2009.372.

Lee, J. H. *et al.* (2021) 'Poly-ADP-ribosylation drives loss of protein homeostasis in ATM and Mre11 deficiency', *Molecular Cell*. Elsevier Inc., 81(7), pp. 1515-1533.e5. doi: 10.1016/j.molcel.2021.01.019.

Lee, M. J., Lee, J. H. and Rubinsztein, D. C. (2013) 'Tau degradation: The ubiquitin-proteasome system versus the autophagy-lysosome system', *Progress in Neurobiology*. Elsevier Ltd, 105, pp. 49–59. doi: 10.1016/j.pneurobio.2013.03.001.

Lee, Y. J. *et al.* (2017) 'Keap1/Cullin3 Modulates p62/SQSTM1 Activity via UBA Domain Ubiquitination', *Cell Reports*. Elsevier, 20(8), p. 1994. doi: 10.1016/j.celrep.2017.08.019.

Li *et al.* (2019) 'Cytoplasmic restriction of mutated SOD1 impairs the DNA repair process in spinal cord neurons', *Cells*. MDPI AG, 8(12), p. 1502. doi: 10.3390/cells8121502.

Li, G. M. (2008) 'Mechanisms and functions of DNA mismatch repair', *Cell Research*, 18(1), pp. 85–98. doi: 10.1038/cr.2007.115.

Li, M. *et al.* (2015) 'RECQ5-dependent SUMOylation of DNA topoisomerase I prevents transcription-associated genome instability', *Nature Communications*. Nature Publishing Group, 6, pp. 1–13. doi: 10.1038/ncomms7720.

Li, S.-H. *et al.* (2002) 'Interaction of Huntington Disease Protein with Transcriptional Activator Sp1', *Molecular and Cellular Biology*, 22(5), pp. 1277–1287. doi: 10.1128/mcb.22.5.1277-1287.2002.

Lin, L. *et al.* (2015) 'In Vitro Differentiation of Human Neural Progenitor Cells Into Striatal GABAergic Neurons', *Stem Cells Translational Medicine*, 4(7), pp. 775–788. doi: 10.5966/sctm.2014-0083.

Lin, Y. *et al.* (2010) 'R loops stimulate genetic instability of CTG·CAG repeats', *Proceedings of the National Academy of Sciences*. National Academy of Sciences, 107(2), pp. 692–697. doi: 10.1073/PNAS.0909740107.

Lin, Y., Dion, V. and Wilson, J. H. (2006) 'Transcription promotes contraction of CAG repeat tracts in human cells', *Nature Structural and Molecular Biology*, 13(2), pp. 179–180. doi: 10.1038/nsmb1042.

Lin, Y. and Wilson, J. H. (2012) 'Nucleotide Excision Repair, Mismatch Repair, and R-Loops Modulate Convergent Transcription-Induced Cell Death and Repeat Instability', *PLoS ONE*, 7(10), pp. 1–9. doi: 10.1371/journal.pone.0046807.

Lin, Z. and Fang, D. (2013) 'The Roles of SIRT1 in Cancer', *Genes and Cancer*, 4(3–4), pp. 97–104. doi: 10.1177/1947601912475079.

Liu, J. and Zeitlin, S. O. (2017) 'Is Huntingtin Dispensable in the Adult Brain?', *Journal of Huntington's Disease*, 6(1), pp. 1–17. doi: 10.3233/JHD-170235.

Liu, T. *et al.* (2010) 'FAN1 acts with FANCI-FANCD2 to promote DNA interstrand cross-link repair', *Science*, 329(5992), pp. 693–696. doi: 10.1126/science.1192656.

Liu, W. J. *et al.* (2016) 'P62 Links the Autophagy Pathway and the Ubiqutin-Proteasome System Upon Ubiquitinated Protein Degradation', *Cellular and Molecular Biology Letters*. Cellular & Molecular Biology Letters, 21(1), pp. 1–14. doi: 10.1186/s11658-016-0031-z.

Liu, Y. *et al.* (2009) 'Coordination between polymerase β and FEN1 can modulate CAG repeat expansion', *Journal of Biological Chemistry*, 284(41), pp. 28352–28366. doi: 10.1074/jbc.M109.050286.

Löbrich, M. *et al.* (2010) 'γH2AX foci analysis for monitoring DNA double-strand break repair: Strengths, limitations and optimization', *Cell Cycle*, 9(4), pp. 662–669. doi: 10.4161/cc.9.4.10764.

Lombardi, P. M., Matunis, M. J. and Wolberger, C. (2017) 'RAP80, ubiquitin and SUMO in the DNA damage response', *Journal of Molecular Medicine*. Journal of Molecular Medicine, 95(8), pp. 799–807. doi: 10.1007/s00109-017-1561-1.

Lopes, C. *et al.* (2016) 'Dominant-negative effects of adult-onset huntingtin mutations alter the division of human embryonic stem cells-derived neural cells', *PLoS ONE*, 11(2), pp. 1–16. doi: 10.1371/journal.pone.0148680.

Lu, T. *et al.* (2004) 'Gene regulation and DNA damage in the ageing human brain', *Nature*, 429(6994), pp. 883–891. doi: 10.1038/nature02661.

Lu, X. *et al.* (2021) 'RNF8-ubiquitinated KMT5A is required for RNF168-induced H2A ubiquitination in response to DNA damage', *FASEB Journal*, 35(4), pp. 1–18. doi: 10.1096/fj.202002234R.

Lu, X. H. *et al.* (2014) 'Targeting ATM ameliorates mutant Huntingtin toxicity in cell and animal models of Huntington's disease', *Science Translational Medicine*, 6(268), p. 268ra178. doi: 10.1126/scitranslmed.3010523.

Luijsterburg, M. S. *et al.* (2012) 'A new non-catalytic role for ubiquitin ligase RNF8 in unfolding higher-order chromatin structure', *EMBO Journal*. Nature Publishing Group, 31(11), pp. 2511–2527. doi: 10.1038/emboj.2012.104.

Luijsterburg, M. S. *et al.* (2017) 'A PALB2-interacting domain in RNF168 couples homologous recombination to DNA break-induced chromatin ubiquitylation', *eLife*, 6, pp. 1–26. doi: 10.7554/eLife.20922.

Luo, K., Yuans, J. and Lous, Z. (2011) 'Oligomerization of MDC1 protein is important for proper DNA damage response', *Journal of Biological Chemistry*, 286(32), pp. 28192–28199. doi: 10.1074/jbc.M111.258087.

Luthi-Carter, R. *et al.* (2000) 'Decreased expression of striatal signaling genes in a mouse model of Huntington's disease', *Human Molecular Genetics*, 9(9), pp. 1259–1271. doi: 10.1093/hmg/9.9.1259.

Ma, S., Attarwala, I. Y. and Xie, X. (2019) 'SQSTM1/p62: A Potential Target for Neurodegenerative Disease', *ACS Chemical Neuroscience*, 10(5), pp. 2094–2114. doi: 10.1021/acschemneuro.8b00516.

MacDonald, M. E. *et al.* (1993) 'A novel gene containing a trinucleotide repeat that is expanded and unstable on Huntington's disease chromosomes', *Cell*, 72(6), pp. 971–983. doi: 10.1016/0092-8674(93)90585-E.

Machiela, E. *et al.* (2020) 'The Interaction of Aging and Cellular Stress Contributes to Pathogenesis in Mouse and Human Huntington Disease Neurons', *Frontiers in Aging Neuroscience*, 12(September), pp. 1–17. doi: 10.3389/fnagi.2020.524369.

MacKay, C. *et al.* (2010) 'Identification of KIAA1018/FAN1, a DNA Repair Nuclease Recruited to DNA Damage by Monoubiquitinated FANCD2', *Cell*, 142(1), pp. 65–76. doi: 10.1016/j.cell.2010.06.021.

Madabhushi, R. *et al.* (2015) 'Activity-Induced DNA Breaks Govern the Expression of Neuronal Early-Response Genes', *Cell*. Elsevier, 161(7), pp. 1592–1605. doi: 10.1016/j.cell.2015.05.032.

Madabhushi, R., Pan, L. and Tsai, L. H. (2014) 'DNA damage and its links to neurodegeneration', *Neuron*. Elsevier Inc., 83(2), pp. 266–282. doi: 10.1016/j.neuron.2014.06.034.

Mah, L. J., El-Osta, A. and Karagiannis, T. C. (2010) 'γH2AX: A sensitive molecular marker of DNA damage and repair', *Leukemia*. Nature Publishing Group, 24(4), pp. 679–686. doi: 10.1038/leu.2010.6.

Mailand, N. *et al.* (2007) 'RNF8 Ubiquitylates Histones at DNA Double-Strand Breaks and Promotes Assembly of Repair Proteins', *Cell*, 131(5), pp. 887–900. doi: 10.1016/j.cell.2007.09.040.

Maiuri, T. *et al.* (2017) 'Huntingtin is a scaffolding protein in the ATM oxidative DNA damage response complex', *Human Molecular Genetics*, 26(2), pp. 395–406. doi: 10.1093/hmg/ddw395.

Maiuri, T. *et al.* (2019) 'DNA Damage Repair in Huntington's Disease and Other Neurodegenerative Diseases.', *Neurotherapeutics : the journal of the American Society for Experimental NeuroTherapeutics*. Neurotherapeutics, 16(4), pp. 948–956. doi: 10.1007/s13311-019-00768-7.

Mangiarini, L. *et al.* (1996) 'Exon 1 of the HD Gene with an Expanded CAG Repeat Is Sufficient to Cause a Progressive Neurological Phenotype in Transgenic Mice', *Cell*, 87(3), pp. 493–506. doi: 10.1016/S0092-8674(00)81369-0.

Manley, K. *et al.* (1999) 'Msh2 deficiency prevents in vivo somatic instability of the CAG repeat in Huntington disease transgenic mice', *Nature Genetics*, 23(4), pp. 471–473. doi: 10.1038/70598.

Manzo, S. G. *et al.* (2018) 'DNA Topoisomerase I differentially modulates R-loops across the human genome', *Genome Biology*. Genome Biology, 19(1), pp. 1–18. doi: 10.1186/s13059-018-1478-1.

Marchina, E. *et al.* (2014) 'Gene expression profile in fibroblasts of Huntington's disease patients and controls', *Journal of the Neurological Sciences*, 337(1–2), pp. 42–46. doi: 10.1016/j.jns.2013.11.014.

Maréchal, A. and Zou, L. (2013) 'DNA damage sensing by the ATM and ATR kinases', *Cold Spring Harbor Perspectives in Biology*, 5(9), pp. 1–18. doi: 10.1101/cshperspect.a012716.

Martí, E. (2016) 'RNA toxicity induced by expanded CAG repeats in Huntington's disease', *Brain Pathology*, 26(6), pp. 779–786. doi: 10.1111/bpa.12427.

Martin, D. D. O. *et al.* (2015) 'Autophagy in Huntington disease and huntingtin in autophagy', *Trends in Neurosciences*. Elsevier Ltd, 38(1), pp. 26–35. doi: 10.1016/j.tins.2014.09.003.

Martinez-Vicente, M. *et al.* (2010) 'Cargo recognition failure is responsible for inefficient autophagy in Huntington's disease', *Nature Neuroscience*. Nature Publishing Group, 13(5), pp. 567–576. doi: 10.1038/nn.2528.

Marzban, H. *et al.* (2015) 'Cellular commitment in the developing cerebellum', *Frontiers in Cellular Neuroscience*, 8(JAN), pp. 1–26. doi: 10.3389/fncel.2014.00450.

Massey, T. H. and Jones, L. (2018) 'The central role of DNA damage and repair in CAG repeat diseases', *Disease Models & Mechanisms*, 11(1), p. dmm031930. doi: 10.1242/dmm.031930.

Mastrocola, A. S. *et al.* (2013) 'The RNA-binding protein fused in sarcoma (FUS) functions downstream of poly(ADP-ribose) polymerase (PARP) in response to DNA damage.', *The Journal of Biological Chemistry*. American Society for Biochemistry and Molecular Biology, 288(34), pp. 24731–41. doi: 10.1074/jbc.M113.497974.

Mattiroli, F. *et al.* (2012) 'RNF168 ubiquitinates K13-15 on H2A/H2AX to drive DNA damage signaling', *Cell*. Elsevier Inc., 150(6), pp. 1182–1195. doi: 10.1016/j.cell.2012.08.005.

Mattson, M. P. and Arumugam, T. V. (2018) 'Hallmarks of Brain Aging: Adaptive and Pathological Modification by Metabolic States', *Cell Metabolism*. Elsevier Inc., 27(6), pp. 1176–1199. doi: 10.1016/j.cmet.2018.05.011.

McColgan, P. and Tabrizi, S. J. (2018) 'Huntington's disease: a clinical review', *European Journal of Neurology*, 25(1), pp. 24–34. doi: 10.1111/ene.13413.

McFarland, K. N. *et al.* (2013) 'Genome-wide increase in histone H2A ubiquitylation in a mouse model of huntington's disease', *Journal of Huntington's Disease*, 2(3), pp. 263–277. doi: 10.3233/JHD-130066.

McKinnon, P. J. (2009) 'DNA repair deficiency and neurological disease', *Nature Reviews Neuroscience*, 10(2), pp. 100–112. doi: 10.1038/nrn2559.

McKinnon, P. J. (2013) 'Maintaining genome stability in the nervous system', *Nature Neuroscience*. Nature Publishing Group, 16(11), pp. 1523–1529. doi: 10.1038/nn.3537.

McKinnon, P. J. (2016) 'Topoisomerases and the regulation of neural function', *Nature Reviews Neuroscience*, 17(11), pp. 673–679. doi: 10.1038/nrn.2016.101.

McKinnon, P. J. (2017) 'Genome integrity and disease prevention in the nervous system',

Genes & Development, 31(12), pp. 1180–1194. doi: 10.1101/gad.301325.117.

McKinstry, S. U. *et al.* (2014) 'Huntingtin is required for normal excitatory synapse development in cortical and striatal circuits', *Journal of Neuroscience*, 34(28), pp. 9455–9472. doi: 10.1523/JNEUROSCI.4699-13.2014.

Mealer, R. G. *et al.* (2014) 'Rhes, a Striatal-selective Protein Implicated in Huntington Disease, Binds Beclin-1 and activates autophagy', *Journal of Biological Chemistry*, 289(6), pp. 3547–3554. doi: 10.1074/jbc.M113.536912.

Mei, C. *et al.* (2020) 'The role of single strand break repair pathways in cellular responses to camptothecin induced DNA damage', *Biomedicine and Pharmacotherapy*, 125(January). doi: 10.1016/j.biopha.2020.109875.

Meisenberg, C. *et al.* (2015) 'Clinical and cellular roles for TDP1 and TOP1 in modulating colorectal cancer response to irinotecan.', *Molecular cancer therapeutics*, 14(2), pp. 575–85. doi: 10.1158/1535-7163.MCT-14-0762.

Mellott, A. J., Forrest, M. L. and Detamore, M. S. (2013) 'Physical non-viral gene delivery methods for tissue engineering', *Annals of Biomedical Engineering*, 41(3), pp. 446–468. doi: 10.1007/s10439-012-0678-1.

Menon, M. B. and Dhamija, S. (2018) 'Beclin 1 phosphorylation - at the center of autophagy regulation', *Frontiers in Cell and Developmental Biology*, 6(OCT), pp. 1–9. doi: 10.3389/fcell.2018.00137.

Menzies, F. M. *et al.* (2017) 'Autophagy and Neurodegeneration: Pathogenic Mechanisms and Therapeutic Opportunities', *Neuron*, 93(5), pp. 1015–1034. doi: 10.1016/j.neuron.2017.01.022.

Mercado-Uribe, H. *et al.* (2020) 'Analyzing structural alterations of mitochondrial intermembrane space superoxide scavengers cytochrome-c and SOD1 after methylglyoxal treatment', *PLoS ONE*, 15(4), pp. 1–14. doi: 10.1371/journal.pone.0232408.

Milakovic, T. and Johnson, G. V. W. (2005) 'Mitochondrial respiration and ATP production are significantly impaired in striatal cells expressing mutant huntingtin', *Journal of Biological Chemistry*, 280(35), pp. 30773–30782. doi: 10.1074/jbc.M504749200.

Mirkin, S. M. (2007) 'Expandable DNA repeats and human disease', *Nature*, 447(7147), pp. 932–940. doi: 10.1038/nature05977.

Mitra, J. *et al.* (2019) 'Motor neuron disease-associated loss of nuclear TDP-43 is linked to DNA double-strand break repair defects', *Proceedings of the National Academy of Sciences*, p. 201818415. doi: 10.1073/pnas.1818415116.

Mitra, S., Tsvetkov, A. S. and Finkbeiner, S. (2009) 'Single neuron ubiquitin-proteasome dynamics accompanying inclusion body formation in Huntington disease', *Journal of Biological Chemistry*, 284(7), pp. 4398–4403. doi: 10.1074/jbc.M806269200.

Mizushima, N. and Yoshimori, T. (2007) 'How to interpret LC3 immunoblotting', *Autophagy*, 3(6), pp. 542–545. doi: 10.4161/auto.4600.

Moily, N. S. *et al.* (2017) 'Transcriptional profiles for distinct aggregation states of mutant Huntingtin exon 1 protein unmask new Huntington's disease pathways', *Molecular and Cellular Neuroscience*. Elsevier, 83(July), pp. 103–112. doi: 10.1016/j.mcn.2017.07.004.

Moldovan, G. L. and D'Andrea, A. D. (2009) 'How the fanconi anemia pathway guards the genome', *Annual Review of Genetics*, 43, pp. 223–249. doi: 10.1146/annurev-genet-102108-134222.

Møllersen, L. *et al.* (2012) 'Neil1 is a genetic modifier of somatic and germline CAG trinucleotide repeat instability in R6/1 mice', *Human Molecular Genetics*, 21(22), pp. 4939–4947. doi: 10.1093/hmg/dds337.

Mollica, P. A. *et al.* (2016) 'DNA Methylation Leads to DNA Repair Gene Down-Regulation and Trinucleotide Repeat Expansion in Patient-Derived Huntington Disease Cells', *American Journal of Pathology*. American Society for Investigative Pathology, 186(7), pp. 1967–1976. doi: 10.1016/j.ajpath.2016.03.014.

Mori, F. *et al.* (2012) 'Autophagy-related proteins (p62, NBR1 and LC3) in intranuclear inclusions in neurodegenerative diseases', *Neuroscience Letters*. Elsevier Ireland Ltd, 522(2), pp. 134–138. doi: 10.1016/j.neulet.2012.06.026.

Morris, E. J. and Geller, H. (1996) 'Induction of neuronal apoptosis by camptothecin, an inhibitor of DNA topoisomerase-I: evidence for cell cycle-independent toxicity', *The Journal of cell biology*. J Cell Biol, 134(3), pp. 757–770. doi: 10.1083/JCB.134.3.757.

Mosbech, A. *et al.* (2013) 'The deubiquitylating enzyme USP44 counteracts the DNA double-strand break response mediated by the RNF8 and RNF168 ubiquitin ligases', *Journal of Biological Chemistry*, 288(23), pp. 16579–16587. doi: 10.1074/jbc.M113.459917.

Moss, D. J. H. *et al.* (2017) 'Identification of genetic variants associated with Huntington's disease progression: a genome-wide association study', *The Lancet Neurology*, 16(9), pp. 701–711. doi: 10.1016/S1474-4422(17)30161-8.

Moumné, L., Betuing, S. and Caboche, J. (2013) 'Multiple Aspects of Gene Dysregulation in Huntington's Disease', *Frontiers in Neurology*, 4(October), pp. 1–10. doi: 10.3389/fneur.2013.00127.

Moyal, L. *et al.* (2011) 'Requirement of ATM-Dependent Monoubiquitylation of Histone H2B for Timely Repair of DNA Double-Strand Breaks', *Molecular Cell*, 41, pp. 529–542. doi: 10.1016/j.molcel.2011.02.015.

Mozaffari, N. L., Pagliarulo, F. and Sartori, A. A. (2021) 'Human CtIP: A "double agent" in DNA repair and tumorigenesis', *Seminars in Cell and Developmental Biology*. Elsevier Ltd, 113Mozaffa(September 2020), pp. 47–56. doi: 10.1016/j.semcdb.2020.09.001.

Mrakovcic, M. and Fröhlich, L. F. (2018) 'P53-mediated molecular control of autophagy in tumor cells', *Biomolecules*, 8(2). doi: 10.3390/biom8020014.

Myeku, N. and Figueiredo-Pereira, M. E. (2011) 'Dynamics of the degradation of ubiquitinated proteins by proteasomes and autophagy: Association with sequestosome 1/p62', *Journal of Biological Chemistry*, 286(25), pp. 22426–22440. doi: 10.1074/jbc.M110.149252.

Nagaoka, U. *et al.* (2004) 'Increased expression of p62 in expanded polyglutamine-expressing cells and its association with polyglutamine inclusions', pp. 57–68. doi: 10.1111/j.1471-4159.2004.02692.x.

Nakada, S. (2016) 'Opposing roles of RNF8/RNF168 and deubiquitinating enzymes in ubiquitination-dependent DNA double-strand break response signaling and DNA-repair pathway choice', *Journal of Radiation Research*, 57(S1), pp. i33–i40. doi: 10.1093/jrr/rrw027.

Nakatani, R. *et al.* (2015) 'Large expansion of CTG·CAG repeats is exacerbated by MutSβ in human cells', *Scientific Reports*. Nature Publishing Group, 5, pp. 1–11. doi: 10.1038/srep11020.

Nasir, J. *et al.* (1995) 'Targeted disruption of the Huntington's disease gene results in embryonic lethality and behavioral and morphological changes in heterozygotes', *Cell*, 81(5), pp. 811–823. doi: 10.1016/0092-8674(95)90542-1.

Ng, H. M. *et al.* (2016) 'The Lys63-deubiquitylating enzyme BRCC36 limits DNA break processing and repair', *Journal of Biological Chemistry*, 291(31), pp. 16197–16207. doi: 10.1074/jbc.M116.731927.

Nihei, Y. *et al.* (2019) 'Poly-glycine–alanine exacerbates C9orf72 repeat expansion - mediated DNA damage via sequestration of phosphorylated ATM and loss of nuclear hnRNPA3', *Acta Neuropathologica*. Springer Berlin Heidelberg, 139(1), pp. 99–118. doi: 10.1007/s00401-019-02082-0.

Nishitoh, H. *et al.* (2008) 'ALS-linked mutant SOD1 induces ER stress- and ASK1-dependent motor neuron death by targeting Derlin-1', *Genes and Development*, 22(11), pp. 1451–1464. doi: 10.1101/gad.1640108.

Nóbrega, C. *et al.* (2013) 'Silencing Mutant Ataxin-3 Rescues Motor Deficits and Neuropathology in Machado-Joseph Disease Transgenic Mice', *PLoS ONE*, 8(1). doi: 10.1371/journal.pone.0052396.

Noguchi, T. *et al.* (2018) 'ALIS act as microdomains sensing cellular stresses and triggering oxidative stress- induced parthanatos', *Cell Death and Disease*. Springer US. doi: 10.1038/s41419-018-1245-y.

Nopoulos, P. C. *et al.* (2011) 'Smaller intracranial volume in prodromal Huntington's disease: Evidence for abnormal neurodevelopment', *Brain*, 134(1), pp. 137–142. doi: 10.1093/brain/awq280.

Novak, M. J. U. and Tabrizi, S. J. (2011) 'Huntington's disease: Clinical presentation and treatment', in *International Review of Neurobiology*. Elsevier Inc., pp. 297–323. doi: 10.1016/B978-0-12-381328-2.00013-4.

Nucifora, L. G. *et al.* (2012) 'Identification of novel potentially toxic oligomers formed in vitro from mammalian-derived expanded huntingtin exon-1 protein', *Journal of Biological Chemistry*, 287(19), pp. 16017–16028. doi: 10.1074/jbc.M111.252577.

Nybo, K. (2012) 'GFP imaging in fixed cells.', *BioTechniques*, 52(6), pp. 359–360. doi: 10.2144/000113872.

O'Regan, G. C. *et al.* (2020) 'Wild-type huntingtin regulates human macrophage function', *Scientific Reports*. Nature Publishing Group UK, 10(1), pp. 1–12. doi: 10.1038/s41598-020-74042-8.

O'Regan, G. C. *et al.* (2021) 'Human Huntington's disease pluripotent stem cell-derived microglia develop normally but are abnormally hyper-reactive and release elevated levels of reactive oxygen species', *Journal of Neuroinflammation*. Journal of Neuroinflammation, 18(1), pp. 1–17. doi: 10.1186/s12974-021-02147-6.

Orr, A. L. *et al.* (2008) 'N-terminal mutant huntingtin associates with mitochondria and impairs mitochondrial trafficking', *Journal of Neuroscience*, 28(11), pp. 2783–2792. doi: 10.1523/JNEUROSCI.0106-08.2008.

Ouyang, S. *et al.* (2015) 'RNF8 deficiency results in neurodegeneration in mice', *Neurobiology of Aging*, 36(10), pp. 2850–2860. doi: 10.1016/j.neurobiolaging.2015.07.010.

Owen, B. A. L. *et al.* (2005) '(CAG)n-hairpin DNA binds to Msh2-Msh3 and changes properties of mismatch recognition', *Nature Structural and Molecular Biology*, 12(8), pp. 663–670. doi: 10.1038/nsmb965.

Paine, H. (2015) 'Does loss of the normal protein function contribute to the pathogenesis of Huntington's disease?', *Bioscience Horizons*, 8, pp. 1–9. doi: 10.1093/biohorizons/hzv005.

Pal, S. and Tyler, J. K. (2016) 'Epigenetics and aging', *Science Advances*, 2(July). doi: 10.1007/978-3-319-55530-0_123.

Paldino, E. *et al.* (2017) 'Selective Sparing of Striatal Interneurons after Poly (ADP-Ribose) Polymerase 1 Inhibition in the R6/2 Mouse Model of Huntington's Disease', *Frontiers in Neuroanatomy*, 11(August), pp. 1–11. doi: 10.3389/fnana.2017.00061.

Panigrahi, G. B. *et al.* (2005) 'Slipped (CTG)•(CAG) repeats can be correctly repaired, escape repair or undergo error-prone repair', *Nature Structural and Molecular Biology*, 12(8), pp. 654–662. doi: 10.1038/nsmb959.

Panigrahi, G. B. *et al.* (2010) 'Isolated short CTG/CAG DNA slip-outs are repaired efficiently by hMutSβ, but clustered slip-outs are poorly repaired', *Proceedings of the National Academy of Sciences of the United States of America*, 107(28), pp. 12593–12598. doi: 10.1073/pnas.0909087107.

Paraskevopoulou, F., Herman, M. A. and Rosenmund, C. (2019) 'Glutamatergic innervation onto striatal neurons potentiates GABAergic synaptic output', *Journal of Neuroscience*, 39(23), pp. 4448–4460. doi: 10.1523/JNEUROSCI.2630-18.2019.

Patel, P. S. *et al.* (2021) 'RNF168 regulates R-loop resolution and genomic stability in BRCA1/2-deficient tumors', *Journal of Clinical Investigation*, 131(3). doi: 10.1172/JCI140105.

Pei, H. *et al.* (2011) 'MMSET regulates histone H4K20 methylation and 53BP1 accumulation at DNA damage sites', *Nature*. Nature Publishing Group, 470(7332), pp. 124–129. doi: 10.1038/nature09658.

Petr, M. A. *et al.* (2020) 'Protecting the Aging Genome', *Trends in Cell Biology*. Elsevier Inc.,

30(2), pp. 117–132. doi: 10.1016/j.tcb.2019.12.001.

Pietrucha, B. *et al.* (2017) 'Clinical and biological manifestation of RNF168 deficiency in two polish siblings', *Frontiers in Immunology*, 8(DEC), pp. 4–11. doi: 10.3389/fimmu.2017.01683.

Pinato, S. *et al.* (2009) 'RNF168, a new RING finger, MIU-containing protein that modifies chromatin by ubiquitination of histones H2A and H2AX', *BMC Molecular Biology*, 10, pp. 1–14. doi: 10.1186/1471-2199-10-55.

Pinto, R. M. *et al.* (2013) 'Mismatch repair genes Mlh1 and Mlh3 modify CAG instability in Huntington's disease mice: genome-wide and candidate approaches.', *PLoS genetics*, 9(10), p. e1003930. doi: 10.1371/journal.pgen.1003930.

Pircs, K. *et al.* (2018) 'Huntingtin Aggregation Impairs Autophagy, Leading to Argonaute-2 Accumulation and Global MicroRNA Dysregulation', *Cell Reports*, 24(6), pp. 1397–1406. doi: 10.1016/j.celrep.2018.07.017.

Pluciennik, A. *et al.* (2013) 'Extrahelical (CAG)/(CTG) triplet repeat elements support proliferating cell nuclear antigen loading and MutLa endonuclease activation', *Proceedings of the National Academy of Sciences of the United States of America*, 110(30), pp. 12277–12282. doi: 10.1073/pnas.1311325110.

Podhorecka, M., Skladanowski, A. and Bozko, P. (2010) 'H2AX phosphorylation: Its role in DNA damage response and cancer therapy', *Journal of Nucleic Acids*, 2010. doi: 10.4061/2010/920161.

Poetsch, A. R. (2020) 'The genomics of oxidative DNA damage, repair, and resulting mutagenesis', *Computational and Structural Biotechnology Journal*. The Author, 18, pp. 207–219. doi: 10.1016/j.csbj.2019.12.013.

Pommier, Y. *et al.* (2003) 'Repair of and checkpoint response to topoisomerase I-mediated DNA damage', *Mutation Research - Fundamental and Molecular Mechanisms of Mutagenesis*, 532(1–2), pp. 173–203. doi: 10.1016/j.mrfmmm.2003.08.016.

Pommier, Y. *et al.* (2006) 'Repair of Topoisomerase I-Mediated DNA Damage', *Progress in nucleic acid research and molecular biology*. NIH Public Access, 81, p. 179. doi: 10.1016/S0079-6603(06)81005-6.

Pommier, Y. (2006) 'Topoisomerase I inhibitors: camptothecins and beyond', *Nature Reviews Cancer*, 6(10), pp. 789–802. doi: 10.1038/nrc1977.

Pommier, Y. *et al.* (2014) 'Tyrosyl-DNA-phosphodiesterases (TDP1 and TDP2)', *DNA Repair*. Elsevier B.V., 19, pp. 114–129. doi: 10.1016/j.dnarep.2014.03.020.

Popiel, H. A. *et al.* (2007) 'Protein transduction domain-mediated delivery of QBP1 suppresses polyglutamine-induced neurodegeneration in vivo', *Molecular Therapy*. The American Society of Gene Therapy, 15(2), pp. 303–309. doi: 10.1038/sj.mt.6300045.

Porro, A. *et al.* (2021) 'FAN1-MLH1 interaction affects repair of DNA interstrand cross-links and slipped-CAG/CTG repeats', *Science Advances*, 7(31), pp. 1–13. doi: 10.1126/sciadv.abf7906.

Pourquier, P., Ueng, L. M., *et al.* (1997) 'Effects of uracil incorporation, DNA mismatches, and abasic sites on cleavage and religation activities of mammalian topoisomerase I', *Journal of Biological Chemistry*, 272(12), pp. 7792–7796. doi: 10.1074/jbc.272.12.7792.

Pourquier, P., Pilon, A. A., *et al.* (1997) 'Trapping of mammalian topoisomerase I and recombinations induced by damaged DNA containing nicks or gaps. Importance of DNA end phosphorylation and camptothecin effects', *Journal of Biological Chemistry*, 272(42), pp. 26441–26447. doi: 10.1074/jbc.272.42.26441.

Pourquier, P. and Pommier, Y. (2001) 'Topoisomerase I-mediated DNA damage', *Advances in Cancer Research*. Academic Press, 80, pp. 189–216. doi: 10.1016/S0065-230X(01)80016-6.

Prasad Tharanga Jayasooriya, R. G. *et al.* (2018) 'Camptothecin induces G2/M phase arrest through the ATM-Chk2-Cdc25C axis as a result of autophagy-induced cytoprotection: Implications of reactive oxygen species', *Oncotarget*, 9(31), pp. 21744–21757. doi: 10.18632/oncotarget.24934.

Qi, Y. *et al.* (2016) 'ATM mediates spermidine-induced mitophagy via PINK1 and Parkin regulation in human fibroblasts', *Scientific Reports*. Nature Publishing Group, 6, pp. 1–11. doi: 10.1038/srep24700.

Qiu, H. *et al.* (2014) 'ALS-associated mutation FUS-R521C causes DNA damage and RNA splicing defects', *Journal of Clinical Investigation*. American Society for Clinical Investigation, 124(3), pp. 981–999. doi: 10.1172/JCI72723.

Quigley, J. (2017) 'Juvenile Huntington's Disease: Diagnostic and Treatment Considerations for the Psychiatrist', *Current Psychiatry Reports*. Current Psychiatry Reports, 19(2), pp. 17–20. doi: 10.1007/s11920-017-0759-9.

Rahman, S. and Islam, R. (2011) 'Mammalian Sirt1: Insights on its biological functions', *Cell Communication and Signaling*. BioMed Central Ltd, 9(1), p. 11. doi: 10.1186/1478-811X-9-11.

Ramachandran, S. *et al.* (2021) 'Hypoxia-induced SETX links replication stress with the unfolded protein response', *Nature Communications*, 12(1), pp. 1–14. doi: 10.1038/s41467-021-24066-z.

Ramesh, N. and Pandey, U. B. (2017) 'Autophagy dysregulation in ALS: When protein aggregates get out of hand', *Frontiers in Molecular Neuroscience*, 10(August), pp. 1–18. doi: 10.3389/fnmol.2017.00263.

Ratovitski, T. *et al.* (2012) 'Huntingtin protein interactions altered by polyglutamine expansion as determined by quantitative proteomic analysis', *Cell Cycle*, 11(10), pp. 2006–2021. doi: 10.4161/cc.20423.

Reddy, K. *et al.* (2011) 'Determinants of R-loop formation at convergent bidirectionally transcribed trinucleotide repeats', *Nucleic Acids Research*. Oxford Academic, 39(5), pp. 1749–1762. doi: 10.1093/NAR/GKQ935.

Reid, D. A. *et al.* (2021) 'Incorporation of a nucleoside analog maps genome repair sites in postmitotic human neurons', *Science*, 372(6537), pp. 91–94. doi: 10.1126/science.abb9032.

Renkawitz, J., Lademann, C. A. and Jentsch, S. (2014) 'Mechanisms and principles of homology search during recombination', *Nature Reviews Molecular Cell Biology*. Nature Publishing Group, 15(6), pp. 369–383. doi: 10.1038/nrm3805.

Rigamonti, D. *et al.* (2000) 'Wild-type huntingtin protects from apoptosis upstream of caspase-3', *Journal of Neuroscience*, 20(10), pp. 3705–3713. doi: 10.1523/jneurosci.20-10-03705.2000.

Rigamonti, D. *et al.* (2001) 'Huntingtin's Neuroprotective Activity Occurs via Inhibition of Procaspase-9 Processing', *Journal of Biological Chemistry*, 276(18), pp. 14545–14548. doi: 10.1074/jbc.C100044200.

Rinaldi, C. *et al.* (2021) 'Sensing R-Loop-Associated DNA Damage to Safeguard Genome Stability', *Frontiers in Cell and Developmental Biology*, 8(January), pp. 1–13. doi: 10.3389/fcell.2020.618157.

Roos, R. A. C. (2010) 'Huntington's disease: A clinical review', *Orphanet Journal of Rare Diseases*. BioMed Central Ltd, 5(1), p. 40. doi: 10.1186/1750-1172-5-40.

Roy, A., George, S. and Palli, S. R. (2017) 'Multiple functions of CREB-binding protein during postembryonic development: Identification of target genes', *BMC Genomics*. BMC Genomics, 18(1), pp. 1–14. doi: 10.1186/s12864-017-4373-3.

Roy, J. C. L. *et al.* (2021) 'Somatic CAG expansion in Huntington's disease is dependent on the MLH3 endonuclease domain, which can be excluded via splice redirection', *Nucleic Acids Research*. Oxford University Press, 49(7), pp. 3907–3918. doi: 10.1093/nar/gkab152.

Rué, L. *et al.* (2013) 'Brain region- and age-dependent dysregulation of p62 and NBR1 in a mouse model of Huntington's disease', *Neurobiology of Disease*. Elsevier Inc., 52, pp. 219–228. doi: 10.1016/j.nbd.2012.12.008.

Rué, L. *et al.* (2016) 'Targeting CAG repeat RNAs reduces Huntington's disease phenotype independently of huntingtin levels', *Journal of Clinical Investigation*, 126(11), pp. 4319–4330. doi: 10.1172/JCI83185.

Rui, Y. N. *et al.* (2015) 'Huntingtin functions as a scaffold for selective macroautophagy', *Nature Cell Biology*, 17(3), pp. 262–275. doi: 10.1038/ncb3101.

Runwal, G. *et al.* (2019) 'LC3-positive structures are prominent in autophagy-deficient cells', *Scientific Reports*. Springer US, 9(1), pp. 1–14. doi: 10.1038/s41598-019-46657-z.

Sahl, S. J. *et al.* (2012) 'Cellular inclusion bodies of mutant huntingtin exon 1 obscure small fibrillar aggregate species', *Scientific Reports*, 2, pp. 1–7. doi: 10.1038/srep00895.

Salguero, I. *et al.* (2019) 'MDC1 PST-repeat region promotes histone H2AX-independent chromatin association and DNA damage tolerance', *Nature Communications*. Springer US, 10(1), pp. 1–11. doi: 10.1038/s41467-019-12929-5.

Salim, S. (2017) 'Oxidative stress and the central nervous system', *Journal of Pharmacology and Experimental Therapeutics*, 360(1), pp. 201–205. doi: 10.1124/jpet.116.237503.

Sánchez-Martın, P. and Komatsu, M. (2018) 'p62/SQSTM1 – Steering the cell through health

and disease', *Journal of Cell Science*, pp. 1–13. doi: 10.1242/jcs.222836.

Sap, K. A. and Reits, E. A. (2020) 'Strategies to Investigate Ubiquitination in Huntington's Disease', *Frontiers in Chemistry*, 8(June), pp. 1–15. doi: 10.3389/fchem.2020.00485.

Sartori, A. A. *et al.* (2007) 'Human CtIP promotes DNA end resection', *Nature*, 450(7169), pp. 509–514. doi: 10.1038/nature06337.

Sathasivam, K. *et al.* (2013) 'Aberrant splicing of HTT generates the pathogenic exon 1 protein in Huntington disease', *Proceedings of the National Academy of Sciences of the United States of America*, 110(6), pp. 2366–2370. doi: 10.1073/pnas.1221891110.

Saudou, F. and Humbert, S. (2016) 'The Biology of Huntingtin', *Neuron*, 89(5), pp. 910–926. doi: 10.1016/j.neuron.2016.02.003.

Schiefer, J., Werner, C. J. and Reetz, K. (2015) 'Clinical diagnosis and management in early Huntington's disease: a review', *Degenerative Neurological and Neuromuscular Disease*, Volume 5, pp. 37–50. doi: 10.2147/DNND.S49135.

Schmid, J. A. *et al.* (2018) 'Histone Ubiquitination by the DNA Damage Response Is Required for Efficient DNA Replication in Unperturbed S Phase', *Molecular Cell*. Elsevier Inc., 71(6), pp. 897-910.e8. doi: 10.1016/j.molcel.2018.07.011.

Schmidt, M. H. M. and Pearson, C. E. (2016) 'Disease-associated repeat instability and mismatch repair', *DNA Repair*. Elsevier B.V., 38, pp. 117–126. doi: 10.1016/j.dnarep.2015.11.008.

Schwab, R. A. *et al.* (2015) 'The Fanconi Anemia Pathway Maintains Genome Stability by Coordinating Replication and Transcription', *Molecular Cell*. Elsevier Inc., 60(3), pp. 351–361. doi: 10.1016/j.molcel.2015.09.012.

Schwertman, P., Bekker-Jensen, S. and Mailand, N. (2016) 'Regulation of DNA double-strand break repair by ubiquitin and ubiquitin-like modifiers', *Nature Reviews Molecular Cell Biology*. Nature Publishing Group, 17(6), pp. 379–394. doi: 10.1038/nrm.2016.58.

Scott, P. *et al.* (2019) 'Spinocerebellar ataxia with axonal neuropathy type 1 revisited', *Journal of Clinical Neuroscience*. Elsevier Ltd, 67, pp. 139–144. doi: 10.1016/j.jocn.2019.05.060.

Seidel, K. *et al.* (2010) 'Axonal inclusions in spinocerebellar ataxia type 3', *Acta Neuropathologica*, 120(4), pp. 449–460. doi: 10.1007/s00401-010-0717-7.

Sengupta, S. *et al.* (2020) 'Ligand-induced gene activation is associated with oxidative genome damage whose repair is required for transcription', *Proceedings of the National Academy of Sciences of the United States of America*, 117(36), pp. 22183–22192. doi: 10.1073/pnas.1919445117.

Seong, I. S. *et al.* (2009) 'Huntingtin facilitates polycomb repressive complex 2', *Human Molecular Genetics*, 19(4), pp. 573–583. doi: 10.1093/hmg/ddp524.

Shaikh, A. Y. and Martin, L. J. (2002) 'DNA base-excision repair enzyme apurinic/apyrimidinic endonuclease/redox factor-1 is increased and competent in the brain and spinal cord of individuals with amyotrophic lateral sclerosis', *NeuroMolecular Medicine*.

Springer Science and Business Media LLC, 2(1), pp. 47–60. doi: 10.1007/s12017-002-0038-7.

Sharma, A. *et al.* (2018) 'USP14 regulates DNA damage repair by targeting RNF168-dependent ubiquitination', *Autophagy*. Taylor & Francis, 14(11), pp. 1976–1990. doi: 10.1080/15548627.2018.1496877.

Sharma, N. *et al.* (2014) 'USP3 counteracts RNF168 via deubiquitinating H2A and γH2AX at lysine 13 and 15', *Cell Cycle*, 13(1), pp. 106–114. doi: 10.4161/cc.26814.

Sharma, P. M. *et al.* (2015) 'High throughput measurement of γH2AX DSB repair kinetics in a healthy human population', *PLoS ONE*, 10(3), pp. 1–18. doi: 10.1371/journal.pone.0121083.

Shelbourne, P. F. *et al.* (2007) 'Triplet repeat mutation length gains correlate with cell-type specific vulnerability in Huntington disease brain', *Human Molecular Genetics*, 16(10), pp. 1133–1142. doi: 10.1093/hmg/ddm054.

Shiloh, Y. and Ziv, Y. (2013) 'The ATM protein kinase: regulating the cellular response to genotoxic stress, and more', *Nature Reviews Molecular Cell Biology*. Nature Publishing Group, 14(4), pp. 197–210. doi: 10.1038/nrm3546.

Shirasaki, D. I. *et al.* (2012) 'Network organization of the huntingtin proteomic interactome in mammalian brain', *Neuron*, 75(1), pp. 41–57. doi: 10.1016/j.neuron.2012.05.024.

Shirendeb, U. *et al.* (2011) 'Abnormal mitochondrial dynamics, mitochondrial loss and mutant huntingtin oligomers in Huntington's disease: Implications for selective neuronal damage', *Human Molecular Genetics*, 20(7), pp. 1438–1455. doi: 10.1093/hmg/ddr024.

Shoaib, M. *et al.* (2018) 'Histone H4K20 methylation mediated chromatin compaction threshold ensures genome integrity by limiting DNA replication licensing', *Nature Communications*. Springer US, 9(1). doi: 10.1038/s41467-018-06066-8.

Sikora, E. *et al.* (2021) 'Cellular Senescence in Brain Aging', *Frontiers in Aging Neuroscience*, 13(February), pp. 1–23. doi: 10.3389/fnagi.2021.646924.

Singh, A. N. *et al.* (2019) 'The p97-Ataxin 3 complex regulates homeostasis of the DNA damage response E3 ubiquitin ligase RNF8.', *The EMBO journal*, 38(21), p. e102361. doi: 10.15252/embj.2019102361.

Skourti-Stathaki, K., Proudfoot, N. J. and Gromak, N. (2011) 'Human Senataxin Resolves RNA/DNA Hybrids Formed at Transcriptional Pause Sites to Promote Xrn2-Dependent Termination', *Molecular Cell*. Elsevier Inc., 42(6), pp. 794–805. doi: 10.1016/j.molcel.2011.04.026.

Sobczak, K. *et al.* (2010) 'Structural diversity of triplet repeat RNAs', *Journal of Biological Chemistry*, 285(17), pp. 12755–12764. doi: 10.1074/jbc.M109.078790.

Sobhian, B. *et al.* (2007) 'RAP80 targets BRCA1 to specific ubiquitin structures at DNA damage sites', *Science*, (May), pp. 1198–1203.

Sollier, J. *et al.* (2014) 'Transcription-Coupled Nucleotide Excision Repair Factors Promote R-Loop-Induced Genome Instability', *Molecular Cell*, 56(6), pp. 777–785. doi:

10.1016/j.molcel.2014.10.020.

Sordet, O. *et al.* (2008) 'Topoisomerase I Requirement for Death Receptor-induced Apoptotic Nuclear Fission', *Journal of Biological Chemistry*, 283(34), pp. 23200–23208. doi: 10.1074/jbc.M801146200.

Sordet, O. *et al.* (2009) 'Ataxia telangiectasia mutated activation by transcription- and topoisomerase I-induced DNA double-strand breaks', *EMBO reports*, 10(8), pp. 887–893. doi: 10.1038/embor.2009.97.

Sordet, O. *et al.* (2010) 'DNA double-strand breaks and ATM activation by transcription-blocking DNA lesions', *Cell Cycle*, 9(2), pp. 274–278. doi: 10.4161/cc.9.2.10506.

Stagni, V. *et al.* (2021) 'ATM Kinase-Dependent Regulation of Autophagy: A Key Player in Senescence?', *Frontiers in Cell and Developmental Biology*, 8(January), pp. 1–6. doi: 10.3389/fcell.2020.599048.

Steffan, J. S. *et al.* (2000) 'The Huntington's disease protein interacts with p53 and CREB-binding protein and represses transcription', *Proceedings of the National Academy of Sciences of the United States of America*, 97(12), pp. 6763–6768. doi: 10.1073/pnas.100110097.

Stewart, G. S. *et al.* (2007) 'RIDDLE immunodeficiency syndrome is linked to defects in 53BP1-mediated DNA damage signaling.', *Proceedings of the National Academy of Sciences of the United States of America*, 104(43), pp. 16910–5. doi: 10.1073/pnas.0708408104.

Stewart, G. S. *et al.* (2009) 'The RIDDLE Syndrome Protein Mediates a Ubiquitin-Dependent Signaling Cascade at Sites of DNA Damage', *Cell*, 136(3), pp. 420–434. doi: 10.1016/j.cell.2008.12.042.

Stout, J. C. *et al.* (2012) 'Neurocognitive Signs in Prodromal Huntington Disease', *Neuropsychology*, 25(1), pp. 1–14. doi: 10.1037/a0020937.Neurocognitive.

Su, X. A. and Freudenreich, C. H. (2017) 'Cytosine deamination and base excision repair cause R-loop–induced CAG repeat fragility and instability in Saccharomyces cerevisiae', *Proceedings of the National Academy of Sciences of the United States of America*, 114(40), pp. E8392–E8401. doi: 10.1073/pnas.1711283114.

Suberbielle, E. *et al.* (2013) 'Physiologic brain activity causes DNA double-strand breaks in neurons, with exacerbation by amyloid-β', *Nature Neuroscience*. Nature Publishing Group, 16(5), pp. 613–621. doi: 10.1038/nn.3356.

Sugars, K. L. and Rubinsztein, D. C. (2003) 'Transcriptional Abnormalities in Huntington's Disease', *Trends in Genetics*, 19(5), pp. 417–440. doi: 10.1002/3527608036.ch20.

Suk, T. R. and Rousseaux, M. W. C. (2020) 'The role of TDP-43 mislocalization in amyotrophic lateral sclerosis', *Molecular Neurodegeneration*. Molecular Neurodegeneration, 15(1), pp. 1–16. doi: 10.1186/s13024-020-00397-1.

Sun, X. *et al.* (2017) 'Conformation-dependent recognition of mutant HTT (huntingtin) proteins by selective autophagy', *Autophagy*, 13(12), pp. 2111–2112. doi: 10.1080/15548627.2017.1382783.

Sun, Y. *et al.* (2021) 'PARylation prevents the proteasomal degradation of topoisomerase I DNA-protein crosslinks and induces their deubiquitylation', *Nature Communications*. Springer US, 12(1), pp. 1–16. doi: 10.1038/s41467-021-25252-9.

Tabrizi, S. J. *et al.* (1999) 'Biochemical abnormalities and excitotoxicity in Huntington's disease brain', *Annals of Neurology*, 45(1), pp. 25–32. doi: 10.1002/1531-8249(199901)45:1<25::AID-ART6>3.0.CO;2-E.

Tabrizi, S. J. *et al.* (2020) 'Huntington disease: new insights into molecular pathogenesis and therapeutic opportunities', *Nature Reviews Neurology*. Springer US, 16(10), pp. 529–546. doi: 10.1038/s41582-020-0389-4.

Tang, J. *et al.* (2013) 'Acetylation limits 53BP1 association with damaged chromatin to promote homologous recombination', *Nature Structural and Molecular Biology*. Nature Publishing Group, 20(3), pp. 317–325. doi: 10.1038/nsmb.2499.

Tasdemir, E. *et al.* (2008) 'Regulation of autophagy by cytoplasmic p53', *Nature Cell Biology*, 10(6), pp. 676–687. doi: 10.1038/ncb1730.

Taylor, A. M. R., Groom, A. and Byrd, P. J. (2004) 'Ataxia-telangiectasia-like disorder (ATLD) - Its clinical presentation and molecular basis', *DNA Repair*, 3(8–9), pp. 1219–1225. doi: 10.1016/j.dnarep.2004.04.009.

Thorslund, T. *et al.* (2015) 'Histone H1 couples initiation and amplification of ubiquitin signalling after DNA damage', *Nature*, 527(7578), pp. 389–393. doi: 10.1038/nature15401.

Tobias, F. *et al.* (2013) 'Spatiotemporal Dynamics of Early DNA Damage Response Proteins on Complex DNA Lesions', *PLoS ONE*, 8(2), pp. 17–21. doi: 10.1371/journal.pone.0057953.

Toro, D. del *et al.* (2009) 'Mutant Huntingtin Impairs Post-Golgi Trafficking to Lysosomes by Delocalizing Optineurin/Rab8 Complex from the Golgi Apparatus', *Molecular biology of the cell*, 20, pp. 1478–1492. doi: 10.1091/mbc.E08.

Träger, U. *et al.* (2014) 'HTT-lowering reverses Huntington's disease immune dysfunction caused by NFκB pathway dysregulation', *Brain*, 137(3), pp. 819–833. doi: 10.1093/brain/awt355.

Tresini, M. *et al.* (2015) 'The core spliceosome as target and effector of non-canonical ATM signalling', *Nature*, 523(7558), pp. 53–58. doi: 10.1038/nature14512.

Tresini, M. *et al.* (2016) 'Bidirectional coupling of splicing and ATM signaling in response to transcription-blocking DNA damage', *RNA Biology*. Taylor & Francis, 13(3), pp. 272–278. doi: 10.1080/15476286.2016.1142039.

Trinkaus, V. A. *et al.* (2021) 'In situ architecture of neuronal α-Synuclein inclusions', *Nature Communications*. Springer US, 12(1), pp. 1–10. doi: 10.1038/s41467-021-22108-0.

Trushina, E. *et al.* (2004) 'Mutant Huntingtin Impairs Axonal Trafficking in Mammalian Neurons In Vivo and In Vitro', *Molecular and Cellular Biology*, 24(18), pp. 8195–8209. doi: 10.1128/mcb.24.18.8195-8209.2004.

Tsoi, H. and Chan, H. Y. E. (2013) 'Expression of expanded CAG transcripts triggers nucleolar

stress in huntington's disease', *Cerebellum*, 12(3), pp. 310–312. doi: 10.1007/s12311-012-0447-6.

Tsuburaya, N. *et al.* (2018) 'A small-molecule inhibitor of SOD1-Derlin-1 interaction ameliorates pathology in an ALS mouse model', *Nature Communications*. Springer US, 9(1), p. 2668. doi: 10.1038/s41467-018-05127-2.

Tulino, R. *et al.* (2016) 'SIRT1 activity is linked to its brain region-specific phosphorylation and is impaired in Huntington's disease mice', *PLoS ONE*, 11(1), pp. 1–25. doi: 10.1371/journal.pone.0145425.

Typas, D. *et al.* (2015) 'The de-ubiquitylating enzymes USP26 and USP37 regulate homologous recombination by counteracting RAP80', *Nucleic Acids Research*, 43(14), pp. 6919–6933. doi: 10.1093/nar/gkv613.

Uckelmann, M. and Sixma, T. K. (2017) 'Histone ubiquitination in the DNA damage response', *DNA Repair*. Elsevier, 56(June), pp. 92–101. doi: 10.1016/j.dnarep.2017.06.011.

Usdin, K., House, N. C. M. and Freudenreich, C. H. (2015) 'Repeat instability during DNA repair: Insights from model systems', *Critical Reviews in Biochemistry and Molecular Biology*. Informa Healthcare, 50(2), pp. 142–167. doi: 10.3109/10409238.2014.999192.

Uziel, T. *et al.* (2003) 'Requirement of the MRN complex for ATM activation by DNA damage', *EMBO Journal*, 22(20), pp. 5612–5621. doi: 10.1093/emboj/cdg541.

Valentin-Vega, Y. A. *et al.* (2012) 'Mitochondrial dysfunction in ataxia-telangiectasia', *Blood*, 119(6), pp. 1490–1500. doi: 10.1182/blood-2011-08-373639.The.

Velimezi, G. *et al.* (2018) 'Map of synthetic rescue interactions for the Fanconi anemia DNA repair pathway identifies USP48', *Nature Communications*. Springer US, 9(1). doi: 10.1038/s41467-018-04649-z.

Ventura-Clapier, R., Garnier, A. and Veksler, V. (2008) 'Transcriptional control of mitochondrial biogenesis: The central role of PGC-1α', *Cardiovascular Research*, 79(2), pp. 208–217. doi: 10.1093/cvr/cvn098.

Vicencio, E. *et al.* (2020) 'Implications of Selective Autophagy Dysfunction for ALS Pathology', *Cells*, 9(2), p. 381. doi: 10.3390/cells9020381.

Vis, J. C. *et al.* (2005) 'Expression pattern of apoptosis-related markers in Huntington's disease', *Acta Neuropathologica*, 109(3), pp. 321–328. doi: 10.1007/s00401-004-0957-5.

Voisin, J. *et al.* (2020) 'FOXO3 targets are reprogrammed as Huntington's disease neural cells and striatal neurons face senescence with p16INK4a increase', *Aging Cell*, 19(11), pp. 1–15. doi: 10.1111/acel.13226.

Waaijer, M. E. C. *et al.* (2016) 'DNA damage markers in dermal fibroblasts in vitro reflect chronological donor age', *Aging*, 8(1), pp. 147–157. doi: 10.18632/aging.100890.

Waelter, S. *et al.* (2001) 'Accumulation of mutant huntingtin fragments in aggresome-like inclusion bodies as a result of insufficient protein degradation.', *Molecular biology of the cell*, 12(5), pp. 1393–407. doi: 10.1091/mbc.12.5.1393.

Wahba, L. *et al.* (2011) 'RNase H and Multiple RNA Biogenesis Factors Cooperate to Prevent RNA:DNA Hybrids from Generating Genome Instability', *Molecular Cell*. Elsevier, 44(6), pp. 978–988. doi: 10.1016/j.molcel.2011.10.017.

Walker, C. *et al.* (2017) 'C9orf72 expansion disrupts ATM-mediated chromosomal break repair', *Nature Neuroscience*, 20(9), pp. 1225–1235. doi: 10.1038/nn.4604.

Walker, C. and El-Khamisy, S. F. (2018) 'Perturbed autophagy and DNA repair converge to promote neurodegeneration in amyotrophic lateral sclerosis and dementia.', *Brain : a journal of neurology*, 141(5), pp. 1247–1262. doi: 10.1093/brain/awy076.

Walser, F. *et al.* (2020) 'Ubiquitin Phosphorylation at Thr12 Modulates the DNA Damage Response', *Molecular Cell*, 80(3), pp. 423-436.e9. doi: 10.1016/j.molcel.2020.09.017.

Wang, B. and Elledge, S. J. (2007) 'Ubc13/Rnf8 ubiquitin ligases control foci formation of the Rap80/Abraxas/Brca1/Brcc36 complex in response to DNA damage', *Proceedings of the National Academy of Sciences*, 104(52), pp. 20759–20763. doi: 10.1073/pnas.0710061104.

Wang, J. *et al.* (2014) 'PTIP associates with artemis to dictate DNA repair pathway choice', *Genes and Development*, 28(24), pp. 2693–2698. doi: 10.1101/gad.252478.114.

Wang, L. *et al.* (2019) 'p62-mediated Selective autophagy endows virus-transformed cells with insusceptibility to DNA damage under oxidative stress', *PLOS Pathogens*. Edited by P. M. Lieberman, 15(4), p. e1007541. doi: 10.1371/journal.ppat.1007541.

Wang, W.-Y. *et al.* (2013) 'Interaction of FUS and HDAC1 regulates DNA damage response and repair in neurons', *Nature Neuroscience*. Nature Publishing Group, 16(10), pp. 1383–1391. doi: 10.1038/nn.3514.

Wang, X. and Ge, P. (2020) 'Parthanatos in the pathogenesis of nervous system diseases', *Neuroscience*. IBRO, 449, pp. 241–250. doi: 10.1016/j.neuroscience.2020.09.049.

Wang, Y. *et al.* (2016) 'Autophagy Regulates Chromatin Ubiquitination in DNA Damage Response through Elimination of SQSTM1/p62', *Molecular Cell*, 63(1), pp. 34–48. doi: 10.1016/j.molcel.2016.05.027.

Wang, Z. *et al.* (2016) 'USP51 deubiquitylates H2AK13, 15ub and regulates DNA damage response', *Genes & development*, 30(8), pp. 946–959. doi: 10.1101/gad.271841.115.5.

Watroba, M. and Szukiewicz, D. (2016) 'The role of sirtuins in aging and age-related diseases', *Advances in Medical Sciences*, 61(1), pp. 52–62. doi: 10.1016/j.advms.2015.09.003.

Wei, H. and Yu, X. (2016) 'Functions of PARylation in DNA Damage Repair Pathways', *Genomics, Proteomics & Bioinformatics*. Beijing Institute of Genomics, Chinese Academy of Sciences and Genetics Society of China, 14(3), pp. 131–139. doi: 10.1016/j.gpb.2016.05.001.

Wellington, C. L. *et al.* (2002) 'Caspase cleavage of mutant huntingtin precedes neurodegeneration in Huntington's disease', *Journal of Neuroscience*, 22(18), pp. 7862–7872. doi: 10.1523/jneurosci.22-18-07862.2002.

Wheeler, V. C. and Dion, V. (2021) 'Modifiers of CAG/CTG Repeat Instability: Insights from Mammalian Models', *Journal of Huntington's Disease*, 10(1), pp. 123–148. doi: 10.3233/JHD-

200426.

White, J. K. *et al.* (1997) 'Huntingtin is required for neurogenesis and is not impaired by the Huntington's disease CAG expansion', *Nature Genetics*, 17(december), pp. 404–410.

Wilson, D. M. and Bohr, V. A. (2007) 'The mechanics of base excision repair, and its relationship to aging and disease', *DNA Repair*, 6(4), pp. 544–559. doi: 10.1016/j.dnarep.2006.10.017.

Wilson, M. D. *et al.* (2016) 'The structural basis of modified nucleosome recognition by 53BP1', *Nature*. Nature Publishing Group, 536(7614), pp. 100–103. doi: 10.1038/nature18951.

Wojcik, F. *et al.* (2018) 'Functional crosstalk between histone H2B ubiquitylation and H2A modifications and variants', *Nature communications*, 1394(9), pp. 1–11. doi: 10.1038/s41467-018-03895-5.

Wold, M. S. *et al.* (2016) 'ULK1-mediated phosphorylation of ATG14 promotes autophagy and is impaired in Huntington's disease models', *Molecular Neurodegeneration*. Molecular Neurodegeneration, 11(1), pp. 1–13. doi: 10.1186/s13024-016-0141-0.

Wong, Y. C. and Holzbaur, E. L. F. (2014) 'The regulation of autophagosome dynamics by huntingtin and HAP1 is disrupted by expression of mutant huntingtin, leading to defective cargo degradation', *Journal of Neuroscience*, 34(4), pp. 1293–1305. doi: 10.1523/JNEUROSCI.1870-13.2014.

Wright, G. E. B. *et al.* (2019) 'Length of Uninterrupted CAG, Independent of Polyglutamine Size, Results in Increased Somatic Instability, Hastening Onset of Huntington Disease', *American Journal of Human Genetics*, 104(6), pp. 1116–1126. doi: 10.1016/j.ajhg.2019.04.007.

Wright, G. E. B. *et al.* (2020) 'Interrupting sequence variants and age of onset in Huntington's disease: clinical implications and emerging therapies', *The Lancet Neurology*. Elsevier Ltd, 19(11), pp. 930–939. doi: 10.1016/S1474-4422(20)30343-4.

Wu, W. *et al.* (2021) 'Neuronal enhancers are hotspots for DNA single-strand break repair', *Nature*. Springer US, 593(7859), pp. 440–444. doi: 10.1038/s41586-021-03468-5.

Xi, W. *et al.* (2016) 'Multiple discrete soluble aggregates influence polyglutamine toxicity in a Huntington ' s disease model system', *Nature Publishing Group*. Nature Publishing Group, (September), pp. 1–14. doi: 10.1038/srep34916.

Xia, J. *et al.* (2003) 'Huntingtin contains a highly conserved nuclear export signal', *Human Molecular Genetics*, 12(12), pp. 1393–1403. doi: 10.1093/hmg/ddg156.

Yan, W. X. *et al.* (2017) 'BLISS is a versatile and quantitative method for genome-wide profiling of DNA double-strand breaks', *Nature Communications*, 8. doi: 10.1038/ncomms15058.

Yang, J. L. *et al.* (2020) 'Oxidative DNA damage is concurrently repaired by base excision repair (BER) and apyrimidinic endonuclease 1 (APE1)-initiated nonhomologous end joining (NHEJ) in cortical neurons', *Neuropathology and Applied Neurobiology*, 46(4), pp. 375–390. doi: 10.1111/nan.12584.

Yang, Z. and Klionsky, D. J. (2010) ‘Eaten alive: A history of macroautophagy’, *Nature Cell Biology*. Nature Publishing Group, 12(9), pp. 814–822. doi: 10.1038/ncb0910-814.

Ye, J. *et al.* (2016) ‘CPP-assisted intracellular drug delivery, what is next?’, *International Journal of Molecular Sciences*, 17(11), pp. 1–16. doi: 10.3390/ijms17111892.

Yehuda, A. Ben *et al.* (2017) ‘Ubiquitin accumulation on disease associated protein aggregates is correlated with nuclear ubiquitin depletion, histone De-ubiquitination and impaired DNA damage response’, *PLoS ONE*, 12(1), pp. 1–17. doi: 10.1371/journal.pone.0169054.

Yoshii, S. R. and Mizushima, N. (2017) ‘Monitoring and measuring autophagy’, *International Journal of Molecular Sciences*, 18(9), pp. 1–13. doi: 10.3390/ijms18091865.

Yu, C. *et al.* (2018) ‘Decreased BDNF Release in Cortical Neurons of a Knock-in Mouse Model of Huntington’s Disease’, *Scientific Reports*. Springer US, 8(1), pp. 1–11. doi: 10.1038/s41598-018-34883-w.

Yu, M. *et al.* (2017) ‘Suppression of MAPK11 or HIPK3 reduces mutant Huntingtin levels in Huntington’s disease models’, *Cell Research*, 27(12), pp. 1441–1465. doi: 10.1038/cr.2017.113.

Zaksauskaite, R. *et al.* (2021) ‘Tdp1 protects from topoisomerase 1–mediated chromosomal breaks in adult zebrafish but is dispensable during larval development’, *Science Advances*, 7(5), p. eabc4165. doi: 10.1126/sciadv.abc4165.

Zeitler, B. *et al.* (2019) ‘Allele-selective transcriptional repression of mutant HTT for the treatment of Huntington’s disease’, *Nature Medicine*, 25(7), pp. 1131–1142. doi: 10.1038/s41591-019-0478-3.

Zhang, J. *et al.* (2015) ‘ATM functions at the peroxisome to induce pexophagy in response to ROS’, *Nature Cell Biology*, 17(10), pp. 1259–1269. doi: 10.1038/ncb3230.

Zhang, Q. *et al.* (2018) ‘A peptidylic inhibitor for neutralizing expanded CAG RNA-induced nucleolar stress in polyglutamine diseases.’, *RNA*, 24(4), pp. 486–498. doi: 10.1261/rna.062703.117.

Zhang, Y. *et al.* (2006) ‘Huntingtin inhibits caspase-3 activation’, *EMBO Journal*, 25(24), pp. 5896–5906. doi: 10.1038/sj.emboj.7601445.

Zhao, H. *et al.* (2018) ‘RNase H eliminates R-loops that disrupt DNA replication but is nonessential for efficient DSB repair’, *EMBO reports*, 19(5), pp. 1–10. doi: 10.15252/embr.201745335.

Zheng, P. and Kozloski, J. (2017) ‘Striatal Network Models of Huntington ’ s Disease Dysfunction Phenotypes’, *Frontiers in Computational Neuroscience*, 11(July), pp. 1–12. doi: 10.3389/fncom.2017.00070.

Zimmermann, M. and De Lange, T. (2014) ‘53BP1: Pro choice in DNA repair’, *Trends in Cell Biology*. Elsevier Ltd, 24(2), pp. 108–117. doi: 10.1016/j.tcb.2013.09.003.

Zou, Z.-Y. *et al.* (2017) ‘Genetic epidemiology of amyotrophic lateral sclerosis: a systematic review and meta-analysis.’, *Journal of Neurology, Neurosurgery, and Psychiatry*. BMJ

Publishing Group Ltd, 88(7), pp. 540–549. doi: 10.1136/jnnp-2016-315018.

Zuccato, C. *et al.* (2001) 'Loss of huntingtin-mediated BDNF gene transcription in Huntington's disease', *Science*, 293(5529), pp. 493–498. doi: 10.1126/science.1059581.

Zuccato, C. *et al.* (2003) 'Huntingtin interacts with REST/NRSF to modulate the transcription of NRSE-controlled neuronal genes', *Nature Genetics*, 35(1), pp. 76–83. doi: 10.1038/ng1219.